

**ELLYBEN  
ÖLVASHATÓ**

**ACTA UNIVERSITATIS SZEGEDIENSIS**

# **ACTA MINERALOGICA-PETROGRAPHICA**

**Tomus XXVIII**

**SZEGED, HUNGARIA**

**1986**

## NOTE TO CONTRIBUTORS

### General

The Acta Mineralogica—Petrographica publishes original studies on the field of geochemistry, mineralogy and petrology, first of all studies of Hungarian researchers, papers resulted in by co-operation of Hungarian researchers and those of other countries and, in a limited volume, papers from abroad on topics of global interest.

Manuscripts should be written in English and submitted to the Editor-in-chief, Institute of Mineralogy, Geochemistry and Petrography, Attila József University, H-6701 Szeged, Pf. 651 Hungary.

The authors are responsible for the accuracy of their data, references and quotations from other sources.

### Manuscript

Manuscripts should be typewritten with double spacing, 25 lines on a page and space for 50 letters in a line. Each new paragraph should begin with an indented line. Underline only words that should be typed in italics.

Manuscripts should generally be organized in the following order:

Title

Name(s) of author(s) and their affiliations, in foot-note the address of the author to whom the correspondence should be sent.

Abstract

Introduction

Methods, techniques, material studied, description of the area investigated, etc.

Results

Discussion or conclusions

Acknowledgement

Explanation of plates (if any)

Tables

Captions of figures (drawings, photomicrographs, etc.)

### Abstract

The abstract cannot be longer than 500 words.

### Tables

The tables should be typewritten on separate sheets and numbered according to their sequence in the text, which refers to all tables.

The title of the table as well as the column headings must be brief, but sufficiently explanatory.

The tables generally should not exceed the type-area of the journal, i.e. 12.5×18.5 cm. Fold-outs can only exceptionally be accepted



HELYBEN  
OLVASHATÓ

B 120234

ACTA UNIVERSITATIS SZEGEDIENSIS

# ACTA MINERALOGICA-PETROGRAPHICA

Tomus XXVIII

SZEGED, HUNGARIA

1986

HU ISSN 0365—8066

HU ISSN 0324—6523

Adjuvantibus

BÉLA MOLNÁR et TIBOR SZEDERKÉNYI

Redigit

GYULA GRASSELLY

Edit

Institutum Mineralogicum, Geochimicum et Petrographicum  
Universitatis Szegediensis de Attila József nominatae

Nota

Acta Miner. Petr., Szeged

Szerkeszti

GRASSELLY GYULA

A szerkesztőbizottság tagjai

MOLNÁR BÉLA és SZEDERKÉNYI TIBOR

Kiadja

a József Attila Tudományegyetem Ásványtani, Geokémiai és  
Kőzettani Tanszéke

H—6722 Szeged, Egyetem u. 2—6.

Kiadványunk címének rövidítése  
Acta Miner. Petr., Szeged



**B120234**



## CONTENTS

KOTSIS, T.: Penninic ophiolites at the eastern margin of the Eisenberg-group (Felsőcsatár, W-Hungary) .....	5
ALLAM, AHMED and SHAMAH, KAMAL: Microfacial analysis and environmental development of the Duwi (phosphate) formation, Quseir-Safaga District, Eastern Desert, Egypt.....	11
MSTIVSLAVSKIY, M. M.: Regularities in the formation of manganese deposits on continents....	21
VEIMARN, A. B., ROZHN OV, A. A. and SCHIBRIK, V. I.: Iron and manganese ores in the geological history of Central Kazakhstan.....	37
TOMSCHEY, O.: Trace elements in metamorphic and granitoid rocks of the basement in the Central Danube—Tisza Interfluve (Hungary).....	47
GUIRGUIS, L. A.: Infrared vibrational sulphate band shift correlation in alkaline sulphate minerals .....	57
BÉRCZI, SZ. and <u>BÉRCZI, J.</u> : Rare earth element content in the Szentbék kála series of peridotite inclusions .....	61
BALOGH, KADOSA, ÁRVA-SÓS, E., PÉCSKAY, Z. and RAVASZ-BARANYAI, L.: K/Ar dating of post-Sarmatian alkali basaltic rocks in Hungary.....	75
HETÉNYI, M. and KEDVES, M.: Organic geochemical characterization of brown coals by thermal degradation and modified Rock-Eval method.....	95
HETÉNYI, M. and PÁPAY, L.: Type and evolution stage of Hungarian oil shale kerogens.....	109

1. The first step in the process of creating a new product is to identify a market need. This involves conducting market research to determine what consumers want and what problems they are trying to solve. Once a need is identified, the next step is to develop a concept for a product that addresses that need.

2. The second step is to create a prototype of the product. This involves building a physical model of the product that can be used to test the concept and gather feedback from potential customers.

## **PENNINIC OPHIOLITES AT THE EASTERN MARGIN OF THE EISENBERG-GROUP (FELSŐCSATÁR, W-HUNGARY)**

**T. KOTSIS**

Department of Petrology and Geochemistry, Loránd Eötvös University

### **ABSTRACT**

At the Eastern termination of the Alps there are various greenstones of basaltic origin, ultramafites and a meta-ultrabasic rocks exposed in the tectonic windows of the Eisenberg-Group. The paper gives detailed description of the mineralogy and mineral chemistry of this rock suite.

### **INTRODUCTION**

In the "Rechnitzer Penninikum" (PAHR, 1977, 1980a, 1980b) there is ample evidence of an igneous activity, the age of which apparently coincides with the early stage of the Cretaceous sedimentation. Predominant products of this activity are lavas and tuffs of basaltic composition with gabbros and various ultramafics. The magmatic centers were found in Austrian territory, whereas in Hungary mainly pyroclastics were detected by mapping in the areas adjoining the Austro-Hungarian frontier. The original depth and character of the igneous activity is not yet fully disclosed and need more detailed research the first result of which are presented here.

### **GEOLOGICAL SETTING**

The Eisenberg-Window is built up by Mesozoic metasediments (*i.e.* quartzphyllites, phyllites, carbonate-phyllites and calcareous shales) with some metamorphic ophiolites (metabasalts, ultramafites, meta-ultrabasics). Their lithostatigraphic setting was established on the basis of information supplied by outcrops, exploration-drifts and bore holes (SZEÉNYI, 1948, VARRÓK, 1953, KOTSIS, 1957, 1982, VENDEL and KISHÁZI, 1967, KUBOVICS, 1983). The deepest known members of the sequence are organic-rich graphite-bearing phyllites and quartzphyllites overlain by carbonate phyllites at places with a characteristic conglomerate (the Cák-conglomerate) which are covered by carbonate phyllites, calcareous phyllites, calcareous shales and crystalline limestone. The uppermost member of the sequence is a thick series of greenschist. The phyllite series contains large complexes of serpentinite to have been intruded in solid state. Along the margins of the serpentinite mass there are meta-ultrabasics of various composition.

## PETROLOGY OF OPHIOLITES

The ophiolites are represented by 1. greenstones, 2 ultramafics (serpentinized), 3. meta-ultrabasites.

*1. Greenstones of basaltic origin.* These rocks are usually of pale-green color, compact and — at places — exhibit more or less pronounced schistosity. Their major constituents are albite, epidote, tremolite-actinolite and chlorite. The mafic minerals are characteristically poor in iron: both the clinozoisite-epidote and tremolite-actinolite series are represented by their iron-poor members. It is the amount of chlorites which fluctuates most, also it never exceeds the amount of the afore-mentioned two other components. The only felsic mineral is albite, occurring as large porphyroblasts. Minor components: quartz, titanite as common constituents of sedimentary origin, pyrite slightly altered to limonite and secondary vermiculite, rare carbonate.

On the basis of 28 modal analyses of the basaltic greenstones the mineralogical composition is as follows: albite 30% (19—37), chlorite 18% (6—33), epidote-clinozoisite 23% (5—35), tremolite-actinolite 27% (16—36), titanite 5% (3—6). Detailed mineralogical data (after LORENZ, 1976) are shown Fig. 1.

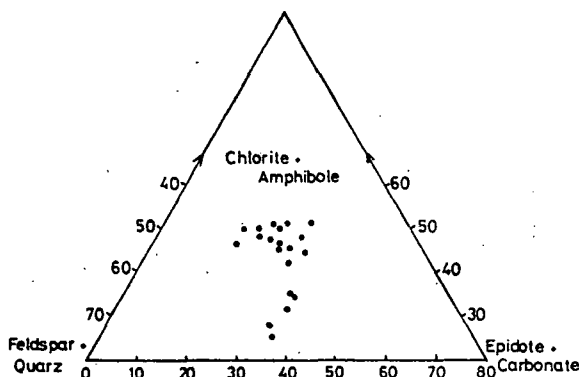


Fig. 1. Mineral composition of basaltic greenstones.

The possible pyroclastic origin of greenstones is reflected also by the relative high fluctuations of some elements from the chemical analyses (e.g.  $\text{SiO}_2$ ,  $\text{Na}_2\text{O}$ ). Their whole rock chemical composition is shown in Table 1.

## 2. SERPENTINITES

Serpentinites are medium green, blackish-green rocks with Al-bearing antigorite and lizardite as major constituents. Monomineralic serpentinites are rare. They usually contain minor components as talc or fibrous silica minerals (lussatite, chalcedony). At places relict aggregates of olivin, grains of ilmenite, magnetite and chromite also occur.

There were no relict pyroxenes in any of the Hungarian rocks; whereas in Austria W. POLLAK (1962) identified ones in the Badersdorf serpentinite. The antigorite-lizardite aggregates, however, nicely preserve the shape of the olivine grains.

Chemical analyses of some selected samples are shown in Table 2. That clearly

Chemical composition of the greenschists of the Eisenberg Group

TABLE 1

	1	2	3	4	5	6	7	8	9	10	11	12	13*
SiO <sub>2</sub>	47.25	48.76	49.85	51.80	42.40	53.60	53.11	48.26	45.73	48.67	50.57	48.84	38.75
TiO <sub>2</sub>	1.52	1.57	1.57	2.33	0.92	0.95	0.69	1.57	1.12	1.60	1.20	1.13	6.23
Al <sub>2</sub> O <sub>3</sub>	16.23	13.77	17.40	14.02	17.26	19.58	16.55	16.77	17.04	15.75	13.83	17.68	13.55
Fe <sub>2</sub> O <sub>3</sub>	10.36	7.80	9.94	8.23	10.55	9.61	2.33	7.80	7.13	1.00	0.90	2.24	8.83
FeO	—	3.32	—	—	—	—	6.02	3.72	3.38	—	7.09	4.65	8.50
MgO	6.55	7.60	7.55	10.45	11.30	3.15	7.60	7.60	8.50	9.84	5.58	6.45	5.29
MnO	0.32	—	0.29	0.12	0.28	0.34	—	0.27	0.15	—	0.15	0.12	0.19
CaO	9.30	7.57	6.60	9.46	7.95	6.10	9.54	7.57	11.95	7.84	12.16	12.56	11.25
Na <sub>2</sub> O	3.11	3.42	2.41	0.18	1.34	2.56	0.22	3.42	2.70	2.94	4.49	2.77	1.95
K <sub>2</sub> O	0.65	0.75	0.28	0.37	0.47	0.55	0.14	0.65	0.18	0.57	0.13	0.05	0.26
H <sub>2</sub> O	4.95	3.23	4.32	3.36	7.27	3.67	0.45	2.73	2.20	2.77	2.61	1.43	5.03
Σalk	3.76	4.17	2.69	0.55	1.81	3.11	0.36	4.07	2.88	3.51	4.62	2.82	2.21

1—9 Felsőcsatár; 10 Badersdorf; 11 Pinkatal-Burg; 12 Woppendorf; 13\* crossit-greenschist Felsőcsatár

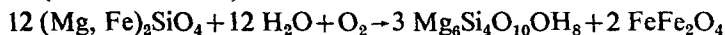
Chemical composition of the Felsőcsatár serpentinites

TABLE 2

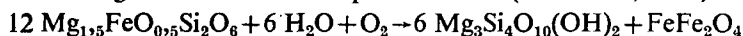
	1	2	3	4	5	6	7	8	9	10
SiO <sub>2</sub>	39.30	37.85	39.28	36.31	39.05	36.45	36.86	38.80	46.00	56.3
TiO <sub>2</sub>	0.19	0.06	0.01	0.01	0.02	0.01	0.01	2.67	0.10	0.1
Al <sub>2</sub> O <sub>3</sub>	4.58	6.05	1.52	1.63	1.69	1.28	1.28	1.53	2.52	1.0
Fe <sub>2</sub> O <sub>3</sub>	10.28	10.98	8.52	7.45	7.19	4.50	6.86	12.32	1.40	1.9
FeO	—	—	—	—	—	—	—	—	4.40	3.5
MgO	29.45	30.91	36.83	35.45	36.45	33.62	32.85	27.90	32.30	26.3
MnO	0.10	0.09	0.08	0.14	0.08	0.25	0.19	0.13	0.10	—
CaO	1.32	0.90	0.91	1.06	0.91	3.54	1.84	4.41	—	0.8
Na <sub>2</sub> O	—	0.38	0.14	—	0.39	0.64	0.24	0.14	—	—
K <sub>2</sub> O	—	0.26	0.32	—	0.12	0.43	0.30	0.53	0.05	—
H <sub>2</sub> O	13.41	12.32	12.32	17.02	14.10	17.02	19.10	11.15	12.90	9.8

indicate the peridotitic pyroxenitic character of the parent rock: sample No. 9 is unusually low in CaO, which calls for orthorhombic pyroxenes and olivine to be supposed as parent minerals (neither monoclinic pyroxenes nor Ca-amphiboles could provide for such a Ca-poor mineral assemblage when metamorphosed). The normative composition of their protolith rock (calculated on dry basis) probably comprises forsterite-rich olivine (cca 30 percent) and bronzitic pyroxene (cca 70 percent).

The formation of the major constituents of these ultrabasic rocks (*i. e.* antigorite, lizardite and secondary magnetite) and the alteration of the serpentine minerals into talc and local silification of the serpentinite can be reconstructed and deduced from the equation (KUBOVICS, 1983):



Talc occurs mainly along the margins of the serpentinite bodies, thus reflecting the late metamorphic-metasomatic character of talc formation. It is accompanied by silica minerals and carbonates indicating that talc itself was formed by metamorphic-metasomatic alteration also of serpentinites of ultramafic origin. It seems to be highly probable, however, that the reaction producing talc took place at a temperature somewhat higher than that of serpentinization (KUBOVICS, 1983):



It can be supposed that the proportion of ferrous iron in the original pyroxene was somewhat higher than indicated by the equation above and thus the alteration may have resulted in the release of silica, which then contributed to the formation of talc and to silification. During serpentinization of the ultrabasites also some chlorites (chloritites, chlorite-schists) were formed in the marginal parts, the character of which is a sensitive indicator of the varying nature of the metamorphism.

The chlorite schists consist mainly of Mg-rich chlorite minerals of various iron content, part of which can be deduced from the original material of the parent ultrabasics (particularly when locally within the ultramafic suite the presence of some Al-rich rocks, such as hornblendites, can be supposed).

Hornblendites often forming the marginal facies of peridotite-pyroxenite complexes offer an attractive explanation for the formation of the chlorite-schists by their metamorphic alteration.

This idea seems to be supported by the presence of titanite-chlorite, a peculiar variety of chlorite-schists in the area concerned (see also below).

### 3. META-ULTRABASICS

According to the latest results of mapping in the Felsőcsatár area there are titanium- and iron-bearing meta-ultrabasics of various origin in the scree covering the SE slopes of the Nagyvilágos-hill. As to petrology they are titanite-crossitites (1, 2, 3) titanite-chloritites (4) and crossite-epidote-greenstones (5).

The titanite-crossitites consist of alkali-amphiboles of centimeter size with titanite-pseudomorphs after ilmenite. There is an inverse relationship between crossite, epidote, chlorite and albite: the less the percentage of crossite the higher the percentages of epidote+chlorite+albite. It is remarkable that as to composition most crossite crystals are inhomogeneous and along their cleavage planes sometimes even glaucophane may occur.

The titanite-chloritite consist of titanite and rhipidolite with accessory magnetite and apatite in certain varieties (Table 3).

	1	2	3	4	5
Crossite	70	40	33	55	
Albite	5	12	7	18	
Epidote	3	13	13	6	
Titanite	21			21	35
Magnetite		2		1	10
Chlorite		2	10		54
Ilmenite	1	2			1
Leucoxene		29	36		
Calcite			1		

Mineralogical and chemical variations of the above described metamorphics are supposed to be due to the inhomogeneous nature of metamorphism on the one hand and to the differences between the equilibrium states of the parent mineral assemblages on the other. This means that chemical changes of metamorphic origin did most probably not affect the studied igneous complex as a whole. Unlike normal ultrabasics all the investigated titanite-crossitites are of a definite tholeiitic character which suggest a hornblendite or some similar ultramafic rock as the parent material. All evidences point to the fact that the formation of the ultrabasics in the Hungarian part of the Rechnitzer Penninikum must have taken place under rather unusual conditions.

## REFERENCES

- HERITSCH, H. (1956): Der Natrium-Amphibol aus dem Glasbachgraben bei Schlaining, Burgenland. *Tschermaks Min. Petr. Mitt.*, **10**, p. 209—217.
- KOLLER, F. (1979): Die Zusammensetzung der Amphibole in Penninikum des Ostalpenrandes. *Fortschr. Min.*, **57**, Bb. 1, p. 70—71.
- KOLLER, F. and PAHR, A. (1980): The Penninic ophiolites on the Eastern End of the Alps. *Ophioliti* **5**, p. 65—72.
- KOTSIS, T. (1957): Minerals of the Vashegy. Dissertation. (in KOCH, S: Minerals of Hungary. Budapest, 1966)
- KOTSIS, T. (1982): Gesteinswelt und Bau der Eisenberggruppe. *Vasi Szemle* **36**, p. 83—88.
- KUBOVICS, I. (1983): Petrological characteristics and genetic features of crossit from Western Hungary. *Földt. Közl.*, **113**, p. 207—224.
- LELKES-FELVÁRY, GY. (1982): A contribution to the knowledge of the Alpine metamorphism in the Kőszeg-Vashegy area (Western Hungary). *Neues Jb. Geol. Paleont. Mh.*, **5**, p. 297—305.
- PAHR, A. (1977): Ein neuer Beitrag zur Geologie des Nordostsporns der Zentralalpen. *Verh. Geol. B. A. Wien Jg.*, 1977, p. 23—33.
- PAHR, A. (1980): Die Fenster von Rechnitz, Bernstein und Möltern. (In: Der geologische Aufbau Österreichs. Springer Verlag Wien, New York, p. 320—326.
- SZEBÉNYI, L. (1948): Geology of the Hungarian Vashegy. *Jel. Jöv. Mélykut. Munk. Budapest*, p. 45—50.
- VARRÓK, K. (1954): Constitution géologique et les occurrences de talc et de minerai de fer des environs de Felsőcsatár. *MÁFI Évi Jel.*, 1953/II, p. 479—490.
- VENDEL, M. and KISHÁZI, P. (1967): Die Genese der Talklagerstätte von Felsőcsatár. *Bány. Kut. Int. Közl.*, Sonderheft, p. 1—153.

Manuscript received, 8 May, 1986







## **MICROFACIAL ANALYSIS AND ENVIRONMENTAL DEVELOPMENT OF THE DUWI (PHOSPHATE) FORMATION, QUSEIR-SAFAGA DISTRICT, EASTERN DESERT, EGYPT**

AHMED ALLAM<sup>1</sup> and KAMAL SHAMAH<sup>2</sup>

- 1) Geology Department, Faculty of Science, Tanta University, Egypt  
2) Department of Natural History: Faculty of Education, Fayoum, Egypt

### **ABSTRACT**

Microfacial analysis, based on six stratigraphic sections, were carried out to the Duwi (Phosphate) Formation at the coastal plain of Quseir-Safaga along the Red Sea coast. The study showed that the main rock types are: phosphorite, organic-rich shale, siliceous claystone, glauconitic sandstone, chert, dolomite, and oyster limestone. Detailed field and microfacial investigations of these rock types were done.

The paleogeographical distribution of the Duwi (Phosphate) Formation was found to be influenced by biological and chemical parameters which was necessary for the precipitation of calcium phosphates. Other factors controlling the areal extent include water depth, wave base and current velocity.

### **INTRODUCTION AND PREVIOUS WORK**

The Duwi (Phosphate) Formation occurs as a thin widespread shallow marine sediments which were deposited in an east-west trending belt spanning the middle latitudes of Egypt. These rocks lie near the base of a transgressive marine sequence, which was deposited during Late Cretaceous time on the northern edge of the Arabo-African craton. The formation comprises a shallow marine heterogenous sediment which overlies the Variegated Shales and underlies the Dakhla Shales. The present study is restricted at the Duwi (Phosphate) Formation in the Quseir-Safaga district and along the Red Sea coast where these rocks are well exposed, and the six sections were taken (*Fig. 1* and *2*). The main task is to reconstruct the depositional history and environmental development of the Duwi (Phosphate) Formation.

BARRON and HUME (1902) studied the topography and structure of the central portion of the Eastern Desert including the Quseir-Safaga region. They considered the whole series of Esna Shales (Dakhla Shale, Chalk and Esna Shale of Said, 1962) as Eocene and they determined the unconformity between the Cretaceous and Eocene. BALL (1913) examined the Safaga district, around Um El-Huetat mines. He regarded the phosphate beds as Upper Cretaceous. HUME *et al.* (1920) studied the area between Quseir and Safaga. They regarded the phosphate beds as Campanian. BEADNELL (1924) dealt with the coastal plain of the Red Sea between Quseir and Wadi Ranga. The phosphate beds in the *Ostrea villie* limestones were given as Upper Senonian (Campanian) age. YOUSSEF (1957) described the stratigraphy of the Upper Cretaceous rocks in the Quseir area. A Campanian-Maastrichtian age was assigned to the Duwi (Phosphate) Formation, which confirmed by SAID (1962).



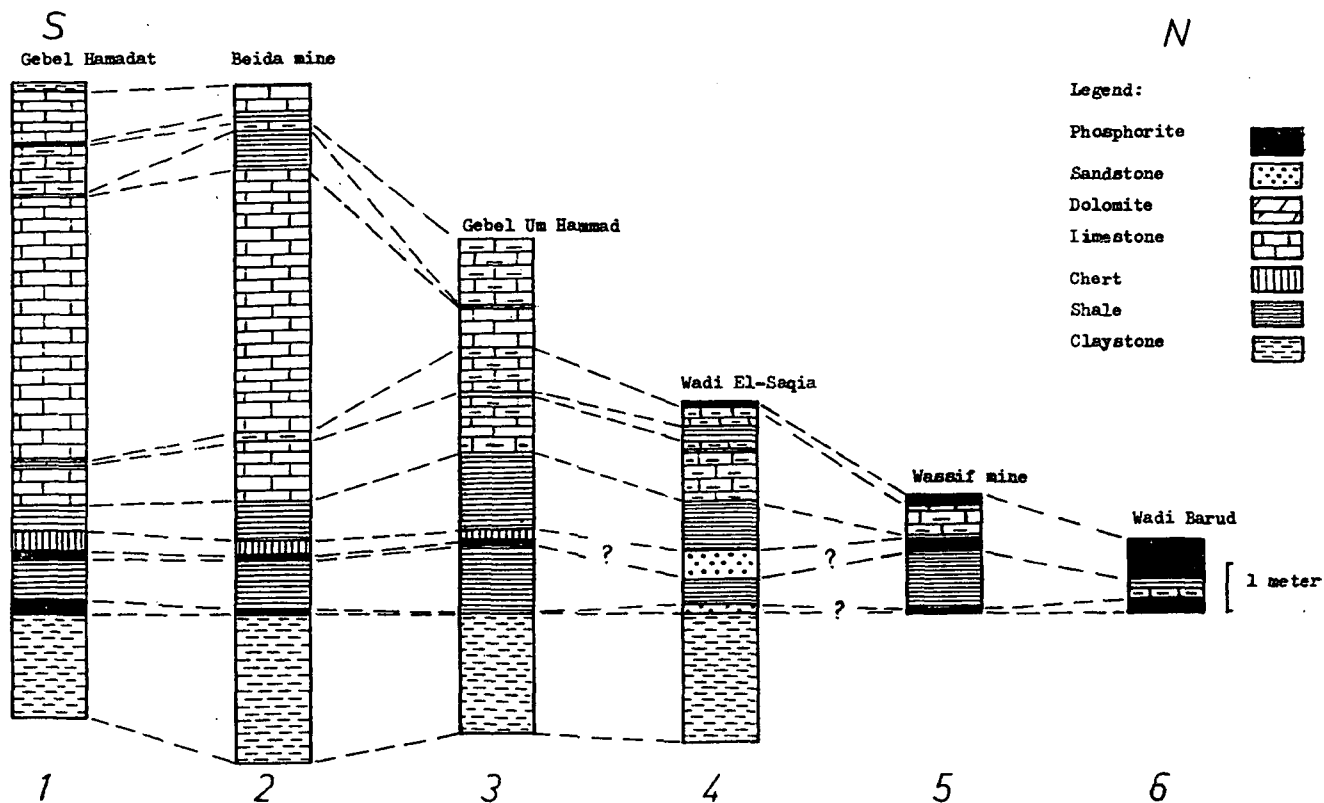


Fig. 2. Correlation chart of the studied sections of the Duwi (Phosphate) Formation, Quseir-Safaga district, Eastern Desert, Egypt

*cana aegyptiaca*. Herewith, the presence of the *Globotruncana aegyptiaca* zone is confirmed. This zone characterizes the top of the lower Maastrichtian. Furthermore, the nannoplankton zone *Quadrum trifidum* in association with *Micula staurophora* is present at the top of the formation. Therefore, the Duwi (Phosphate) Formation is considered of Campanian age in its lower part and of Maastrichtian age in its upper part, which conforms with the age assigned, to the Duwi (Phosphate) Formation in Quseir area, by YOUSSEF (1957), SAID (1962), WILLIAM and SHETA (1967, in ALLAM *et al.*, 1981: Fig. 1), and BARAKAT and EL-DAWOODY (1973).

#### MICROFACIAL ANALYSIS

The rocks of the Duwi (Phosphate) Formation include many varieties, e.g. phosphorite, organic-rich shale, siliceous claystone, glauconitic sandstone, chert, dolomite, and oyster-limestone. Field observations in the Quseir-Safaga district showed, that these rocks are lense shaped terminating both to the north and south, and thinning also to the east. The depositional environment deduced from lateral and vertical distribution of the facies could be either: a) an environment primarily controlled by hemipelagic deposition, or b) an environment favourable to the deposition of calcareous sediment. Hemipelagic environments are likely to be represented by shales and siliceous claystone, whereas limestone, dolomite, and marl facies are characteristic of environments dominated by calcareous deposition.

##### *Siliceous claystone*

The siliceous claystones are characteristically finely laminated or thinly bedded, predominantly siliceous fine-grained claystones which often contain scattered cryptocrystalline collophane intraclasts. The silica in these rock-types is usually present as microcrystalline cement. Other constituents include very fine silicate or carbonate grains together with some glauconite.

Study of the stratigraphic limits of the Duwi (Phosphate) Formation, revealed that the claystones are predominantly laterally confined to the exposures along Gebel Um Hammad, Gebel Duwi, and Gebel Hamadat. The siliceous claystones are generally confined to the base of the Duwi (Phosphate) Formation. These rocks appear to have been deposited within a relatively terrigenous free, low energy hemipelagic environment. The presence of glauconite and phosphate grains indicates that these rocks were probably deposited under a slightly reducing conditions.

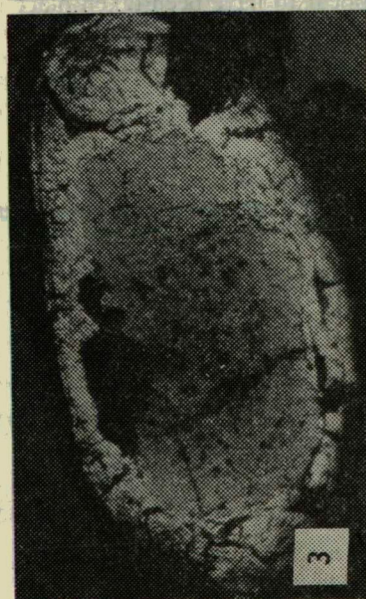
---

*Fig. 3.* Photomicrograph of a polished section showing crystalline envelope of pyrite surrounding the pyrite grain, the core is formed of finely dispersed minute cryptocrystalline pyrite. (reflected light,  $6.3 \times 30$ )

*Fig. 4.* Photomicrograph of thin section showing collophane grains and skeletal remains embedded in the ground mass (crossed nicols,  $2.5 \times 12.5$ )

*Fig. 5.* Photomicrograph of a thin section showing a collophane grain embedded in a ground mass totally composed of dolomite (crossed nicols,  $2.5 \times 12.5$ )

*Fig. 6.* Photomicrograph of a thin section showing collophane grains of different shapes, sizes, and structures (crossed nicols,  $2.5 \times 12.5$ )



### *Organic-rich shale*

The shales are black to grey, finely laminated to thinly bedded, fissile, organic-rich, and containing some intercalated siltstones. The shales contain abundant fish fragments and scattered pyrite grains (Fig. 3). These shales are found to contain small collophane nodules which have white to brown colour and form a shabby surface texture. The collophane grains (Fig. 4) reside either as scattered intraclasts that float within the groundmass or mixed with fish fragments and bone remains.

Within the Duwi (Phosphate) Formation, the organic-rich shale is laterally widespread throughout the investigated area, reaching maximum thickness along Gebel Um Hammad, thinning in southeast exposures, and disappearing to the north and south. However, the shales of the Duwi (Phosphate) Formation is lithologically very similar to the shale beds comprising the Variegated Shale, and that those units might actually be time-transgressive facies equivalents. The presence of organic-matter, pyrite, phosphate grains, and the general lack of bioturbation structures, indicates that these shales were deposited in a reducing, marginal marine or even shallow-marine environment.

### *Chert*

The rock type consists of dark grey banded cherts, silicified fine-grained claystones, and silicified phosphorites. The remarkable feature of these rocks is the common occurrence of fissured bedding. The chert is widespread throughout all the areas north and south of Gebel Duwi. The presence of rock fragment intercalations is restricted in northern localities, which indicate high current velocities. The depositional environments of these cherts appear to have been taken place in conditions of low-energy hemipelagic deposition intermittently disrupted by high-energy current activity.

### *Oyster limestone*

This type of limestone consists of a heterogenous assemblages of faunal communities in which *Ostrea villie* predominates. Oyster valves are unusually rugged. The limestone beds thin towards the east and northwest, but lacking in the north.

Actually, the oyster assemblages are largely restricted to the southwestern exposures, and it is apparently observed that the thick oyster beds are developed in southerly area.

The accumulation of thick bioclastic remains forming the limestone of these deposits, together with the development of low-angle cross bedding, suggest that these faunal communities lived in a relatively high energy environment.

---

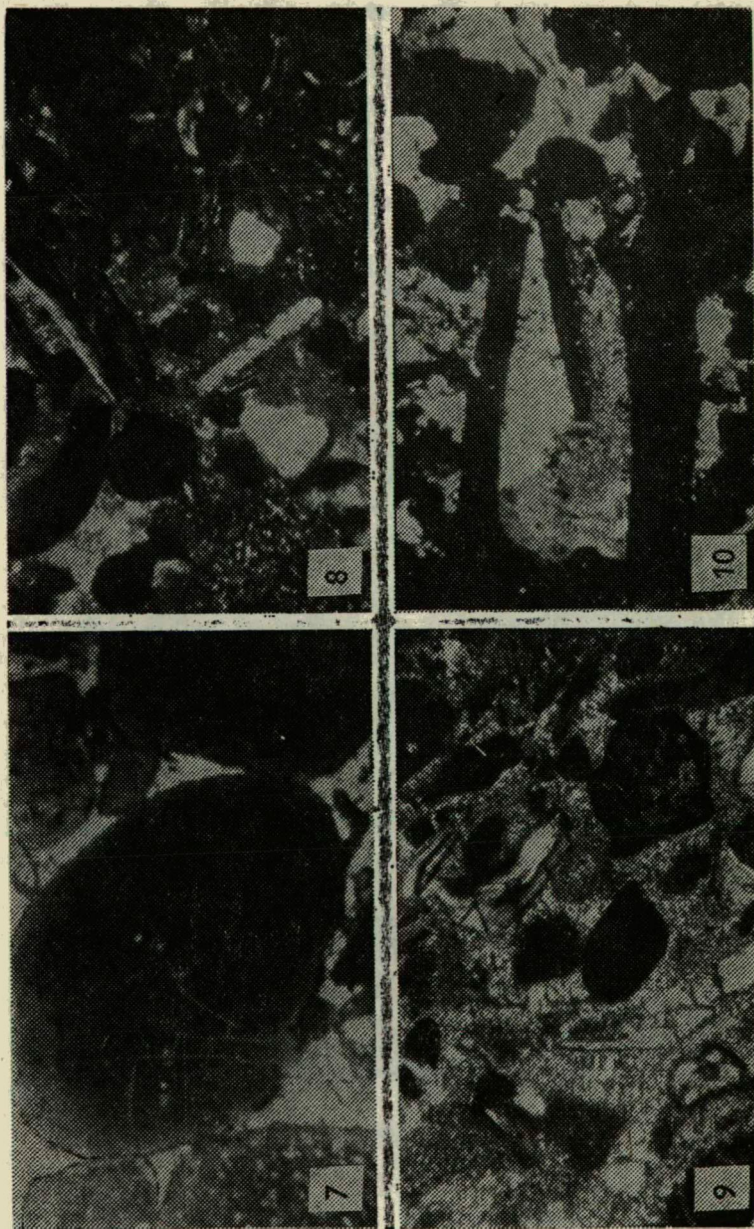
Fig. 7. Photomicrograph of a thin section showing coarse grained coprolite (crossed nicols,  $2.5 \times 12.5$ )

Fig. 8. Photomicrograph of thin section showing collophane grains and skeletal fragments embedded in the ground mass (crossed nicols,  $2.5 \times 12.5$ )

Fig. 9. Photomicrograph of a thin section showing fine crystalline calcite forming the ground mass (crossed nicols,  $2.5 \times 12.5$ )

Fig. 10. Photomicrograph of a thin section showing fine crystals of calcite enclosed in collophane (crossed nicols,  $2.5 \times 12.5$ )







## *Dolomite*

This rock type is characterized by ochre-yellow colour and has a finely laminated appearance. Microscopic investigation reveals that these rocks consist of very fine crystalline dolomite rhombs (Fig. 5). Regardless to the presence of several dolomite concretions found throughout the investigated area, the rocks of this type are found to be mainly restricted to southeastern localities. These dolomite are most probably formed by metasomatic replacement.

## *Glaucinite sandstone*

Although glauconitic sandstones appear to be widely dispersed throughout the upper part of the Variegated Shale, however, they are found to be of very limited occurrence within the Duwi (Phosphate) Formation. These rocks are mainly associated with black fissile shales. The glauconitic deposits are fine to medium-grained, well sorted, and consist of friable green glauconite-intraclast bearing quartz sandstones bound with a ferruginous cement. Observation of bedding surfaces has shown that they are characterized by a small scale ripple laminations indicating moderately high energy levels during deposition. The formation of glauconite requires slightly reducing conditions, weakly oxidizing and therefore may be linked to the upper- or lowermost levels of the oxygen-minimum zone.

## *Phosphorite*

Particular attention was previously given to these phosphate bands by ALLAM *et al.* (1981, 1982 and 1983). The phosphorites are found to range from phosphatic fossiliferous pelmicrites to biosparites, i.e., phosphatic and carbonate allochemical constituents reside in a micrite matrix and/or a sparry cement (Fig. 6, 7, 8, 9, 10 and 11). Siliceous and sometimes phosphatic cement was noticed. This rock type contains 30–60% collophane grains together with minor amounts of detrital quartz and/or feldspar grains. Phosphatic grains are primarily of skeletal, pelletal, or intraclast types. Skeletal grains include marine vertebrate bone fragments, fish teeth, and remains of phosphatized shell fragments. Intraclast types are commonly composed of pellets and fish remains bound by phosphatic cement. Pelletal grains range from silt to pebble size with subangular to well rounded shape. Ovoid-shaped grains

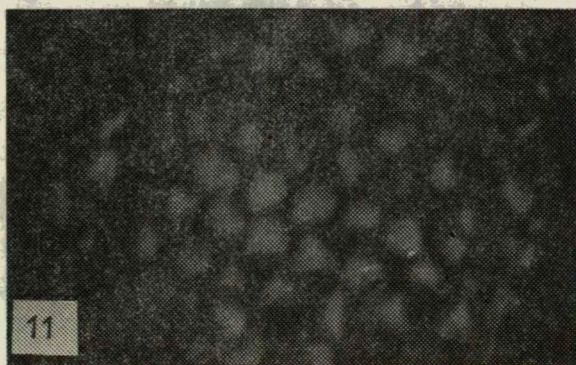


Fig. 11. Photomicrograph of a polished section showing an enlarged collophane grain containing an advanced stage of the globular pyrite network with organic material filling (reflected light,  $6.3 \times 30$ )



resemble phosphatized fecal pellets. Shallow scour-fill structures are common at the lower part and basal contacts and are commonly highly bioturbated. The phosphorite beds are widely distributed both laterally and vertically throughout the investigated area. They may range from few millimeters to few meters in thickness. Phosphorite deposits are usually intercalated with other rock types presented, but mainly associated with the siliceous claystones and organic-rich shales.

The phosphorite rocks of the Duwi (Phosphate) Formation are clastic sedimentary deposits that have probably accumulated through mechanical winnowing, reworking, and concentration of pre-existing phosphatic sediments. As previously mentioned siliceous claystones contain scattered phosphatic grains and skeletal fragments. These hemipelagic deposits represent a suitable source rocks from which the phosphorite beds were derived. Therefore, the relatively quiet, low-energy depositional environment of these hemipelagic sediments must have been interrupted from time to time by extensive high energy conditions. Such high-energy conditions seem to be attributed to wind- and wave-induced currents. Such currents can remove and rework the seafloor well below fair weather wave base. The fact that basal contacts of phosphorite beds are commonly highly bioturbated suggests that intermittent storm currents helped to oxygenate the anaerobic (or anoxic) bottom waters.

### CONCLUSION

The study obviously indicate that the Duwi (Phosphate) Formation, in general has been mostly deposited in a marine environment. This marine environment is most probably poor in oxygen content. The deposition of the Duwi (Phosphate) Formation (phosphorite, siliceous claystone, and organic-rich shale) agrees with such conditions. However, the oyster limestone reflect the depositional settings isolated from such anaerobism. Such isolation must have been the result of either vertical or lateral distance from the oxygen-minimum-zone. Vertical effects could be attributable to such phenomenon as development of oyster reefs on topographic accumulations, whereas lateral isolation may be linked to a shore-ward development or reefal communities. Many differences exist between the general hydrologic, geographic, and tectonic environments associated with the recent phosphorite sea floor deposits and those of the Duwi (Phosphate) Formation. However, these modern deposits appear to be very similar to the siliceous claystone and shale facies associated with the origin of the Duwi (Phosphate) Formation phosphorites.

A highly generalized sequence of events leading to the formation of the Duwi (Phosphate) Formation phosphorite deposits can be summarized as follows: a) Nutrient-rich oxygenated waters are brought to the basin of deposition which resulted in high rates of biological productivity. These nutrient-rich waters may be associated with upwelling of bottom currents from the Tethyan seaway at the north during Late Cretaceous time. b) Large amounts of biogenic sedimentation in the form of diatoms, coprolites, and other organic remains. Biogenic debris settling within the oxygen-minimum-zone, is largely removed from the biochemical cycle. c) Oxidation of organic remains along the borders of the oxygen-minimum-zone due to sulphate reduction which mobilizes dissolved phosphate ions in pore waters. d) Collophane precipitation in anoxic sediments was most probably achieved, by: either rise in pH due to decomposition of organic matter, or deficiency of magnesium ion due to replacement of  $\text{Fe}^{3+}$  in clays of authigenic formation of dolomite and/or magnesium-rich silicates. e) These deposits are then winnowed and concentrated into phosphorite beds by currents generated during storm activities.

## REFERENCES

- ABDEL RAZIK, T. M. (1967): Stratigraphy of the sedimentary cover of Anz-Atshan-South Duwi District. — Bulletin Fac. Sc., Cairo University, No. 41
- ALLAM, A., EL-ASSALY, F. M. & EL-SHARNOUBY, A. K. (1981): Geological and Radioactive Studies on Wadi Teban Phosphates, Hamrawein Area, Eastern Desert, Egypt. — Delta J. Sci. Tanta Univ., 6a
- ALLAM, A. & EL-SHARNOUBY, A. K. (1982): X-Ray Diffraction and Infrared Spectrometric Studies on the Safaga Mining District, Eastern Desert, Egypt. — Delta J. Sci. Tanta Univ., 6b
- ALLAM, A. & EL-SHARNOUBY, A. K. (1983): X-Ray Diffraction and Infrared Spectrometric Studies on Wadi Teban Phosphates, Hamrawein Area, Eastern Desert, Egypt. — Delta J. Sci. Tanta Univ., 7 (2)
- AWAD, G. H. (1964): Palaeontological zoning of the Upper Cretaceous — Lower Tertiary in the U. A. R. — Geol. Soc. of Egypt, Second annual meeting, Cairo, May, 1964
- BALL, J. (1913): Topography and Geology of the Phosphate District of Safaga. — Survey Department, Paper No. 29
- BARAKAT, M. G. & EL-DAWOODY, A. S. (1973): A Microfacies Study of the Upper Cretaceous-Paleocene-Lower Eocene Sediments at Duwi and Gurnah Sections, Southern Egypt. — MAFI évi jelentés, 26, Budapest
- BARRON, T. & HUME, W. F. (1902): Topography and Geology of the Eastern Desert of Egypt. — Survey Department
- BEADNELL, H. J. L. (1924): Report on the Geology of the Red Sea coast between Quseir and Wadi Ranga. — Petroleum Research Bulletin, No. 13, Survey Department, Egypt
- EL-AKKAD, S. & DARDIER, A. A. (1966): Geology and Phosphate Deposits of Wassif, Safaga Area. — Geological Survey, Egypt, Paper No. 36
- HUME, W. F., MAGDWICK, T. G., MOON, F. W. & SADEK, H. (1920): Preliminary Geological Report on the Quseir-Safaga District Particularly the Wadi Mureikha Area. — Survey Department, Petroleum Research Bull. No. 5
- ISSAWI, B., FRANCIS, M., EL-HINNAWI, & MEHANNI A. (1969): Contribution to the structure and Phosphate deposits of Quseir area. — Geological Survey, Paper No. 50
- MOHAMED, M. F. (1982): Micropaléontologie et biostratigraphie du Crétacé supérieur et de l'Eocene inférieur de l'Egypte centrale. — Thèse Doc. ès Sc., Univ. Pierre et M. Curie, Paris
- SAID, R. (1962): The Geology of Egypt. — Elsevier Publishing Co., Amsterdam—New York
- YOUSSEF, M. I. (1957): Upper Cretaceous Rocks in Kosseir Area. — Bulletin De L'Institute Du Desert d'Egypte, T. VII No. 2

*Manuscript received, 20 February, 1986*

## REGULARITIES IN THE FORMATION OF MANGANESE DEPOSITS ON CONTINENTS

M. M. MSTISLAVSKIY\*

Ministry of Geology of the USSR, Department of Base Metals, Moscow

### ABSTRACT

The destructive type of tectonic regimes directly controlled the formation of the larger part of primary manganese deposits. Recurrences of these regimes in the history of the Earth marked the periodicity of the active manganese-forming epochs. The main body of the manganese ores was deposited in as late as the Early Proterozoic, after the protoplatforms have appeared. In the Archean, the formation of the lowermost crust (lithosphere) stimulated the isomorphic dissemination of manganese, thus raising the clark of the metal in basites and ultrabasites. The taphrogenic rifting on cratons was the major ore-forming regime during the thalassocratic periods in the evolution of the Earth. On the contrary, the geocratic accretive period of the Pangaea formation was less favourable for manganese concentration. On the supercontinents, the manganese deposits practically did not appear in the orogenic and trappian magmatic zones and in the regions of hypergenic crustal formation. The latter regions are favourable for bauxite formation, but not for manganese concentration in the original rocks with the clark of the metal. Secondary manganese deposits appear only in the originally specified manganese-bearing formations. The epochs of bauxite formation and of initial manganese concentration are antipathic. The separation of iron from manganese in the formation of deposits occurred mostly under endogenic conditions. The accumulation of ferruginous ores is characterised by tholeiite, spilite-keratophyric magmatism, whereas the manganese deposits require a more acid and alkalic geochemical regime with a higher effect of fluids. The described genetic conception provides ways of elaborating new criteria for prospecting of manganese deposits.

### INTRODUCTION

Manganese deposits are found in the rocks of different geological epochs, from the Precambrian to Anthropogene. They occur in geosynclinal and platform rock assemblages, in crusts of weathering, and in metamorphic layers. Though widely scattered, the distribution of the deposits, however, is specific; they are mostly bedded among marine deposits, whereas commercial manganese ores are almost completely absent from the continental series and the facies of largest lakes. Are there general regularities in the formation of manganese deposits on continents and what are the causes of these regularities? The researchers are as yet unable to give a positive answer.

The author believes that manganese orebodies and the periodicity of their appearance is primarily controlled by tectonic events; the formulation of the problem was first advanced by I. M. VARENTSOV as far back as in 1962 (VARENTSOV, 1962). The author proposed arguments in favour of the dependence of manganese concentration on destructive endogenous regimes and on their recurrence in the history of the Earth (MSTISLAVSKIY, 1984a).

\* Bolshaya Grusinskaya str. 4/6, Moscow, 123813, USSR

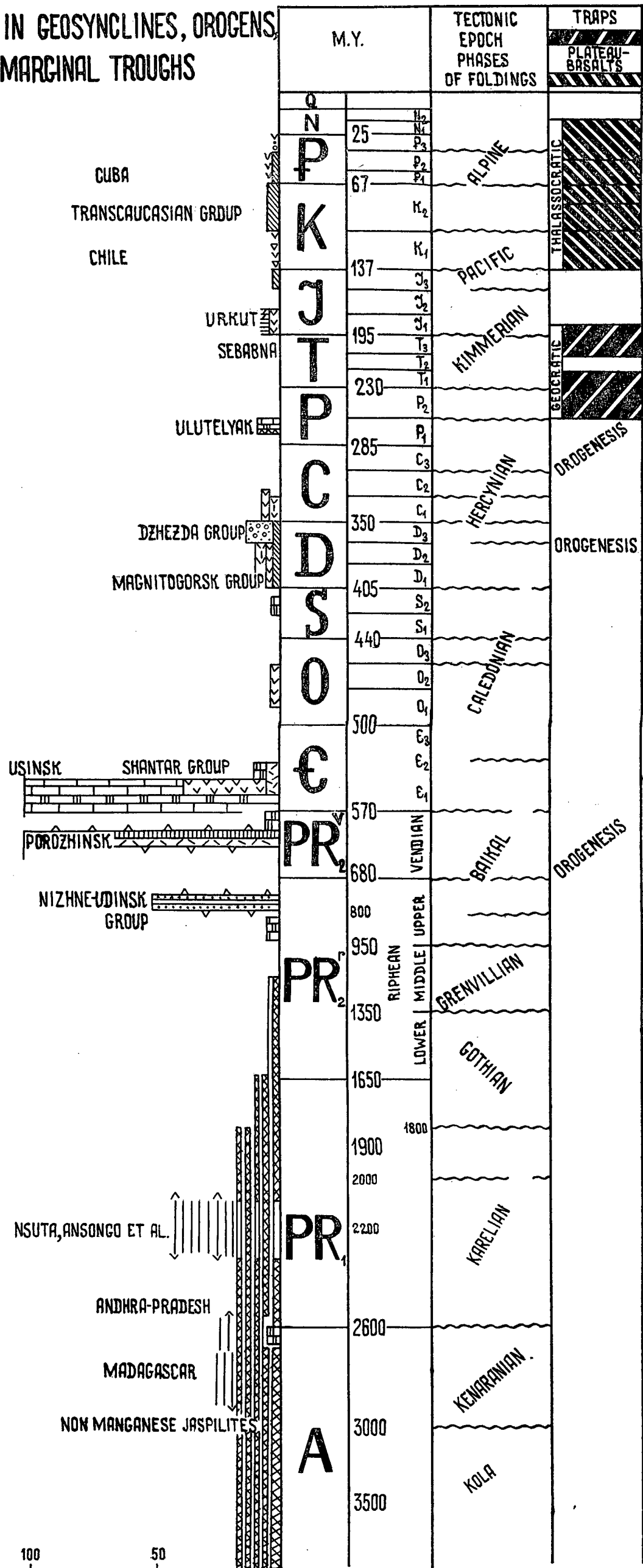
The pre-Riphean megachrone has two distinct stages of manganese formation: Archean and Early Proterozoic. As universally known, the protocontinents (proto-platforms) appeared about 2600 m.y. ago, between the Archean and Early Proterozoic. The manganese accumulation, very low in the Archean, is mainly dated from that period and is found only in a few locations: gondites of Madagascar, gondites of Andhra-Pradesh in India, the manganese and carbon-bearing formation of Rio das Velhas in Brazil and other smaller manganese deposits (VARENTSOV, 1962; *Geology and genesis...*, 1972; *Geology and minerals...*, 1973).

Contrary to manganese, the ferruginous concentration was a common process in the Archean. The jaspilite concentrations of the greenstone belts constitute such deposits. An important conclusion can be derived that as far back as the Archean and actually in the endogenic conditions, the ferruginous concentration was separated from the manganese deposition. Manganese was in a diffused state and enriched vast amounts of basites and ultrabasites. We may therefore state that the Archean cannot be considered as the manganese metallogenic epoch (MSTISLAVSKIY, 1984a).

In contrast to that epoch, the Early Proterozoic stage of the pre-Riphean megachrone is one of the most productive in manganese; it is characterised as the **Early Proterozoic epoch of manganese ore formation**. The deposits of the gondite formation are numerous in the Lower Proterozoic (2200 m.y.) geosynclinal Birrimian system of Central and Western Africa: Nsuta, Ansongo, Tambao, etc. (*Geology and minerals...*, 1973; *Explanatory...*, 1980). The gondites are found in the Lower Proterozoic Baram and Paramak groups in Guiana, French Guiana and Surinam in South America, and also in India (1700—2000 m.y. old) (*Geology and genesis...*, 1972; *Explanatory...*, 1979). But gondites are technologically difficult and manganese is derived from them by the varieties of lateritically oxidised supergenic ores. However, the commercially important Early Proterozoic deposits are composed not of gondites, but of the ores of the itabiritic (dolomite-manganese-jaspilite) formation of the active zones in the old cratons. To these formations belong the ores of Kalahari, Postmasburg, South Africa, and the explored rich (44% Mn) ores with reserves amounting to 311 m.t., the total tonnage of predicted resources of the South African Republic reaching 12.6 billion tons (*Discovery...*, 1982). In the Kalahari region there are Kuruman, Middelwit, Rooisloot and other deposits which together with Kwarkwe and Ootsi of Botswana belong to the Transvaal system more than 2000 m.y. old (DU TOIT, 1957; *Geology and minerals...*, 1973). On the Brazilian shield, the Morro do Mina deposit of the itabiritic formation is confined to the Minas rock group 2200—1900 m.y. old, whereas on the Guiana shield the Serra do Navio carbonate-siliceous formation is located in the Amapa group. Its age, after ALMEIDA and J. V. N. DORR II, is 1800 m.y. (*Geology and genesis...*, 1972). The lateritically enriched Moanda deposit in Gabon, after J. BOULADON, F. WEBER and others, is confined to the sand-siliceous-pelitic volcanogenic-sedimentary Francevillian rock group 1704 m.y. old (*Geology and genesis...*, 1972) (*Fig. 1*).

The gondites are characteristic features of greenstone belts, but the manganese-bearing itabirites with large commercial manganese deposits are located in the mature parts of the continental crust within old cratons of the Southern Hemisphere. The tectonic regime of the ore-forming epoch, however, was different from the regime of slow epeirogenic movements of stable platforms. In the Early Proterozoic, a tremendous destruction of the crust of the protocontinents took place and the processes of rifting were extensively manifested with the appearance of structures of the oceanic

# IN GEOSYNCLINES, OROGENS, MARGINAL TROUGHS



# ON ACTIVIZED PLATFORMS, ANCIENT CRATONS, THE MIDDLE MASSIVES

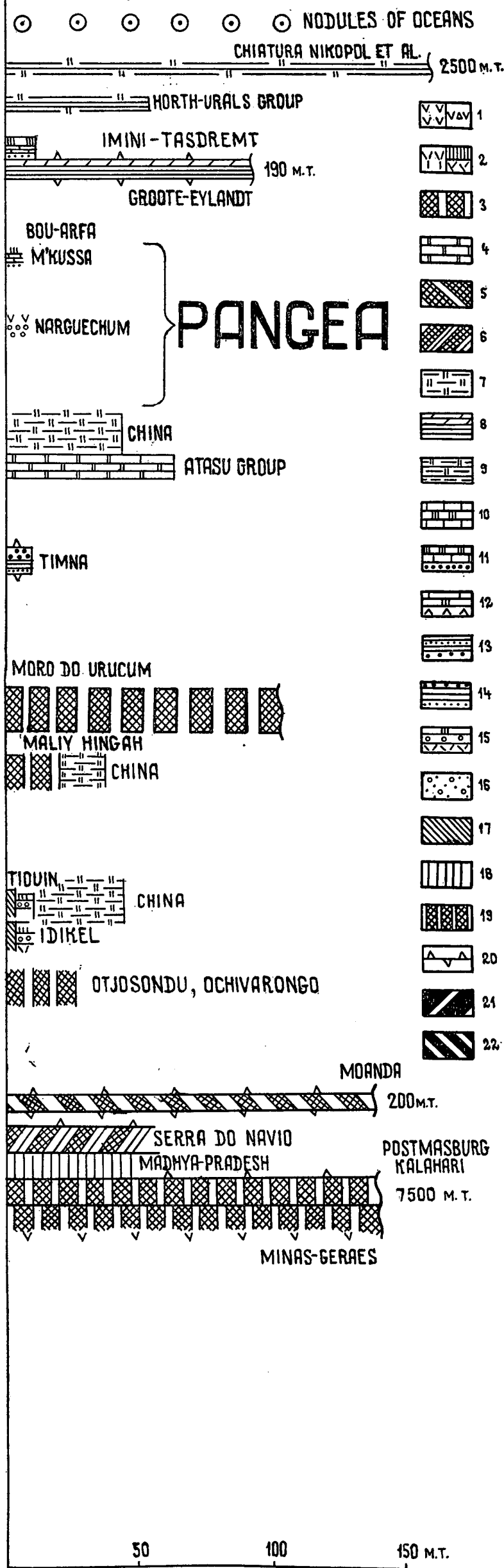


Fig. 1. Diagram of manganese forming epochs, formations and endogenous regimes. Compiled after: VARENTSOV, 1962; VARENTSOV and RAKHMANOV, 1974; DU TOIT, 1957; PEIVE et al., 1980; BOULADON and JOURAVSKY, 1952, 1956; FRANKS and BOLTON, 1984; RUIZ, 1965; SIMONS and STRACZEK, 1958; and others, supplemented.

**Marine manganese formations:** volcanogenic-siliceous: 1-splite-keratophyre-siliceous (a), tholeiite-siliceous-greywacke (b); 2-porphry-siliceous (a); tuffite-porphry-siliceous (b). Carbonate-siliceous formations: 3-dolomite-manganese-ferruginous-siliceous (itabirite); 4-dolomite-siliceous-limestone ferro-manganese (Atasu). Siliceous-shale, siliceous-clay and argillaceous (predominantly) formations: 5-dolomite-siliceous-sandy-argillaceous ferro-manganese; 6-limestone-siliceous-graphitic-shale; 7-siliceous-shale-orthocquartzite; 8-marl-clay; 9-sandy-glaucinite-siliceous-clay. Carbonate formations: 10-dolomite-limestone; 11-limestone-dolomite; 12-halogenic-carbonate.

**Terrigenous formations:** 13-glaucinite-quartz sandy-clay; 14-sandy-clay (lagoon).

**Continental formations:** 15-volcanogenic-carbonate-terrigenous; 16-molassic and volcanogenic-molassic.

**Post-magmatic formations:** 17-hydrothermal-metasomatic ores in a variety of formations **Metamorphic formations:** 18-gondite.

**Ferro-manganese formations:** 19-jaspilite (not in scale of ore sources); 20-laterite-enriched deposits **Stages of manifestation:** 21-traps; 22-oceanic plateau-basalts

type (PEIVE *et al.*, 1980) or geosynclinal belts. In the Early Proterozoic, jaspilites were deposited on a global scale within the geosynclines, whereas the manganese-bearing itabiritic formations appeared with dolomites in the active taphrogenic structures\* and rifts on the old cratons of the Southern Hemisphere (Fig. 1). The distribution of the manganese-bearing itabirites in the Southern Hemisphere is apparently one of the indications of a dissymmetry in the Earth's evolution connected with the breakup of Gondwana and formation of intracraton geosynclines (BOZHKO, 1984). The appearance of manganese-bearing intracraton geosynclines was synchronous with the proto-Thetys opening and has much in common with the phenomenon of reflected tectono-magmatic activation.

**The Riphean is the next manganese forming epoch**, which has two stages associated with the initial phases of the Grenvillian and Baikalian epochs of tectogenesis (Fig. 1). In the Riphean, the geosynclinal manganese-bearing formation, which produced gondites in the process of metamorphism, has almost disappeared and the number of manganese-bearing itabirites was sharply reduced. The latter are found in Namibia in the Damara group, the Otjosondou and Ochivarongo deposits (Geology and minerals..., 1973; Explanatory..., 1980). At the same time, the manganese deposits have appeared on the African craton but as constituents of the continental series associated, after G. CHOUVERT, with the acid platform volcanites; such are the Idikel (1,350—900 m.y.), Tiouin, Migouden, Offremt deposits and more than 200 manganese veins pervading the Ouazazate group 927—832 m.y. old (Geology and genesis..., 1972). After J. BOULADON and G. JOURAVSKY (Geology and genesis..., 1972), the Idikel deposit of braunite, psilomelane ores is a metamorphosed hydrothermal sedimentary limnetic formation. On the Chinese platform, the manganese deposits also appeared in the Riphean, whereas in the USSR, there are the Nizhneudinsk group of deposits in the Sayan foredeep and the manganese ores in the geosynclinal units of the Baikal region and the Enisei Range (VARENTSOV, 1962; VARENTSOV, RAKHMANOV, 1978).

**The Vendian-Cambrian manganese metallogenic epoch** occurred between the Proterozoic and Paleozoic. The Vendian rocks of the Enisei Range contain the Porozhinsk deposit of oxide and carbonate (oxidised in the Meso-Cenozoic) manganese ores in the siliceous tuffites and silicites. To Cambrian time belong the Lower Cambrian Usinsk deposit in the eugeosynclinal zone of the Kuznetsk Alatau, the Gornoshorsk, Arghinsk, Shantarsk groups of deposits and the Durnovsk deposit in Salair (Fig. 1). On active platforms, the Lower Cambrian deposits are located in China, the manganese itabirites in the Maly Khingan median mass, and others (VARENTSOV, 1962; VARENTSOV, RAKHMANOV, 1978). One of the largest regions in the world of manganese-ferro-siliceous formations, situated on the Central Brazilian shield, is characterised by a "typically tectonic position"; the Moró do Urucum deposit located in this region is confined to the lower part of the Jacadigo group of the undifferentiated Cambrian-Ordovician rocks also observed in the geosynclinal complex of the Andes (Explanatory..., 1979). As described by J. V. N. DORR II (Geology and genesis..., 1972), unlike itabirites in other regions, the rocks of the Jacadigo group on the Brazilian shield are only slightly crumpled and unmetamorphosed; the degree of their weathering and hypergenic manganese and iron enrichment is low. This is a positive evidence of the primary nature of commercial manganese ores in jaspilites.

\* Taphrogenesis here means contrasting and geologically short-lived subsidences or collapses of crustal blocks along deep ruptures.

The Cambrian epoch of manganese accumulation, the first most productive epoch after the Early Proterozoic one, is coeval with the processes of global destruction during the opening of Proto-Atlantic and in the Vendian-Early Cambrian with the processes of destruction during the formation of the Asian paleo-ocean between the Siberian, East European and Chinese Precambrian continents (PEIVE *et al.*, 1980).

In the Ordovician-Silurian, both oceans closed, which is manifested also in the absence of corresponding epochs of manganese accumulation and in the activity of only secondary manganese metallogenic stages. By the beginning of the Devonian, vast areas of continental crust were formed in these regions, and only in the Urals and Irtysh-Zaisan zone new linear oceanic structures appeared (PEIVE *et al.*, 1980). The geosynclinal manganese deposits of the Mugodzhär Ordovician group and the Magnitogorsk Lower and Middle Devonian group with deposits in the Bugulygyr jasper stratum are actually confined to these structures (GAVRILOV, 1972) (*Fig. 1*).

The Devonian metallogenic epoch produced the commercial deposits of the active zones. The most important is the Atasu group of ferromanganese deposits of Central Kazakhstan (Karazhal, Ushkatyn, Zhairam, etc.). A. A. ROZHNOV and co-authors (Geology and geochemistry..., 1982; New data..., 1980) indicate, that these afacial deposits were formed at the same time as the basalt-liparite high alkalinity formation during the active tectono-magmatic stage of the Famennian and in the beginning of the Tournaisian. In the adjacent Dzhezda region, the Upper Devonian red limestones are superimposed by the hydrothermal ferro-manganese ores of the Dzhezda Nazaitas and other deposits (KALININ, New data..., 1980). The Atasu and Dzhezda group of deposits reveals the more contrasting Late Devonian Early Carboniferous epoch. The Early Carboniferous stage of this epoch is extensively represented in many regions of the world: on the active Chinese platform, in the geosynclines of the Urals (Akkerman) and Morocco (Glib an Nam) (VARENTSOV, 1962). After Said, the Suez graben developed on the African craton in the Upper Devonian-Early Carboniferous and continued in the Red Sea area (MILANOVSKIY, 1976). Along this rift zone in Egypt, the carbonate rocks of Carboniferous age contain the Umm-Bogma and Umm-Rina manganese deposits and the vein manganese ores at Wadi Malik, Agwampt, etc. (Geology and minerals..., 1973) (*Fig. 1*).

In the middle of Carboniferous age, the continental crust was formed on the vast area of Eurasia. Eurasia and North America composed Laurasia, which at the end of the Paleozoic joined with Gondwana into the Pangaea supercontinent. The geocratic continental regime was now developing on a planetary scale. It should be emphasised, that the geocratic period of formation and the existence of Pangaea from the Middle Carboniferous to the middle of the Early Jurassic was the least favourable for manganese accumulations not only on orogens and the plates themselves, but also in the areas of trapp magmatism and regional hypergenic formation of the crust. For example, in Triassic-Jurassic epoch of the hypergenic formation of the crust the manganese accumulations were not deposited on the territory of the USSR. This was the situation not only in Eurasia, but practically on the entire territory of Pangaea (*Fig. 1*).

Triassic-Jurassic (particularly  $T_3-J_1$ ) and Permian-Triassic ( $P_2-T_1$ ) epochs experienced intensive trapp magmatism in a number of large regions of the globe, such as the Tungusssk syncline of Siberia ( $P_2-T_1$ ), the Parana syncline in South America ( $T_3$ ) and other structures with the areas of trapp formation over the Gondwana relicts in South Africa (the Karroo syncline), Antarctica, and Tasmania ( $T_3-J_1$ ) (BELOUSSOV, 1976). These regions are almost without manganese ores, whereas the ferruginous deposits in trapp formation are fairly numerous.

Therefore, the territory of Pangaea in the Permian-Triassic continental geocratic period of trapp magmatism and in Triassic-Jurassic epoch of regional hypergenic formation of the crust had practically no manganese accumulations (MSTISLAVSKIY, 1984a). In Morocco, the Nargeuchum group of deposits in the Permian-Triassic red limestones is associated, after J. BOULADON and G. JOURAVSKY (1956), with distal volcanism (VARENTSOV, 1962) (Fig. 1).

The taphrogenic leptogeosynclinal subsidences of several aquatories in the northern part of Pangaea in the Early Permian, however, caused the activity of the Lower Permian manganese accumulative stage, for example, in the northern continuation of the Urals within the Pay-Khoy and on the Novaya Zemlya. In this region of the Arctic, a new manganese-bearing province of carbonate manganese ores of hydrothermal-sedimentary origin, after V. S. ROGOV and co-authors, is located in the black carbonaceous argillites and aleurolites interbedded with phtanites and limestones (Manganese..., 1984). In Fig. 1 this Lower Permian ore deposit is not shown, because it can misrepresent the actual absence of manganese deposits on the Pangaea supercontinent itself during the geocratic regime of continental sedimentation and hypergenic formation of the crust inside the continent. The Lower Permian manganese accumulation on Novaya Zemlya and Pay-Khoy was probably associated with the cracks of the rift which penetrated to the northern margin of Pangaea from the Arctic Ocean. The Ulutelyak deposit of manganoous limestones with alabandite is described as the sedimentary deposit bedded in the marly-dolomite-anhydrite Lower Permian stratum in the junction zone between the East European platform and the marginal foredeep of the Urals (GRIBOV, 1972).

As soon as Pangaea began to break up, the manganese ores resumed their accumulation in different parts of the globe. For example, in the second half of the Early Jurassic and in the Middle Jurassic the geosynclinal regime is revived in the Alpine belt (BELOUSSOV, 1976) synchronously with the formation of manganese deposits in Hungary (Úrkút), in the northern margin of the African craton in Morocco (Bou Arfa, M'Kussa) (VARENTSOV, 1962), and in the regenerated geosyncline on the southern slope of the Caucasus Major with large pyrite-polymetallic manganese deposits and ores (SMIRNOV, 1982). It is assumed, that in the Late Jurassic the modern Atlantic and Indian oceans started to open, thus predicting the Late Jurassic stage to be a manganese-forming time period. The opening increased in the Cretaceous, when great volumes of plateau-basalts were erupted in the oceans. The available data implies that the initial stages of riftogenesis and taphrogenesis of the oceanic stage of development were productive in manganese accumulation.

**The Cretaceous-Paleogene thalassocratic epoch** confirms this regularity by accumulating tremendous amounts of manganese in different regions of the world (Fig. 1). For example, the formation of the largest Groote Eylandt Lower Cretaceous (Albian) manganese deposit in Australia (MCINTOSH *et al.*, 1975; FRANKS, BOLTON, 1984) was nearly synchronous with the contrasting block subsidences and basaltic effusions in the eastern part of the Indian Ocean. On the African craton in Morocco, the Imini-Tasdremt deposit in the Cenomanian-Turonian limestone-dolomite stratum was also formed nearly synchronous with a burst of the large Late Cretaceous effusions of oceanic plateau-basalts. This stratified deposit of high-quality oxide ores is occasionally accompanied by manganese veins and, after J. BOULADON and G. JOURAVSKY, has hydrothermal-sedimentary origin.

The numerous small Paleocene deposits of Northern Urals (Polunochnoye, Ivdel, etc.) stretch 200 km along the eastern slope in a narrow intermittent band (RABINOVICH, 1971). In the Paleocene, the rifting and the oceanic plateau-basalt



effusions were also manifested, the latter being particularly large in Briton-Arctic province. This province was probably related to the Urals belt through the zones of deep ruptures, which surround in the northeast the epi-Paleozoic East European platform and its northern part, the Barents platform. This is also indicated by the rapid transgression of the Paleocene sea from the Arctic to the south along the eastern slope of the Urals (RABINOVICH, 1971).

Such gigantic deposits of manganese ores as Nikopol and Chiatura (BETEKHTIN, 1946; Nikopol..., 1964; Chiatura..., 1964; AVALIANI, 1982; VARENTSOV, RAKHMANOV, 1974) and other deposits of Southern Ukraine, Western Georgia, the Varna region of Bulgaria and Mangyshlak form a single metallogenic province of the southern part of the USSR and Bulgaria. All these deposits and the entire manganese-bearing province appeared during one short Early Oligocene metallogenic epoch (Fig. 1), when the sub-oceanic Maikop basin of the marginal type appeared in the southern part of the USSR (MSTISLAVSKIY, 1972, 1982). The basin took form in the global epoch of crustal destruction simultaneously with the taphrogenic rifting between the Eocene and Oligocene. At that time, one of the spreading stages of the Red Sea graben occurred (Recent..., 1974), whereas in the south of the USSR the geologically instantaneous taphrogenic subsidence of the Black Sea deepwater basin took place with the amplitude of 4—5 km in the very beginning of the Oligocene (YANSHIN *et al.*, 1980; MSTISLAVSKIY, 1972, 1982).

This vast taphrogenesis coincided in time with the impressive accumulation of manganese ores within one metallogenic province in the time interval of a single metallogenic Early Oligocene epoch. We believe, that this circumstance reflects the unity of the appearance of the manganese metallogenic province and of the manganese metallogenic epoch controlled by one factor, i.e., the endogenous tectonic regime of taphrogenesis.

The endogenous metallogenic regime also controls the endogenous source of manganese in the Early Oligocene sea basin under discussion. G. S. DZOTSENIDZE (1965) and his followers A. I. MAKHARADZE, V. G. GOGISHVILI, N. I. KHAMKHADZE and others (New data..., 1980) for the Chiatura deposit (Chiatura..., 1964), N. I. KHAMKHADZE, G. P. TUMANISHVILI for the Kvirili depression (Manganese..., 1984), B. ALEKSIEV and KR. BOGDANOVA (1974) for the Obrochishte deposit in the Varna ore region of Bulgaria determined the hydrothermal source of manganese and the volcanogenic-sedimentary type of manganese accumulation. These and other data provide grounds to debate the origin of the Chiatura and Nikopol deposits (RAKHMAMOV, CHAIKOVSKY, 1983) considered earlier as "classically sedimentary" (STRAKHOV *et al.*, 1968). The solution of the problem shall have a general importance for the understanding of the genesis of manganese deposits on continents.

In this connection we shall discuss the recently obtained observation material of local order on the presence in the past of an ore-supplying hydrothermal channel for the Chiatura manganese deposit formed in the sea basin (MSTISLAVSKIY *et al.*, 1984). On the western slope of the Perevis Highlands, under the Oligocene manganese layer in the zone of the Major Deep Fault, the vein metasomatic-block lenslike manganese ore deposit is bedded in the Upper Cretaceous limestones (Fig. 2). This deposit consists of the oxide-oxidised pyrolusite ores with residual manganite. The ores have higher Mo and V content, and the clarks of concentrations of manganese, the major ore-forming element, and its accessories Ni, Co, Cu, Ba in the ores sharply increase: tenfold for Cu, hundredfold for Ni and Co, and up to three orders for Ba. On the area, the high values of Ni, Co contents from the Upper Cretaceous limestones of the fault zone appear in the field III of the highest Ni and Co concentrations in the

# CHIATURA DEPOSIT

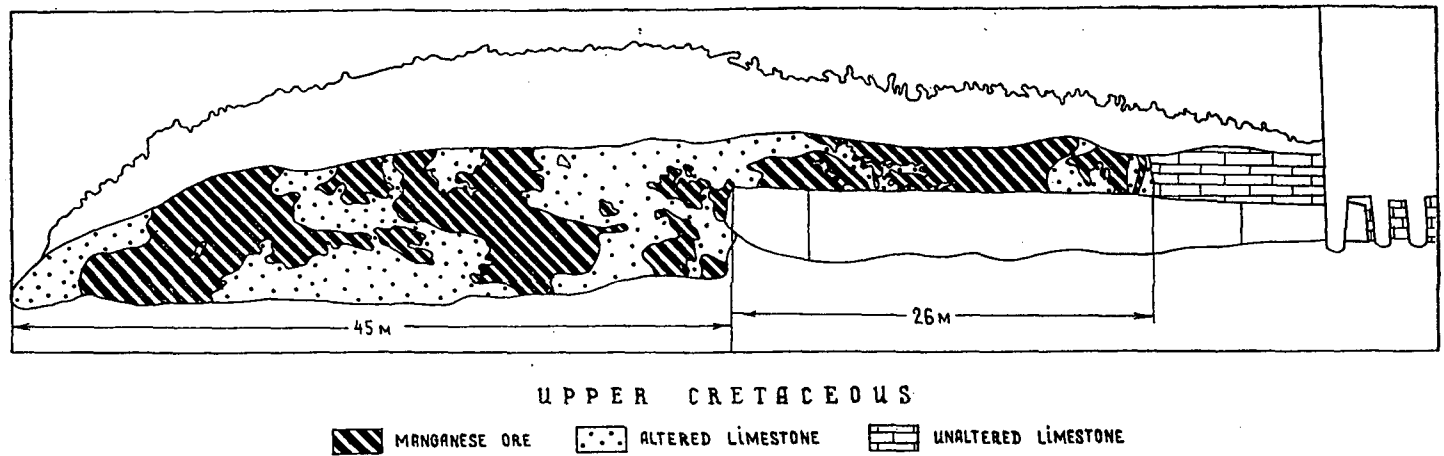


Fig. 2. Denuded fragment of the manganese ore column in the Upper Cretaceous limestones from the Chiatura deposit of the Major Fault on the Perevis Highlands 1-denudation contour; 2-manganese ores and manganised limestones; 3-loose hydrothermally altered limestones, 4-unaltered solid limestones

Oligocene stratified ores (STRAKHOV *et al.*, 1968) confined to the Major Fault (*Fig. 3*). At the intersections of the fault with the transversal co-sedimentation faults, the mineralizing channels probably appeared; along them the manganese-bearing solutions filtered into the Oligocene sea basin and formed the hydrothermal Chiatura deposit during the period of taphrogenic destruction in the Early Oligocene. The Early Oligocene was the second most important manganese-forming epoch, as also the contrasting metallogenic stages of the Early Proterozoic, when the largest formations, such as Kalahari and Postmasburg, appeared in South Africa (*Fig. 1*).

Therefore, the available observation material on the Chiatura and Varna groups of deposits implies the hydrothermal source of manganese in the Early Oligocene sea basin. Similar evidence for the Nikopol and Mangyshlak deposits is as yet to be collected. This circumstance still allows certain researchers to classify them as the properly sedimentary type, the more so since at first sight the tectonic position of all these Early Oligocene deposits seems different, i.e., the Nikopol group is deposited in the covering layer of the ancient craton of the Ukrainian shield, the Chiatura deposit is situated within the Alpine fold belt, and the Varna group and the Mangyshlak deposit are confined to the covering layers of the epi-Paleozoic plates, Misian and Turanian. Though the named deposits are confined to different structural blocks, the tectonic causes of their origin were the same. For instance, after tectonic stabilisation in the Late Eocene and the formation on the entire indicated territory of the shallow epi-continental sea basin, where mostly marls and limestones accumulated, a tremendous taphrogenic subsidence of the Black Sea depression took place, as noted above, in the very beginning of the Early Oligocene. These events positively imply a powerful synchronous manganese accumulation in the Early Oligocene in the southern part of the USSR, including the Early Oligocene stage of endogenic destruction of the type of the region's oceanisation. As the result of this process, the synchronous Early Oligocene manganese deposits were bedded in the periphery of the newly formed suboceanic Maikop basin or marginal sea. The author believes that the size of the deposit was actually controlled by the variations in the influence of taphrogenic processes on structurally different blocks. For example, in the regions with a thick platform layer on the epi-Paleozoic plates only small deposits were formed, as in the Varna and Mangyshlak regions, whereas the largest manganese accumulations were deposited in the regions of the denuded (or covered by a thin layer) crystalline basement of the old craton of the Ukrainian shield (Nikopol) or the Dziruli prominence of the median mass (Chiatura) (MSTISLAVSKIY, 1982). V. G. GOGISHVILI, N. I. KHAMKHADZE, V. D. GUNIAVA, from another aspect, discussed the structural confinement of manganese deposits to the Caucasus under effect of hydrothermal processes; the structural location of the Chiatura deposit in the Dziruli region was analysed by G. S. DZOTSENIDZE in the book "Recent data on manganese deposits of the USSR" (1980). All these arguments lead to the conclusion that the processes of endogenous destruction (taphrogenesis, rifting) directly affecting the crystalline basement (or the basement covered by a thin layer) of old cratons and median masses have caused, in the process of sedimentation in these structures, the formation of large and gigantic manganese deposits within the individual cosedimentary depressions (*Fig. 1*).

Consequently, as already mentioned, the absence of intracontinental manganese accumulations during constructive accretion against the background of geocratic building of Pangaea is symptomatic. Let us note, that the regimes of tectonic stabilisation and cratonisation of the regions, together with climate, control the development of processes of hypergenic crustal and bauxite formation. We should particularly emphasise the circumstance that the manganese-forming epochs, on the one hand,

# CHIATURA DEPOSIT

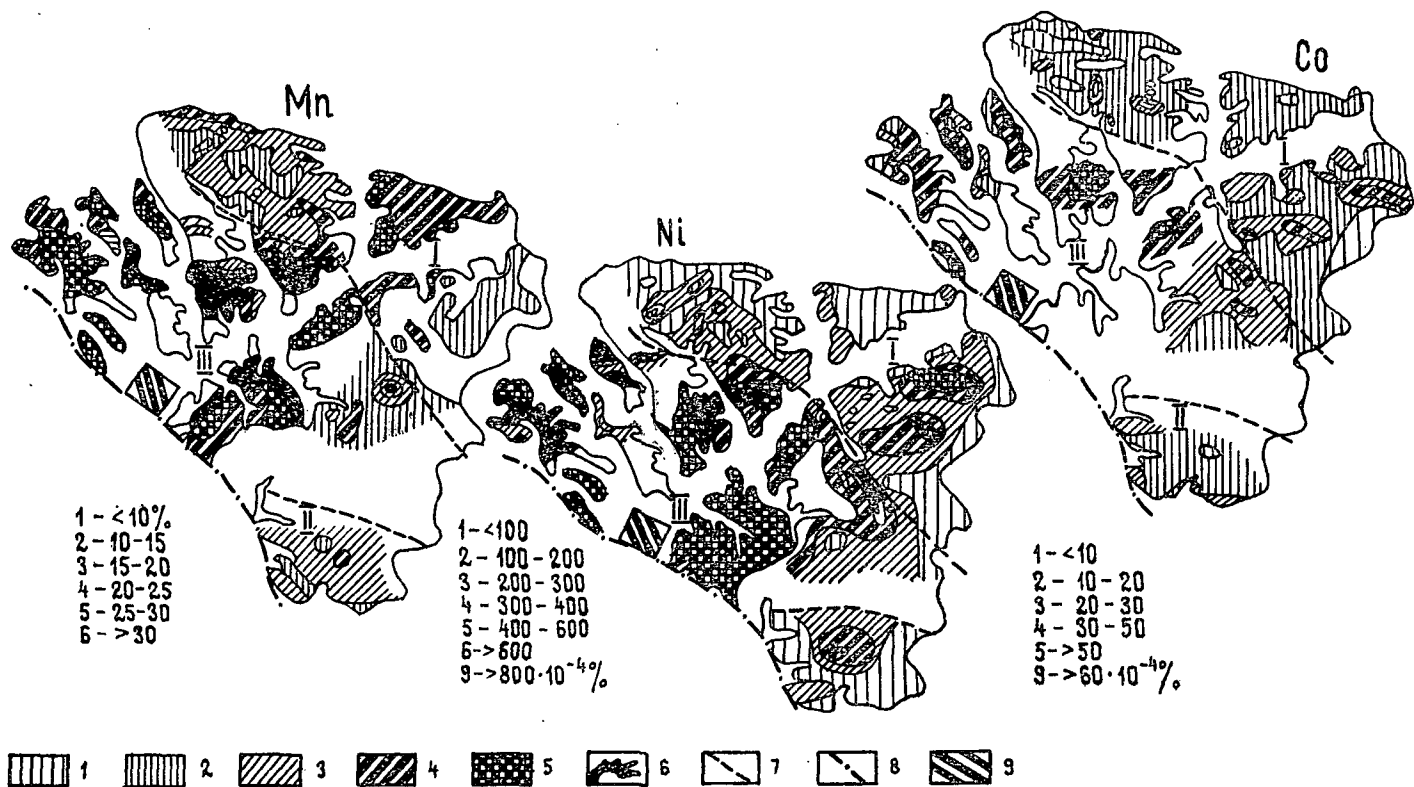


Fig. 3. Distribution of Mn (%), Ni and Co ( $10^{-4}\%$ ) on the Chiatara deposit, after L. E. STERENBERG (STRAKHOV *et al.*, 1968), supplemented: A Mn content: 1: up to 10; 2: 10-15; 3: 15-20; 4: 20-25; 5: 25-30; 6: >30; B Ni content: 1: up to 100; 2: 100-200; 3: 200-300; 4: 300-400; 5: 400-600; 6: >600; C Co content: 1: up to 10; 2: 10-20; 3: 20-30; 4: 30-50; 5: >50; 7: boundary between the fields of different concentrations of Mn, Ni, Co in the Lower Oligocene Ores; 8: Major Fault; 9: contents of Mn (more than 10%); Ni (more than  $800 \cdot 10^{-4}\%$ ), Co (more than  $60 \cdot 10^{-4}\%$ ) in the Upper Cretaceous limestones of the Major Fault zone on the western slope of the Perevis Highlands. I, II, III-principal ore fields

and the epochs of hypergenic crustal and bauxite formation, on the other, are essentially antipathic. In the crust of weathering the bauxite and not manganese deposits are bedded in primary oreless rocks. The infiltration residual commercial manganese deposits appear only during the hypergenic enrichment and ennobling of manganese primary deposits of other genetic types formed earlier. This is particularly apparent in the lateritic transformation of technologically unfavourable gondite deposits into the manganese oxide ores of the crust of weathering. Therefore, combined manganese-bauxite deposits, suitable for commercial extraction of manganese, are unknown. Consequently, we presume that the geochemical triad Al-Fe-Mn considered earlier (STRAKHOV *et al.*, 1968), collapses during the formation of deposits (but not of geochemical aureoles) of these metals in the crust of weathering: manganese falls out because it forms neither hypergenic crustal deposits in oreless rocks with the clark of metal (for example, the hypothetical bauxite manganese bodies), nor the sedimentary continental deposits unaffected by volcanism. The manganese ores are more often characterised by a different geochemical triad, i.e., manganese-iron-phosphorus. Its analysis, however, is beyond the scope of this paper.

J. BOULADON, G. JOURAVSKY (1952, 1956), G. CHOUBERT (Geology and genesis..., 1972) have used the typically continental manganese deposits on the African craton (Idikel, Nargeuchum, and others, see *Fig. 1*) to show their hydrothermal-sedimentary and properly sedimentary origin in lake basins associated with manifestations of continental volcanism. Such manganese accumulations on continents are usually spatially connected with the hydrothermal-metasomatic vein manganese ores, for example, in the Quarzazate province (Geology and genesis..., 1972). The Golconda Pleistocene continental volcanogenic-sedimentary manganese deposit is also associated with volcanism. The ores of this deposit have high contents of trace elements: tungsten up to 6.19%  $\text{WO}_3$  (average 0.5%), lead up to 5%, and copper up to 0.3% (KERR, 1940).

The unquestionably sedimentary manganese deposits are apparently only those belonging to the type of manganese recent "embryonic" accumulations found in the lakes of Karelia and Finland and in the Baltic and Beloye inner seas; they derive this metal from the crystalline rocks of the Baltic shield (STRAKHOV *et al.*, 1968 SAPOZHNIKOV in: "Geology and geochemistry...", 1982). Other present-day inner seas do not reveal manganese accumulations not being in the zones of volcanism or having no discharge regions for brines. Even the modern Black Sea cannot be regarded, from our viewpoint, as the prototype of the basin, where the sedimentary manganese can accumulate in commercial concentrations. The reason is that during the Neogene-Quaternary, within the drainage area of the Black Sea basin, not only the common rocks with the clark of the metal were eroded, but also the denuded manganese deposits themselves, including those of Nikopol and Chiatura. For example, almost 50% of the Chiatura deposit was eroded and the denudation products were washed out into the Black Sea impounded basin. But new sedimentary manganese accumulations were not re-deposited in the Black Sea in the Neogene-Quaternary, and the submarine deltas of the Rioni and Dnieper rivers, whose tributaries wash out the Chiatura and Nikopol deposits, contain only non-commercial manganese aureoles. Moreover, the waters of the Black Sea, in the hydrogen sulphide zone, have collected up to 100 million tons of dissolved manganese (SAPOZHNIKOV, 1967). In order to obtain 100 million tons of manganese in one deposit, the total volume of the Black Sea water should be somehow "evaporated" and the whole amount of manganese "precipitated" in one locality. It is nonsensical even to suggest this hypothetical "geological

process" for the formation of sedimentary manganese deposits, let alone such giants as Nikopol and Chiatura.

All this evidence, we believe, testifies that without volcanism and plutonism the continental basins-lakes and inner seas are genetically unfavourable for the formation of commercial manganese deposits. Proceeding from tectonic conceptions, these deposits are formed in the marginal seas, which appear during taphrogenesis, or in the regions of rifting, when the oceanic crust opens, i.e., in the destruction areas. The cause of the predominance of marine manganese deposits over continental ones is, therefore, apparent if viewed from these concepts. Both taphrogenesis and spreading control the rapid deepening of epi-continental sea basins in the regions of subsidence and of crustal spreading during the formation of deepwater basins. The manganese deposits synchronous with tectonic destruction actually occur in the periphery of these structures, in the intersections of differently oriented cosediment faults within newly formed separate foredeeps or depressions (MSTISLAVSKY, 1982). All Early Oligocene manganese deposits in the south of the USSR and in Bulgaria, the metalliferous sediments of the Red Sea graben, etc., are examples of these accumulations.

How are the processes of destruction manifested in the manganese-bearing regions and in the local parts of the deposits themselves? Besides the mineralising zones of cosedimentary faults with vein and hydrothermal-metasomatic manganese ores, several deposits reveal the lenslike layered sedimentary breccias of tectonic breakup and destruction. They are often thick and contain ore lumps of different size, even blocks. The destruction breccias are observed in the Porozhinsk Vendian deposit of the Enisei Range (MSTISLAVSKIY, 1984b), in the Usinsk Lower Cambrian deposit of the Kuznetsk Alatau, after I. M. VARENTSOV (1962), in the itabirites of the Malyi Khingan (Geology and genesis..., 1972), in the Karazhal Famennian deposit of Central Kazakhstan, after A. A. ROZHN OV *et al.* (New data..., 1980), and in other regions. We also tend to classify as the manganese destruction breccias, preceding the supply of hydrothermal ore-bearing solutions into the basin, the Blinkklip Lower Proterozoic basal manganese-bearing breccia of the Postmasburg deposit in South Africa, after A. Du TOIT (1957), the intraformational breccias of the El Cobre Cretaceous-Eocene manganese formation of Cuba, after F. SIMONS and J. STRACZEK (1958), the Imini-Tasdremt breccias, after J. BOULADON and G. JOURAVSKY (1956), V. P. RAKHMANOV, I. K. TCHAIKOVSKY (1980), and other deposits.

The structural position of the breccias is peculiar. They are confined to the roof and near-roof parts in the sides of the anticlinal structures. The comparison of the bedding of the basal manganese-bearing breccias in the Postmasburg deposit, South Africa, and in the Porozhinsk deposit, the Enisei Range, has revealed similar features of their occurrence. Both of them are deposited unconformably and with washout on the underlying dolomites in the near-roof parts of the structures. The breccias wedge out towards the central parts of the depressions, whereas the angular unconformities and erosions between the two contacting layers disappear (MSTISLAVSKIY, 1984b). The analogous bedding of sedimentary breccias is typical of the Karazhal deposits in Central Kazakhstan and probably of other manganese-bearing regions as well. The sedimentary character of breccias with lumps of manganese ores are discussed in detail by F. SIMONS and J. STRACZEK (1958) in terms of evidence of the syngenetic manganese lenslike occurrence in the El Cobre Late Cretaceous-Eocene formation of Cuba.

Besides their stratified lenslike bedding, the manganese-bearing breccias of tectonic destruction in the mentioned deposits are also characterised by other sedimen-

tary features. They are chaotically heaped and without orientation; the ore lumps have different size and habit ranging from several millimeters to decimeters in diameter. The dominating irregular sharply angular habit and the variety of dimensions of lumps of rocks mostly from the enclosing formations, a small amount or absence of gravels of other rocks positively imply the destruction of lithified deposits and intraformational redeposition, chaotic heaping of fragments without remote transportation, rounding or hydrodynamical differentiation.

This kind of breccias is characteristic of volcanogenic-sedimentary deposits with notable domination of pyroclastic and siliceous rocks. The cement of the breccias themselves is mostly composed of the carbonate-siliceous substance, whereas the manganese mineralisation in the non-metamorphosed strata predominantly contains manganite and rhodochrosite with accessory goethite. Manganite also dominates among breccias of redeposited manganese ore lumps, as for example in the Porozhinsk deposit (MSTISLAVSKIY, 1984b). At the Porozhinsk deposit, the hydrothermal-metasomatic mineralisation with hausmannite and rarely occurring manganosite was cored at the intersections of faults. These minerals apparently indicate ore shoots, relicts of mineralising channels, which supplied manganese-bearing solutions through the underlying rocks to the basin.

The Porozhinsk deposit in the taphrogenic-siliceous formation, after D. I. MUSATOV, V. V. USTALOV *et al.*, (New data..., 1980) is located in the Vendian orogenic foredeep of the Enisei Range. It was formed, however, not in the orogenic regime, but during the taphrogenic activity which followed tectonic stabilisation and accumulation of the dolomite layer in the interval between the lower and upper molassic deposits. In a similar manner the hydrothermal-metasomatic ores of the adjacent region were deposited with the formation of the Atasu graben-syncline during the taphrogenic tectono-magmatic activity; these ores are superimposed on the Upper Devonian red limestones of the Dzhesda and Nazaitas deposits (KALININ, in: "New data...", 1980). The same tectonic position probably occupy the Barremian-Albian manganese stratified deposits of the Arqueros and Quebrada Marquesa formations in the Cocuimbo province, Chile, after C. RUIZ (1965), F. PEEBLES (1970), E. A. SOKOLOVA (1982).

To emphasise the regularity of confinement of manganese deposits to the regions of crustal destruction, let us recall that manganese-bearing metalliferous sediments of the present-day oceans are found in rifts (the Red Sea grabens, the Gulf of Aden, etc.), in tectonic depressions (the Hess and Bauer depressions), on the slopes of the mid-oceanic ridges, which were formed, as generally acknowledged, by the spreading of the lithospheric plates. The direct observations of the hydrothermal manifestations on the Pacific bottom in the Galapagos active zone and in the Hess depression, after G. KLINKHAMMER *et al.* (1977), V. V. GORDEEV, L. L. DEMINA (1979), have shown the Mn content to reach 24 mkg/kg at the spouts of the hydrotherms in the bottom water, where the deep isotopes  $^3\text{He}$ ,  $^{222}\text{Rn}$  were also detected. All known regions of metalliferous ferro-manganese sediments, with the accessory microelements Ni, Cu, Co, Zn, V are associated with the regions of crustal destruction in the zones of spreading and taphrogenesis. The latter process evidently controls the appearance of large depressions in the ocean bottom several hundreds of kilometers long (the Hess depression and others). The destruction processes in transform faults cause the appearance of zones analogous to the Clarion-Clipperton interdiff zone in the Pacific. In this zone, after D. CRONAN (1973), M. BENDER, I. DYMOND (1973), I. M. VARENTSOV (1976), the ferromanganese concretions are found having high Mn content 22.33% and contents of Fe 9.44%, Ni 1.08%, Cu 0.63%, Co 0.19%.

## CONCLUSIONS

By using the available data on the relation between the manganese-bearing capacity and the destruction processes, we classified the manganese deposits according to their confinement to the basic commonly acknowledged tectonic regimes: 1-platform proper, plate or epeirogenic; 2-platform with trapp magmatism (geocratic); 3-geosynclinal; 4-orogenic; 5-taphrogenic activation of platforms and ancient cratons; 6-oceanic (thalassocratic). The last regime should probably be described as mostly the taphrogenic-rifting endogenous one. The most manganese productive are the oceanic regime and the regime of taphrogenic activity of platforms and particularly of ancient cratons and median masses. Among the geosynclinal regimes, the most favourable is the island arc regime with a sufficiently intensive explosivity. The regime of early geosynclinal large troughs usually produces only small manganese deposits. In the troughs, the ferro-manganese accumulations are normally deposited during the formation of undifferentiated tholeiitic basalts. These deposits are also typical of the trapp formation.

We should emphasise, therefore, the different character of volcanism, during which the iron and manganese ores could accumulate. Manganese ores are often characterised by the differentiated andesite-basalt-liparite series with high alkalinity. For example, as stated by A. A. ROZHNOV and A. B. VEIMARN, this is typical of contrasting differentiated subalkaline-basalt—alkaline-liparite formation of the Atasu group of ferro-manganese deposits in Central Kazakhstan; the formation is associated with the potassic metasomatism (New data..., 1980; *Geology and geochemistry...*, 1982). In Chiatura and Western Georgia, the pronounced alkalic nature of magmatism on the Okribo-Dziruli prominence directly preceded manganese accumulation during the period from the Late Cretaceous to the end of the Late Eocene (DZORSENIDZE, 1965). The subalkalic volcanism characterises a number of other manganese-bearing regions.

The genetic positions described above form the basis of systematic classification of criteria for prospecting manganese deposits on continents. Of major importance are the syngenetic criteria on a regional scale and first of all the manganese forming epochs.

The manganese forming epochs, considered as strictly stratigraphical intervals and used as prospecting criteria, still cannot serve as direct indications of manganese accumulations for any territory. We believe, that the epochs are metallogenic for manganese only in the regions, which experienced a special kind of endogenous regime, i.e., taphrogenic or taphrogenic-rifting. Consequently, the stratigraphic indication is combined with the tectonic factor into a single tectono-stratigraphic criterion. The author notes the unity of metallogenic manganese forming epochs and provinces and emphasises their common genetic causes controlled by the manifestations of the taphrogenic-rifting regime. To conclude, the manganese-metallogenic zoning of the territory is based on the specific tectonic properties of the regions derived from the formational and genetic principles controlling ore-prospective areas.

## ACKNOWLEDGEMENT

The author acknowledges his thanks to I. M. VARENTSOV for the constructive and kindly given criticism.



## REFERENCES

- AVALIANI, G. A. (1982): Manganese deposits of Georgia. p. 3—138, M., "Nauka", (in Russ.).
- ALEKSIEV, B. BOGDANOVA, KR. (1974): The manganese deposit of Obrochishte. — In: "Twelve ore deposits in Bulgaria", p. 144—156, Sofia, (in Russ.).
- BELOUSSOV, V. V. (1976): Geotectonics. Publ. of Moscow State University, (in Russ.).
- BETEKHTIN, A. G. (1946): Commercial manganese ores of the USSR. M. L., Publ. House of USSR Academy of Sciences, (in Russ.).
- BOULADON J., JOURAVSKY, G. (1952): Manganese. Géologie des gites minéraux marocains. Dans: XIX Congrès géologique international. — Monographies régionales, 3e sér., Maroc, N 1, Rabat.
- BOULADON, J. JOURAVSKY, G. (1956): Les gites des manganese du Maroc. (Suivi d'une description des gisements du Précambrien III). In: XX Congreso geológico internacional. — Symposium sobre Yacimiento de manganese. T.2. Africa, Mexico.
- BOZHKO N. A. (1984): The Late Precambrian of Gondwana. M., "Nedra" (in Russ.).
- The Chiatura manganese deposit. M., "Nedra", 1964, p. 3—101 (in Russ.).
- CRONAN, D. S. (1973): Basal ferruginous sediments cored during Leg 16 of the Deep Sea Drilling Project. Initial Reports of the Deep Sea Drilling Project. Washington, US Government Printing Office.
- Discovery of a number of new commercial manganese deposits in the SAR. Ref. Journ. "Geology of ore deposits", v.2, 1982 (in Russ.).
- DU TOIT, ALEX L. (1954): The geology of South Africa. (S. H. HAUGHTON, ed.), Oliver and Boyd Publ., London.
- DYMOND, I. *et al.* (1973): Origin of metalliferous sediments from the Pacific Ocean. Geol. Soc. Amer. Bull., 84, N 10.
- DZOTSENIDZE, G. S. (1965): Effect of volcanism on sedimentation. M., "Nedra", p. 79—109, (in Russ.).
- Explanatory note to the geological map of South America, scale 1:5,000,000. M., VNII Zarubezhgeologia, 1979 (in Russ.).
- Explanatory note to the geological map of Africa, scale 1:5,000,000. M., VNII Zarubezhgeologia, 1980 (in Russ.).
- FRAKES, L. A., BOLTON, B. R. (1984): Origin of manganese giants.: sea-level change and anoxic-oxic history. Geology, v 12, p. 83—86.
- GAVRILOV, A. A. (1972): Exhalation-sedimentary manganese ore accumulation. M., "Nedra" (in Russ.).
- Geology and genesis of the Precambrian ferro-siliceous and manganese formations of the world. Kiev, "Naukova dumka", 1972 (in Russ.).
- Geology and geochemistry of manganese. M., "Nauka", 1982 (in Russ.).
- Geology and commercial minerals of Africa. p. 468—473, M., "Nedra", 1973 (in Russ.).
- GORDEEV, V. V., DEMINA, L. L. (1979): Direct observations of hydrotherms on the Pacific bottom (the Galapagos active zone, the Hess depression). — Geochemistry, N 6, p. 902—917, (in Russ.).
- GRIBOV, E. M. (1972): Alabandite from the Ulutelyak manganese deposit (the Bashkir Urals). — "High School News" (Izvestia vuzov), Geology and Prospecting, N 8, p. 134—136, (in Russ.).
- KERR, P. E. (1940): Tungsten-bearing manganese deposits at Golconda, Nevada. — Geol. Soc. Amer. Bull., 51.
- KLINKHAMMER, G., BENDER, M., WEISS, R. F. (1977): Hydrothermal manganese in the Galapagos Rift. Nature, v. 269, N. 5626.
- MCINTOSH, J. L., FARAG, J. S., and SLEE, K. J. (1980): Groote Eylandt manganese deposits. In: "Economic Geology of Australia and Papua New Guinea". 1. Metals (C. L. KNIGHT, ed.), Austral. Inst. Min. Metal. Monograph 5, pp. 815—821.
- Manganese ore formation on the territory of the USSR. M., "Nauka", 1984 (in Russ.).
- MILANOVSKIY, E. E. (1976): The rift zones of continents. M., "Nedra", 1976 (in Russ.).
- MSTISLAVSKIY, M. M. (1972): The origin and morphological type of the Maikop basin in the south of the USSR. Doklady AN SSSR, v. 202, N. 5, p. 1151—1154, (in Russ.).
- MSTISLAVSKIY, M. M. (1982): The Oligocene manganese accumulation in the south of the USSR and oceanisation. In: "Geology and geochemistry of manganese", M., "Nauka", (in Russ.).
- MSTISLAVSKIY, M. M. (1984 a): Manganese accumulation and the epochs of crustal destruction. Doklady AN SSSR, v. 275, N 2, p. 435—439, (in Russ.).
- MSTISLAVSKIY, M. M. (1984 b): The breccias produced by tectonic destruction of the top layers in manganese deposits. Doklady AN SSSR, v. 275, N. 3, p. 700—703, (in Russ.).
- MSTISLAVSKIY, M. M., POTKONEN, N. I., TABAGARI, D. V. (1984): The mineralising channel of the Chiatura manganese deposit. Geology of ore deposits. N. 2, p. 68—76, (in Russ.).

- New data on the manganese deposits of the USSR. M., "Nauka", 1980 (in Russ.).
- The Nikopol manganese basin. M., "Nedra", 1964 (in Russ.).
- PEEBLES, F. L., KLOHN, E. N. (1970): Geología de los yacimientos de manganeso de Corral Quemado, Arrayan y Fragua, Provincia de Coclé. — Bol. Inst. Invest. Geol., Chile, N. 27.
- PEIVE, A. V. *et al.* (1980): Tectonics of Northern Eurasia. M. "Nauka", (in Russ.).
- RABINOVICH, S. D. (1971): The North Urals manganese ore basin. M., "Nedra", (in Russ.).
- RAKHMANOV, V. P., TCHAIKOVSKY, V. K. (1980): Manganese ores in activated platforms.-Proc. of the Fifth Quadrennial IAGOD Symposium, E. Schweizerbartische Verlagsbuchhandlung (Nägele u. Obermiller) FRG, Stuttgart, p. 135.
- RAKHMANOV, V. P., CHAIKOVSKIY, V. K. (1983): Geochemistry of manganese and the evolution of manganese-bearing formations during geological history.-In: "Geochemistry of platform and geosynclinal sedimentary rocks and ores". p. 234—242, M., "Nauka", (in Russ.).
- Recent hydrothermal ore deposition. M., "Mir", 1974 (in Russ.).
- RUIZ, C. F. (1965): Geología y yacimientos metalíferos de Chile. — Inst. Invest. Geol., Chile.
- SAPOZHNIKOV, D. G. (1967): Conditions for the formation of manganese deposit, in the south of the Russian platform and in the Crimean-Caucasus geosyncline.-Geology of ore deposits, N. 1, p. 74—87, (in Russ.).
- SIMONS, F. S., STRACZEK, J. A. (1958): Geology of the manganese deposits of Cuba.-Bull. U.S. Geol. Surv., 1057.
- SMIRNOV, V. I. (1982): Geology of minerals.-p. 392—403, M., "Nedra", (in Russ.).
- SOKOLOVA, E. A. (1982): Manganese sources in volcanogenic-sedimentary formations, — M., "Nauka", (in Russ.).
- STRAKHOV, N. M., STERENBERG, L. E., KALINENKO, V. V., TICHOMIROVA, E. S. (1968): Geochemistry of sedimentary manganese accumulation process. — M., "Nauka", (in Russ.).
- VARENTSOV, I. M. (1962): The major manganese-bearing formations.-In: "Sedimentary iron and manganese ores". Trans. Geological Inst., USSR Academy of Sciences, issue 70, p. 117—173, (in Russ.).
- VARENTSOV, I. M. (1976): Geochemistry of transitional metals in the process of formation of ferromanganese ores in present-day basins. In: "Mineral deposits". p. 79—96, M., Nauka, (in Russ.).
- VARENTSOV, I. M., RAKHMANOV, V. P. (1974): Manganese deposits. In: "Ore deposits of the USSR", v. 1, p. 109—167, M., "Nedra", (in Russ.).
- YANSHIN, A. L., BASENTSIAN, SH. A., PILIPENKO, A. I., SHLEZINGER, A. E. (1980): New data on the time of formation of the Black Sea deepwater depression. Doklady AN SSSR, v. 253. N. 1, p. 223—227, (in Russ.).

*Manuscript received, 17 February, 1986*



## IRON AND MANGANESE ORES IN THE GEOLOGICAL HISTORY OF CENTRAL KAZAKHSTAN

A. B. VEIMARN<sup>1</sup>, A. A. ROZHN OV<sup>2</sup> and V. I. SCHIBRIK<sup>2</sup>

<sup>1</sup>Geological Department, Moscow State University

<sup>2</sup>Ministry of Geology of Kazakhskaya SSR, Industrial Geological  
Association "Centrkazgeologiya"

### ABSTRACT

The history of iron and manganese accumulation in Kazakhstan has been analysed by identifying ore formations and revealing geological conditions of their generation. A quantitative assessment of the ore contents of the formations identified has been carried out. Epochs of maximum ore accumulation and regimes most favourable for ore genesis have been distinguished.

### INTRODUCTION

At present, Central Kazakhstan has become the second manganese ore base in the USSR after the Ukraine (ROZHN OV *et al.*, 1985). 321 deposits and ore manifestations of iron and manganese are discovered on the territory of Central Kazakhstan. Specialised metallogenic works carried out at the mentioned objects and on an entire territory allow us to characterize history of iron and manganese accumulations of the region (*Fig. 1*). A metallogenic analysis was carried out on the basis of the identification of ore formations, i.e. sets of ore deposits and manifestations common in mineralogical-geochemical composition, geological conditions of origin and age. Paleotectonic constructions were used to characterize geological conditions in terms of the ore formation generation.

### ORE FORMATIONS

Studying a process of the iron and manganese accumulation it is only advisable to consider its development in time (*Fig. 1*).

Pre-Cambrian series different in age contain horizons of iron quartzites. However, all the deposits of commercial value occur only among rocks of the Early Proterozoic Karsakpayskaya series, making up the *Early Karelian regionally-metamorphosed hydrothermal (volcanic) — sedimentary formation of iron quartzites (jaspilitic)*.

After S. B. ROSANOV (1976) and L. I. FILATOVA (1983) Karsakpayskaya series is characterised with a rough rhythm. There are four suites which may be considered

<sup>1</sup> University place 1, 119899 Moscow, USSR

as microrhythms. Porphyritoids and greenschists make 50% of the section whereas high-iron basalts dominate in composition. The latter is isolated in the lower part of each suite, and its upper parts are formed by phyllite bands with iron quartzite horizons. Nine horizons of iron quartzites have been revealed, part of which is traced in a submeridional direction at a distance of 200 km (the Karsakpayskaya ore zone in Fig. 1). Quartzites are mostly of hematite, rarely of magnetite-hematite. Ore varieties transit into ore-free ones, sometimes into graphitite microquartzites. Marble may also occur. Thickness of ore bodies within a deposit drastically changes achieving 25 m depending on the confinement to limbs or curves of folds. A mean iron content in the ore is of 40%,  $\text{SiO}_2$  — 35%. The Karsakpayskaya series is considered to be a greenschist basalt-spilitic jaspilite-bearing early geosynclinal early Karelian formation generated within the intracratonal trough.

Non-commercial, though the most ancient manganese ore manifestation is Utegsensor in the Chingiz mountains in the East of the region. Quartzites with 2—12% iron content and that of the 29—37% manganese occur in the band of sericitic-quartz microquartzites being in themselves the metamorphosed (greenschist facies) tuffogene siliceous sediments with volcanites of predominantly acid composition referred to the Late Proterozoic Murzhikskaya series.

Three ore formations were generated during the Early Caledonian geosynclinal cycle.

The deposits of the *Early Caledonian iron-manganese hydrothermal (volcanic) — sedimentary formation* are confined to the early geosynclinal Caledonian troughs (Fig. 2). The ore generation is probably connected with processes accompanying volcanism displayed in these troughs against the background of the siliceous-terrigenous sedimentation in  $O_1$   $\alpha$ . Volcanites are represented, predominantly, by homogeneous basalt series of tholeiitic composition. The Kosagalinskaya ore zone deposits are typical ones (Fig. 1). They occur among sandstone suites of the Middle Ordovician, sections of which reveal rare horizons of basalts and siliceous rocks. The latter contains ore bodies 1—32 m thick (6 m in average), the iron content is of 18—42%, that of the manganese is of 0.1—7%. The main ore minerals here are magnetite and hematite. The deposits in terms of size are small ones. Conditions involved into the ore formation generation characterized with a high tectonic activity did not assist in forming large deposits. A quality of ores occurring in zones of the contact with the later granitoid intrusions becomes slightly higher.

A small deposit of Otaydy-Karasu represents the *Early Caledonian titanomagnetite late-magmatic formation*. After E. M. SPIRIDONOV (1979), an ilmenite-titanomagnetite mineralization is confined to most large differential bodies of ultrabasites o

---

**Fig. 1.** Iron and manganese deposits in Central Kazakhstan. I — ore formations: 1 — oligocene platformal chemogenic-sedimentary oölitic (siderite-leptochlorite-hydrogoethitic); 2 — Late Hercynian skarn-copper-magnetite; 3 — Early Hercynian skarn-magnetite; 4 — Early Hercynian magnetite-titanomagnetite of coastal-marine placers; 5 — Early Hercynian iron-manganese hydrothermal (volcanic)-sedimentary; 6 — Late Caledonian skarn-magnetite; 7 — Early Caledonian skarn-magnetite; 8 — Early Caledonian titanomagnetite late magmatic; 9 — Early Caledonian iron-manganese hydrothermal (volcanic)-sedimentary; 10 — Early Karelian regionally-metamorphosed hydrothermal (volcanic)-sedimentary formation of iron quartzites (jaspilitic). II — IV — deposits (II — small, III — middle, IV — large). V — age of mineralization. VI — iron and manganese ore zones: A — Atansor-Kuzganskaya, B — Karsakpayskaya, C — Dzhezdzinskaya, D — Zhailminskaya, E — Kosagalinskaya, F — East-Karkaralinskaya. VII — a boundary of the epipaleozoic platform mantle spread within Central Kazakhstan. VIII — a boundary of the area to carry out specialized metallogenic works.

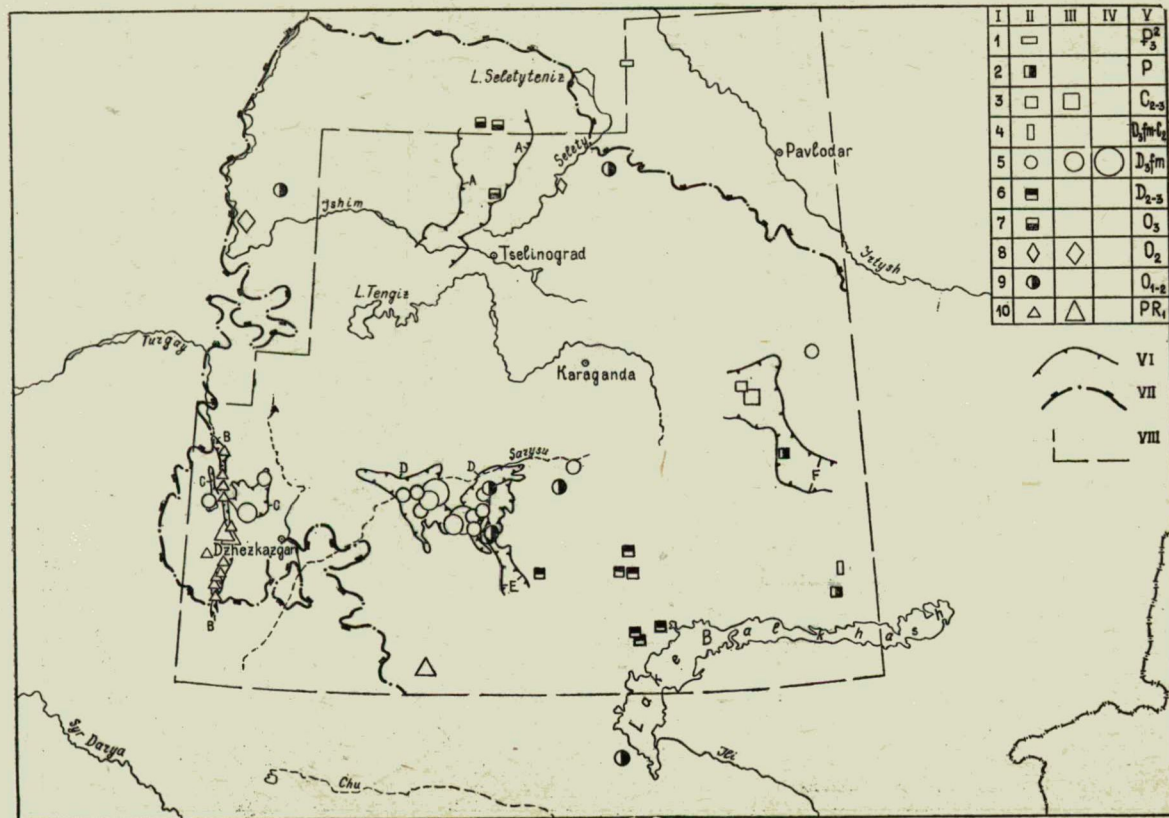


Fig. 1



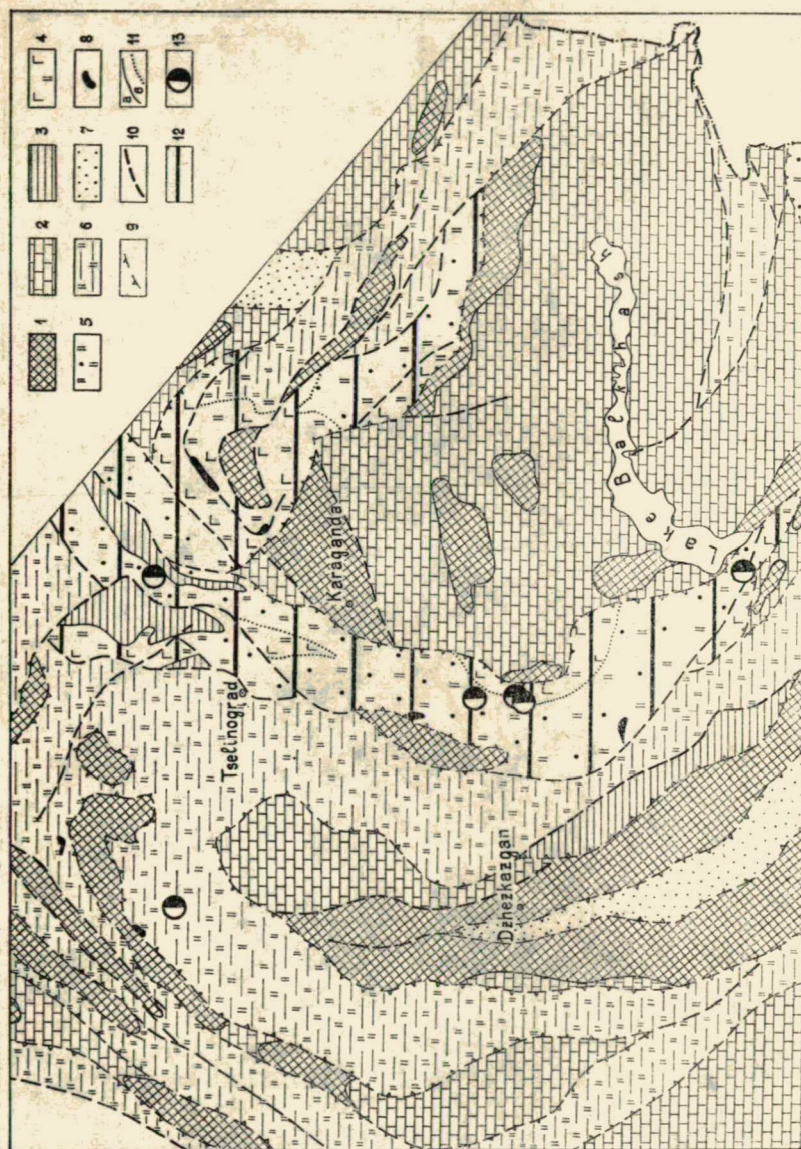


Fig. 2

the phase II of intrusion (clinopyroxenites are often olivine one) of the Middle Ordovician intrusive complex. The latter being comagmatic to high aluminium basalts of Sagskaya series ( $O_2$ ) formed under conditions of a mature geosynclinal regime is represented with small stock and funnel-shaped massifs. The iron content in ores is of 12—19% (up to 37% by section),  $TiO_2$  — of 0,5—3% (up to 7%).

The Early Caledonian skarn-magnetite formation was generated on the verge of the geosynclinal stage proper and is associated with intrusions of granodiorites forming within the Taconic folding phase ( $O_3$ ). Deposits are confined to contacts of diorites and granodiorites with volcanogenic sedimentary rocks of the Sagskaya series ( $O_2$ ) and grouped into Atansor-Kuzganskaya ore zone (Fig. 1). By composition of metasomatites, these deposits are of calc-skarn, small in size; ores are of magnetite with the mean iron content of 45%.

The Late Caledonian skarn-magnetite formation is typical for a region of the Telbessian-Middle Devonian folding occurrence and is associated with Devonian granitoid massifs widely spread over that region. Two subformations have been identified: calc-skarn and magnesian-skarn. A small deposit of Bapy refers to the second subformation, lizardite-magnetite ores of which have been probably formed under metasomatism of dolomite.

The Early Hercynian iron-manganese hydrothermal (volcanic) — sedimentary formation is the most important for Central Kazakhstan. All the known manganese and main iron deposits formed in the Famennian and occurring, basically, among Famennian sediments appertain to the mentioned formation.

Main deposits are concentrated in Zhailminskaya ore zone (Fig. 1) (Atasuysky region). The largest deposit — Western Karazhal is confined to the southern part of the zone. It is represented with beds of hematite, magnetite and manganese (braunite-hausmannite) ores occurring in the band of knot-bedded red-coloured limestones of the Upper Famennian substage. The mean content of components in corresponding ores is of Fe — 50%, Mn — 20%. The majority of deposits in the northern part of the zone are complex. They contain iron-manganese and barite-polymetallic ores. By this sign, they are identified as deposits of Atasuysky type (ROZHNOV, 1967). A most large manganese deposit among them is Ushkatyn III, ores of which are also confined to red-coloured limestones of the Upper Famennian.

The majority of the Zhailminskaya zone deposits occur within siliceous-carbonate rocks and are singled out into a separate subformation (Karazhalsky type). Deposits confined to terrigenous rocks (Dzhezdzinsky type) appertain to another subformation. They are typical for Dzhezdzinskaya ore zone (Fig. 1), and occur in the conglomerate-sandstone Uytasskaya suite of the Lower Famennian manifesting the beginning of the Famennian transgression. Their size is not large.

Fig. 2. Paleotectonic scheme of the Early-Middle Ordovician of Central Kazakhstan (after ZAITSEV *et al.*, 1987) and iron-manganese deposits of the given age. 1—2 — residual median massifs (1 — erosion areas, 2 — covered by a mantle of limestone, terrigenous, siliceous-terrigenous and volcanic formations); 3 — new geosynclinal uplifts (erosion areas); 4—5 — troughs with eugeosynclinal development regime (4 — filled with basalt, andezite-basalt and jasper-basaltic formations; 5 — terrigenous-siliceous formation); 6 — troughs with chemi-eugeosynclinal development regime, filled with siliceous-terrigenous, volcanic-siliceous-terrigenous, carbonate formation; 7 — troughs with inverse development regime filled with terrigenous, carbonate-terrigenous flyschoid formations; 8 — massifs of hyperbasits; 9 — boundaries of median massifs; 10 — regional faults; 11 — geological boundaries (a) and facial boundaries (b); 12 — regions of the highest tectonic activity; 13 — iron-manganese deposits



Famennian weakly differential subalkaline olivine basalts are locally revealed in almost all the ore fields of the formation. Established in time and space, the proximity of processes involved into the basalt magmatism, potassic metasomatism and ore formation constitutes a united hydrothermal-magmatic system (VEIMARN *et al.*, 1981).

A paleotectonic analysis (Fig. 3) showed that the majority of deposits in the formation is confined to a latitudinally oriented paleotrough which had occupied a cross-cutting position relative to earlier existed structures, and had a heterogeneous basement (VEIMARN *et al.*, 1986). The tectonic regime within its limits is a geosynclinal activation (regeneration of geosynclinal conditions) after a preceding orogenic stage in the development. The comparison of the trough with modern rifting zones is quite possible. Most large deposits were forming under conditions of the sea-floor stagnant depressions where a siliceous-coaly-clay-carbonate flyschoid formation under a regime of the miogeosynclinal activation had accumulated. Iron-manganese deposits of commercial value in quazi-platform regions and Hercynides which did not experience previous Caledonian folding and characterized by an early geosynclinal and mature geosynclinal tectonic regime are not fixed.

*The Early Hercynian formation of coastal-marine placers* is represented by titanomagnetite sandstones. Ultrabasic rocks eroded on adjacent uplifts constitute a principal source of ore minerals. Poor ores prevail.

*The Early Hercynian (C<sub>2-3</sub>) skarn-magnetite and Late Hercynian (P) skarn copper-magnetite ore formations* are associated with widespread orogenic magmatism of corresponding time. Deposits of these formations are grouped into Eastern-Karkaralinskaya iron zone (Fig. 1) ("Geology and metallogeny...", 1971). The location of the zone is determined by an intersection of the edge part in Dzhungaro-Balkhashskaya geosyncline with deep fault. A most significant deposit here is Kentobe, rich massive magnetite ores of which contain 62% of iron.

Thick crusts of weathering formed during the Mesozoic-Cenozoic in Central Kazakhstan have been, mainly, eroded later. Most probably, the latter served as a source of metals for *Oligocene platformal chemogenic-sedimentary oolitic (siderite-leptochlorite-hydrogoethitic) formation*, commercial deposits of which within Central Kazakhstan have not been singled out.

## ORE CONTENT OF FORMATIONS

A quantitative assessment of the ore contents of formations identified as performed allowing for forecasting data is presented in a relative scale in Fig. 4. As, only a modern structure of the region was analysed, ore contents of formations character-

---

Fig. 3. The paleotectonic scheme of the Famennian in the Central Kazakhstan. 1 — erosion areas; geological formations and associations: 2 — salt-bearing; 3 — terrigenous, red, continental; 4 — carbonaceous-gypsiferous-terrigenous lagoon type; 5 — carbonaceous (prevailing dolo-mitic) marine; 6 — limestone marine; 7 — calciferous-terrigenous coastal-marine; 8 — terrigenous carbonaceous marine; 9 — red knot-bedded limestones forming upper parts of the sections in a number of structures; 10 — clay-siliceous-carbonaceous flyschoid; 11 — aleurite-clay; 12 — terrigenous marine; 13 — carbonaceous-tuffaceous-terrigenous-flyschoid; 14 — tuffaceous-terrigenous; 15 — terrigenous-siliceous; 16 — porphyric dacite-liparite; 17 — consedimentation faults; 18 — younger faults; 19 — the boundaries of the Kazakhstan-Tien Shan epi-Caledonian median massif; 20 — the boundaries of the areas which had experienced the pre-Famennian folding; 21 — isopachytes; 22 — manifestations of basaltic volcanism; 23 — iron-manganese deposits

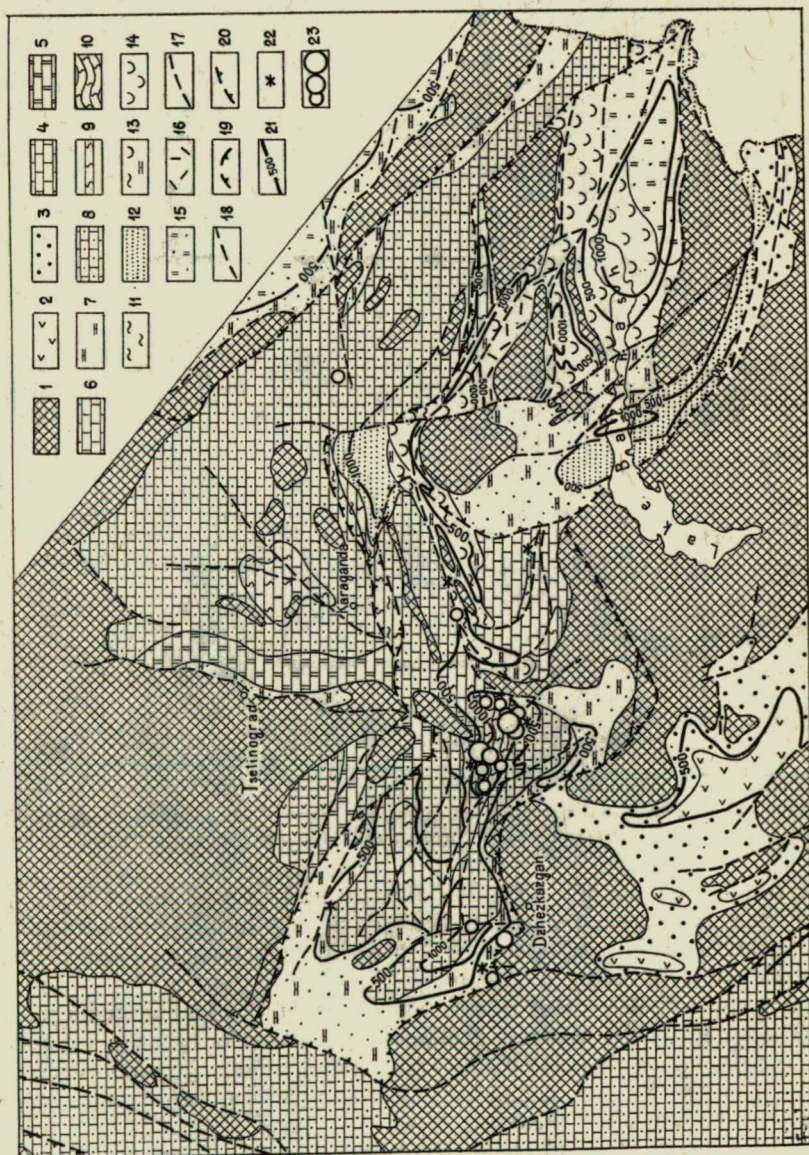


Fig. 3

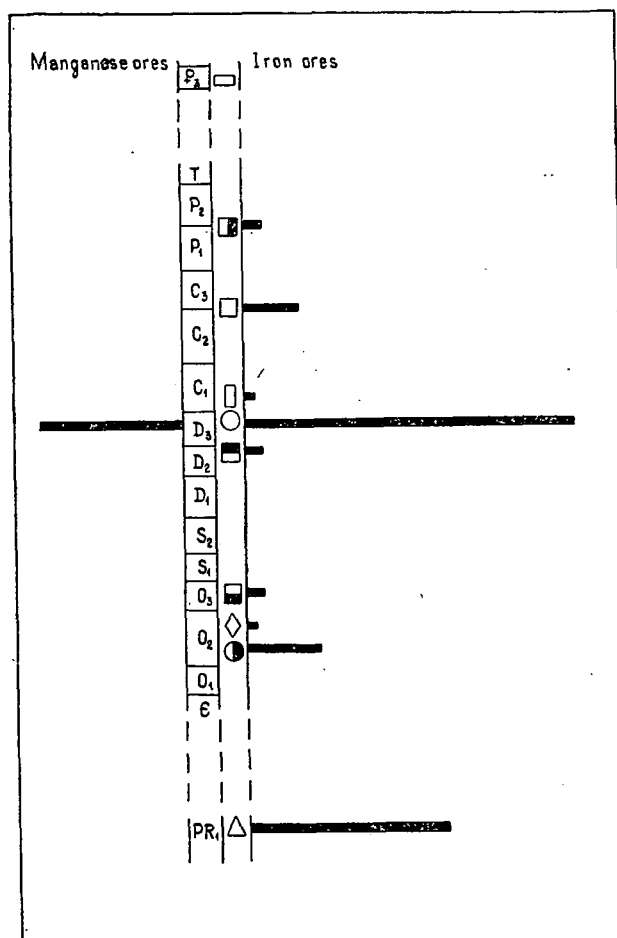


Fig. 4. Ore content of iron and manganese formations. Signs of ore formations located along the stratigraphic scale correspond to signs in Fig. 1.

ize an erosional section of Central Kazakhstan up to 0,5—1 km of depth and not absolute scales of ore accumulation in the time of each formation generation.

Following a given assessment, only hydrothermal (volcanic)-sedimentary and skarn deposits are of commercial value.

Skarn-magnetite deposits various in age contain ores of a high quality but small in size. The latter may be probably explained by a character of magmatic rocks with which the deposits are associated. They are predominantly granodiorite complexes derivative from the granite magma as opposed to gabbro-plagiogranite ore-bearing intrusions of the Urals and the Turgai.

The generation of hydrothermal (volcanic)-sedimentary deposits in the geological history of the region took place three times. In the Early Proterozoic a considerable number of ores, though, of low quality has been formed. Geological conditions typical for early geosynclinal troughs of the Early-Middle Ordovician were not favourable for ore concentration. Small in size, iron-manganese deposits, rarely the

manganese ones have generated. Similar deposits are typical for the Urals geosyncline. The Famennian is the time of all the commercial manganese concentrations along with most large ones of the iron ore in Central Kazakhstan being formed.

A study of the changes in the endogenic tectonic regimes both in time and space within Central Kazakhstan show that the miogeosynclinal activation regime (regeneration of geosynclinal conditions, rifting) for areas which experienced a considerable previous consolidation of the earth crust is most favourable for iron-manganese accumulation.

The interrelationship between iron and iron-manganese ore zones of various age is most peculiar. With a general latitudinal orientation of the expansion range of the Early Hercynian hydrothermal (volcanic)-sedimentary iron-manganese formation, a most important in the region, its main ore zones are conjugated in space with more ancient ones (*Fig. 1*).

## CONCLUSIONS

Metallogenic analysis of Kazakhstan territory showed that virtually all the commercial manganese deposits are of Famennian age and appertain to the Early Hercynian hydrothermal (volcanic)-sedimentary iron-manganese formation. Studies on geological settings of the deposit formation have allowed us to identify epochs and tectonic regimes most favourable for ore concentration ensuring a substantial approach to prospecting, evaluating and predicting mineralization. Comparison with other regions serves to prove the relationships established, to a certain degree, to be of a common nature.

## REFERENCES

- FILATOVA, L. I. (1983): Stratigraphy and historical geological (formational) analysis of the Pre-Cambrian metamorphic series in Central Kazakhstan. M., Nedra, 160 p. (in Russ.)
- Geology and metallogeny of eastern part of Tokrauskaya depression and south-western Chingiz (1971): Data on geology of Central Kazakhstan. IX, M., Moscow University, 214—281. (in Russ.)
- ROZANOV, S. B. (1976): Spilitic jaspilite-bearing formation of the Early Proterozoic in Kazakhstan. In: Geology and tectonics of the Pre-Cambrian in Central Kazakhstan. M., Moscow University, 11—181. (in Russ.)
- ROZHN OV, A. A. (1967): On geological genetic peculiarities of manganese mineralization in western part of Dzhaibinskaya syncline, and manganese mineralization rank with iron and polymetals occurrences in the region. In: Manganese deposits in the USSR. M., Nauka, 311—324. (in Russ.)
- ROZHN OV, A. A., SEREDA, V. YA., BUZMAKOV, YE. I., KNYAZHEV, S. S., SCHIBRIK, V. I. (1985): Manganese ore base in Central Kazakhstan. — Prospection and mineral resources protection. No. 8, 16—22.
- SPIRIDOV, E. M., SERGEEVA, N. YE., SOKOLOVA, N. F., SHADE, B. (1979): Iron-titanium mineralization of clinopyroxenite-gabbro intrusion of Otaydy-Karasu in Central Kazakhstan. — Geology of ore deposits. No. 1, 23—35. (in Russ.)
- VEIMARN, A. B., KAPSAMUN, V. I. (1981): Famennian volcanism in Central Kazakhstan related to iron-manganese mineralization. In: Volcanic-sedimentary litho- and ore genesis. Alma-Ata, Nauka, 88—96. (in Russ.)
- VEIMARN, A. B., BUZMAKOV, YE. I., ROZHN OV, A. A., SCHIBRIK, V. I. (1986): Famennian iron-manganese epoch in Kazakhstan. — Geology of ore deposits, No. 4. (in Russ.)
- ZAITSEV, YU. A., APOLLONOV, M. K., BABICHEV, YE. A., YERGALIEV, G. KH., ZVONTSOV, V. S., ROZANOV, S. B. (1987): Megastages in generating Kazakhstan-Tien-Shan geosynclinal system. In: Geology and mineral resources of Central Kazakhstan. M., Nauka (in the press). (in Russ.)

*Manuscript received, 15 August, 1986*



## TRACE ELEMENTS IN METAMORPHIC AND GRANITOID ROCKS OF THE BASEMENT IN THE CENTRAL DANUBE—TISZA INTERFLUVE (HUNGARY)

O. TOMSCHEY

Laboratory for Geochemical Research,  
Hungarian Academy of Sciences, Budapest

### ABSTRACT

Trace elements of the metamorphic and granitoid rocks of the Kiskunhalas—Tázlár—Szank—Jászszentlászló region lying in the central part of the Danube—Tisza Interfluve were studied. By means of the trace element diagrams the trace element distribution of different rock types can be compared and the premetamorphic rocks can be identified with satisfactory approximation, as well. In the region in question the gneisses are of pelitic, the amphibolites of basic igneous origin, with high probability. Migmatization and milonitization did not cause considerable changes in the trace element compositions of the rocks. The trace element distribution pattern of granitoids remarkably differs from that of the metamorphic rocks.

Keywords: metamorphic rocks, granitoid rocks, trace element geochemistry, petrogenesis.

### INTRODUCTION

The basement of the central and southern part of the Danube — Tisza Interfluve consists predominantly of non-equilibrium rocks. Tectonically, the Danube — Tisza-Interfluve is dissected by a dislocation line of roughly W—E direction into two parts (JUHÁSZ, 1966). North of this line only a few data are available while the basement of the southern one has been explored by numerous hydrocarbon exploration wells. In this latter region different metamorphites (mica schists, gneiss, granite-gneiss, amphibolite) are found that based on their variegated texture can be grouped, as well (e.g. milonites, phyllonitic milonites, see SZEPESHÁZY, 1966). In the subsequent comprehension of the Hungarian Oil and Gas Trust (JUHÁSZ, 1969) the rock groups of the regions are represented by: a) granite and associated magmatites; b) paleo-volcanites and paleo-subvolcanites; and c) metamorphites. Based on the metamorphic grade and compositional differences, the latter ones can be divided into sub-groups. In this comprehension the trace elements are discussed also according to this classification but no petrogenetic conclusions are drawn. The metamorphites underlying the Cenozoic or Mesozoic formations can be identified as the metamorphites of highest age in the Carpathians (SZEPESHÁZY, 1973).

Based on the mineral paragenetic studies, on the composition zoning and element partition ratios of the rock-forming minerals a three-phase evolution model was established (ÁRKAI *et al.*, 1975, 1977). The metamorphic basement of the Danube — Tisza Interfluve consists of strips of SW-NE direction (SZALAY, 1977a, 1977b) the development of which is related to three tectonometamorphic cycles (in this sense the studied area belongs to the central strip consisting of polymetamorphic gneisses and amphibolites).

Address: H-1112 Budapest, Budaörsi út 45, Hungary

In harmony with the comparative petrological investigations (CSEREPES-MESZÉNA, B., 1980) in the formations of the Danube — Tisza Interfluvium older than Carboniferous two formations can be distinguished: the Kecskemét Formation (the Soltvadkert region belongs to this unit) and the Jászszentlászló Formation (in the area in question the Kiskunhalas — Szank — Jászszentlászló region represents this unit).

Based on up-to-date analytical methods two main groups, i.e. anchimetamorphites and polymetamorphites have been distinguished (ÁRKAI, 1978, 1980, 1981). The trace element analyses of these works were carried out by myself and this will be discussed below having accepted the nomenclature and terminology elaborated so far (ÁRKAI, 1981).

My studies aimed the characterization of the metamorphic and granitoid rocks according to their trace element concentrations as well as the determination of the premetamorphic rocks based on the trace element composition and changes, respectively.

### SAMPLES AND METHODS

119 samples of 70 boreholes of the Kiskunhalas — NE, Tázlár and Szank — Jászszentlászló regions (*Fig. 1*) were studied (including two granite samples from the Soltvadkert area). The determination of the mineral composition as well as the petrographic description were carried out earlier (ÁRKAI, 1978, 1980, 1981).

Trace elements (B, Co, Cr, Ga, Mn, Ni, Pb, Ti, V and Zn) were determined by means of emission spectrography (PGS — 2 type Zeiss spectrograph).

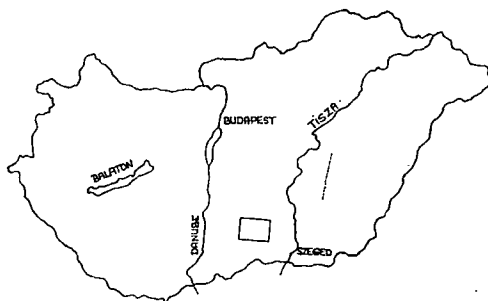


*Fig. 1.* Geographical setting of the studied region

Recording conditions: grate position: 6.22; split: 15 microns; blende: 2; nominal amperage: 7 A; exposition time: 164 s; electrodes: Al 9999; collimator: 10.6; electrode distance: 1 mm; arc source: BIG — 100 AC generator; plates: AGFA GEVAERT 23D56; development: AGFA — L at 20 °C, 5 min.

Evaluation: at least three records were made from each sample. Quantitative evaluation was made based on comparative standards (GM granite and TB clay from the Staatsekretariat für Geologie, Berlin) and on internal standards determined by chemical analyses (AAS). The maximal deviation proved to be  $\pm 15$  percent, the ranges of measurements are given in Table 1.



TABLE 1

## Trace element contents of the rocks of the Kiskunhalas-NE region (ppm)

Rock unit		B	Co	Cr	Ga	Mn	Ni	Pb	Ti	V	Zn
Measurement range (ppm)		5— 500	3— 500	1— 500	3— 500	20— 2500	5— 500	5— 500	50— 7000	5— 500	10— 500
Quartz-phyllite (4)	$\bar{x}$ $s_k$	82 11	42 35	181 123	35 14	158 141	18 8	11 7	4037 1850	46 29	53 40
Carbonate-phyllite (7)	$\bar{x}$ $s_k$	147 87	45 31	172 126	48 31	306 395	97 99	72 79	2925 2018	148 114	122 118
Chloritic muscovite-gneiss (6)	$\bar{x}$ $s_k$	54 22	43 31	134 79	50 22	224 67	91 102	26 22	5765 1030	157 131	134 82
Chloritic muscovite-biotite-gneiss (10)	$\bar{x}$ $s_k$	59 21	34 18	209 86	71 28	346 352	38 43	12 7	6670 480	93 11	74 30
Chloritic muscovite-gneiss (19)	$\bar{x}$ $s_k$	64 21	21 11	208 95	56 21	167 88	18 8	11 7	5170 1980	73 46	60 31

Note:  $s_k$  = denotes the corrected deviation

TABLE 2

## Trace element content of the rocks in the Tázlár region (ppm)

Rock unit		B	Co	Cr	Ga	Mn	Ni	Pb	Ti	V	Zn
Carbonate-phyllite		160	10	295	41	2500	135	36	4300	105	83
Chloritic biotite-gneiss (12)	$\bar{x}$ $s_k$	46 25	28 19	183 68	29 11	1260 1055	67 35	39 23	5500 1950	135 78	102 46
Migmatitic biotite-gneiss (1)		30	16	140	36	320	57	54	6430	65	150
Amphibolite (1)		33	53	295	40	925	98	32	6330	305	155

TABLE 3

## Trace element contents of the rocks from the Szank region (ppm)

Rock unit		B	Co	Cr	Ga	Mn	Ni	Pb	Ti	V	Zn
Muscovite-gneiss (2)	$\bar{x}$	24	18	148	35	453	92	24	4750	235	26
Chlorite biotite-muscovite-gneiss (7)	$\bar{x}$ $s_k$	21 8	26 14	159 85	25 9	591 197	68 56	25 13	5865 2055	300 138	40 27
Biotite-gneiss (22)	$\bar{x}$ $s_k$	19 7	24 18	120 80	29 29	1023 600	80 72	17 11	6180 1208	285 91	54 81
Granite (2)	$\bar{x}$	10	104	59	62	437	15	46	992	39	41
Amphibolite (11)	$\bar{x}$ $s_k$	20 6	57 31	144 99	18 11	1635 430	139 128	10 3	6100 1690	254 110	72 60

TABLE 4

## Trace element contents of the Szank-gneisses taking into account the garnet content and the subsequent effects (ppm)

Rock unit		B	Co	Cr	Ga	Mn	Ni	Pb	Ti	V	Zn
Non-migmatitic biotite-gneiss (12)	$\bar{x}$ $s_k$	21 7	25 23	136 76	24 9	1190 600	80 63	19 12	5960 1400	292 96	65 107
Migmatitic biotite-gneiss (10)	$\bar{x}$ $s_k$	15 4	23 8	102 85	34 31	1025 456	65 88	16 11	6450 930	277 88	40 33
Garnetiferous biotite-gneiss (8)	$\bar{x}$ $s_k$	17 5	38 39	126 55	28 21	1010 400	60 47	20 15	5990 2400	315 130	47 24
Milonitized biotite-gneiss (8)	$\bar{x}$ $s_k$	23 10	18 13	135 89	100 78	760 365	82 62	15 8	4925 1875	234 97	22 13
Migmatitized biotite—, muscovite- and muscovite-biotite-gneiss (16)	$\bar{x}$ $s_k$	18 8	24 11	113 77	32 34	870 420	73 72	21 12	6090 1485	264 89	37 29

TABLE 5

## Trace element contents of the rocks from the Soltvadkert—Jászszentlászló region (ppm)

Rock unit		B	Co	Cr	Ga	Mn	Ni	Pb	Ti	V	Zn
Soltvadkert granite (2)	$\bar{x}$	21	97	102	36	191	24	29	5950	86	14
Jászszentlászló-granite (7)	$\bar{x}$ $s_k$	13 2	97 76	54 46	52 6	222 149	26 24	48 13	2580 1795	82 41	55 27
Migmatitic biotite-gneiss (1)		15	30	168	25	890	110	11	5300	365	18
Biotite-gneiss (1)		17	22	138	30	915	30	20	4000	200	70
Amphibolite (2)	$\bar{x}$	12	78	253	20	2220	390	8	5900	310	170



## RESULTS

The trace element concentrations of 46 samples from 18 boreholes of the Kiskunhalas — NE region are found in Table 1, those of 15 samples from 12 boreholes of the Tázlár region in Table 2, those of 44 samples from 27 boreholes of the Szank region in Tables 3 and 4, finally the trace element data of 13 samples from the Soltvadkert — Jászszentlászló region are demonstrated in Table 5.

Formations of lowest metamorphic grade are represented by quartz-phyllites (Kiskunhalas) and by carbonate phyllites (Kiskunhalas and Tázlár). Based on their trace element contents the (carbonatic) quartz-phyllites considerably differ from the carbonate phyllites their trace element concentrations being much lower. The carbonate phyllites of the two regions are similar and based on their trace element contents may represent the same rock type.

Muscovite gneisses are found essentially in the Kiskunhalas region, the Szank samples (2 pieces) are somewhat more abundant in trace elements (e.g. Mn, Ni, Pb and V) only their Zn concentrations are lower than that of the Kiskunhalas samples. Due to the rather high concentration differences the formations of the two regions cannot be regarded to be the same. Nevertheless, in harmony with the fact that the formations of the Szank region are usually always of higher trace element amounts, these will be discussed together.

Among the biotite-gneiss samples of the three regions the V, Zn and Mn values show the highest dispersion. In spite of this and based on the similarities in their mineral composition these rocks will be dealt with as one unit.

No amphibolites are found in the Kiskunhalas region, in the Tázlár area only one borehole revealed amphibolite. The amphibolites of Szank and Jászszentlászló are rather similar, except their Zn-contents. The Tázlár samples show higher Ga and Pb contents as compared with the two other regions. By all means, the amphibolites of the three regions are more or less similar, disregarding some smaller differences.

Granites are found only in the Szank and Jászszentlászló areas lying north-northeast of the Kiskunhalas and Tázlár regions. The granites of the two regions are conspicuously similar.

### *Premetamorphic rocks*

Based on petrological-geochemical data efforts were made to determine the characteristics of the premetamorphic rocks (ÁRKAI, 1978, 1980, 1981). Due to the small number of samples, in each region the premetamorphic starting rocks were only probalitized, except amphibolites the major part of which proved to be of mafic igneous origin.

It can be stated that, in spite of the smaller deviations or differences, the individual rock types can be considered to be the same rock type affected by local alterations. In this sense I try to reconstruct the premetamorphic rocks on the basis of their trace element contents.

The different gneiss varieties derive with high probability from sedimentary, first of all from pelitic rocks. In Fig. 2 the trace element composition of the biotite-gneisses and muscovite-biotite-gneisses are compared with the mean values of the clayey and basic igneous rocks (TUREKIAN and WEDEPOHL, 1961). Except the values of Co and Ga the trace element concentrations are close to the clayey composition. The Co-content showing sometimes anomalously high values may be due to granitization (the Co concentrations of granites are very high as compared to the granitic



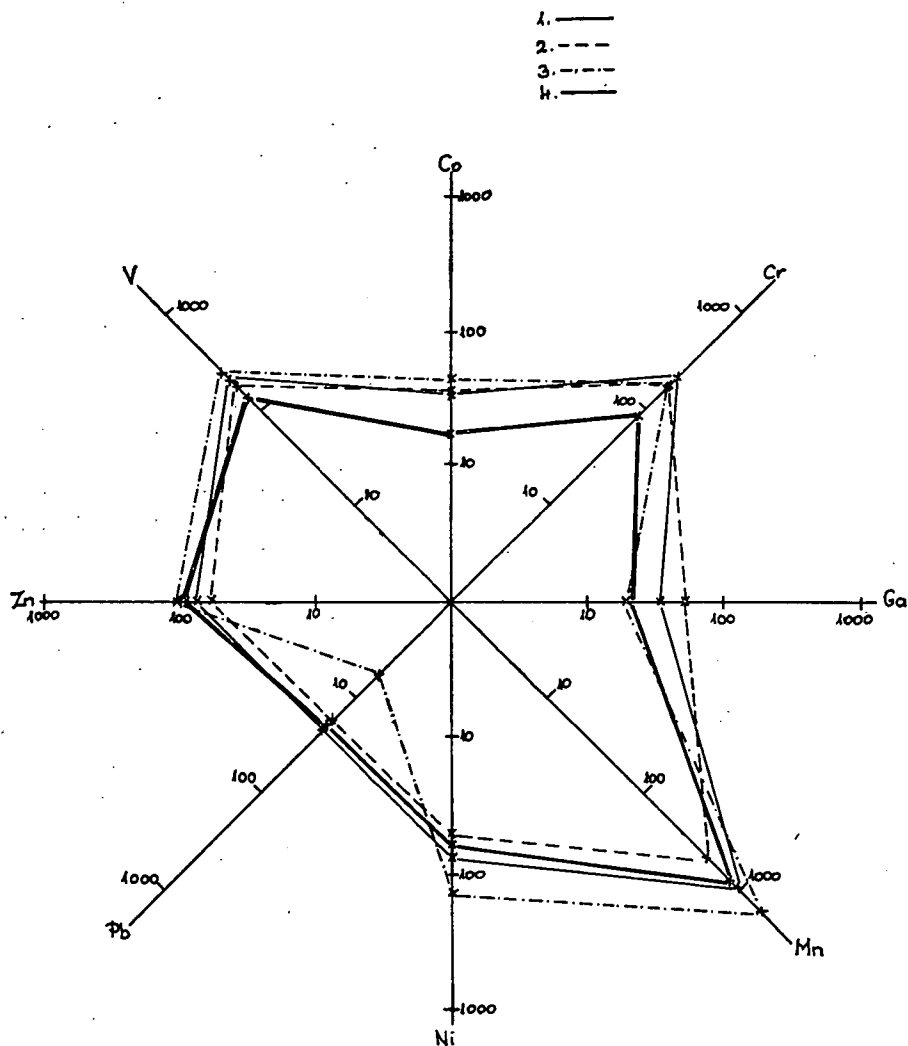


Fig. 2. Trace element composition of biotite-gneisses (1), muscovite-biotite-gneisses (2) as compared to the basic igneous average (3) and clayey average (4) of TUREKIAN and WEDEPOHL (1961)

average). The rocks are characterized always by higher Ga contents than usual, thus when deciding the origin of the rocks the Ga-values were neglected.

□ In case of the Szank—Jászszentlászló—Soltvadkert region the trace elements of the biotite-gneiss group and of granites are demonstrated (Fig. 3) and the average values of TUREKIAN and WEDEPOHL (1961) are also shown. There is no significant difference between the non-migmatitic and migmatitic biotite-gneisses, thus migmatitization itself did not cause remarkable change in the trace element concentrations. The process of granitization conspicuously increased the Co, Ga and Pb, and decreased the Mn, Ni and V concentrations. The Cr and Zn value do not show changes. In harmony with these data, the clayey origin comes to the lamelight again.

Several methods are available to determine the origin of amphibolites, though not all of them proved to be suitable in case of amphibolites of the region in question. E.g. the ' diagrams constructed after VAN DE CAMP (1969) and based on the Ni-mg and Cr-mg values of BURRI and NIGGLI (1945), referring to the origin of eruptive basic rocks, proved to be unsuitable to determine the premetamorphic rocks.

In the V-Cr discrimination diagram constructed after SCHWEDER (1968) the average values computed for all amphibolites are located unambiguously in the ortho-field, close to the zone of migmatitic amphibolites but outside the sedimentary range

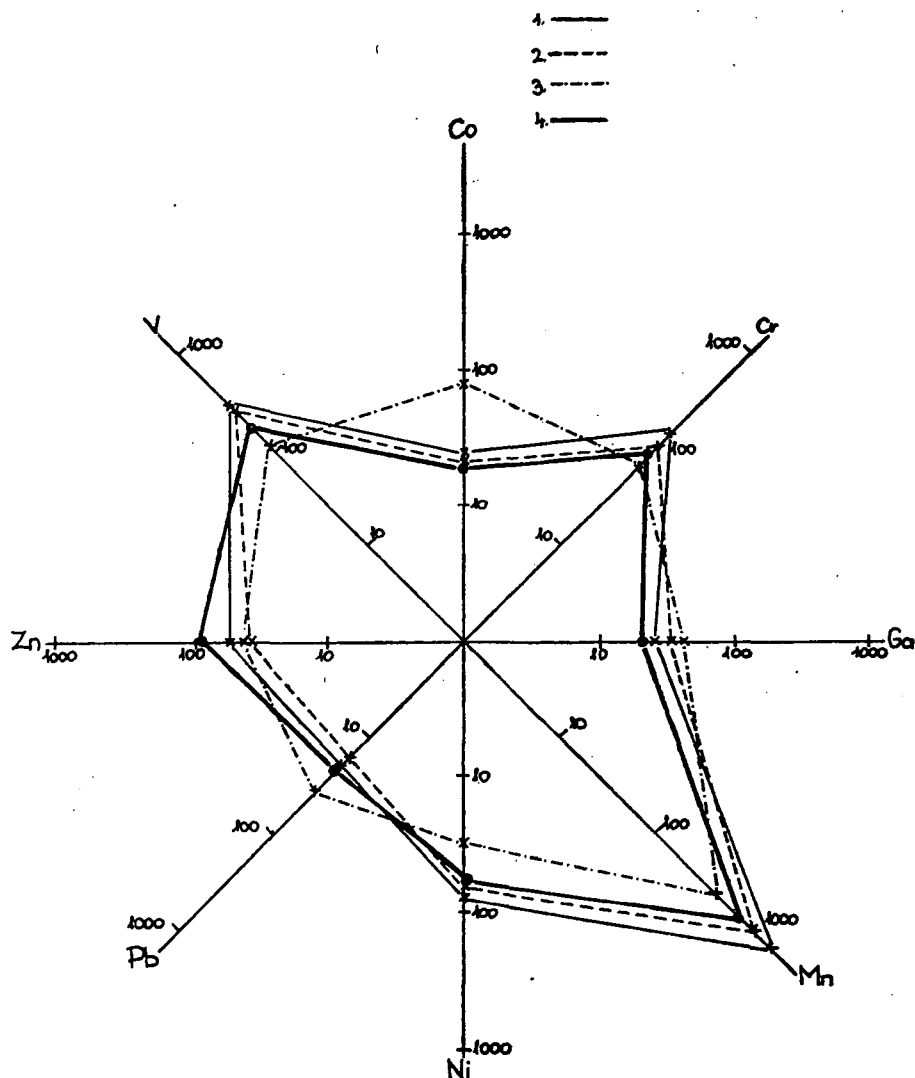


Fig. 3. Trace elements of non-migmatitized biotite-gneisses (1), migmatitized biotite-gneisses (2), granites (3) and the clayey average (4) of TUREKIAN and WEDEPOHL (1961)

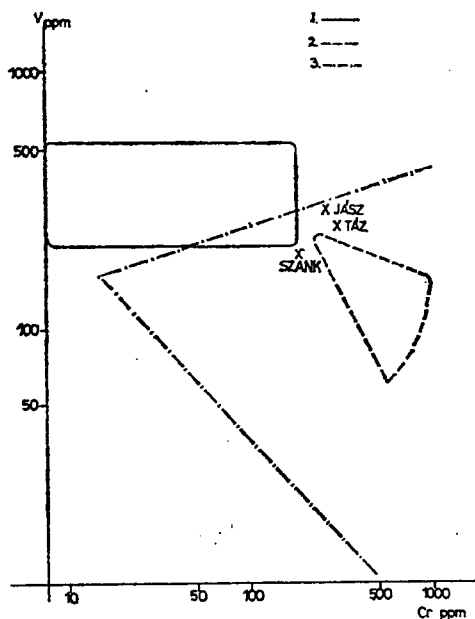


Fig. 4. Average values of amphibolites in the V-Cr discrimination diagram of SCHWEDER (1968), 1 — para-/sedimentary/amphibolites, 2 — migmatitic amphibolites, 3 — ortho-/basic igneous/-amphibolite.

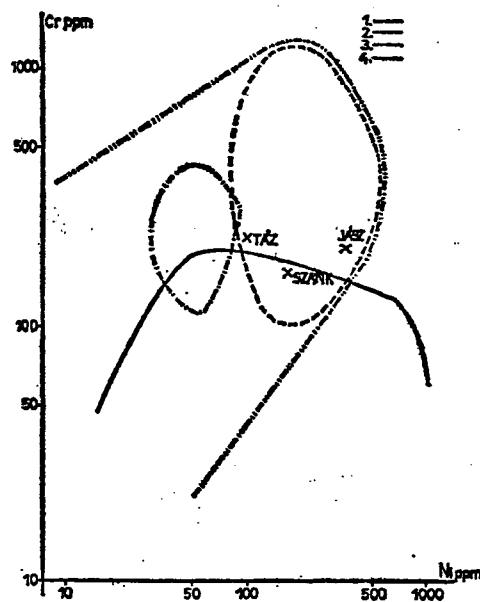


Fig. 5. Average values of amphibolites in the Cr-Ni discrimination diagram of WALKER *et al.* (1960). 1 — clays, 2 — ortho-/basic igneous/-amphibolites, 3 — para-/sedimentary/-amphibolites, 4 — migmatitic amphibolites

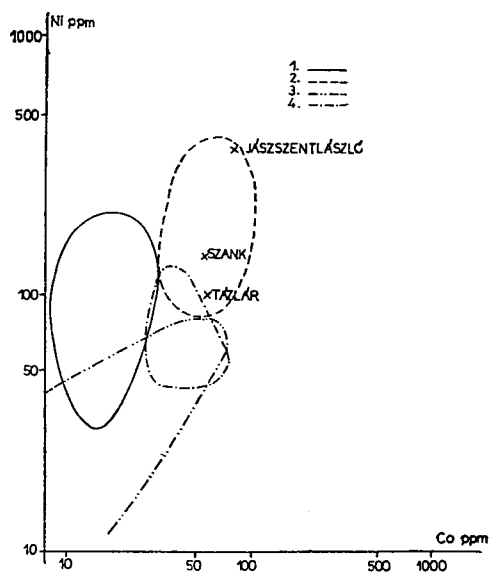


Fig. 6. Average values of amphibolites in the Ni-Co discrimination diagram of WALKER *et al.*, (1960). 1 — clays, 2 — ortho-/basic igneous/-amphibolites, 3 — para-/sedimentary/-amphibolites, 4 — migmatitic amphibolites

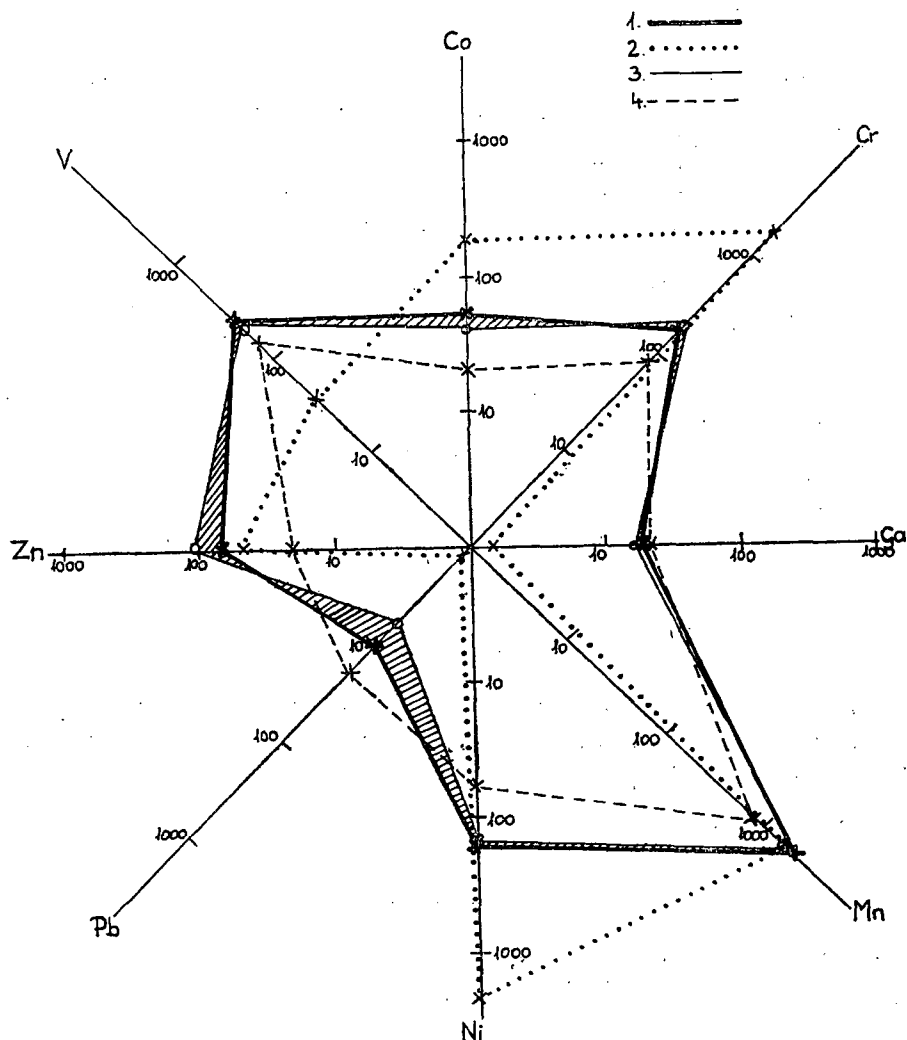


Fig. 7. Average trace element composition of amphibolites from the Szank—Jászszentlászló—Soltvadkert region (1) as compared to the average values of ultrabasic rocks (2), basic igneous rocks (3) and clays (4) of TUREKIAN and WEDEPOHL (1961).

(Fig. 4). In the Cr-Ni discrimination diagram (Fig. 5) constructed after WALKER *et al.*, (1960) there is some uncertainty due to the overlapping of the sedimentary field, but according to the Ni-Co discrimination diagram (Fig. 6) the amphibolites fall to the ortho-field, i.e. are of igneous origin.

In Fig. 7 the trace element concentrations of amphibolites of the Szank—Jászszentlászló region are demonstrated for the ultrabasic, basic igneous and clayey sedimentary rocks in addition to the average values given by TUREKIAN and WEDEPOHL (1961). The ultrabasic origin can be fairly well excluded and except the Ga-values none of the elementary concentrations refer to clayey origin, i.e. the distribution of the total trace element contents indicates basic igneous origin.

## CONCLUSIONS

Based on the trace element investigations carried out in the Kiskunhalas—Tázlár—Szank—Jászszentlászló—Soltvadkert region, concerning the metamorphic and granitoid rocks it can be stated that

- the applied trace element discrimination diagrams are suitable to compare the trace element contents of different rock types on the one hand, and are suitable to identify with good approximation the premetamorphic rocks, on the other;
- the different gneiss types of the region are most probably of sedimentary, i.e. of pelitic origin;
- the amphibolites are of igneous (basic igneous) origin, this statement reinforcing the previous conclusions;
- migmatitization in itself did not cause considerable change in the trace element contents of the rocks;
- milonitization is represented by textural and/or mineral compositional alterations, the trace element distribution pattern shows no remarkable change due to this effect;
- granitization concentrated certain elements (e.g. Co) independently of the type of the granitization process.

## ACKNOWLEDGEMENTS

I am highly indebted to the leading authorities of the National Oil and Gas Trust for permitting the publication of the results and for making possible to analyze the samples, further to DR. PÉTER ÁRKAI, senior researcher of the Laboratory for Geochemical Research of the Hungarian Academy of Sciences, for his valuable assistance and consultations.

## REFERENCES

- ÁRKAI, P., NAGY, G. and PANTÓ, GY. (1975): Types of composition zoning in the garnets of polymetamorphic rocks and their genetic significance. — *Acta Geol. Acad. Sci. Hung.*, **19**, 17—42.
- ÁRKAI, P. (1978): Report "On the mineralogical-petrological investigations of the igneous and metamorphic formations of the Kiskunhalas — NE region older than Mesozoic". OKGT-Library, manuscript (in Hungarian).
- ÁRKAI, P. (1980): Report "On the mineralogical-petrological and geochemical investigation of the igneous and metamorphic rocks of the Tázlár region older than Mesozoic". OKGT-Library, manuscript (in Hungarian).
- ÁRKAI, P. (1981): Report "On the investigation results of metamorphites revealed by the boreholes of Szank, Soltvadkert, Jászszentlászló and Álmosd". OKGT-Library, manuscript (in Hungarian).
- BURRI, C. and P. NIGGLI (1945): *Die jungen Eruptivgesteine des mediterranen Orogens*. I. Schweizer Spiegel Verl. Zürich.
- CSEREPES-MESZÉNA, B. (1981): Migmatite zones in the basement of the Danube—Tisza Interfluve. — *Proc. of the 12th Congress of the CBGA, Bucharest*.
- FÖLDVÁRI-VOGL, M. (1978): *Theory and Practice of Regional Geochemical Exploration*. Akad. Kiadó, Budapest.
- GHONEIM, M. A. and SZEDERKÉNYI, T. (1977): Preliminary petrological and geochemical studies of the Ófalu area, Mecsek Mountains, Hungary. — *Acta Miner. Petr. Univ. Szeged*. **XXIII**, 1. 29—39.
- JUHÁSZ, Á. (1966): Formations older than Tertiary in the Szank environment. — *Földt. Közl.* **96**, 3. 427—435. (in Hungarian).

- JUHÁSZ, Á. (1969): Igneous and metamorphic formations of the Danube—Tisza Interfluve. — *Földt. Közl.*, **99**, 4, 320—336. (in Hungarian).
- LEAKE, B. E. (1964): The chemical distinction between ortho- and para-amphibolites. — *J. Petr.*, **5**, 238—253.
- SCHWEDER, P. (1968): Geochemische Untersuchungen im Kiffhauser — kristallin. — *Chemie der Erde* **27**, 1.
- SZÁDECZKY-KARDOSS, E. (1955): Geochemistry. Akad. Kiadó, Budapest (in Hungarian).
- SZALAY, Á. (1977): Metamorphic-granitogenic rocks of the basement complex of the Great Hungarian Plain, Eastern Hungary. — *Acta Miner. Petr. Univ. Szeged*, **23**, 49—69.
- SZALAY, Á. (1977): Igneous and metamorphic formations of the basement of the Great Plain. OGIL-report, Szolnok (in Hungarian).
- SZEDERKÉNYI, T. (1983): Origin of amphibolites and metavolcanics of crystalline complexes of South Transdanubia, Hungary. — *Acta Geol. Acad. Sci. Hung.*, **26**, 1—2, 103—136.
- SZEPESHÁZY, K. (1969): Main rock types of the crystalline basement in the central and southern part of the Danube—Tisza Interfluve. — *MÁFI Évi Jel.* 257—289. (in Hungarian).
- TUREKIAN, K. K. and WEDEPOHL, K. H. (1961): Distribution of the elements in some major units of the Earth's crust. — *Bull. Soc. Geol. Amer.*, **72**, 175—191.
- TUREKIAN, K. K. and WEDEPOHL, K. H. (1969): Distribution of the elements in some major units of the Earth's crust. — *Geol. Soc. Amer. Bull.*, **80**, 641—664.
- VINOGRADOV, A. P. (1962): Average occurrences of chemical elements in the main magmatic rock formations of the Earth's crust. — *Geokhimiya*, 1962. 555—572 (in Russian).
- WALKER, K. R. and G. A. JOPLIN (1960): Metamorphic and metasomatic convergence of basic igneous rocks and lime-magnesia sediments of the Precambrian of North-Western Queensland. — *J. Geol. Soc. Austr.*, **6**, No. 2.
- WEDEPOHL, K. H. (1971): Chemical composition of shales and clays. — *Physics and Chemistry of the Earth*. Pergamon Press **8**, 304—305.

*Manuscript received. 22 February, 1986*





## INFRARED VIBRATIONAL SULPHATE BAND SHIFT CORRELATION IN ALKALINE SULPHATE MINERALS

L. A. GUIRGUIS

Nuclear Materials Corporation, Cairo, Egypt

### ABSTRACT

Infrared spectra of anhydrite, celestine and barite minerals had been measured in the range 4000—400  $\text{cm}^{-1}$  and discussed.

The shift of the  $\text{SO}_4^{2-}$  stretching modes to lower frequency on passing from anhydrite to barite minerals could be explained by the difference in the ionization potential of the cation.

### INTRODUCTION

The absorption spectra of several sulphate minerals has been shown by WACHTER and LYON (1970). From a fundamental approach Ross (1972) has presented assignments of sulphate vibrations in anhydrous, hydrated, and hydroxyl containing sulphate minerals. Low frequency lattice vibrations for several sulphate minerals have been studied by MORANDAT *et al.*, (1966).

Differences of opinion exist between various authors dealing with the structural factors which influence molecular vibrations in sulphate minerals. Thus, ADLER and KERR (1965) have discussed the spectra of anhydrous sulphates  $\text{MSO}_4$  ( $\text{M} = \text{Sr, Ba, Pb}$ ) and band shifts of the stretching modes toward lower frequencies with increasing cation mass. On the contrary, the frequency shift of  $\text{SO}_4^{2-}$  stretching modes in a homologous hafnium and zirconium sulphate tetrahydrates is evidently caused by a slight change in ionic radius produced by cation substitution (ADLER, 1965). Lately POVARENENYKH (1978) summarized in a formula the main factors which affect the position of fundamental and characteristic absorption bands in IR spectra of minerals. These factors are as follows: valencies of cation and anion, coordination number of cation, interatomic distance cation—anion, the reduced mass of cation and the coefficient of relative bond strength.

The present work aims to correlate the value of the shift in absorption frequency observed in structurally related alkaline-earth minerals having a common functional ionic molecule.

### MATERIALS AND METHOD

Three alkaline-earth sulphate minerals are collected from El Baharia area at the Western Desert of Egypt. These samples are anhydrite ( $\text{CaSO}_4$ ), barite ( $\text{BaSO}_4$ ), and celestine ( $\text{SrSO}_4$ ), and denoted in this work by the letters A, B and C, respectively.

Each sample is prepared for infrared analysis using the pressed potassium bromide disc technique (FARMER, 1974). A known amount (2 mg) of the mineral was

carefully ground and mixed with 198 mg of spectroscopically pure dry potassium bromide for 10 sec in a vibrator, and this mixture pressed so as to give a disc of 12 mm diameter and about 0.2 mm thickness. The obtained KBr pellets were dried for four hours at 110 °C.

All spectra have been registered between 4000—400  $\text{cm}^{-1}$  with a Perkin-Elmer 398 double-beam spectrophotometer. The maximum of absorption bands were reproducible within  $\pm 0.5 \text{ cm}^{-1}$ .

## RESULTS AND DISCUSSION

IR spectra of the studied samples are shown in *Fig. 1*. The spectra are remarkably alike and appear to contain no anomalies except for small differences in the position of the absorption frequency.

In the spectrum of celestine, the strong frequencies at 1110, 1150 and 1200  $\text{cm}^{-1}$  are due to triply asymmetric S-O stretching mode  $\nu_3$  in ionic sulphates while  $\nu_1$  occurs as a small ridge at 1015  $\text{cm}^{-1}$ . Corresponding mode of barite are at 1100 1130 and 1190  $\text{cm}^{-1}$ , respectively. Also its  $\nu_1$  occurs as a small ridge at 1020  $\text{cm}^{-1}$ . The non degenerate S-O-S bending mode  $\nu_4$  occurs at 650 and 620  $\text{cm}^{-1}$  in the spectrum of celestine. Corresponding value for barite occurs at 670 and 610  $\text{cm}^{-1}$ .

The splitting of the fundamental sulphate stretching mode  $\nu_3$  in both the spectra of celestine and barite arises from the partial resolution of its triply degenerate vibrations of this mode, normally have exactly the same frequency when the  $\text{SO}_4^{2-}$  molecule is perfectly tetrahedron. However, they assume different frequencies if the molecular symmetry is lowered in conforming to the symmetry of the site. According to the relationships between molecular symmetry, site symmetry and vibrational activity of the sulphate ion, the three  $\nu_3$  bands and single  $\nu_1$  band for celestine and barite are indicative of  $C_{3v}$  or lower symmetry of the sulphate ion (ADLER, 1965).

In the spectrum of calcium sulphate (anhydrite) the bands due to ionic stretching vibrations  $\nu_3$  and its bending mode  $\nu_2$  and  $\nu_4$  differ in shape and/or position from that of celestine and barite. Thus the strong absorption band between 1120 and 1210  $\text{cm}^{-1}$  are due to S-O stretching mode  $\nu_3$  in ionic sulphates, this band shows tendency of splitting to its three components at 1120, 1170 and 1210  $\text{cm}^{-1}$ . The  $\nu_1$  mode occurs as small ridge at 1030  $\text{cm}^{-1}$ . The O-S-O bending mode  $\nu_4$  occurs as a medium well defined peak at 670  $\text{cm}^{-1}$  while  $\nu_2$  bending mode splits into two components at 610 and 559  $\text{cm}^{-1}$ .

In going from one mineral to the other, there is a shift of 20  $\text{cm}^{-1}$  between the  $\nu_3$   $\text{SO}_4^{2-}$  stretching and from 20 to 10  $\text{cm}^{-1}$  in the  $\nu_4$   $\text{SO}_4^{2-}$  bending vibration. The following discussion is made in hopes of clarifying this problem.

All the studied sulphate minerals crystallise in the orthorhombic system. The space group for anhydrite is *Amma*, while that for barite and celestine is *Pnma*. Anhydrite got an anhydrite structure while celestine and barite got a barite structure. For anhydrite the *a*, *b* and *c* are 6.991, 6.996, 6.238 Å, while those for barite are 8.878, 5.450 7.152 Å, respectively, and for celestine 8.359, 5.352, 6.866 Å (DEER *et al.*, 1962).

It was found by VELDE and MARTINEZ (1981) that an increase in cell dimensions decreases the frequency vibrations of the Mg-OH vibrations in kaolinite. The value is about 7  $\text{cm}^{-1}$  per 0.01 Å change in cell dimensions. However, in the present case there is no clear relation between the unit cell dimensions and the frequency shift.

Also, the shift to lower frequency observed for both  $\nu_3$  and  $\nu_4$  of the  $\text{SO}_4^{2-}$  ion on passing from anhydrite to barite minerals could not be explained by the difference

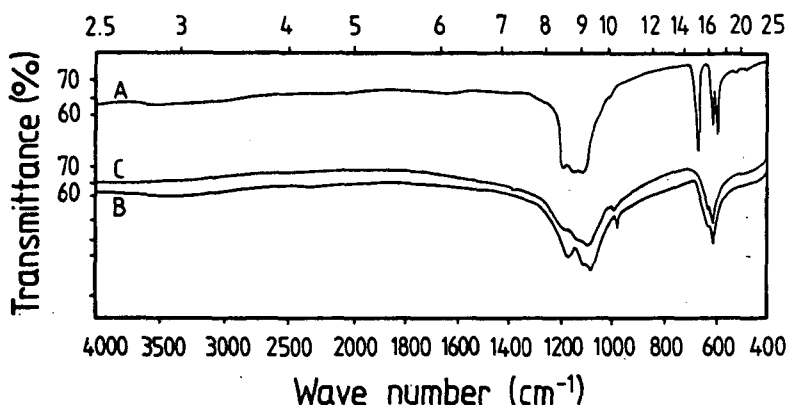


Fig. 1. Infrared absorption spectra of some alkaline earth sulphate minerals: anhydrite (A), barite (B) and celestine (C) in the range of 4000—400  $\text{cm}^{-1}$

in ionic radius (SHANNON and PREWITT, 1969) produced by  $\text{Ca}^{2+}$  (1.12 Å),  $\text{Sr}^{2+}$  (1.4 Å) and  $\text{Ba}^{2+}$  (1.60 Å) cation substitution, respectively. If the ionic radius of the cation were effective in producing a change in the frequency of the  $\text{SO}_4^{4-}$  vibration, the  $\nu_3$  and  $\nu_4$  mode would occur at higher rather than lower frequencies (ADLER, 1965).

The polarizing power of a cation is proportional to the ratio of its charge divided by its radius, and the charge of all the studied cations is +2 and their ionic radius appear to be a non functional property. Accordingly, the polarising power for Ca, Sr, and Ba is not useful in explaining the bathochromic shift, shown in the frequency, of the  $\text{SO}_4^{4-}$  vibration.

It is repeatedly mentioned in the literature (ADLER and KERR, 1965; FARMER 1974; SHANNON and PREWITT, 1969) that the frequency of valence stretching vibration varies inversely with the atomic mass. However, no evidence of a correlative shift obtained between the atomic weight of  $\text{Ca}^{2+}$  (40.08),  $\text{Sr}^{2+}$  (97.52),  $\text{Ba}^{2+}$  (137.34) and their sulphate frequencies.

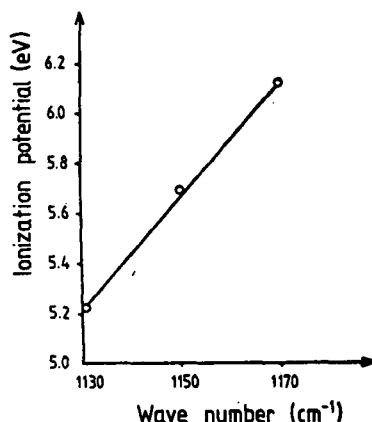


Fig. 2. Correlation of ionization potential and band frequency of  $\text{SO}_4^{2-}$  stretch  $\nu_3$  for anhydrite, barite and celestine

The vibrational frequency is affected also by the force constant which was found to vary directly with electronegativity and inversely with the internuclear distance in some tectosilicates (MILKEY, 1960). The electronegativity values for Ca, Sr, Ba are 1.0, 1.0, and 0.9 respectively, as given by BLOSS (1971). It seems that the effect of the electronegativity change is not valid for the presently studied sulphate band shift.

According to POVARENENYKH (1978) the valency vibrations  $\nu_3$  in minerals shift to higher frequency with decreasing coordination number due to the increase in both atomic distances and quantum-mechanical interaction. The coordination number is 8 for anhydrite, 14 and 12 for celestine and barite (PHILLIPS and GRIFFEN, 1981). Definitely there should be another factor to account for the observed shift between celestine and barite, having the same coordination number.

Correlation of the ionization potential of the element atoms taken from OSLER (1972) appears to best account for the observed shifts shown in the frequency of the  $\text{SO}_4^{2-}$  vibration of the presently studied minerals. A relation which gives a straight line fits between the ionization potential of Ca (6.11), Sr (5.65), Ba (5.21) and the position of the sulphate vibration frequency  $\nu_3$  as shown in Fig. 2.

So the regularities in the frequency variation of this sulphate minerals could be attributed to the change in ionic character of the cation-oxygen bond with increasing covalency of the bonded polyatomic anions ( $\text{SO}_4^{2-}$ ). This will possibly affects the relative bond strength between the adjacent atoms in their structure.

#### REFERENCES

- ADLER, H. H. (1965): Examination of mass radius effects, hydrogen bonding and splitting in infrared spectra of Zr-Hf homologs. *Amer. Miner.*, **50**, 1553—1562.
- ADLER, H. H. and KERR, P. F. (1965): Variation in IR spectra, molecular symmetry and site symmetry of sulphate minerals. *Amer. Miner.*, **50**, 132—147.
- BLOSS, E. D. (1971): Crystallography and crystal chemistry. Rinehart and Winston Inc., 194.
- DEER, W. A., HOWIE, R. A. and ZUSSMAN, J. (1962): An introduction to the rock forming mineral. John Wiley and Sons Inc., 462—472.
- EVANS, R. C. (1952): An introduction to crystal chemistry. Cambridge University Press. 258.
- FARMER, W. C. (1974): The infrared spectra of minerals. Adlard and Son Ltd. Dorking, Surrey. 12—15.
- MILKEY, R. G. (1960): Infrared spectra of some tectosilicates. *Amer. Miner.*, **45**, 990—1007.
- MORANDAT, J., LORENZELLI, V. and PAQUET, H. (1966): Far infrared absorption spectra of some metallic sulphates. *C. R. Acad. Sci., Paris, ser. A, B*, **263 B**, 697.
- OSLER, H. J. and LANGE, H. (1972): Geochemical tables. Elsevier Publ. Co., Amsterdam.
- PHILLIPS, W. R. and GRIFFEN, D. T. (1981): Optical mineralogy of non-opaque minerals. Freeman Co., San Francisco, 90.
- POVARENENYKH, A. S. (1978): The use of infrared spectra for the determination of minerals. *Amer. Miner.*, **63**, 956—959.
- ROSS, S. O. (1972): Inorganic infrared and Raman-spectra. McGraw-Hill, London, 414.
- SHANNON, R. D. and PREWITT, C. D. (1969): Effective ionic radii in oxides and fluorides. *Acta Cryst.*, **925—946**.
- VELDE, B. (1983): Infrared OH-stretch bands in potassic micas, talcs and saponites, influence of electronic configuration and site of charge compensation. *Amer. Miner.*, **68**, 1169.
- VELDE, B. and MARTINEZ, G. (1981): Effect of pressure on OH-stretching frequencies in kaolinite and ordered aluminous serpentine. *Amer. Miner.*, **66**, 196—200.
- WACHTER, B. G. and LYON, R. T. P. (1970): Infrared mineralogical techniques for ore search. Dept. Mineral. Eng. Stanford University, Stanford, California.

*Manuscript received, 14 January, 1986.*

## RARE EARTH ELEMENT CONTENT IN THE SZENTBÉKKÁLA SERIES OF PERIDOTITE INCLUSIONS

Sz. BÉRCZI<sup>1</sup> and J. BÉRCZI<sup>2</sup>

<sup>1</sup> Department of General Technics, Loránd Eötvös University

<sup>2</sup> Nuclear Training Reactor, Technical University of Budapest

### ABSTRACT

The genetic relations of four nonfrequent xenolith inclusion groups (dunite, layered lherzolite, websterite and spinel-pyroxenite) to the hypothetical mantle source spinel-lherzolite (the most frequent inclusion) and to the host alkali basalts have been investigated. The concentrations of rare-earth elements (REE) in the basalts, in the peridotite inclusions and in the mineral separates of spinel-lherzolites and spinel-pyroxenites were determined by instrumental neutron activation analysis. The REE abundance patterns of peridotite inclusions show increasing REE concentrations in the order: dunite, spinel-lherzolite, layered lherzolite, websterite and spinel-pyroxenite. Except spinel-pyroxenite this series of inclusions represents a gradation from depleted (the former two groups) to enriched (the later two groups) remnants of source mantle material. The enrichment of REE in spinel-pyroxenites and alkali basalts are in accord with their 17 percent and 3 percent partial melting from a chondritic mantle source. On the basis of our REE concentration measurements on alkali basalts containing peridotite inclusions (Szigliget, Szentbékálka, Kapolcs) we suggest the introduction of a new group, the peridotite inclusion containing basalt group into Gy. PANTÓ's classification of Hungarian basalts.

### INTRODUCTION

Ultramafic inclusions keep on to be in the centre of interest as they are the carriers of many information about the constitution of upper mantle. They are the most ultramafic representatives of a differentiatinal series of which the varieties of basalts are the most frequent products on the surface of the Earth. From ultramafic mantle rocks to the basalts there are a lot of branching pathways during the differentiation. The stations of these pathways can be found in the form of rare, nonfrequent inclusions which have been enclosed and conveyed in small xenolithic ammounts mainly by alkali basalts penetrating the upper mantle and crust. With our measurements we intended to sketch some steps of processes which had formed the upper mantle and lower crust under the NW Balaton region and which can be deciphered from the xenolith inclusions after their arrangement along a hypothetical evolutionary chain.

Two previous works must be referred here. The olivine dominated inclusions of Hungarian alkali basalts were investigated comprehensively for the first time by EMBEY-ISZTIN, A. (1976), who identified their xenolithic nature, showed their mineral composition to have been a four phase spinel-lherzolitic one and proved their upper mantle origin. The other work is that of PANTÓ's one (1981), who has measured by

<sup>1</sup> H-1088 Budapest, Rákóczi út 5, Hungary

mass-spectrometric method the REE abundances of different Hungarian volcanic rocks from the Cenozoic era. Among his measurements some results about the REE pattern of some basalts from this NW Balaton region occurred, although no those one which contain lherzolite xenoliths.

The major purpose of the present paper is to report concentrations for rare earth elements in selected (frequent and mainly monofrequent) ultramafic inclusions, in their separated constituent minerals and in the host basalts, and to discuss briefly the genetic implications of these data. The REE determinations presented here were all made by instrumental neutron activation analysis (INAA) in the reactor of Budapest Technical University and the reactor of the Central Physical Institute of the Hungarian Academy of Sciences; the electron microsonda analyses were carried out on the JXA—50A type instrument of Department of Petrology and Geochemistry, Eötvös Loránd University.

### SAMPLES

The source region of our samples is situated in a triangle bordered by the Balaton Lake from SE, by the Bakony Mountains from NE and by the Little Hungarian Plain from west (*Fig. 1*). The NW Balaton basalt occurrences consist of tuff and lava type flecks (some kilometers in diameter) of alkali basalts forming an arc of a half-ring around the southern Little Plain. The rocks of this half-ring frequently contain

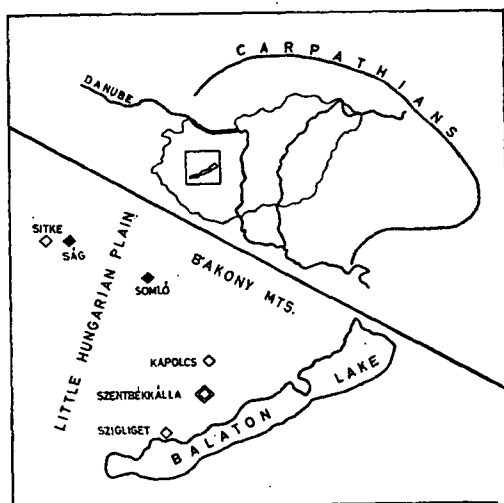


*Fig. 1.* Location of the NW Balaton region in Hungary, where the peridotite inclusions and host basalts were collected. (◇ — source of samples, ◆ — source of greatest part of samples, ♦ — sources of samples from literature (see GY. PANTÓ, 1981/))

lherzolite inclusions as xenoliths in the rocks from other parts of the arc. The detailed petrological description of the occurrences has been given by EMBEY-ISZTIN, A. (1976).

The list of Table 1 shows the rock types investigated and the measurements carried out on them. The series of nonfrequent ultramafic inclusions in from Szentbékáll,

The list of rock and xenolith types investigated and the measurements carried out on them

TABLE 1

Name of rock	REE (INAA)	REE (INAA) on separated minerals	Electron microsonda analyses
Basalt (Szentbékállá) (Kapolcs)	+		cpx-megacryst
(Szigliget)	+		
Lherzolite (Szentbékállá) (Kapolcs) (Szigliget) (Sitke)	+ + + +		
THE SZENTBÉKKÁLLA SERIES			
Spinel-pyroxenite	+	+	+
Wehrlite	+		+
Layered lherzolite	+		
Average lherzolite		+	
Dunite	+		
Progran lherzolite		+	+

the most rich source region. Sample pairs of lherzolite and host basalt are from Szentbékállá, Szigliget and Kapolcs, and only lherzolite sample is from Sitke. There are clinopyroxene megacrystals from Szentbékállá and Kapolcs.

#### REE ABUNDANCES IN ROCKS

The results of our neutron activation analyses are given in Table 2 for basalts and lherzolites, in Table 3 for the Szentbékállá series of nonfrequent peridotite inclusions.

#### Alkali basalts

The total REE content is given by an estimation of  $\frac{3}{2}$  times the sum of measured.

lanthanide content, because we have results from about  $\frac{3}{2}$  rd of all lanthanides only.

This estimated total REE content varies within a limited range between 240—340 ppm as compared to the 220—880 ppm (PANTÓ, GY., 1981) range of Hungarian basalts characteristic to the Southern Bakony and Balaton Highland group and the Mt. Ság in the Little Plain group in PANTÓ's classification. The chondrite normalized REE patterns of our three xenolith containing basalts are very similar to each other. (Fig. 2.) They exhibit a marked enrichment of light REE (LREE) and a moderate enrichment of heavy REE (HREE). The La/Lu ratio which roughly express the gradient of the slope is relatively high and varies between 160—220. These La/Lu ratio values are characteristic to the Little Plain group (PANTÓ, GY., 1981).

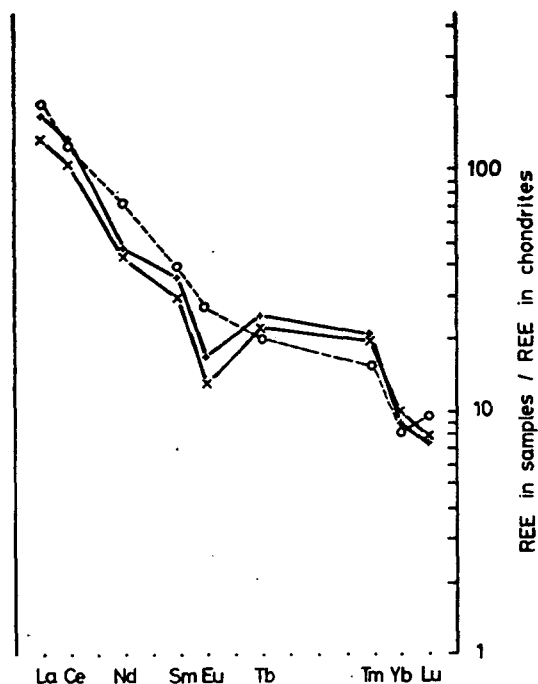


Fig. 2. Chondrite normalized REE abundances in three basalt samples (○—Szigliget, +—Kaposcs, ×—Szentbékállá)

TABLE 2  
REE content of rocks basalts and lherzolite inclusions (data in ppm)

	Basalts			Lherzolites				Average of 20 chondrites
	Szigliget	Kaposcs	Szentbékállá	Sitke	Szigliget	Kaposcs	Szentbékállá	
La	56.6	50.9	39.7	0.6	0.4	1.4	1.2	0.30
Ce	107.0	110.8	87.8	3.1	1.5	4.0	2.7	0.84
Nd	42.0	25.6	25.4	1.2	0.5	1.3	<2.0	0.58
Sm	8.32	7.40	6.20	0.08	0.30	0.09	0.23	0.21
Eu	1.99	1.22	0.96	0.02	0.08	0.02	0.04	0.074
Tb	1.0	1.20	1.10	0.2	0.1	0.07	0.06	0.049
Tm	0.5	0.68	0.65	0.1	0.05	0.04	0.03	0.033
Yb	1.5	1.5	1.69	—	0.14	—	<0.5	0.17
Lu	0.30	0.24	0.24	0.05	0.06	0.05	<0.02	0.031
(Cr)	620						3200	
$\Sigma$ La-Lu	219.2	199.5	163.7	5.4	3.1	7.0	<6.0	2.3
$\frac{3}{2}\Sigma$ La-Lu	328.8	299.3	245.6	8.0	4.7	10.5	<9.0	3.4
La/Lu	188.6	212.1	165.4					

Rare-earth element concentration was a good criteria to distinguish basalt groups. PANTÓ has performed this classification, and he has found that the REE patterns of rocks from a geographical region are similar to each other, therefore his groups were named after geographical regions. The locations of our basalt samples



REE content of the series of inclusions from Szentbékállá (data in ppm)

TABLE 3

REE	Spinel-pyroxenite	Wehrlite	Layered lherzolite	Dunite
La	5.1	6.6	0.6	0.5
Ce	9.4	14.9	1.5	1.8
Nd	8.7	13.6	1.8	<0.5
Sm	2.76	3.25	0.56	0.08
Eu	0.81	1.17	0.19	0.03
Tb	0.45	1.0	0.14	0.04
Tm	0.2	0.5	0.06	0.02
Yb	0.9	1.5	0.2	<0.5
Lu	0.16	0.38	0.07	<0.02
(Cr)	50	9400	4400	1100
$\Sigma$ La-Lu	28.5	42.9	5.1	<3.5
$3/2 \Sigma$ La-Lu	42.7	64.4	7.6	<5.2

are near to his type-rocks, but do not match exactly with them. Although the place of occurrence of our three basalt samples fall onto his Southern Bakony Mountains and Balaton Highlands group's region (Szentbékállá, Szigliget, Kapolcs), the REE abundance patterns of our samples (that of xenolith-containing basalts) show closer relation to the patterns of samples from the Little Plain group: Mt. Ság and Mt. Somló, on the basis of their steeper slopes with decreasing enrichment in LREE and marked Eu anomaly (except Szigliget). This contradiction forced us to suggest a completion of PANTÓ's classification with a transient new group of xenolith-containing basalts determined only on the basis of REE abundance pattern. This transient group should consist of those alkali basalts (and tuffs), which has

- total REE content similar to that of rocks from the Southern Bakony and Balaton Highlands group,
- La/Lu ratio similar to that of the basalts from the Little Plain group,
- inclusion content from the upper mantle (lherzolite xenolith inclusions).

#### Lherzolites

The total REE content of lherzolites is very low. The  $\frac{3}{2}$  times sum of La-Lu values varies between 4,7 and 10,5 ppm which range falls between the 1,5 to 3 times of chondritic sum. These low values are in accord with the petrological results (EMBEY-ISZTIN, A., 1975) on their upper mantle origin. The chondrite normalized REE patterns of samples from the four source regions are scattering in a range shown on Fig. 3 and show considerable fluctuations. The patterns are characterized by marked Eu and sometimes Sm negative anomaly.

#### The Szentbékállá series

There were five selected rare inclusions which had REE abundances transitional from lherzolitic to basaltic values. One of them which were named as Progran — because of its protogranular texture according to the classification of MERCIER and NICOLAS (1975) — has not been measured for REE content as a whole sample, but only in separated minerals. (In order to get real average from the mixture of component minerals we should have needed a greater piece of this xenolith, which has large mineral grains.) The four xenolith inclusions are: a dunite, a layered lherzolite, a

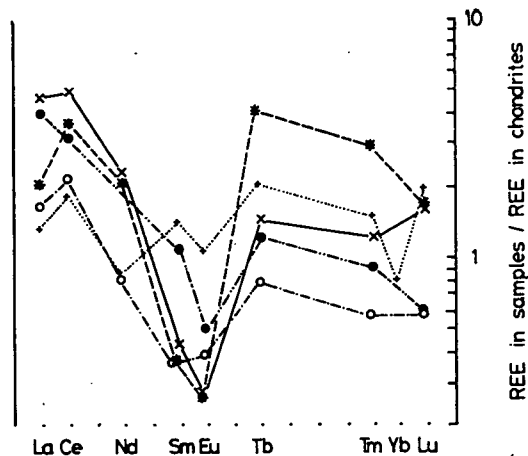


Fig. 3. Chondrite normalized REE abundances in Hungarian lherzolite xenolites, (x — Kapolcs, ● — Szentbékálla /equigranular/, \* — Sitke, ○ — Szentbékálla /dunite/, + — Szigliget).

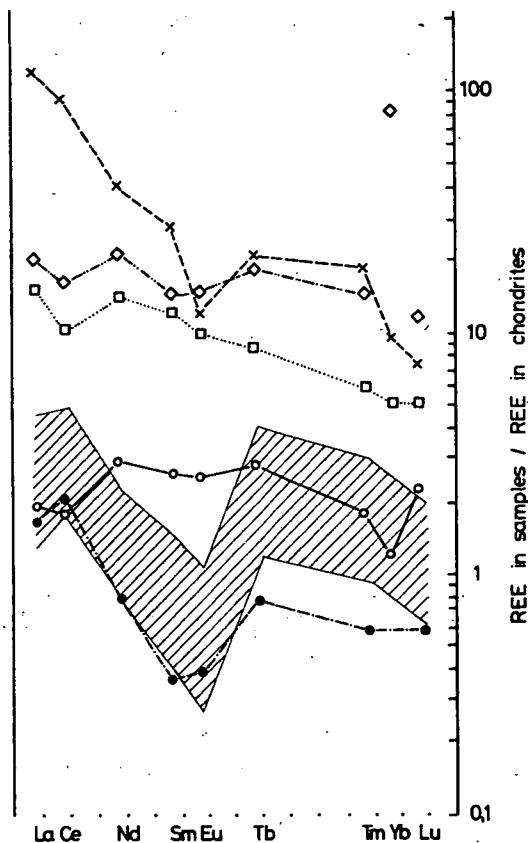


Fig. 4. Chondrite normalized REE abundances in the peridotite inclusions of the Szentbékálla series and compared to the lherzolitic range, (x — Basalt, ◇ — Wehrlite, □ — Spinel-pyroxenite, ● — Dunite, ○ — Layered lherzolite).

wehrlite and a spinel-pyroxenite. Their chondrite normalized REE patterns are given on Fig. 4 and ordered according to their increasing REE content. (The REE abundances are listed in Table 3) They represent different evolutionary stages of parental rocks and melts as will be discussed later.

# REE ABUNDANCES OF MINERAL SEPARATES OF THE PERIDOTITE INCLUSIONS OF THE SZENTBÉKKÁLLA SERIES

The four mineral phases of average lherzolite and three of the Progran sample (lacking the fourth phase in measurable amount) were separated by handpicking, the two phases of spinel-pyroxenites were separated by magnetic separator. Optical and X-ray diffractonal identification also belonged to the sample preparations. The REE content of mineral separates of rocks referred in Table 1 are given in Table 4 for the two lherzolites and in Table 5 for spinelpyroxenites and basaltic megacrystals.

REE content of mineral fractions I (data in ppm)

TABLE 4

	Average lherzolite				Progran sample		
	Olivine	Enstatite	Diopside	Spinel	Olivine	Enstatite	Diopside
La	0.14	0.12	1.10	3.0	0.3	0.2	1.5
Ce	0.34	0.28	3.8	42.2	0.7	0.6	4.6
Nd	0.5	0.07	2.8	23.1	—	—	3.0
Sm	0.03	0.05	1.65	0.33	0.06	0.06	0.7
Eu	0.01	0.004	0.31	0.42	0.02	0.02	0.18
Tb	<0.02	<0.02	0.33	0.4	0.06	0.1	0.3
Tm	<0.02	<0.02	0.16	2.0	0.02	0.05	0.2
Yb	0.04	0.14	0.56	0.7	—	—	0.50
Lu	0.14	0.03	0.09	0.17	0.01	0.02	0.13
(Cr)				16.2%			
$\Sigma$ La-Lu	0.6	0.6	10.8	72.3	1.2	1.0	11.0
$3/2\Sigma$ La-Lu	1.6	0.9	16.2	108.5	1.8	1.5	16.5

REE content of mineral fractions II (data in ppm)

TABLE 5

REE	Spinel pyroxenites (Szentbékállá)				Megacryst from basalts	
	Spinel A	Cpx A	Spinel D	Cpx D	Szent- békállá	Kapolcs
La	4.3	2.9	0.5	3.2	2.3	3.3
Ce	5.7	5.8	2.0	8.9	8.3	8.8
Nd	<5.0	7.0	<2.0	5.8	6.0	10.9
Sm	0.40	3.34	0.09	3.88	3.10	3.7
Eu	0.10	0.98	0.04	0.04	0.55	0.96
Tb	0.09	0.55	0.03	0.7	0.52	0.6
Tm	0.07	0.16	0.02	0.36	0.29	0.23
Yb	<0.5	<0.5	<0.5	<0.5	0.92	1.5
Lu	<0.05	0.17	<0.02	0.08	0.12	0.12
(Cr)	240	29	44	430		10
$\Sigma$ La-Lu	16.2	21.4	5.2	23.5	22.0	30.1
$3/2\Sigma$ La-Lu	24.3	32.1	7.8	35.2	33.0	45.1

The chondrite normalized REE abundance patterns of minerals in average lherzolite (Fig. 5a) clearly follows the order of partial melting determined from high pressure melting experiments (see. e.g. MYSEN and HOLLOWAY, 1977, or PRESNALL *et al.*, 1978). The spinel component has the highest REE content, it is followed by that of clinopyroxene. During partial melting these two components go into the melt firstly in the order: 1. spinel, 2. clinopyroxene (diopside). There are no considerable differences between the REE patterns of average lherzolite and that of Progran sample (Fig. 5b). The very high point at Tm of spinel component is noteworthy. MYSEN and KUSHIRO (1977) concluded from their high pressure melting experiments on peridotites that the role of garnets in the high pressure field is taken up by spinels (as the highest  $Al_2O_3$  containing phase) in the lower pressure field after the garnet-peridotite  $\rightarrow$  spinel-peridotite transformation. This outstanding Tm data point could be interpreted as the "remembering" of spinel to his "garnet past".

We can follow how partitional relations changes between the spinel and clinopy-

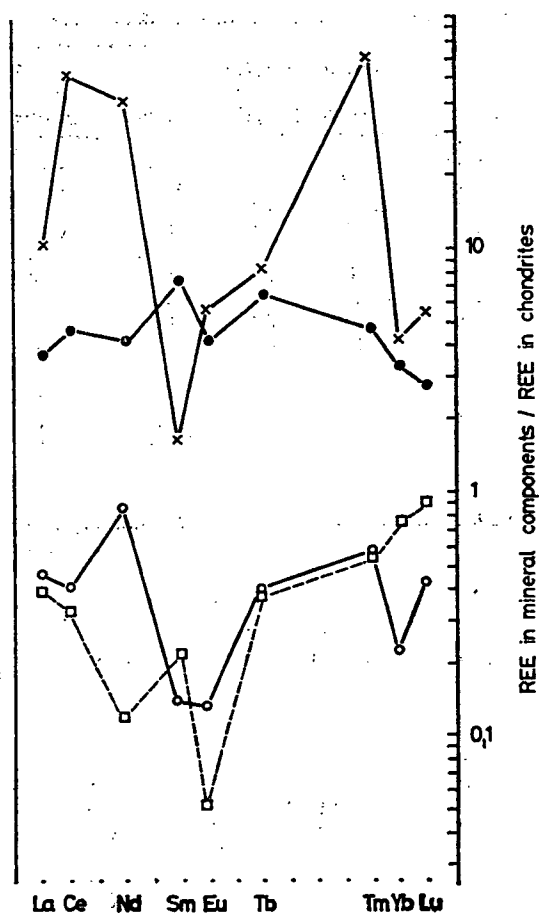


Fig. 5a. Chondrite normalized REE abundances in the mineral components of the average lherzolite, (X — Spinel, ● — Diopside, ○ — Olivine, □ — Enstatite).

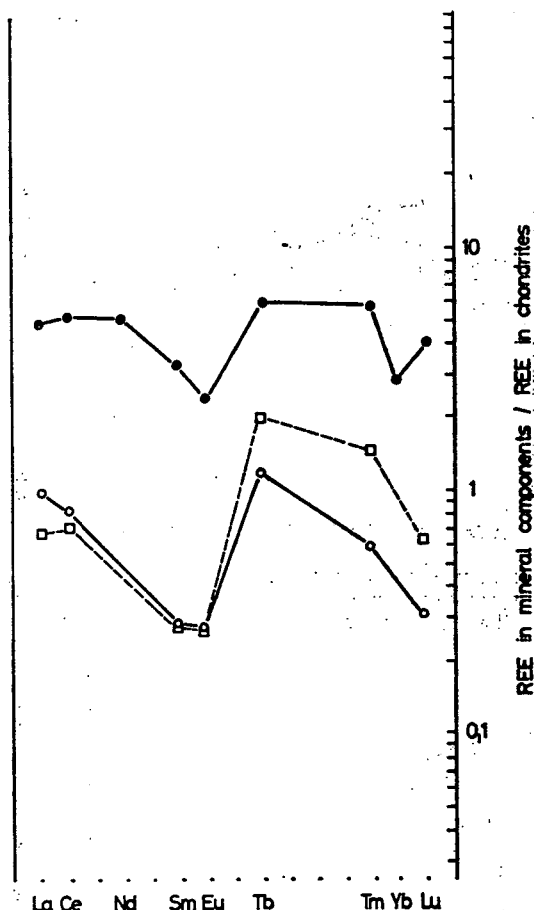


Fig. 5b. Chondrite normalized REE abundances in the mineral components of the Progran sample, (● — Diopside, ○ — Olivine, □ — Enstatite)

roxene components during partial melting when we compare the REE patterns of the spinel and clinopyroxene pair in the average lherzolite with that of in the spinel-pyroxenite. In lherzolitic mineral environment (and upper mantle pressures) spinel is the latest mineral component during crystallization and the first in partial melting: it is characterized with the highest REE content. After a higher degree of partial melting, when clinopyroxenes also went into the melt, and the melt withdrawn from the lherzolitic environment (pressure decreased) the roles between spinel and clinopyroxenite are inverted. (Fig. 7) Spinel is the first components during crystallization and clinopyroxenes has higher REE content.

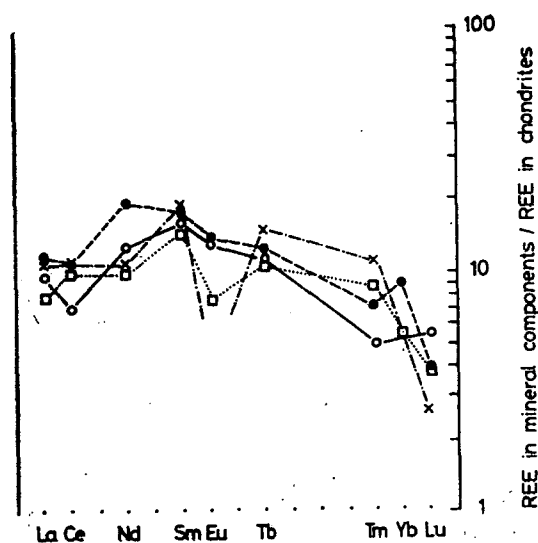


Fig. 6. Comparison of chondrite normalized REE abundances of cpx megacrystals from basalt and cpx components of spinel-pyroxenite samples, (○ — cpx of spinel-pyroxenite A, □ — cpx megacryst. /Szentbékállá/, ● — cpx megacryst. /Kápolcs/, × — cpx of spinel-pyroxenite D)

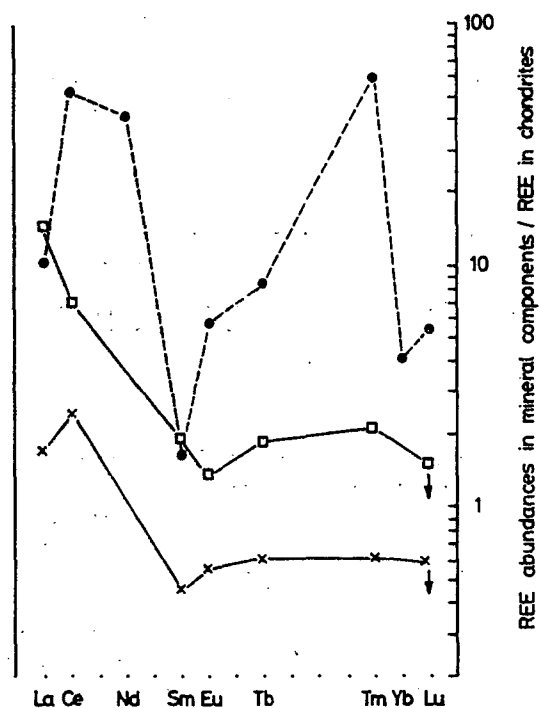


Fig. 7. Comparison of chondrite normalized REE abundances of spinel components of average lherzolite and of spinel-pyroxenites, (● — spinel of average lherzolite, □ — spinel of spinel-pyroxenite A, × — spinel of spinel-pyroxenite D).

## RESULTS FROM ELECTRON MICROSONDA ANALYSES

Electron microsonda analyses were carried out on some mineral components of Progran sample, of wehrlite, of spinel-pyroxenite and on clinopyroxene megacrysts of two basalts (Kapolcs and Szentbékállá) in order to determine the tectonical settings of these samples. The data are given on Table 6.

TABLE 6

*Results of electron microsonda analysis on mineral components of Progran  
lherzolite, wehrlite, spinel-pyroxenite and the clinopyroxene megacryst  
(K. G. SOLYMOS and Cs. SZABÓ)*

	Progran lherzolite			Wehrlite		Spinel-pyroxenite A		Cpx megacryst (Kapolcs)
	olivine	enstatite	diopside	olivine	cpx	spinel	cpx	
SiO <sub>2</sub>	38.58	54.00	52.20	38.31	50.10	—	49.22	48.84
TiO <sub>2</sub>	—	—	0.07	—	0.47	0.49	1.17	0.97
Al <sub>2</sub> O <sub>3</sub>	—	2.26	3.25	0.07	3.36	61.98	7.87	7.63
FeO	8.24	6.23	2.97	13.90	4.51	16.50	6.24	5.82
MnO	0.10	0.15	0.10	0.27	0.16	0.06	0.18	0.10
MgO	51.94	36.48	17.68	47.12	17.29	21.41	15.10	16.12
CaO	0.08	0.93	20.98	0.05	22.66	—	18.64	18.94
Na <sub>2</sub> O	—	—	0.48	—	0.16	—	1.24	1.17
Cr <sub>2</sub> O <sub>3</sub>	—	0.50	0.80	—	0.31	—	—	0.12
Sum	98.94	100.52	98.52	99.72	99.02	100.44	99.66	99.71
100 Mg	91.8	91.3	91.4	85.8	87.2	69.8	81.2	83.2
Fe + Mg								

### *Progran*

The 100 Mg/Mg+Fe values of Progran sample showed the equilibrium character of this lherzolite. We have calculated the p-T conditions of its source region from the Ca and Al content of its diopside and enstatite (according to the method of MERCIER and CARTER, 1975). The mean temperature from the values from enstatite and diopside was 1150 °C (in the spinel-pyroxenite field). For the pressure region a range within 27—37 kbar (80—120 km) has been determined.

Taking into considerations of PRESNALL's attention to be cautious with using of the Al content of enstatite in determination of pressure in the spinel-lherzolite field we can conclude, that our sample, Progran falls onto the oceanic geotherm in the garnet-lherzolite field in MACGREGOR's diagram (MACGREGOR, 1974). As I know our Progran sample is the only one from this zone in Hungary, investigated till now.

### *Wehrlite*

The 100 Mg/Mg+Fe values of the components of wehrlite are more controversial. They are near equilibrium, but the values are a little bit lower than it should be necessary to their upper mantle origin. In the conclusion we point to its transitional character between lherzolitic samples with trapped melt (layered lherzolites) to products which were originated from crystallization of partial melts (but got stuck in deep). This latter type is represented by our spinel-pyroxenites.

### *Spinel-pyroxenite and clinopyroxene megacryst from basalt*

The clinopyroxene of spinel-pyroxenite inclusion strongly resembles in composition, in REE content and pattern and 100 Mg/Mg+Fe value to the clinopyroxene megacryst from the basalt. But the two types represent two types of liquids: The estimated degree of partial melting of their source region as calculated from the ratios of their REE content to that of average lherzolitic one, was: 17 percent for spinel-pyroxenite and 3 percent for basalt. The spinel-pyroxenite originated in a zone, where all mafic liquid could have been crystallized, while clinopyroxene megacryst from basalt characterizes a liquid, where crystallization had begun only.

### CONCLUSIONS

There are two important factors which have affected and formed the REE abundance characteristics of the ultramafic inclusions of the Szentbékállá series investigated in this work. These two factors are partial melting and partial separation of melted liquids from the parental environment.

Rare-earth elements, as other incompatible elements, almost totally partition into the melt during partial melting processes. The high REE concentrations originated in this way are transported with the melt. If melt separates and crystallizes, it is easy to calculate the degree of partial melting, because the REE abundance is inversely related to the degree of partial melting (see e.g. the lunar series, RINGWOOD, 1975).

But the melt rarely separates totally from its parental environment. The arisen partial melt leaving the parental rocks in part only, its higher REE concentration is also retained partly with the residual melt. Changing p-T conditions may cause the recrystallization of this residual melt at the parental environment. This way the partial melting and partial retaining process can increase the concentration of REE on those places where the partial melt accumulated and decrease from where more melt had been withdrawn than had had been there earlier.

Our Szentbékállá series of ultramafic inclusions can be arranged when we take into considerations these two mechanisms changing the REE concentrations. The highest REE abundances characterize those samples which had originated by separation of partial melt, i.e. the basalt and the spinel-pyroxenite samples. The second group of samples consists of rocks which retained more (e.g. layered lherzolites) or less (wehrlite) their lherzolitic character in spite of the fact that more partial melt had accumulated — and later crystallized — in them than originated from them. The third group consists of lherzolitic samples which in some degree has depleted in those components which had gone into the partial melt. The average lherzolite and the dunite sample with Progran sample belong to this group from our samples (Fig. 8).

We can summarize our results in the following items:

1. Considering the lherzolites to be representative to the source region of basalts, the alkali basalts investigated by us were the products of 3 percent partial melting (average value).
2. During the partial melting of average lherzolite first spinel then clinopyroxene goes into the melt.
3. Spinel-pyroxenite inclusions represent a source region, where 15 percent partial melt of the lherzolitic source region was accumulated and solidified in deep.
4. In spinel-pyroxenite the partition of REE in spinel and clinopyroxene is inverted as compared to the lherzolitic case.



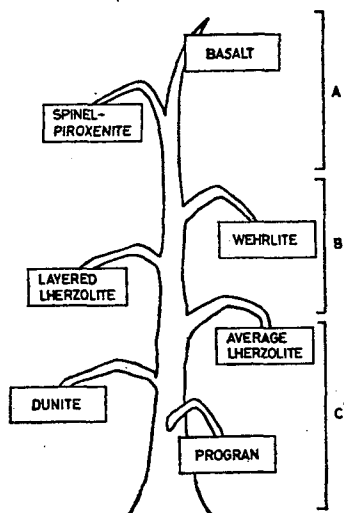


Fig. 8. Evolutionary model about the origin of different peridotite inclusions in the Szentbékálla series. In this model the different degree of partial melting and the different degree of partial retainment of melted liquid determines the REE abundances of the members of the series. A' — Great enrichment of REE. Partial melting separation of highest REE containing components and withdrawal of melt from the parental peridotitic environment. B — Enrichment of REE in the bulk sample (as compared to primary lherzolitic) mainly because of partial enrichment of the clinopyroxene component. C — Partial depletion of REE (as compared to primary lherzolitic) because of partial withdrawal of high REE containing mineral components, the spinel and clinopyroxene

5. Layered lherzolites and especially our wehrlite sample represent source regions enriched in high REE containing melt which then solidified in them.
6. In the Progran sample equilibrium of constituent minerals characteristic to the garnet-pyroxenite state has been preserved.

#### SUMMARY

Our REE measurements with INAA are, as we know, the first ones carried out on Hungarian peridotite inclusions. According to our model the series of ultramafic inclusions — with the supplementary host basalt — from Szentbékálla represents different transitional or terminal stages of evolution of magma in the presence of parental mantle rocks. The results and the model discussed are in accord with earlier works on such types of inclusions from different parts of the world, and with the melting experiments. It may have greater importance for the Carpathian Basin geology contributing to the understanding of processes which has origin in upper mantle regions.

#### ACKNOWLEDGEMENTS

The authors are indebted to K. GÁL-SOLYOS and Cs. SZABÓ for the microsonda analyses, to G. ZSOLT for X-ray measurements, to I. DÓDONY for a spinel-pyroxenite sample and also to Cs. SZABÓ for the worthy discussions.

## REFERENCES

- EMBEY-ISZTIN, A. (1976): Felsőköpeny eredetű lherzolitzárványok a magyarországi alkáli olivinbazaltos bazanitos vulkanizmus közeteiben. *Földtani Közl. (Bull. Hung. Geol. Soc.)* **106**, 42—51.
- EMBEY-ISZTIN, A. (1978): On the petrology of spinel lherzolite nodules in basaltic rocks from Hungary and Auvergne, France. *Ann. Histo-Nat. Musei Nat. Hung.*, **70**, 27—44.
- LOUBET, M., ALLÈGRE, C. J. (1982): Trace elements in orogenic lherzolites reveal the complex history of the upper mantle. *Nature* **298**, 809—814.
- MACGREGOR, I. D. (1974): The system  $\text{MgO-Al}_2\text{O}_3\text{-SiO}_2$ : solubility of  $\text{Al}_2\text{O}_3$  in enstatite for spinel and garnet peridotite compositions. *Am. Mineralogist* **59**, 110—119.
- MERCIER, J.-C., CARTER, N. L. (1975): Pyroxene geotherms. *J. Geophys. Res.*, **80**, 3349—3362.
- MERCIER, J.-C., NICOLAS, A. (1975): Textures and fabrics of upper mantle peridotites as illustrated by xenoliths from basalts. *J. Petrol.*, **16**, 454—487.
- MYSEN, B. O., HOLLOWAY, J. R. (1977): Experimental determination of rare earth fractionation patterns in partial melts from peridotite in the upper mantle. *Earth Planet. Sci. Lett.*, **34**, 231—237.
- MYSEN, B. O., KUSHIRO, I. (1977): Compositional variations of coexisting phases with degree of melting of peridotite in the upper mantle. *Am. Mineralogist* **62**, 843—865.
- PANTÓ, GY. (1981): Rare earth element geochemical pattern of the Cenozoic volcanism in Hungary. *Earth Evol. Sci.*, **3—4/1981**, 249—255.
- PRESNALL, D. C. (1976): Alumina content of enstatite as a geobarometer for plagioclase and spinel lherzolites. *Am. Mineralogist* **61**, 582—588.
- PRESNALL, D. C. *et al.*, (1978): Liquidus phase relations on the join diopside-forsterite-anorthite from 1 atm to 20 kbar. *Contrib. Mineral. Petrol.*, **66**, 203—220.
- REID, J. B., FREY, F. A. (1971): Rare earth distributions in lherzolite and garnet pyroxenite xenoliths and the constitution of the upper mantle. *J. Geophys. Res.*, **76**, 1184—1195.
- RINGWOOD, A. E. (1975): Some aspects of the minor element chemistry of lunar mare basalts. *The Moon* **12**, 127—157.

*Manuscript received, 3 September, 1985*

## K/AR DATING OF POST-SARMATIAN ALKALI BASALTIC ROCKS IN HUNGARY

KADOSA BALOGH<sup>1</sup>, E. ÁRVA-SÓS and Z. PÉCSKAY

Institute of Nuclear Research, Hungarian Academy of Sciences

L. RAVASZ-BARANYAI<sup>2</sup>

Hungarian Geological Institute

### ABSTRACT

The systematic K/Ar chronologic study of post-Sarmatian alkali basaltic rocks in Hungary started in 1978. Since then about 250 determinations were carried out on samples representing the majority of occurrences. This work enabled us to establish a numerical time scale for the evolution of basaltic volcanic activity and to estimate the absolute ages of biostratigraphic units.

In order to discover the possible disagreement of radiometric and geologic ages, which are caused by incomplete degassing, presence of xenolites and radiogenic argon loss, the isochron methods were used on cogenetic rocks and/or on fractions of different magnetic susceptibility and/or density of a single piece of basalt.

The oldest basalts erupted in the Lower Pannonian\* in the Danube—Tisza Interfluvium Region. Their ages fall in the range of 8.1—10.4 Ma. The indicated age for the Lower-Upper Pannonian boundary is a bit younger than 8 Ma but due to the absence of basalts in the lower part of Upper Pannonian, this age estimation is uncertain.

In Transdanubia, in the Balaton Highland, Bakony Mts. and Little Plain the oldest basaltic rocks are tuffs in the Pa<sub>2</sub><sup>3</sup> (*Congeria unguicapræ*) level, these are unsuitable for dating. The oldest eruptive basalts are 5.5—6.0 Ma old, these are in a stratigraphically undefined position. Most of the basalts are younger than 5 Ma and volcanism terminated about 3 Ma ago. The age of boundary between the Pa<sub>2</sub><sup>3</sup> (*Congeria balatonica*) and Pa<sub>2</sub><sup>3</sup> (*Unio wetzleri*) levels changes in space. The deposition of Pa<sub>2</sub><sup>3</sup> sediments started 4.5 Ma ago (or even earlier) in certain areas and in other places the end of the Pa<sub>2</sub><sup>3</sup> level is younger than 4 Ma.

At the village of Bár (southeastern part of Transdanubia) jumillite overlies early Pleistocene red clay. Its age is  $2.17 \pm 0.17$  Ma. This shows that deposition of sediments, classed traditionally as Pleistocene in Hungary, started prior to 1.8 Ma.

In North-Hungary, around town Salgótarján, basalts are 2.0—2.5 Ma old. Since they lie on eroded Oligocene and Miocene surfaces, their K/Ar data can not be related to the age of Pliocene-Pleistocene boundary.

\* The term Pannonian is used in this paper in *sensu lato*.

### INTRODUCTION

In the Carpathian-basin intermediate and acid volcanic activity of calc-alkalic type started in the Lower Miocene and continued until the Lower Pannonian. This was followed in the Lower Pannonians, due to the change of structural environment, by an alkali basic volcanism producing volcanic material both of Atlantic and Mediterranean types. The basic volcanic process lasted till the Pleistocene.

In the Danube — Tisza Interfluvium Region Lower Pannonian basalts are known from deep drillings; jumillite occurs on the right bank of Danube, south of town Mohács, near village Bár, which according to the traditional stratigraphy is classed

<sup>1</sup> H—4026 Debrecen, Bem tér 18/C, Hungary

<sup>2</sup> H—1442 Budapest, Népstadion út 14, Hungary

as Early Pleistocene. Basaltic rocks in the Balaton Highland, southern part of Bakony Mountains and Little Plain are among the layers or on the eroded surface of Upper Pannonian sediments. Around the town of Salgótarján on Hungarian territory basaltic rocks lay discordantly on eroded Oligocene and Miocene surfaces. Thus, their radiometric ages lack chronostratigraphic importance and indicate merely the time of volcanic activity.

This paper treats first of all the chronologic interpretation of K/Ar data measured in the Institute of Nuclear Research of the Hungarian Academy of Sciences. As for the stratigraphic and partly petrologic and geochemical data used in this work, the corresponding geological literature is cited. Results of accomplished petrographic investigations indispensable for the evaluation and interpretation of radiometric ages are briefly summarized, too.

Chronologic relations of the Lower Pannonian basalt reached by borehole Sárospatak — 10 (K/Ar age:  $9.4 \pm 0.5$  Ma) have been discussed elsewhere (BALOGH, KADOSA, *et al.*, 1983b). In the Little Plain Lower Pannonian basaltic rocks were reached by boreholes Pásztori—1 and 4 and described by BALÁZS and NUSSZER (1982). The scarcity of available datable material and the extremely high gas content of this rocks prevented a reliable K/Ar study up to now.

Experimental methods, instruments and treatment of measured data are published elsewhere (BALOGH, K., MÓRIK, GY., 1978, 1979; MOLNÁR, J. *et al.*, 1980; BALOGH, K., 1985). Atomic constants suggested by the Subcommittee on Geochronology of IUGS have been used for calculating K/Ar ages (STEIGER, R. H., JÄGER, E., 1977).

#### CHARACTERISTICS AND ORIGIN OF YOUNG BASALTIC MAGMAS

Parallel to the radiometric age determinations, petrographic examinations were made minimum on two thin sections per samples of the dated rock types. Essential mineralogical-petrographical characteristics are summarized in Table 1. Based on the results of earlier researches published by numerous authors as well as on recent observations, conclusions mentioned below can be drawn.

It appears that the young basaltic magmas have been originated from a depth of the spinel-lherzolite pressure regime or from a source, below it. This basic volcanic series comprises rock types of alkali basalts, differentiation products as trachyte and trachybasalt, nepheline basanites and leucite — rich varieties. The two latter highly alkaline as well as youngest members of the series represent two different magma provinces: atlantic and mediterranean.

The spinel-lherzolitic relation from a source below the subcontinental crust of 40—80 km depth is demonstrated by the common xenoliths of the basaltic tuffs (EMBEY-ISZTIN, A., 1984) and by xenoliths and xenocrysts of the analysed rock samples (Table 1 and 2). It seems, that the K/Ar ages of the samples have not been influenced significantly by the xenoliths present in varying amount in the basaltic rocks.

According to our up-to-date knowledge, alkali basalts and trachytic derivatives outpoured over voluminous tuffaceous accumulations during the Lower Pannonian are found in the region of Little Plain, at Sárospatak and in the area of the Danube — Tisza Interfluvium Region, covered by thick, younger Pannonian basin deposits. In the area of the Little Plain the trachyte and trachytic agglomerates are underlying the trachybasalt flows and are crossed by trachybasalt dikes of younger eruptions (BALÁZS, E., NUSSZER, A., 1982).

Texture and mineral constituents of alkali basaltic rocks in Hungary

TABLE 1

Locality	Rock name	Texture	Phenocrysts				Groundmass								opaque min.	Cavity-filling		Secondary					Remarks	Xenoliths
			olivine	pyroxene	plagioclase	kaersutite	olivine	pyroxene	katophorite?	plagioclase	pot. feldspar	nepheline	zeolite	glass		minerals								
																zeolite	calcite	chlorite	iddingsite	serpentine	chlorite montmor.	carbonates		
NE-Hungary Sárospatak—10 Duna—Tisza Interfluve	b	int	x	o	s		x	x		x	m		o		□						o		2. 3. 4	ch.
Kiskunhalas-Ny-3. 1162. 0—1167.0	b	int						x		x			o	x	★	o	o				x	x	1	
Ruzsa—4 2657.0—2666. Om	b	hya-int	(o)				?	?		x			x	x	★	x		o			x			
Kecel—1 1432.0—1434.0	b	hya-int	(o)	o	x		(o)	o		x				x	★						x	o	2	
Balaton Highland Bakony Mts., Little Plain																								
Mencshely, Ragonya börc	b	int	x	x		s	x	x		x			o		●			x					1. 2	di, co, sp, ka, qu
Barnag, Kőhegy	b	int	x	s		s	x	x		x			o		●			x					1. 2	di, ch, sk, li
Zánka, Hegyestő	b	int	x	s			o	x		x			o		●								1. 2	di, qu
Tihany, monk's caves	tr	sub	x	x				x	x	x	m	o			★		o	o			x		1	di, qu, ph, sa
Várkesző—1. 71.5—76.5	b	hya	x	s			o	x		x				x	●								2	
Monostorapáti—1 120.8—122.4 m	b	int	x	o			o	x		x			o		●		o				o		1	sp, co, en, di, sk
Malomsok—1. 40.0—46.5 m	b	sub	x				x	x		x					□		o	o					1	
Malomsok—2. 54.7—58.1 m	b	sub					x	x		x	m				□			x					1	
Kab-hill	b	sub	x				x	x		x	m				□			x					2. 3	
Kab-hill II	b	sub	x				x	x		x					□			x					2	
Kab-hill III	b	sub	x				x	x		x					□			x		o			2	
Kab-hill, toward Őcs village	b	intg	x				x	x		x					□			x					2	
Kab-hill, TV-transmitter	b	intg	x				x	x		x					★			o					2	
Tálod	b	sub	x				o	x		x	m				□			o					2. 3	
Ság-hill	b	intg	x				o	x		x	m				□			o					1. 3	
Ság-hill, basalt underlain by tuff	b	int	x				(o)	x		x					□				o	o			1. 3	
Ság-hill	b	sub	x				o	x		x					□			o					1. 3	
Vigándpetend—1. 7.5 m	b	intg	x				x	x		x	m				□			o					1	
Rábaszentandrás—1. 56.4—58.5 m	b	sub					x	x		x	m				□			x					1	
Marcaltó—1. 51.8—60.5 m	b	sub					x	x		x	m				□			x					1	
Pula—1. 144.0—147.0 m	b	int	x	s			o	x		x			x	●	o	o							2	sa
Pula—8. 51.5—55.0 m	b	int	x	s			o	x		x			x	●		o							2	di, ch
Pula—14. 30.3—34.0 m	b	int	x	s			o	x		x			x	●		o							1. 2	
Kapolcs—1. 0.3—9.0 m	b	hya	x	o			o	x		x			x	□		o							1	qu
Kapolcs—1. 45.0—50.0 m	b	int	x	s			o	x		x	m				●								1	co
70.0—75.0 m	b	int	x	s			s	x		x					●								1	
85.0—91.0 m	b	int	x	s			o	x		x					●								1	sp+ch+en ka+sp
Kissomlyó	b	int	o	x			o	x		x			o		★	o							1	di
Várkesző—4. 94.5 m	b	int	x	s				x		x			x		●		x				o		1	
Sátorma	b	int	x				o	x		x					●								1	ch+sp, qu
Diszel, Délkő	b	int	x	s			o	x		x			o	x	●		o						1	

Table 1. contd.

Locality	Rock name	Texture	Phenocrysts				Groundmass								opaque min.	Cavity-filling		Secondary				Remarks	Xenoliths			
			olivine	pyroxene	plagioclase	kaersutite	olivine	pyroxene	katophorite?	plagioclase	pot. feldspar	nepheline	zeolite	glass		minerals										
																zeolite	calcite	chlorite	iddingsite	serpentine	chlorite montmor.			carbonates		
Badacsony	b	intg	x				x	x		x	m	m	o		★					o					1	
Uzsa-quarry, lower part	b	int	x	s			x	x		x			o		★										1	di
Uzsa-quarry, upper part	b	int	x	s			x	x		x	m		x	m	★	x						o			1.3	
Doba—3. 47.0—48.9 m	b	int	x	s			o	x		x	m		o		□				o			o			1	
Doba—3. 71.0—72.0 m	b	int	x	s			x	x		x	m		o		□				o			o			1	
Doba—3. 115.0—116.0 m	b	int	x	s			o	x		x			o		□		o		o						1.2	
Somló	b	int	x	s			x	x	s	x			o		★						x				1	
Bazsi, quarry	b	sub					x	x		x	m		o		★				x	o					1	ba
Sümegprága	b	int	x		s		x	x		x			o	x	□										1	sa
Felsődörgicse, Sárkút	b	int	x	x			o	x		x			o		●										2	
Mencshely, Halomhegy	b	int	x	o			o	x	s	x			o		●										1	di
Zalaszántó Kovácsi hills	b	sub	x	s			o	x	s	x	m		o		□										1.3	
Várkesző—3. 26.5—33.0 m	b	int	x	o			o	x		x				x	●		o					o			1	
Monostorapáti—1 39.7—41.0 m	b	int	x	s			x	x		x					●				o						2	sp+ch, sk sp+en+di
Hegyesd	b	hya	x	x			o	x		x			x		●										1.2	
Fekete-hill	b	int	x				o	x	s	x			o		★							o			1.3	di+ch
Szt. György hill	b	intg	x	s			x	x		x	m		o		□							o			1	
Zalahaláp	b	intg	x	s			o	x		x					●										2	co, di
Agártető	b	intg	x	o			o	x		x					□				x						2	
Mindszentkál, Kopsz hill	b	int	(x)	o			(o)	x		x			o		●	o	o								2	sp, di, qu
Salgótarján area																										
Somoskőújfalu	bas.	int	x	o		(o)	o	x		x		x	o		●							o			1.2	ol+di-au + +ka+sp
Somoskőújfalu	bas.	int	x	x		(o)	x	x		x		o	x		●										1.2	
Somoskőújfalu, quarry	bas.	int.	o	x		(o)	o	x		x		x	x		●							o			1.2	
Somoskőújfalu, Eresztvény	bas.	int	o	x		(o)	o	x		x		x	o		●	o						o			1.2	ch+co, di + +sp, di + +ol+ch+sp
Medves, Magyarbánya	bas.	int	x	x			o	x	s	x		x	o		●										1.2	ch+co
Medves, Középbánya	bas.	int.	o	x		(o)	o	x		x		o	o		●										1.2	ch, sp

x main constituents  
o constituents 10%  
m minor constituents  
s sporadic  
(o) pseudomorphs  
□ ilmenite  
★ titanomagnetite  
● magnetite-titano-magnetite  
\* titanohematite

Rock names  
b basalt  
tr trachybasalt bomb in tuff  
bas basanite

Spinel: mostly picotite  
Basalt: uniformly alkali basalt  
remarks 1. titanomagnetite  
2. augite, diopside  
augite  
3. minor amount of  
biotite in the  
groundmass  
4. accessory picotite  
texture  
int intersertal  
hya hyalopilitic  
sub subophitic  
intg intergranular

Xenoliths  
ch chromite  
sp spinel  
di diopside  
co corundum  
ka kaersutite  
sk skarn  
li limestone  
pk phyllite  
sa sandstone  
en enstatite  
ba basalt  
ol olivine  
qu quartz



Texture and mineral constituents of jumillite at Bár

TABLE 2

Locality	Texture	Olivine	Pyroxene	Kaesutite	Kataphorite	Biotite	Sanidine-anorthoclase	Leucite	Analcime	Opaque minerals	Cavity filling -zeolites	Secondary minerals	
												Iddingsite	Serpentine
Bár—4. 18.0 m	porphyritic-poikilitic	x	x	(o)		s	x	x	o	★		o	
26.0 m	porphyritic-poikilitic	x	x	(o)	o	s	x	x	x	*		o	
Bár—6. 62.0 m	poikilitic	x	x	(o)		o	x	x	o	★		o	
67.0 m	poikilitic	x	x	o		o	x	x	x	★	s		o

Based on petrographic examinations it can be supposed that the common bombs of trachybasaltic dike rocks found in the Upper Pannonian basaltic tuff at Tihany represent wallrock material of the trachybasalts of earlier volcanic episode. Thus the Lower Pannonian basaltic volcanism seems to be detected in an area of greater expansion in Transdanubia.

Upper Pannonian alkali basalts (some of them are near to the basanites in composition) are outcropping in NW Transdanubia, basanites are occurring in the area of Salgótarján (N-Hungary) while early Pleistocene peralkaline rock type (jumillite) was discovered by drillings at a shallow depth, at Bár (S-Hungary).

The Upper Pannonian alkali basalts of the Transdanubian area (Balaton Highland, Bakony Mts., Little Plain) partly are outcropping overlying Pannonian basin deposits as remnant hills, partly are covered by Pleistocene loess (locally by Upper Pannonian sedimentary rocks) and one part was eroded. Volcanism is supposed to be represented probably by three repeated episodes, each of which can be characterized by a period of higher activity producing pyroclastics in the beginning while during the period of decaying shields, flows, dikes were formed. As a result of gravitational differentiation, lavas of lower setting are enriched in olivine.

The area, characterized by unnumbered young as well as renewed faults and representing a series of sediments with high number of local varieties, makes difficulties regarding determination of relative age of the members of repeated volcanic episodes on stratigraphic base. Petrographic examinations are also proved inadequate for the clear isolation of the roughly contemporaneous basalts due likely to differentiation and fractionation of the magma. Products of the same volcanic episode are represented by members rich in volatiles and poor in olivine followed later by olivine rich lavas poorer in volatiles and free of xenoliths and xenocrysts due to slow upward transit and fusion during the ascent. The latter magma type has been crystallized also under-surface, intruding into the beds of the Upper Pannonian sedimentary rocks.

The youngest volcanic products of Hungary erupted near the Pannonian-Pleistocene boundary are highly alkaline varieties. In the area of Salgótarján nepheline bearing basanites are outcropping enclosing numerous xenoliths and xenocrysts, the same, found in the alkali basalts in Transdanubia. On the contrary, in the southern part of Hungary at Bár, the undersurface basaltic rocks represent a type of high

K-content, product of a Mediterranean magma type. These rocks can hardly be classified (T. SZEDERKÉNYI, 1980); it seems best to be related to the rare jumillite of Spain. Xenoliths of spinel-lherzolitic origine are not observable.

Summarizing, products of the Lower Pannonian volcanic action are widespread within the Hungarian basin while basaltic rocks of the Upper Pannonian volcanic episodes are not yet discovered in the SE part of the country, probably this area devoids of younger Pannonian volcanic phenomenon. Regarding the activity of the volcanic episodes, it can be stated that it seems to be much more explosive during the Lower Pannonian represented by vast pyroclastic accumulations comparing to the Upper Pannonian, the latter can be marked by the growing importance of basaltic flows. Most of the authors publishing data of the Lower Pannonian volcanic rocks agree with the supposition of a clear genetic relation to the magma type of the Upper Pannonian volcanic action. BALÁZS (BALÁZS, E., NUSSZER, A., 1982) regards the trachytic rocks as derivatives of the basaltic magma.

In general, basaltic magmas tend to be more undersaturated with passage of time and also the continental character of the rock types becomes more pronounced by the end of the Pannonian. A chemical diversity can be observed, too, regarding the youngest products as it is well shown in Fig. 1.  $\text{Na}_2\text{O}/\text{K}_2\text{O}$  versus  $\text{Na}_2\text{O} + \text{K}_2\text{O}$  values available from the literature (GYARMATI, P., 1977, BALÁZS, E., NUSSZER, A., 1982, JUGOVICS, L., 1976) are plotted in MIYASHIRO's (1975) diagramm (Fig. 1).

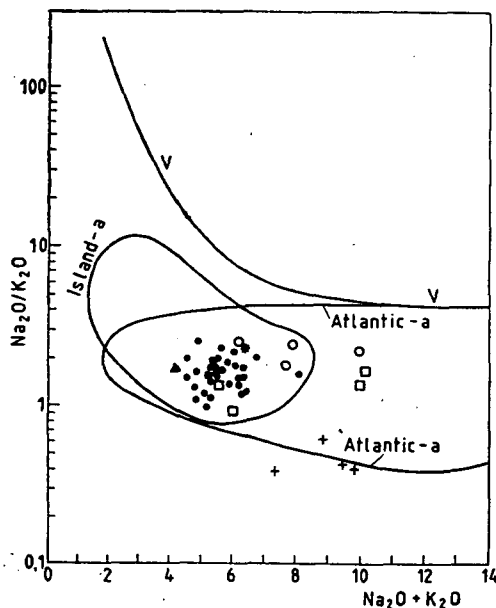


Fig. 1. V—V: upper limit of  $\text{Na}_2\text{O}/\text{K}_2\text{O}$  for all fresh volcanic rocks; Island-a: field of relatively common volcanic rocks in island arcs  
Atlantic-a: alkali rocks on Atlantic islands (except for Island)

- ▲ Sárospatak
  - \* Danube—Tisza Interfluvium
  - Balaton Highland, Bakony Mts., Little Plain
  - Little Plain, trachyte and trachybasalt dikes
  - Salgótarján area, basanites
  - + Bär, Jumillite
- alkali basalts



Comparing the basaltic rock types to the ocean-island alkali magma types of similar composition, it can be noticed that against the alignment, basaltic rocks under consideration have a distinct continental character with  $K_2O/Na_2O$  between 0.4—0.8 included also the trachytic varieties but excepted the jumillite at Bár, the latter characterized by a value about 2.2. It is also worth to notice that the Ba content of the jumillite is unusually high: 2000 ppm (L. RAVASZ-BARANYAI, 1979). Rock types in the area of the Danube—Tisza Interfluve Region and at Sárospatak are represented by the lower values, between 0.4—0.6

Based on the above data, the basanites in the Salgótarján area can be drawn directly from the alkali basaltic source material while the peralkaline jumillite may represent a source of petrochemically different composition. Considering also the trachytic varieties limited to the NW zone of the country, it appears that the subcontinental crust has not been uniformed within the Hungarian basin during the Pannonian. This heterogeneity of the subcontinental crust, or probably of the mantle, could yield to the diversified evolution of magma types in the NE and in the SW zones of Hungary, i. e. the country can be divided into two main structural units from a point of view of volcano-tectonism, regarding the past 10 Ma.

#### LOWER PANNONIAN BASALTS IN THE DANUBE—TISZA INTERFLUVE REGION

Lower Pannonian basaltic rocks have been found by hydrocarbon exploratory boreholes in the Danube—Tisza Interfluve Region (Fig. 2) and were described first by B. CSEREPES-MESZÉNA (1978). Their petrographic investigation and stratigraphic classification were accomplished by A. NUSSZER (BALÁZS, E., NUSSZER, A., 1982) and M. SZÉLES (In: CSEREPES-MESZÉNA, B., 1978), respectively. A greater number of basalt occurrences have been described by S. PAP (1983).

The basalts are syngenetically altered and rocks penetrated by boreholes Kecel — 1 and Kiskunhalas — Ny — 3 are among sediments belonging to the middle-upper part of the Lower Pannonian. The position of basalts in boreholes Kecel — 2 and Ruzsa — 4 can not be specified within the Lower Pannonian.

K/Ar ages are summarized in Table 3. The data contribute to the age estimation of Lower Pannonian, since only a limited number of radiometric ages are available from this substage on the territory of the Paratethys.

Out of the dated rocks, the sample coming from borehole Ruzsa — 4 is the most altered. Its relatively old age supports the syngenetic character of alteration and shows that this rock did not lose a considerable amount of excess argon after its cooling down. K/Ar ages on basalts from boreholes Kecel — 1-2 agree within the limits of experimental errors indicating the similarity of their real ages within the Lower Pannonian. This age is more reliable since it is obtained on samples of different K content; thus, the time given by the K/Ar data falls in the Lower Pannonian substage.

The age of  $9.61 \pm 0.38$  Ma on basalt from borehole Kiskunhalas — Ny — 3 is the most reliable since it is measured on different sample fractions. In the light of this datum and the stratigraphic position an age younger than 11.0 Ma for the Sarmatian/Pannonian boundary is highly unlikely. For the age estimation of Lower-Upper Pannonian boundary the  $9.61 \pm 0.38$  Ma datum, being older, is less suitable than the ages measured on samples from boreholes at Kecel. In borehole Kiskunhalas-Ny-3, basalt is covered by Lower Pannonian sediments in the depth of 523—1120 m, thus its age does not conflict with the younger data measured for basalts at Kecel which are covered with Lower Pannonian sediments with thicknesses of about 200 m.

# MIOCENE-PLIOCENE BASALTIC ROCKS OF HUNGARY

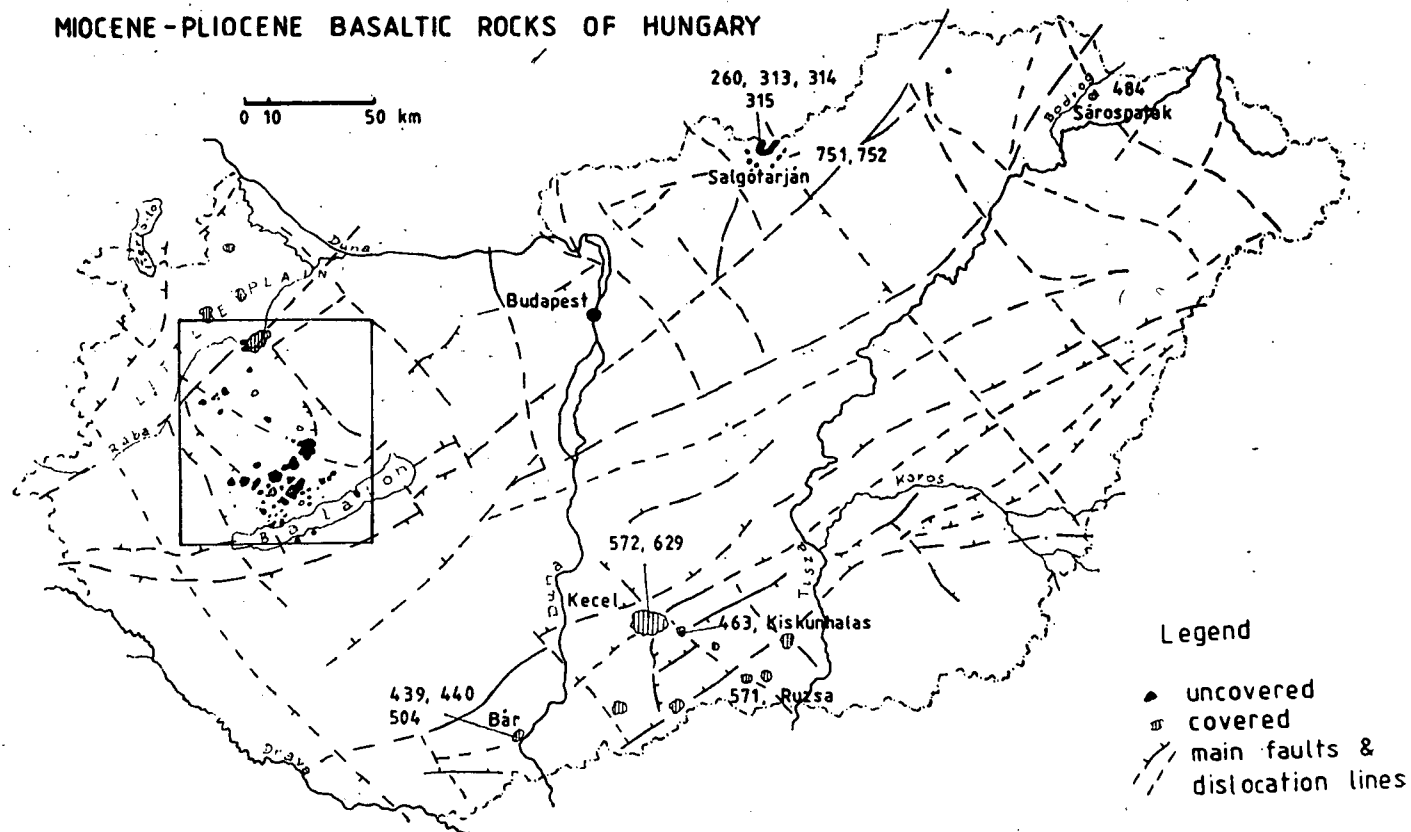


Fig. 2. Locality of post-Sarmatian alkali basaltic rocks in Hungary

TABLE 3.

*K/Ar age of Lower Pannonian basaltic rocks from deep-drillings, Danube-Tisza Interfluve area, Hungary*

No.	Locality Dated fraction	K %	$^{40}\text{Ar}_{\text{rad}}$ %	$10^{-7} \cdot \frac{\text{ccSTP}}{\text{g}}$	Age Ma	Stratigraphy
572	Bh: Kecel—1. 1432—1434 m 1. w. r.	0.77	13 13	2.548 2.533	$8.50 \pm 0.94$ $8.47 \pm 0.77$ $8.34 \pm 0.94$	Lower Pannonian
629	Bh: Kecel—2. 1426—1426,5 m 1. w. r.	1.22	13	3.863	$8.13 \pm 0.71$	Uncertain
463	Bh: Kiskunhalas-Ny—3 1162—1167 m 1. w. r. 2. dnI 3. dnII	1.98 2.12 1.71	24 22 25	7.205 8.065 6.447	$9.35 \pm 0.68$ $9.77 \pm 0.71$ $9.61 \pm 0.38$ $9.68 \pm 0.58$	Middle-Upper part of Lower Pannonia
571	Bh: Ruzsa—4. 2657—2666 m 1. w. r.	0.68	7.8	2.753	$10.4 \pm 1.8$	Uncertain

w. r.: whole rock

dnI, dnII: fraction separated by heavy liquid, numbered in the order of increasing density

## BASALTIC ROCKS IN TRANSDANUBIA

The basaltic remnant hills in the Balaton Highland, the southern part of the Bakony Mountains and the Little Plain attracted the attention of geologists in the first part of the last century. The first works synthetizing the knowledge on the basalts had been prepared in the frame of a project organized by L. Lóczy, having as its aim the scientific study of Lake Balaton and its envidonments (VITÁLIS, I., 1908, Lóczy, L., 1913). Locations of the dated rocks are shown in Fig. 3.

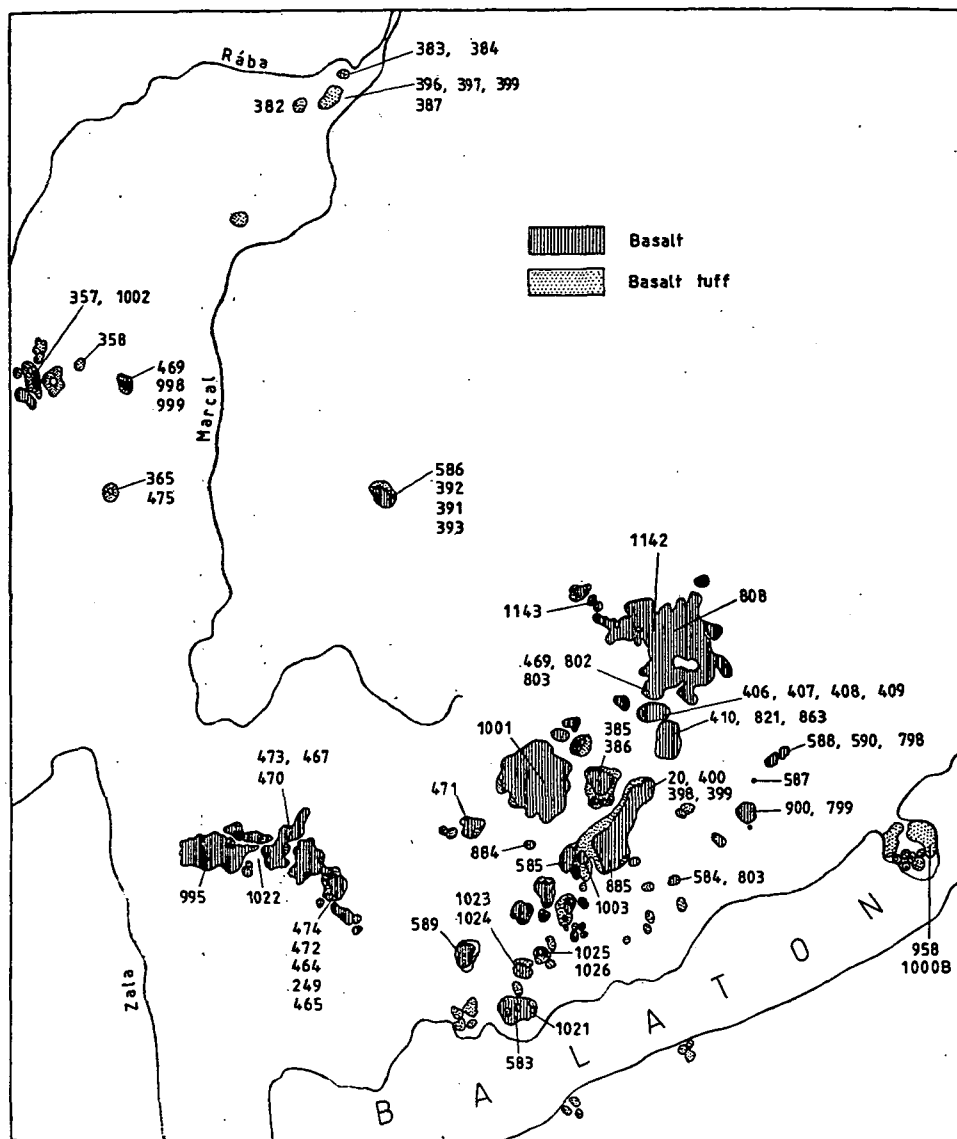


Fig. 3. Locality of post-Sarmatian alkali basaltic rocks in the Balaton Highland, Bakony Mts. and Little Plain. (After Jugovics, L., 1969)

In the last decades a great number of papers have been published dealing with petrologic and geochemical features (VOGL, M., 1979, 1980; PANTÓ, GY., 1981; NAGY, G. 1983; RAVASZ, CS., 1976; KULCSÁR, L., GUZY-SOMOGYI, A., 1962; JUGOVICS, L. 1976; SZÁDECZKY-KARDOSS, E., ERDÉLYI, J., 1957; VICZIÁN, I., 1965; SZEDERKÉNYI, T., 1980) stratigraphic and tectonic position (EMBEY-ISZTIN, A., 1981; JUGOVICS, L., 1969, 1971a, 1971b, 1972; JÁMBOR, Á., SOLTÍ, G., 1976; JÁMBOR, Á., *et. al.*, 1981; VÖRÖS, I., 1966; BARTHA, F., 1959.) paleomagnetism (MÁRTON, P., SZALAY, E., 1968) and the economic importance (BENCE, G., *et. al.*, 1979) of basaltic rocks in this region. These papers were relying on more modern methods of research which were applied also to cores of deep drillings. Instead of reviewing the present knowledge on the basalts, the summarizing work by A. JÁMBOR (1980) is recommended.

This paper discusses first of all the reliability and geologic meaning of radiometric data. Chronostratigraphic consequences of K/Ar dating are also described and still existing problems, where geologic and K/Ar results disagree, are emphasized.

The systematic radiometric dating of Transdanubian basalts started in 1977, but only a minor part of results has been published up to now (JÁMBOR, Á., *et. al.*, 1980; BALOGH, K., *et. al.*, 1983.). This work comprises all the data measured in cooperation between the Hungarian Geological Institute and Hungarian Hydrocarbon Institute before 1985. Results obtained on basaltic rocks in the Tapolca-basin in the frame of a joint project with the Department of Geography, Lajos Kossuth University, Debrecen, will be published elsewhere and are only shortly reviewed here.

K/Ar ages are shown in Table 4.  $^{40}\text{Ar}/^{36}\text{Ar}$ -K/ $^{36}\text{Ar}$  and  $^{40}\text{Ar}_{\text{rad}}$ -K isochron ages are marked with  $I_1$  and  $I_2$ , respectively. The number of samples and/or fractions used for fitting the straight line is indicated in brackets; a number alone denotes all the measured fractions of the relevant sample. Fractions are numbered in the order of increasing magnetic susceptibility and density. Isochron diagrams are shown in the Appendix.

In the territory of the Balaton Highland, the South—Bakony and the Little Plain, neglecting pyroclastics, the basalt hills Kőhegy near the village of Barnag and Hegyestő between Zánka and Monoszló are the oldest. 4 fractions of sample No. 798 and additionally 2 whole rock samples were used for defining isochron ages for Kőhegy. There is a good agreement between the  $I_1$  and  $I_2$  ages ( $5.69 \pm 0.31$  Ma and  $5.67 \pm 1.5$  Ma, respectively). K content of fraction 798/2 greatly differs from that of the other fractions; this increases the reliability of isochron ages. The intercept with y axis indicates complete degassing during solidification. The lack of excess argon is an additional argument for the geological acceptability of measured ages.

Excess argon has been found in the basalt of Hegyestő, therefore isochron ages ( $I_1 = 5.97 \pm 0.41$  Ma and  $I_2 = 5.49 \pm 1.5$  Ma) are less convincing than those of Kőhegy, in spite of the considerably different K content in fraction No. 803/2. The similarity of isochron ages of Kőhegy and Hegyestő is an additional reason to accept them as geologic ages. Positive magnetic polarity has been measured on the basalt of Hegyestő (MÁRTON, P., SZALAY, E., 1968) thus the  $5.57 \pm 5.77$  magnetic polarity zone (MAN-KINEN, E. A., DALRYMPLE, G. B., 1979) is the most likely time of basalt eruption;

An anomalously old age has been obtained in the basalt neck "Ragonya" at the village of Mencshely ( $I_1 = 7.92 \pm 0.33$  Ma). Incomplete degassing is frequent in case of a neck and the K content is nearly the same in its fractions. Therefore, the fitted line is regarded as "mixing line" and the defined age is only a maximum value. On the basis of its strongly eroded character and occurrence along a common line with Kőhegy and Hegyestő, this rock is believed to belong to the oldest basalts in the Balaton Highland.

All these oldest basalts are volcanic necks, the lava flown originally in the surface is fully eroded by now. Their petrographic similarity supports the assumption of a common age.

In Transdanubia, basaltic volcanic activity started with tuff eruptions (unfortunately, tuffs are mostly unsuitable for dating), thus the ages measured on Kőhegy and Hegyestő have to be regarded younger than the commencement of volcanic activity.

Ages of rock samples and their fractions collected from Halomhegy between the villages of Mencshely and Dörgicse (No. 900, 799) are in a good agreement. The  $I_1$  age of  $3.26 \pm 0.16$  Ma shows likely the real time of basalt eruption and excludes the possibility of older volcanic activity.

A small basalt outcrop is known at Sárkút, south of Halomhegy. The  $I_1$  age of  $3.61 \pm 9.52$  Ma should be regarded as maximum age, since the K content of the fractions is very similar. It is clear, however, that this rock is likely coeval with Halomhegy, thus the  $I_1$  value is a real geologic age. We can not decide whether the outcrop is a remnant of an eroded neck or one that slid down from Halomhegy.

The basalt tuff at Tihany is among the layers of the *Congeria balatonica* level (JÁMBOR, Á., 1980). Thus, its absolute age would have a great chronostratigraphic importance. Dating has been attempted on basalt bombs and blocks with very modest results. Part of the fractions contains excess argon and the K contents are very similar. The fitted line is probably a mixing line, thus the formal  $I_1$  age of  $7.56 \pm 0.50$  Ma is an older limit of the geological age. Since considerable amount of excess argon has been detected in a hercynite bomb of mantle origin, a fraction of smaller density has been separated from sample No. 1000B in which less contaminating material of mantle origin has been expected. This fraction appeared to be a little younger ( $7.35 \pm 0.65$  Ma) but its age did not differ significantly from the ages of fractions No. 958/2—3. Thin section investigations of these samples offered an alternative possibility for the explanation of too old ages. According to their textures the trachy-basalt samples are of dike origin, similar to those cut by boreholes at Pásztori, and were torn off and transported to the surface by the basalt tuff eruption. In this case the closure age of dated basalt may be significantly older than the tuff eruption.

The basalt at Tálod-forest is represented by samples from boreholes Vigántpetend — 1 and Put — 2 (No. 410, 821) and by No. 863 collected from the surface. This rock is coeval with the youngest basalt of Kabhegy, and according to Á. JÁMBOR (1980) it is a detached part of it. Both are underlain by the Kabhegy red clay, which covers the Nagyvázsony fresh water limestone under the Tálod-forest. The youngest basalt of Kabhegy has been dated on samples collected from the surface at the television tower and on the slope of the hill toward the village of Öcs. Regarding the stratigraphic importance, repeated, detailed age determination were carried out on these samples. Out of 25 dated fractions, excess argon has been detected in N. 813/2 and 821/2 and argon loss can be supposed from No. 802/2. All these are the least magnetic fractions in which xenolites may accumulate and argon loss may have been caused, too, by weathering. More reasons support the reality of K/Ar ages obtained on these occurrences. A great number of samples, collected from different locations yielded the same age, there is a great difference in the K content of the dated fractions and, according to the intercepts, the basalt degassed completely during its cooling down. A small density fraction (No. 863/4) has been dated, too, and its age is in accordance with that of the other fractions. The K/Ar dating supports the opinion that these basalts are of the same age (JÁMBOR, Á., 1980), but conflicts with the view which regards them as the youngest products of basaltic volcanic activity in the Balaton Highland and Bakony Mountains (JÁMBOR, Á., *et. al.*, 1981). No K/Ar da-

No.	Sample locality	Dated fraction	K %	<sup>40</sup> Ar <sub>rad</sub> %	10 <sup>-7</sup> ccSTP g	<sup>40</sup> Ar <sub>Ar</sub> <sup>36</sup> Ar	$\frac{K/^{36}Ar}{\left(\frac{ccSTP}{g}\right)} \times 10^{-9}$	K/Ar Age Ma
587a	Mencshely, Ragonya	1. w. r.	1.15	53	3.470		7.75±0.50	
587b	Mencshely, Ragonya	1. w. r.	1.12	21	3.06	374.1	0.284	7.02±0.60 I <sub>1</sub> (587):
		2. mgI	1.12	51	3.383	603.1	1.018	7.36±0.50 7.92±0.33
		3. mgII	1.18	44	3.375	527.1	0.811	7.76±0.50
588	Barnag, Kőhegy, Northern slope	1. w. r.	0.79	14	1.789	343.6	0.212	5.82±0.63 I <sub>1</sub> (588+590+798): 5.69±0.31
590	Barnag, W of Kőhegy little outcrop	1. w. r.	0.91	12	2.283	335.8	0.161	6.45±0.53
798	Barnag, Kőhegy	1. w. r.	0.828	33	1.933	441.0	0.623	6.00±0.39 I <sub>1</sub> (588+590+798):
		2. mgI	0.377	6.6	0.919	316.4	0.086	6.27±1.30 5.67±1.50
		3. mgII	0.750	18	1.842	360.4	0.246	6.31±0.57
		4. mgIII	0.894	41	1.955	500.8	0.939	5.62±0.35
584	Hegystő, between Zánka and Monoszló	1. w. r.	2.05	67	6.310	895.5	1.949	7.91±0.51
803	Hegystő, between Zánka and Monoszló	1. w. r.	2.09	61	5.475	757.7	1.764	6.74±0.35 I <sub>1</sub> (803):
		2. mgI	0.613	27	2.427	404.8	0.276	10.20±0.60 5.97±0.41
		3. mgII	2.01	53	4.869	628.7	1.376	6.23±0.35 I <sub>2</sub> (803):
		4. mgIII	2.26	65	5.891	844.3	2.105	6.70±0.30 5.49±1.59
900	Mencshely, Halomhegy	1. w. r.	1.89	48	2.384	568.3	2.163	3.25±0.15
		2. mgI	1.48	50	1.873	591.0	2.335	3.26±0.15
		3. mgII	1.57	45	2.115	537.3	1.795	3.47±0.16
799	Mencshely, Halomhegy	1. w. r.	1.89	26	2.535	399.3	0.775	3.45±0.22 I <sub>1</sub> (799+800):
		2. mgI	1.31	13	1.805	339.7	0.320	3.55±0.39 3.26±0.13
		3. mgII	1.96	19	2.713	364.8	0.501	3.56±0.27
1004	Felső Dörgicse, Sárkút	1. w. r.	0.98	37	1.367	469.0	1.244	3.59±0.18 I <sub>1</sub> (1004):
		2. mgI	0.796	13	1.109	339.7	0.317	3.58±0.24 3.61±0.52
		3. mgII	0.99	23	1.555	383.7	0.562	4.04±0.27
958	Tihany, hermits' caves basalt bomb	1. w. r.	1.79	52	5.852	615.6	0.979	8.40±0.36
		2. mgI	1.84	36	5.524	461.7	0.554	7.72±0.38
		3. mgII	1.87	65	5.428	844.3	1.891	7.46±0.30
1000B	Tihany, hermits' caves basalt block	1. w. r.	1.75	25	5.796	395.0	0.297	8.51±0.45 I <sub>1</sub> (958+1000B/1—3)
		2. mgI	1.53	19	5.797	364.8	0.183	9.73±0.75 7.56±0.50
		3. mgII	1.76	20	5.686	369.4	0.229	8.30±0.61
		4. dnI	1.79	17	5.120	356.0	0.211	7.35±0.65
410a	Bh: Vigántpetend—1. 7.5 m	1. w. r.	1.33	70	2.594	385.0	3.535	5.02±0.30 I <sub>1</sub> (410a):
		2. mgI	1.16	67	2.204	895.5	3.158	4.88±0.25 4.68±0.87
		3. mgII	1.81	74	3.395	1136.5	4.484	4.82±0.20 I <sub>2</sub> (410a): 4.69±0.60
410b	Bh: Vigántpetend—1. 7.5 m	1. w. r.	1.48	35	2.838	454.6	0.830	4.93±0.24 I <sub>1</sub> (410b):
		2. w. r.	1.48	38	2.766	476.6	0.969	4.81±0.23 4.89±0.20
		3. mgI	1.12	34	2.082	447.7	0.819	4.78±0.24 I <sub>2</sub> (410b):
		4. mgII	1.53	84	2.909	1846.9	8.160	4.89±0.20 5.05±0.64
		5. mgIII	1.79	49	3.386	579.4	1.501	4.87±0.20
821	Bh: Put — 2. 3.0 —7.3 m	1. w. r.	1.39	19	2.717	364.8	0.355	5.03±0.39 I <sub>1</sub> (821):5.01±0.68
		2. mgI	0.67	29	1.485	416.2	0.544	5.70±0.31 I <sub>2</sub> (821):4.52±0.39
		3. mgII	1.69	53	3.286	628.7	1.714	5.00±0.23 I <sub>1</sub> (821+863/1—3): 4.84±0.28
863	Forest at Tálod, II	1. w. r.	1.43	51	2.816	603.1	1.562	5.06±0.22 I <sub>1</sub> (821+863/1—3):
		2. mgI	1.03	51	1.854	603.1	1.709	4.97±0.20 4.65±0.72
		3. mgII	1.53	66	2.959	869.1	2.966	4.63±0.20 I <sub>1</sub> (863/1—3): 5.09±1.07
		4. dnI	1.63	29	2.901	416.2	0.679	4.58±0.30 I <sub>2</sub> (863/1—3): 5.87±0.78
469	Kabhegy, slope at village Öcs	1. w. r.	1.43	49	2.584	579.4	1.569	4.65±0.23 I <sub>1</sub> (469+802+803): 5.07±0.81 I <sub>2</sub> (469+802+803): 4.43±0.56
802	Kabhegy II., slope at village Öcs	1. w. r.	1.35	21	2.513	374.1	0.442	4.79±0.39
		2. mgI	0.839	40	1.557	492.5	1.135	4.46±0.21 I <sub>1</sub> (802):4.39±0.49
		3. mgII	1.58	28	2.957	410.4	0.614	4.82±0.23 I <sub>2</sub> (802):5.23±0.58
803	Kabhegy III., slope at village Öcs	1. w. r.	1.39	38	2.567	476.6	0.981	4.75±0.23 I <sub>1</sub> (803):4.92±1.53
		2. mgI	0.425	46	1.037	547.2	1.032	6.27±0.43 I <sub>2</sub> (803):4.38±0.31
		3. mgII	1.81	75	3.458	1182.0	4.640	4.91±0.19 I <sub>1</sub> (469+802+ +803/1,3): 4.82±0.22 I <sub>2</sub> (469+802+ +803/1,3): 5.23±0.35
808	Kabhegy, at the television tower	1. w. r.	1.60	55	2.961	656.7	1.952	4.76±0.20 I <sub>1</sub> (808):4.73±0.46
		2. mgI	1.10	36	2.050	461.7	0.892	4.79±0.27 I <sub>2</sub> (808):4.79±0.64
		3. mgII	1.81	43	3.385	518.4	1.192	4.81±0.22
1142	Kabhegy, lowest lava flow	1. w. r.	1.36	18	2.647			5.01±0.40
1143	Ajka-Padragkut basalt ring	1. w. r.	0.96	15	1.923			5.14±0.50
408	Bh: Pula—1. 40.0—40.5 m	1. w. r.	1.88	34	3.093	447.7	0.925	4.23±0.32 I <sub>1</sub> (408+406+409+ +407):4.25±0.17
406	Bh: Pula—1. 144.5—147.0 m	1. w. r.	1.86	8	2.831	321.2	0.169	3.92±0.96
409	Bh: Pula—8. 51.5—55.0 m	1. w. r.	2.03	46	3.379	547.2	1.512	4.28±0.26
407	Bh: Pula—14. 30.3—34.0 m	1. w. r.	1.61	50	2.599	591.0	1.831	4.16±0.27
20	Bh: Kapolcs—1. 0.3—9.0 m	1. w. r.	2.11	52	3.137			3.82±0.17
		2. mgI	1.95	37	3.116			4.11±0.20
		3. mgII	2.05	34	3.257			4.09±0.21
400a	Bh: Kapolcs—1. 45.0—50.0 m	1. w. r.	1.23	32	1.833			3.94±0.35
400b	Bh: Kapolcs—1. 45.0—50.0 m	1. w. r.	1.16	21	1.934	374.1	0.471	4.29±0.30
		2. w. r.	1.16	31	2.014	428.3	0.765	4.47±0.24
		3. mgI	0.96	25	2.212	394.0	0.427	5.92±0.36
		4. mgII	1.25	32	1.858	434.6	0.936	3.82±0.20
398	Bh: Kapolcs—1. 70.0—75.0 m	1. w. r.	0.75	34	1.263	447.7	0.904	4.33±0.44
399a	Bh: Kapolcs—1. 85.0—91.0 m	1. w. r.	0.98	56	1.758			4.62±0.34
399b	Bh: Kapolcs—1. 85.0—91.0 m	1. w. r.	1.00	11	1.351	332.0	0.270	3.48±0.44 I <sub>1</sub> (399a, b):
		2. mgI	0.99	21	1.716	374.1	0.453	4.46±0.31 4.66±0.36
		3. mgII	0.99	37	1.670	469.0	1.070	4.17±0.20
385	Bh: Monostorapáti—1. 39.7—41.0 m	1. w. r.	0.60	20	0.674			2.90±0.62
386a	Bh: Monostorapáti—1. 120.8—122.4 m	1. w. r.	0.92	61	1.970			5.54±0.40
386b	Bh: Monostorapáti—1. 120.8—122.4 m	1. w. r.	0.914	37	1.925	469.0	0.827	5.42±0.26
		2. mgI	0.244	43	1.603	518.4	0.339	16.80±0.75
		3. mgII	1.16	52	1.740	615.6	2.134	3.86±0.20

TABLE 4. *contd.*

No.	Sample locality	Dated fraction	K %	<sup>40</sup> Ar <sub>rad</sub> %	10 <sup>-7</sup> $\frac{\text{ccSTP}}{\text{g}}$	$\frac{{}^{40}\text{Ar}}{{}^{36}\text{Ar}}$	$\frac{\text{K}/{}^{36}\text{Ar}}{\left(\frac{\text{ccSTP}}{\text{g}}\right)} \times 10^{-9}$	K/Ar age Ma
1003	Sátorma	1. w. r.	1.95	53	3.103		4.09 ± 0.18	
		2. mgI	1.80	53	3.170		4.53 ± 0.20	
		3. mgII	1.87	51	3.112		4.27 ± 0.18	
585a	Diszel, Hajagos Délkő quarry	1. w. r.	1.85	35	2.837	454.5	1.038	3.95 ± 0.20
585b	Diszel, Hajagos Délkő quarry	1. w. r.	1.79	47	2.837	557.5	1.653	4.08 ± 0.18 I <sub>1</sub> (585b):
		2. mgI	1.63	59	2.522	720.7	2.748	3.98 ± 0.17 3.94 ± 0.25
		3. mgII	1.96	57	2.956	687.2	2.597	3.88 ± 0.18
1001	Agártető	1. w. r.	1.60	27	1.855			2.98 ± 0.18
		2. mgI	1.47	29	1.966			3.44 ± 0.19
		3. mgII	1.58	26	1.783			2.90 ± 0.18
471	Haláp	1. w. r.	1.77	18	1.845			2.70 ± 0.36 T <sub>a</sub> (471):
		2. w. r.	1.77	12	2.170			3.16 ± 0.37 2.94 ± 0.34
884	Hegyessd	1. w. r.	2.04	23	2.650	383.8	0.679	3.43 ± 0.22 I <sub>1</sub> (884):2.92 ± 0.40
		2. mgI	0.55	9.6	1.020	326.9	0.169	4.77 ± 0.72 I <sub>2</sub> (884):3.08 ± 0.58
		3. mgII	2.38	19	3.417	364.8	0.482	3.70 ± 0.28
885	Feketehegy Kővágóörs basin	1. w.r.	1.51	18	1.715	360.4	0.571	2.92 ± 0.24
		2. mgI	1.31	23	1.342	383.8	0.862	2.64 ± 0.18
		3. mgII	1.39	18	1.473	360.4	0.604	2.77 ± 0.23
1023	Gulács, NW of the top, 50 m H: 370 m	1. w. r.	1.88	45	2.535			3.47 ± 0.18
1024	Gulács, Northern quarry trapp basalt, H: 220 m	1. w. r.	1.96	40	2.800			3.68 ± 0.20
1025	Tóti-hegy, southern end of the southern peak	1. w. r.	0.94	35	2.184	454.6	0.685	5.71 ± 0.29
		2. mgI	0.96	19	1.681	364.8	0.396	4.51 ± 0.35
		3. mgII	1.01	17	1.644	356.0	0.372	4.19 ± 0.36
1026	Tóti-hegy, northern peak	1. w. r.	1.67	6.9	3.296	317.4	0.111	5.07 ± 1.10
		2. mgI	1.55	6	2.610	314.4	0.112	4.33 ± 1.12
		3. mgII	1.59	7.3	2.981	318.8	0.124	4.82 ± 0.82
583	Badacsony, block field at Rózsakő	1. w. r.	2.12	46	2.817	347.2	1.894	3.42 ± 0.20 I <sub>1</sub> (583):3.45 ± 0.23
		2. mgI	1.60	22	2.229	378.8	0.598	3.58 ± 0.24
		3. mgII	1.94	39	2.738	484.4	1.338	3.63 ± 0.20
1021	Badacsony, quarry at Tördemic, southern court, lower level, H: 315 m	1. w. r.	1.91	30	2.663			3.59 ± 0.20
474	Uzsa-quarry	1. w. r.	2.03	18	2.986	360.4	0.441	4.06 ± 0.34
472	Uzsa-quarry	1. w. r.	2.05	24	2.725	388.8	0.702	3.42 ± 0.25 I <sub>1</sub> (474 + 472 + 464 + + 249 + 465a):
464	Uzsa-quarry	1. w. r.	1.15	3.4	1.916	305.9	0.062	4.29 ± 2.56 3.41 ± 0.84
249	Uzsa-quarry	1. w. r.	1.87	15	3.508	356.0	0.346	4.82 ± 0.66
465a	Uzsa-quarry	1. w. r.	2.07	17	3.622	356.0	0.346	4.50 ± 0.64 I <sub>2</sub> (465a, b):
								4.25 ± 0.59
465b	Uzsa-quarry	2. mgI	1.43	13	2.284	339.7	0.276	4.11 ± 0.45
		3. mgII	1.92	27	3.165	404.8	0.663	4.24 ± 0.25
473	Sümegprága, quarry	1. w. r.	2.38	33	2.869	441.0	1.207	3.10 ± 0.20 I <sub>1</sub> (473 + 467 + 470a):
								2.79 ± 0.29
467	Sümegprága, quarry	1. w. r.	2.82	19	3.853	364.8	0.507	3.52 ± 0.41
470a	Bazsi, quarry	1. w. r.	1.63	15	2.463	347.6	0.345	3.39 ± 0.63
470b	Bazsi, quarry	2. mgI	1.17	13	1.877	339.4	0.275	4.12 ± 0.45 I <sub>2</sub> (470a, b):
		3. mgII	1.42	11	2.174	332.0	0.239	3.94 ± 0.50 3.27 ± 1.70
995	Kovácsi-hegy, quarry	1. w. r.	1.67	17	2.007			3.10 ± 0.26
		2. mgI	1.73	18	1.948			2.90 ± 0.24
		3. mgII	1.63	16	2.024			3.20 ± 0.29
1022	Bh: Zalaszántó—2. 56.3 m	1. w. r.	1.90	25	2.244	394.0	0.834	3.04 ± 0.20
		2. mgI	2.00	34	2.594	447.7	1.174	3.34 ± 0.18
		3. mgII	1.37	13	1.630	339.7	0.371	3.06 ± 0.33
586	Somló	1. w. r.	1.26	5	1.720	316.1	0.114	3.51 ± 0.97 I <sub>1</sub> (586 + 392 + 391):
392	Bh: Doba—3. 47.0—48.9 m	1. w. r.	2.35	37	2.709	469.0	1.505	2.97 ± 0.20 2.98 ± 0.19
391	Bh: Doba—3. 71.0—72.2 m	1. w. r.	1.49	25	1.871	394.0	0.784	3.23 ± 0.36
393a	Bh: Doba—3. 115.4—115.2 m	1. w. r.	1.91	69	3.098	953.2	4.055	4.18 ± 0.20
393b	Bh: Doba—3. 115.4—116.2 m	1. w. r.	2.09	50	3.210	591.0	1.924	3.95 ± 0.20
		2. mgI	1.85	52	3.178	615.6	1.864	4.42 ± 0.20
		3. mgII	2.33	62	2.528	777.6	4.444	2.79 ± 0.20
469	Sághegy	1. w. r.	1.55	41	3.099	500.8	1.027	45.14 ± 0.25
998	Sághegy, base of the level above the lowest court	1. w. r.	1.46	21	3.383	374.1	0.339	5.96 ± 0.42 I <sub>1</sub> (468 + 998 + 999):
		3. mgII	1.32	20	2.768	369.4	0.352	5.39 ± 0.40 6.27 ± 0.58
999	Sághegy, upper basalt	1. w. r.	1.43	60	3.268	738.8	1.940	5.87 ± 0.24
		2. mgI	1.24	49	2.754	579.4	1.278	5.71 ± 0.24
		3. mgII	1.24	63	3.203	798.6	1.948	6.64 ± 0.28
		4. mgIII	1.01	62	2.576	777.6	1.890	6.56 ± 0.27
365	Kissomlyó, quarry	1. w. r.	1.78	54	3.437			4.97 ± 0.31
475a	Kissomlyó, quarry	1. w. r.	2.15	59	3.375	720.7	2.709	4.04 ± 0.17
475b	Kissomlyó, quarry	2. mgI	1.69	48	3.561	568.3	1.295	5.42 ± 0.24
		3. mgII	1.98	21	3.162	374.1	0.492	4.11 ± 0.29
358	Névtelen-hegy, basalt bomb	1. w. r.	1.08	32	1.696			4.04 ± 0.44
357	Sitke, Herczeghegy	1. w. r.	0.80	21	1.416	374.1	0.444	4.55 ± 0.31
1002	Sitke, quarry	1. w. r.	1.63	23	3.554	383.8	0.405	5.60 ± 0.37 I <sub>1</sub> (1002):
		2. mgI	1.70	33	3.636	441.0	0.680	5.50 ± 0.29 4.77 ± 1.8
		3. mgII	1.74	25	4.367	394.0	0.392	6.45 ± 0.40
396	Bh: Várkesző—3. 26.5—33.0 m	1. w. r.	2.09	63	2.435	798.6	4.319	3.00 ± 0.17
397	Bh: Várkesző—1. 71.5—76.5 m	1. w. r.	1.79	61	3.861	757.7	2.168	5.55 ± 0.26
399	Bh: Várkesző—4. 94.5 m	1. w. r.	1.00	51	1.679	603.7	1.832	4.32 ± 0.31
382	Bh: Rábaszentandrás—1.	1. w. r.	1.08	52	1.956	615.6	1.768	4.66 ± 0.30 I <sub>1</sub> (399 + 382 + 383 + + 384 + 387/1):
383	Bh: Malomsok—2. 54.7—58.1 m	1. w. r.	1.20	28	2.502	410.4	0.551	5.36 ± 0.28 4.25 ± 0.32
384	Bh: Malomsok—1. 40.0—46.5 m	1. w. r.	1.52	24	2.913	388.8	0.487	4.93 ± 0.24
387	Bh: Marcaltó—1. 51.8—60.5 m	1. w. r.	1.44	43	2.584	518.4	1.242	4.63 ± 0.33 I <sub>1</sub> (387):
		2. mgI	0.78	39	1.555	447.4	0.764	5.13 ± 0.25 4.15 ± 0.32
		3. mgII	1.78	56	3.124	671.6	2.143	4.52 ± 0.20
439	Bh: Bár—6. 67.0 m	1. w. r.	4.32	14	3.603	343.6	0.577	2.15 ± 0.30 I <sub>1</sub> (439 + 440 + 504):
440	Bh: Bár—4. 18.0 m	1. w. r.	4.20	23	3.181	383.8	1.165	1.95 ± 0.20 2.17 ± 0.17
504	Bh: Bár—6. 62.0 m	1. w. r.	5.17	42	4.370	509.5	2.532	2.18 ± 0.20
		2. pot. fp.	10.07	8	7.386	321.2	0.350	1.89 ± 0.35

w. r.: whole rock  
mgI, mgII, mgIII: magnetically separated fraction, numbered in the order of increasing magnetic susceptibility  
dnI, dnII: fraction separated by heavy liquid, numbered in the order of increasing density  
pot. fp.: potash feldspar





tum indicating a younger age has been measured during this study. On the basis of arguments described above it is felt that radiometric dating is more convincing than stratigraphic classification. Therefore, the deposition of the Nagyvázsony fresh water limestone must have started earlier, at least below the basalt at the Tálod-forest, than the K/Ar age of the basalt. The magnetic polarity of basalt is reversed (MÁRTON, P., SZALAY, E., 1968), thus it can be ascribed to the 4.71—5.26 Ma paleomagnetic zone. (MANKINEN, E. A., DALRYMPLE, G. B., 1979.)

The lowest lava flow of Kabhegy has been dated on a single whole rock sample (No. 1142) and the age of  $5.01 \pm 0.40$  Ma correlates well with the radiometric data measured on the youngest lava flow. The small age difference between the oldest and youngest basalts shows that volcanic activity at Kabhegy lasted for a shorter period, in spite of the red clay layer between the older and younger lava flows. According to the K/Ar dating, the basalt ring at localities Ajka and Padragkút (No. 1143) is similar in age to the oldest lava flow of Kabhegy.

The basalt near the village of Pula is in a stratigraphically well defined position (JÁMBOR, Á., 1980; JÁMBOR, A. *et. al.*, 1981.). The solidified basalt lava pond is underlain by sediments belonging to the middle part of the Upper Pannonian substage (*Congerina balatonica* level,  $Pa_2^2$ ) and the covering layers are characterized by *Unio wetzleri* ( $Pa_2^3$ ). The dated samples (No. 406, 407, 408, 409) are collected from distant point of the basalt body and in the  $I_1$  diagram fit a straight line well. The intercept indicates neither excess argon nor argon loss, and therefore, in spite of the relative uniformity of K contents, the  $I_1$  age of  $4.25 \pm 0.17$  Ma is accepted as a datum marking the end of the  $Pa_2^2$  level in this area.

Borehole Kapolcs — 1, sited at Királykő hill, cut through three basalt lava flows (JÁMBOR, 1980). The sedimentary layers among them are assigned to the  $Pa_2^2$  and  $Pa_2^3$  levels. Two samples (No. 398, 399) have been dated from the first, oldest lava flow.  $4.66 \pm 0.36$  Ma  $I_1$  age has been obtained on fractions of sample No. 399 and the representative point of sample No. 398 fits this isochron, too. The intercept indicates a little argon loss which can be accepted as a consequence of repeated volcanic activity. The second lava flow (sampled by No. 400) is considered, for stratigraphic reasons (JÁMBOR, Á., 1980), to be coeval with the basalt at Pula. Unfortunately, no reliable dating could be accomplished on this rock due to the xenolites accumulating in the least magnetic fraction (No. 400b/3). In this case, the isochron methods are inapplicable since at the time of the rock formation the argon isotopic composition and the amount of excess argon in the fractions were different. When the number of dated samples is small, the representative points may fit a straight line accidentally, and this may lead to erroneous conclusions. This can be observed on fractions 400b/2—4 which define an errorchron age of  $2.19 \pm 0.58$  Ma. This "age" is caused by the excess argon content of fraction 400b/3 and it has been rejected because the intercept indicates a too high ( $>350$ ) initial  $^{40}\text{Ar}/^{36}\text{Ar}$  ratio, which is unacceptable for a lava rock. It can be observed, however, that ages measured on whole rock and on the more magnetic fractions well approximate the age of the basalt at Pula. Thus, K/Ar ages do not disprove the geological correlation.

The youngest basalt lava cut by borehole Kapolcs — 1 is represented by sample No. 20. The uniformity of K content of the fractions frustrates the application of isochron methods, but radiometric ages are in accordance with the stratigraphic position. The real age of this basalt may be younger than their K/Ar data, but this is unlikely since rocks from hills Sátorma (No. 1003) and Hajagos (No. 585) resulted in similar values. It has to be noted, however, that the youngest basalt of Királykő appears to be definitely younger than the basalts of Kabhegy and Tálod-forest.

Borehole Monostorapáti — 1 penetrated the younger (No. 385) and older (No. 386) basalts of Bondoró hill (JÁMBOR, Á., 1980). The older is unsuitable for dating. The extremely old age of fraction 386/b/2 is a joint effect of the high excess argon and low K contents. The representative points are disorderly arranged in both coordinate systems. For stratigraphical reasons this rock is also coeval with the basalt at Pula. It can be noted that geological age is best approximated by the K/Ar age of the most magnetic (No. 386b/3) fraction. The limited sample quantity allowed only one measurement on whole rock for the younger basalt. The analytical error of this datum is great ( $2.90 \pm 0.62$  Ma) but the obtained age does not conflict with stratigraphic observations. As it will be seen later, the possibility of argon loss and, consequently, rejuvenation of radiometric ages, has to be frequently considered for basalts yielding K/Ar ages around 3 Ma. Since postvolcanic activity as a reason for age decrease can not be ruled out, further investigations are desirable on the basalts of Bondoró hill.

The dating of basalts at Pula, Királykő, and Bondoró hills shows that only a part of these rocks is suitable for reliable K/Ar dating. The accepted radiometric ages are in accordance with the geological model elaborated for this area (JÁMBOR, Á. 1980), but there is a disagreement between the geologic and radiometric correlation, of these basalts with the ones of Kabhegy and Tálod-forest. The basalts of the latter area are correlated according to the K/Ar ages with the oldest and on stratigraphic reasons with the youngest basalt of Királykő hill. Radiometric ages for Kabhegy and Tálod-forest are considered to be highly reliable, therefore the settling of this problem might started with the reassessment of stratigraphic arguments.

The basalts forming the hills Sátorma (No. 1003) and Hajagos (No. 585) are similar in age and K content to the youngest lava of Királykő. No fractions of different K contents could be separated from these samples. A small amount of excess argon may be present in fraction 1003/2, but in spite of this the similar K/Ar ages may be regarded as the time of basalt eruption.

Sample No. 884 was collected from the pointed basalt hill west of Hegyesd village. The age of fraction 842/2 is too old but the arrangement of representative points approximate a straight line in both isochron diagrams. The intercept indicate excess argon. There is a good agreement between the two isochron ages and on this ground this basalt is ranged among the products of the youngest (about 3 Ma old) phase of basaltic volcanic activity.

It is likely that the basalt of Haláp hill (No. 471) was also produced during this volcanic phase. This hill has been dated by only 2 whole rock samples. It has to be noted, however, that the magnetic polarity of the basalt is reversed (MÁRTON, P., SZALAY, E., 1968), which is less likely in the time interval defined by the K/Ar age and its error. It has to be admitted that K/Ar system might have been modified by postvolcanic effects and the real time of basalt eruption is similar to that of Badacsony hill, and can be in the paleomagnetic zone ending at 3.40 Ma B. P.

No isochron age can be assigned to the fractions of basalt from Agártető (No. 1001). It is likely that this hill also belongs to the youngest volcanic rocks of the Balaton Highland.

From the Kővágóörs-basin, the hill Fekete-hegy has been dated (No. 885). Similar ages were obtained on the fractions. The distribution of K contents allowed the calculation only of the  $I_1$  age. The too young value and too great error show that the fitted line is an errorchron. The arrangement of representative points makes it likely that argon was lost from fraction No. 885/2; thus, geologic age is better ap-

proximated by the ages of fractions 1 and 3. This rock is ranged among the youngest basalts of the area, too.

Two samples collected from different heights represent the basalt of Gulács hill (No. 1023, 1024). Measured ages correspond to the stratigraphic position and in view of unpublished data by BORSY *et al.* may be accepted as geological ages. The magnetic polarity of basalt is reversed (MÁRTON, P., SZALAY, E., 1968), therefore it is assigned to the 3.40—3.80 Ma zone.

Samples No. 583 and 1021 come from different points of Badacsony hill. Reliable  $I_1$  age has been determined for the first sample, which is confirmed by the whole rock age of sample No. 1021. Radiometric age is in accordance with the reversed magnetic polarity (MÁRTON, P., SZALAY, E., 1968) and fixes the time of basalt eruption in the 3.40—3.80 Ma paleomagnetic zone.

Numerous, still unpublished datings were performed on the basalt hills in and around the Tapolca-basin by BORSY *et al.* The main chronologic results of this work will be only shortly reviewed here.

The oldest reliable ages are a little older than 4 Ma and these were measured on bombs from tuffs forming the hills at Szigliget. Upper Pannonian sand belonging to the *Congeria balatonica* level ( $Pa_2^3$ ) is among the tuff layers, indicating that the deposition of this level in this area did not end prior to about 4 Ma B. P. but likely later. The Csobánc, Gulács and Várhegy hill at Fonyód have been proved to be coeval with Badacsony. The basalt dike of Várhegy at Szigliget intruded 3.3—3.4 Ma ago, so it can be a little younger than Badacsony. According to its reversed paleomagnetic polarity (MÁRTON, P., SZALAY, E., 1968) Szt. György-hill is likely also similar in age to Badacsony; several younger K/Ar ages measured on it may be brought about by postvolcanic effects which can also be detected at Szigliget and Badacsony. Due to the presence of excess argon and radiogenic argon loss, no reliable age could be determined up to now on the basalt of Tóti-hill.

The basaltic rocks of Tátika-group are mostly sills intruding among the sediments of  $Pa_2^3$  level (JÁMBOR, Á., *et al.*, 1981.). The similarity of their geological ages is supported by their uniformly normal magnetic polarity (MÁRTON, P., SZALAY, E., 1968). Samples were collected from Uzsa quarry (Láz-hill), from quarries of villages Bazsi and Sümeprága, from borehole Zalasántó — 2 and Kovácsi hill.

Unfortunately, although several samples have been measured from Láz-hill, the small radiogenic argon enrichment in the only sample of more differing K content (No. 464) frustrated the determination of  $I_2$  and greater uncertainty characterizes the  $I_1$  age of the 5 whole rock samples, too. ( $3.41 \pm 0.84$  Ma). According to the intercept with the  $^{40}\text{Ar}/^{36}\text{Ar}$  axis, the rock did not degass completely during its emplacement. The older  $I_1$  age of sample No. 465 is also inaccurate. The irregular pattern of ages shows that samples contain variable amounts of excess argon and their initial  $^{40}\text{Ar}/^{36}\text{Ar}$  ratios were also different. Therefore, in spite of older K/Ar ages, there is no sufficient cause to regard Láz-hill as older than other members of Tátika-group.  $I_1$  age defined on whole rock samples from the Uzsa quarry is accepted as best approximation of geological age. This agrees with other data obtained for the Tátika group within the limits of experimental error.

Representative points of rocks collected from the quarries at Sümeprága and Bazsi (No. 467, 470, 473) fit a straight line well and the  $I_1$  age assigned to it approximates the youngest ages measured in the Balaton Highland. This age is not substantiated by the older  $I_2$  age determined on the fractions of sample No. 470. The error of this last datum is likely overestimated; it arises from the too great analytical errors of the radiogenic argon contents. (The error calculated on the basis of residuals is

only 0.18 Ma). Considering K/Ar data obtained on samples No. 995 and 1022, the reality of geological ages younger than 3 Ma is unconvincing. Apart from fraction 1022/2, which likely contains excess argon, the ages of samples No. 995 and 1022 agree within the limits of experimental errors and may be regarded as geological ages.

Due to the subsurface solidification, excess argon is frequent in the basalts of Tátika-group. Considering the uniformly normal magnetic polarity (MÁRTON, P., SZALAY, E., 1968) the most likely time of emplacement may be fixed in the 3.15—3.40 Ma paleomagnetic zone. (MANKINON, E. A., DALRYMPLE, G. B., 1979.).

Basalt of Somló-hill in the Little Plain has been dated with samples collected from the surface (No. 586) and taken from three different depths of borehole Doba — 3. The scatter of K/Ar data is great, but 3 whole rock samples define an  $I_1$  age of  $2.98 \pm 0.19$  Ma. The older K/Ar age of sample No. 393 may be explained either by supposing a greater amount of excess argon in it or by accepting the geological reality of older age, though the second assumption is disfavoured for volcanologic reasons (JÁMBOR, Á., 1980). Ages measured on fractions of sample No. 393 do not fit a straight line, but the K/Ar age of fraction 3 is close to the  $I_1$  age of the other three samples of Somló-hill. Older ages may be partly accounted for by the excess argon present at least in sample 393/b/2. On the other hand, radiogenic argon loss from fraction 393b/3, as a consequence of renewed volcanic activity, can not be excluded. Considering radiometric age pattern and volcanologic arguments, the  $I_1$  age of  $2.98 \pm 0.19$  Ma or a little older time interval may be assigned to the basalt eruption.

Seven samples selected from deep-drilling cores have been dated from the Várkesző—Malomsok basalt area. Five whole rock samples define an  $I_1$  isochron of  $4.25 \pm 0.32$  Ma, the reality of which is supported by the  $4.15 \pm 0.34$  Ma  $I_1$  age determined on fractions of greatly different K content of sample No. 387. In both cases little excess argon is indicated by the intercepts of isochrons. The basalt overlies sedimentary layers characterized by *Unio wetzleri* ( $Pa_3^3$ ) (JÁMBOR *et al.*, 1981), thus deposition of this level, at least in this area, started prior to 4.15—4.25 Ma. In the case of samples No. 396 and 397, dating could not be extended to rock fractions due to the insufficient sample quantity available, therefore the too young and too old ages are still unexplained.

A single age has been determined on a basalt bomb from the tuff of Névtelen hill near town Celldömölk. The tuff lies on sediments belonging to the  $Pa_3^3$  level (JÁMBOR, Á., *et al.*, 1981) and the age ( $4.04 \pm 0.44$  Ma) is near the datum determined for the Várkesző—Malomsok area. This shows that a basalt bomb may be completely degassed, too; its K/Ar age does not necessarily surpass the geological one.

Results of repeated efforts to date Ság-hill are still unsatisfactory. The scatter of K/Ar ages convincingly points to the geological error and due to the similarity of K contents  $I_1$  age may be treated only as maximum. The basalt tuff is interlayered with Upper Pannonian sediments and, therefore, the exact knowledge of its age would be of great chronostratigraphic importance. This gives incentive for further investigations.

From ages obtained for Herczeghegy on samples collected from the quarry at Sitke (No. 357, 1002), the geological age can be inferred only with limited certainty. Excess argon is present in sample No. 1002 and the error of the  $I_1$  age is great. The K contents of samples No. 357 and 1002 are highly different, and therefore, the similarity of whole rock and  $I_1$  ages of these samples is remarkable, but their agreement with geological age still has to be confirmed.

Two samples have been dated from the quarry of Kissomlyó. K/Ar ages indicate

excess argon in fraction 475/b/2 and it is likely in sample No. 365, too. Therefore, ages of fractions 475a and 475b/3 may be tentatively related to the geological age.

South of Mohács on the right bank of the Danube at the village of Bár basaltic rock lies on Early Pleistocene red clay (HÖNIG, GY., 1971.). According to the investigations of RAVASZ-BARANYAI (JÁMBOR, Á., *et al.*, 1980), the rock is jumillite. K/Ar ages on 3 whole rock and 1 potash feldspar samples agree well with the  $I_1$  age ( $2.17 \pm 0.17$  Ma) attributed to them and are in accordance with the stratigraphic position. Due to the high atmospheric argon content in fraction 504/2 the accuracy of the  $I_2$  age is unsatisfactory.

#### BASALT AREA AROUND TOWN SALGÓTARJÁN

In the vicinity of Salgótarján, basalts discordantly lie on Miocene and Oligocene surfaces. Therefore, K/Ar ages may be used to study the time relations of volcanic activity and can not be applied for deriving ages of chronostratigraphic units.

K/Ar results are summarized in Table 5. Due to the high atmospheric argon content the measurement error of 4 samples collected from the vicinity of village Somoskőújfalu (No. 260, 313, 314, 315) is great, but ages agree well within the limits of experimental errors. Representative points fit a straight line well, especially in the  $I_2$  diagram. The great error of  $I_2$  age ( $2.30 \pm 0.94$  Ma) arises from the errors assigned to the radiogenic argon contents. This is likely overestimated since, according to the residuals, the error of age is only 0.16 Ma.

Basalt of Medves is represented by samples No. 751 and 752. In the first of them a greater amount of excess argon has been detected. The agreement of  $I_2$  ages ( $2.25 \pm 0.30$  Ma and  $2.30 \pm 0.65$  Ma) with the value derived for basalts at Somoskőújfalu is remarkable.

It can be observed that representative points fit a straight line better in the  $I_2$  diagram. This shows that excess argon is probably incorporated by the ground mass in a more or less uniform concentration. Paleomagnetic polarity of the basalt is reversed (MÁRTON, P., SZALAY, E., 1968) and thus the time of basalt volcanic activity can be fixed at the end of Pliocene in the 2.14—2.48 Ma paleomagnetic zone (MANKINEN, E. A., DALRYMPLE, G. B., 1979.).

In neighbouring Slovakian territory eruption of basalts started earlier and continued until the Early Pleistocene (BALOGH, K., *et al.*, 1981).

#### CHRONOSTRATIGRAPHIC CONCLUSIONS

The  $9.61 \pm 0.38$  Ma age determined on 3 fractions of sample No. 463 is accepted as geological age. Since the basalt ranges in the middle-upper part of the Lower Pannonian an age for the Sarmatian-Pannonian boundary younger than about 11.0 Ma is highly unlikely.

The average age of the youngest Lower Pannonian basalts from boreholes at Kecel (No. 572, 629) is about  $8.3 \pm 0.5$  Ma. Supposing similar rates for the sedimentation and using the age difference between the basalts at Kiskunhalas and Kecel, an age of about 7.5—8.0 Ma might be tentatively assigned to the Lower-Upper Pannonian boundary. This conflicts with unpublished paleomagnetic results indicating ages a bit older than 8 Ma for this event. Considering experimental errors, the possible geological error of samples from Kecel, the uncertainty of rate of sedi-

K/Ar age of basaltic rocks near town Salgótarján, Hungary

TABLE 5

No.	Sample locality	Dated fraction	K %	$^{40}\text{Ar}_{\text{rad}}$ %	$10^{-7} \frac{\text{ccSTP}}{\text{g}}$	$\frac{^{40}\text{Ar}}{^{36}\text{Ar}}$	$\frac{\text{K}/^{36}\text{Ar}}{\left(\frac{\text{ccSTP}}{\text{g}}\right)} \times 10^{-9}$	K/Ar age Ma
260	Somoskőújfalu, quarry	1. w. r.	1.09	6.1	1.181	314.7	0.177	$2.79 \pm 0.64$
313	Somoskőújfalu, quarry lower level	1. w. r.	1.54	7.9	1.522	320.8	0.256	$2.54 \pm 0.45$ $I_s(260+313+314+315):2.49 \pm 0.93$
314	Somoskőújfalu, quarry	1. w. r.	0.836	7.8	0.909	320.5	0.230	$2.80 \pm 0.50$ $I_s(260+313+314+315):2.30 \pm 0.94(\pm 0.16)$
315	Somoskőújfalu, Eresztvény	1. w. r.	1.70	5.5	1.709	312.7	0.171	$2.59 \pm 0.65$
751	Medves, Magyarbánya 5/d	1. w. r.	1.96	29	2.304	416.2	1.027	$3.03 \pm 0.20$ $I_s(751):2.76 \pm 0.34$
		2. mgI	1.06	21	1.569	374.1	0.531	$3.81 \pm 0.27$ $I_s(751):2.25 \pm 0.31$
		3. mgII	2.18	49	2.565	579.4	2.413	$3.03 \pm 0.20$
752	Medves, Középbánya 7/a	1. w. r.	1.47	19	1.295	364.8	0.787	$2.27 \pm 0.20$ $I_s(752):2.01 \pm 0.96$
		2. dnI	2.01	21	1.925	374.1	0.820	$2.47 \pm 0.20$ $I_s(752):2.30 \pm 0.65$
		3. dnII	1.02	16	1.017	351.8	0.565	$2.57 \pm 0.23$

w. r.: whole rock

mgI, mgII: magnetically separated fraction, numbered in the order of increasing magnetic susceptibility

dnI, dnII: fraction separated by heavy liquid, numbered in the order of increasing density

mentation and the variation in time of the Lower-Upper Pannonian boundary, the deviation of radiometric and paleomagnetic results is not too serious.

In several previous papers (JÁMBOR, Á., *et al.*, 1980, BALOGH, L., *et al.*, 1983a) the age value of the Lower-Upper Pannonian boundary has been estimated using the youngest ages from the Lower Pannonian and the oldest age from the  $Pa_2^3$  level measured on sample No. 399 coming from borehole Kaposcs—1 ( $I_1 = 4.66 \pm 0.36$  Ma). These data allowed the correlation of the Lower-Upper Pannonian and the Miocene-Pliocene boundaries at 5.5 Ma ago (BERGGREN, W. W. 1979). However, basaltic volcanic activity in the Balaton Highland started with tuff production in the  $Pa_2^3$  level (*Congerina unguiculaprae*, JÁMBOR, Á., 1980), therefore the oldest tuffs have to be older than the basalts of Hegyestő and Kőhegy and the commencement of the Upper Pannonian must have preceded the time of the first tuff eruption. This is an additional argument to fix the Miocene-Pliocene boundary (according to newer investigations its age is 5.2 Ma (MCDUGALL, J., *et al.*, 1977) within the Upper Pannonian.

$4.25 \pm 0.32$  Ma and  $4.15 \pm 0.34$  Ma  $I_1$  ages were determined on whole rock samples for the basalts of the Little Plain and on fractions of sample No. 387, respectively. The basalts overlie sediments of the *Unio wetzleri* ( $Pa_2^3$ ) level (JÁMBOR, Á., *et al.*, 1981), thus an older age; at least 4.5 Ma has to be assigned to the beginning of  $Pa_2^3$  level in the Little Plain. On the other hand, at Pula the  $I_1$  age of  $4.25 \pm 0.17$  Ma marks the end of the  $Pa_2^3$  level. According to the dating of hills at Szigliget, the tuff eruptions did not start much before 4 Ma but the deposition of  $Pa_2^3$  sediments continued during the tuff accumulation. It has been described earlier that the boundary of  $Pa_2^3$  and  $Pa_2^2$  levels is not an isochron surface (BARTHA, F., 1959). This picture is confirmed by the K/Ar datings which yield for this boundary a time span starting at least 4.5 Ma ago and ending after 4 My or possibly 3.5 Ma before present.

The jumillite at Bár lying on Early Pleistocene red clay is a little older than 2 Ma. Accepting 1.8 Ma for the Pliocene-Pleistocene boundary, part of the sediments classified as Early Pleistocene in Hungary has to be transferred to the Uppermost Pliocene. This has been confirmed by paleomagnetic investigations resulting in ages in excess of 2 Ma for Early Pleistocene sediments (RÓNAI, A., SZEMETHY, A., 1979).

#### ACKNOWLEDGEMENTS

The authors express their gratitude to GÉZA HÁMOR and ÁRON JÁMBOR for initiating and supporting this work and for their continuous interest. The majority of the dated rocks was collected with the help of G. SOLTÍ and additional samples were supplied by B. CSEREPES-MESZÉNA and A. NUSSZER (No. 463, 571, 572, 629), P. MERZICH (No. 1021—1026), Z. BORSY (No. 884, 885), E. SZALAY (No. 1142, 1143) and A. EMBEY — ISZTIN (No. 995); their valuable help is gratefully acknowledged. This research was sponsored primarily by the Central Geological Office, Budapest.

#### REFERENCES

- BALÁZS, E., NUSSZER, A. (1982): Magyarország medenceterületeinek alsópannóniai vulkanizmusa. Manuscript. Hung. Geol. Inst., Archives.
- BALOGH, KADÓSA (1985): K/Ar dating of Neogene volcanic activity in Hungary: Experimental technique, experiences and methods of chronological studies. ATOMKI Rep. (In press)
- BALOGH, KADÓSA, MÓRIK, GY. (1978): Magnetic mass spectrometer for K-Ar dating (In Hungarian). ATOMKI Közl., 20, 215—228.

- BALOGH, KADOSA, MÓRIK, GY. (1979): High capacity argon extraction and purification system (In Hungarian). *ATOMKI Közl.*, **21**, 363—375.
- BALOGH, KADOSA, MIHALIKOVA, A., VASS, D. (1981): Radiometric dating of basalts in Southern and Central Slovakia. *Západné Karpaty, Séria geol.* **7**, Geol. Ust. D. Stura, 113—126.
- BALOGH, KADOSA, JÁMBOR, Á., PARTÉNYI, Z., RAVASZ-BARANYAI, L., SOLT, G., NUSSZER, A. (1983a): Petrography and K/Ar dating of Tertiary and Quaternary basaltic rocks in Hungary. *An. Inst. Geol. Geof. Bucharest*, **LXI**, 365—373.
- BALOGH, KADOSA, PÉCSKAY, Z., SZÉKY-FUX, V., GYARMATI, P. (1983b): Chronology of Miocene volcanism in North-East Hungary. *An. Inst. Geol. Geofiz.*, Bucharest, **LXI**, 149—158.
- BARTHA, F. (1959): Geologische Ergebnisse von feinstratigraphischen Untersuchungen an oberpannonischen Bildungen von der Umgebung des Balatonsees. (In Hungarian). *Földt. Közl.*, **89**, 23—26.
- BENCZE, G., JÁMBOR, Á., PARTÉNYI, Z. (1979): Exploration of alginite (oil-shale) and bentonite deposits between Várkesző and Malomsok. (In Hungarian) *Ann. Rep. of the Hung. Geol. Inst. of 1977*. 257—267. *Műszaki Kiadó*, Budapest.
- BERGGREN, W. A. (1969): Cenozoic chronostratigraphy, foraminiferal zonation and the radiometric time scale. *Nature* **224**, 1072—1074.
- CSEREPES-MESZÉNA, B. (1978): On the Lower Pannonian basalts and Proterozoic migmatites uncovered by the hydrocarbon-exploratory borehole Kiskunhalas — Ny — 3. (In Hungarian). *Földt. Közl.*, **108**, 53—64.
- EMBEY-ISZTIN, A. (1981): Statistical analysis of major element pattern in basic rocks of Hungary: An approach to determine their tectonic setting. (In Hungarian). *Földt. Közl.*, **111**, 43—58.
- EMBEY-ISZTIN, A. (1984): Texture types and their relative frequencies in ultramafic and mafic xenoliths from Hungarian alkali basaltic rocks. *Annales Historico-Naturales Musei Nationalis Hungarici* **LXXXVI**, 43—58.
- GYARMATI, P. (1977): Intermediate volcanism in the Tokaj Mountains. *Ann. Hung. Geol. Inst.*, **LVIII**.
- HÖNIG, GY. (1971): A bári B—4, B—5 és B—6 számú fúrások rétegsora. Manuscript. Hung. Geol. Inst. Archives.
- JÁMBOR, A. (1980): Pannonian in the Transdanubian Central Mountains. *Ann. Hung. Geol. Inst.*, **LXII**, *Műszaki Kiadó*, Budapest.
- JÁMBOR, Á., SOLT, G. (1976): Geological conditions of the Upper Pannonian oil shale deposit recovered in the Balaton Highland and at Kemeneshát. (In Hungarian) *Ann. Rep. of the Hung. Geol. Inst. of 1974*, 193—219. *Műszaki Kiadó*, Budapest.
- JÁMBOR, A., PARTÉNYI, Z., RAVASZ-BARANYAI, L., SOLT, G., BALOGH, K. (1980): K/Ar dating of basaltic rocks in Transdanubia, Hungary. *ATOMKI Közl.*, **22**, 172—190.
- JÁMBOR, Á., PARTÉNYI, Z., SOLT, G. (1981): Geological features of basalt volcanics in Transdanubia. (In Hungarian). *Ann. Rep. of the Hung. Geol. Inst. of 1979*, 225—239. *Műszaki Kiadó*, Budapest.
- JUGOVICS, L. (1969): Basalt und Basalttuffgebiete, Transdanubiens. (In Hungarian). *Ann. Rep. of the Hung. Geol. Inst. of 1967*, 75—82. *Műszaki Kiadó*, Budapest.
- JUGOVICS, L. (1971a): Über die Basaltgebiete von Nordungarn (Umgebung von Salgótarján). (In Hungarian). *Ann. Rep. of the Hung. Geol. Inst. of 1968*, 145—165. *Műszaki Kiadó*, Budapest.
- JUGOVICS, L. (1971b): Über den Bau der Basaltgebiete des Balatonhochlandes und des Tapolcaer Beckens. (In Hungarian). *Ann. Rep. of the Hung. Geol. Inst. of 1968*, 223—244. *Műszaki Kiadó*, Budapest.
- JUGOVICS, L. (1972): Die Basalt und Basalttuffvorkommen der Kleinen Ungarischen Tiefebene. (In Hungarian). *Ann. Rep. of the Hung. Geol. Inst. of 1970*, 29—101. *Műszaki Kiadó*, Budapest.
- JUGOVICS, L. (1976): Chemical features of the basalts in Hungary (In Hungarian). *Ann. Rep. of the Hung. Geol. Inst. of 1974*, 431—470. *Műszaki Kiadó*, Budapest.
- KULCSÁR, L., GUZY-SOMOGYI, A. (1962): Le volcan de Sághegy de Celldömölk. (In Hungarian). *Acta Geogr. Debr.*, **VIII/1**, No. 27, 33—83.
- LÓCZY, L. (1913): A Balaton környékének geológiai képződményei és ezek vidékek szerinti telepedése. A Balaton tudományos tanulmányozásának eredményei. I. I. 1., 1—581, Budapest.
- MANKINEN, E. A., DALRYMPLE, G. B. (1979): Revised Geomagnetic Polarity Time Scale for the Interval 0—5 m. y. *B. P. J. Geophys. Res.*, **84**, 615—626.
- MÁRTON, P., SZALAY, E. (1968): Paläomagnetische Untersuchungen an Basaltlaven von Ungarn. *Acta Geol. Hung.*, **12**, 291—305.
- MCDUGALL, I., SAEMUNDSON, K., JOHANNESSON, H., WATKINS, N. D., KRISTJANSSON, L. (1977): Extension of the geomagnetic polarity time scale to 6.5 m. y.: K-Ar dating, geologic and paleomagnetic study of a 3,500 m lava succession in western Iceland. *Geol. Soc. Am. Bull.*, **88**, 1—13.



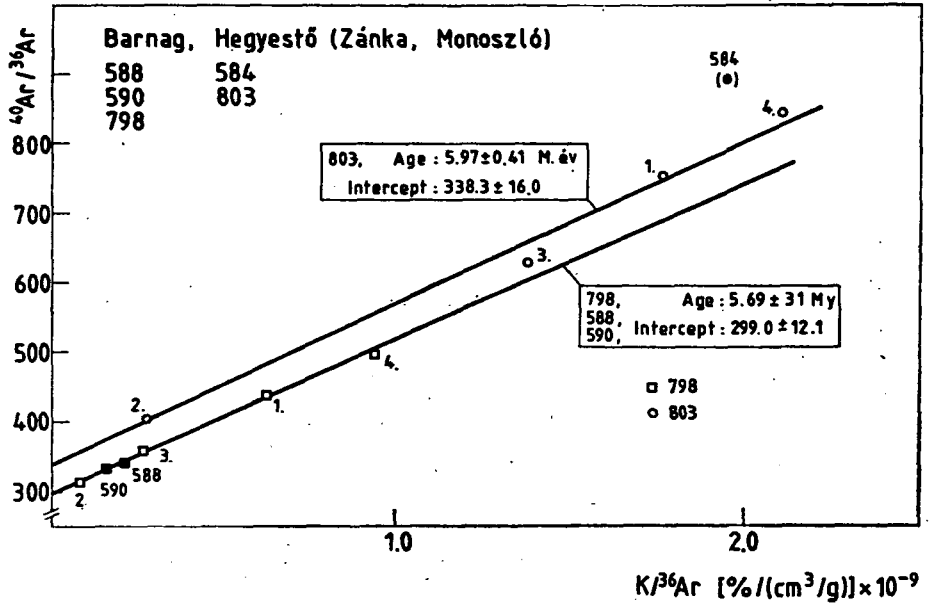
- MIYASHIRO, A. (1975): Classification, characteristics, and origin of ophiolites. *Jour. Geol.*, **85**, 249—276.
- MOLNÁR, J., PAÁL, A., SEPSY, K. (1980): Microprocessor based system for control, data acquisition, and processing. (In Hungarian). *ATOMKI Közl.*, **22**, 369—373.
- NAGY, G. (1983): Cooling history of young Hungarian basalts based on zoning of olivine phenocrysts. *Acta Geol. Hung.*, **26**, 321—339.
- PANTÓ, GY. (1981): Rare earth element geochemical pattern of Cenozoic volcanism in Hungary. *Earth Evol. Sci.*, **3—4**, 249—256.
- PAP, S. (1983): Lower Pannonian basalt volcanism in the Balástya and Üllés—Ruzsa—Zákányszék areas. (In Hungarian). *Földt. Közl.*, **113**, 163—170.
- RAVASZ, CS. (1976): Petrographic examinations of oil-shale at Pula and Gérce. (In Hungarian). *Ann. Rep. of the Hung. Geol. Inst. of 1974*, 221—245. Műszaki Kiadó, Budapest.
- RAVASZNÉ BARANYAI, L. (1979): Bár, alkáli magmás vulkanitok ásvány-kőzettani vizsgálata. Manuscript. Hung. Geol. Inst. Archives.
- RÓNAI, A., SZEMETHY, A. (1979): Latest result of lowland research in Hungary. Palaeomagnetic measurements on unconsolidated sediments. (In Hungarian). *Ann. Rep. of the Hung. Geol. Inst. of 1977*, 67—83. Műszaki Kiadó, Budapest.
- STEIGER, R. H., JÄGER, E. (1977): Subcommittee on Geochronology: Convention on the use of decay constants in geo- and cosmochemistry. *Earth and Plan. Sci. Letters* **36**, 359—362.
- SZÁDECZKY-KARDOSS, E., ERDÉLYI, J. (1957): Über die Zeolithbildungen der Basalte der Balaton-gegend (In Hungarian). *Földt. Közl.*, **87**, 302—308.
- SZEDERKÉNYI, T. (1980): Petrological and geochemical character of the Bár basalt, Baranya county, South Hungary. *Acta Miner.-Petr.*, Szeged, **XXIV/2**, 235—244.
- VICZIÁN, I. (1965): Basalt aus dem Komitat Baranya. (In Hungarian). *Földt. Közl.*, **95**, 448—452.
- VITÁLIS, I. (1908): A balatonfelvidéki bazaltok. A Balaton tudományos tanulmányozásának eredményei I. I. 2., 1—169, Budapest.
- VOGL, M. (1979): Geochemical examination of basalts in Hungary. 1. Little Hungarian Plain. 2. Southern Bakony Mountains. (In Hungarian). *Ann. Rep. of the Hung. Geol. Inst. of 1977*, 343—361. Műszaki Kiadó, Budapest.
- VOGL, M. (1980): Geochemical examination of basalts in Hungary. 3. Tátika group. (In Hungarian). *Ann. Rep. of the Hung. Geol. Inst. of 1978*, 333—341. Műszaki Kiadó, Budapest.
- ~ VÖRÖS, I. (1966): Volcanological and structural relations of the Kabhegy-area. (In Hungarian). *Földt. Közl.*, **96**, 292—300.

*Manuscript received, 10 October, 1985*

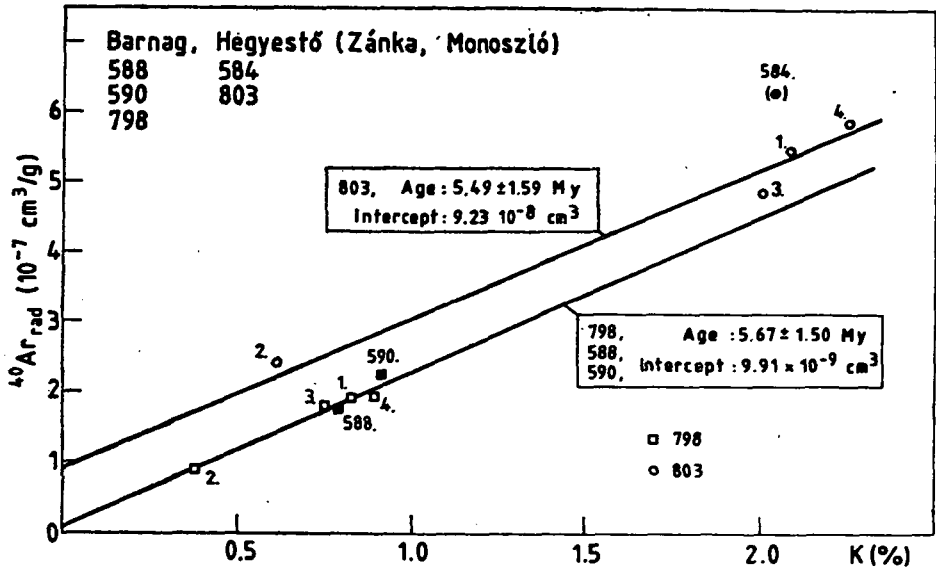
# Appendix

## Isochron diagrams

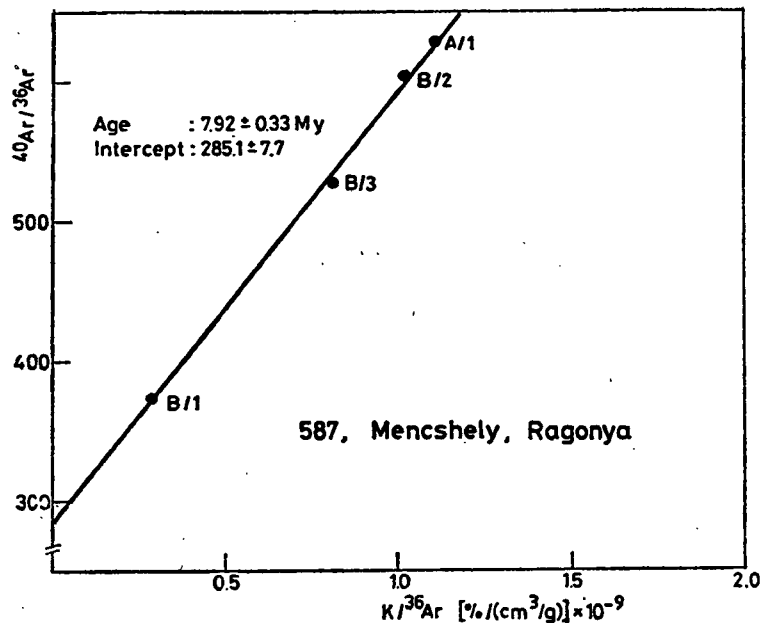
I



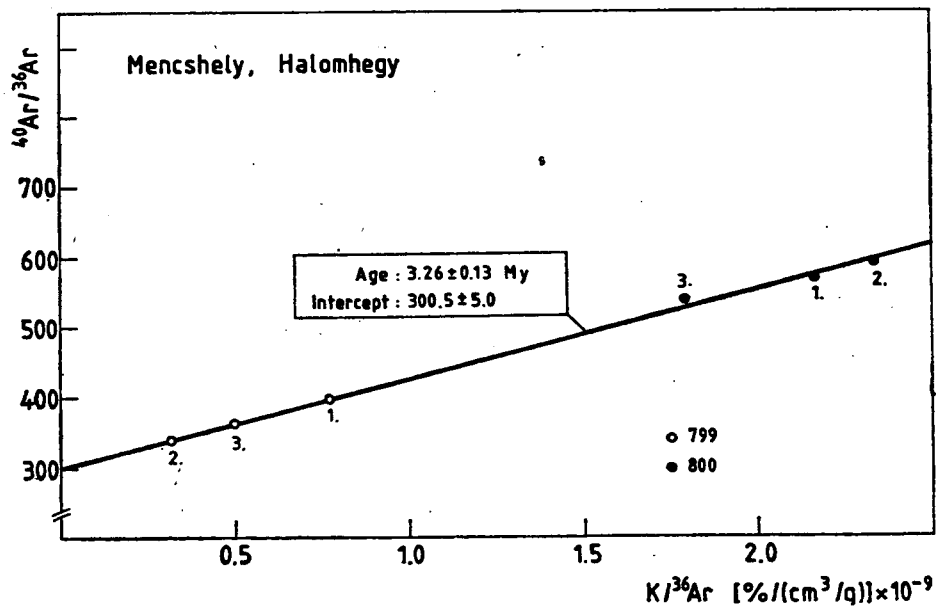
II



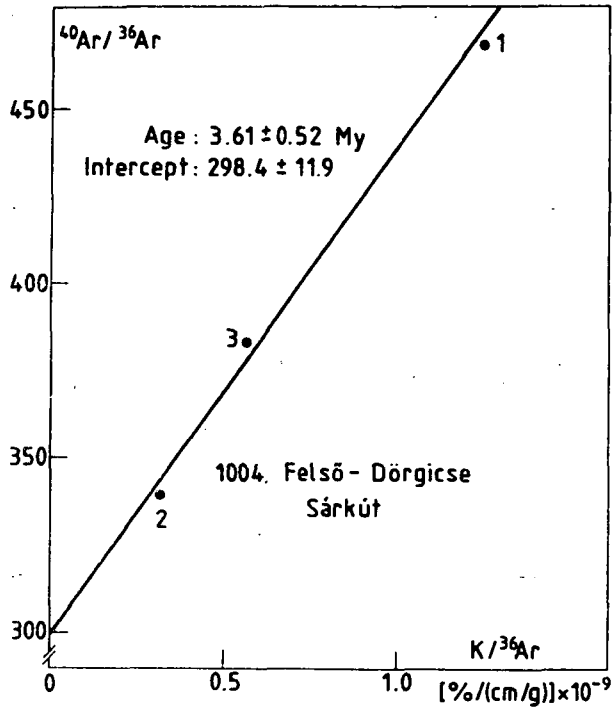
### III



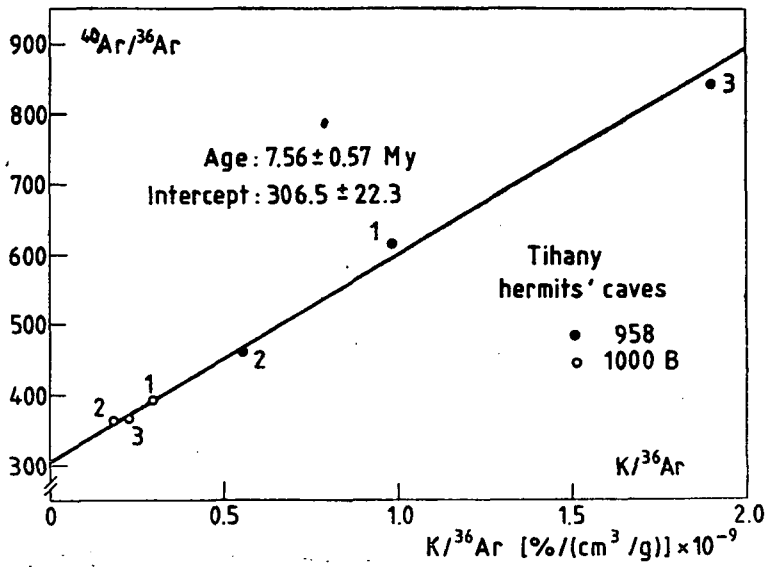
### IV



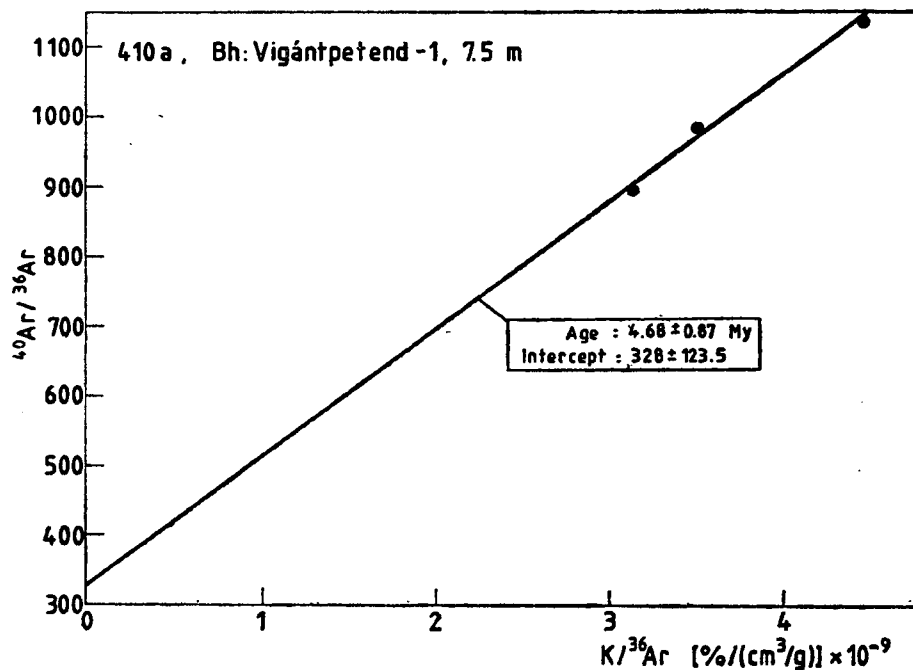
V



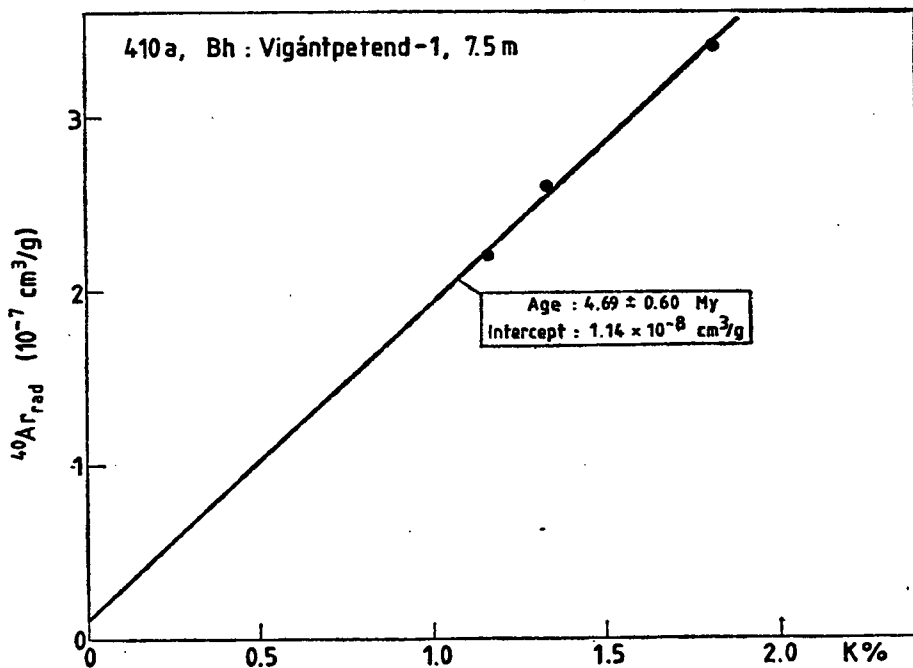
VI



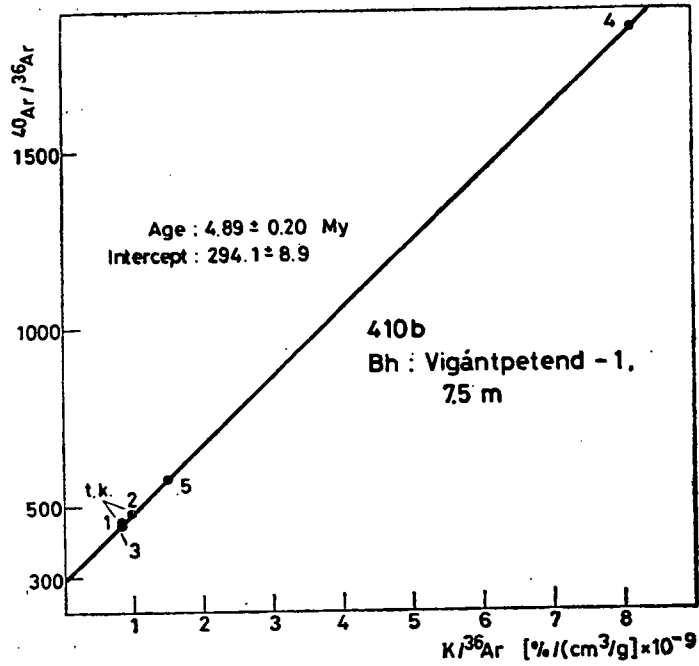
# VII



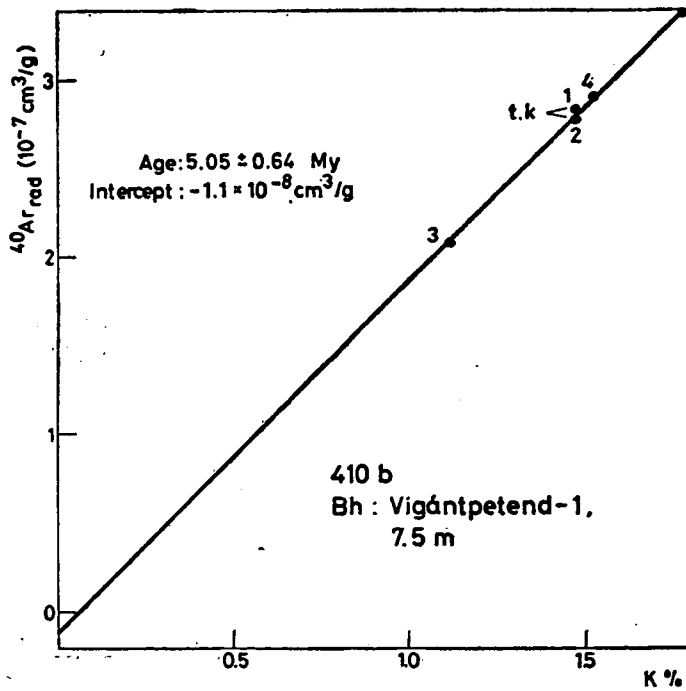
# VIII



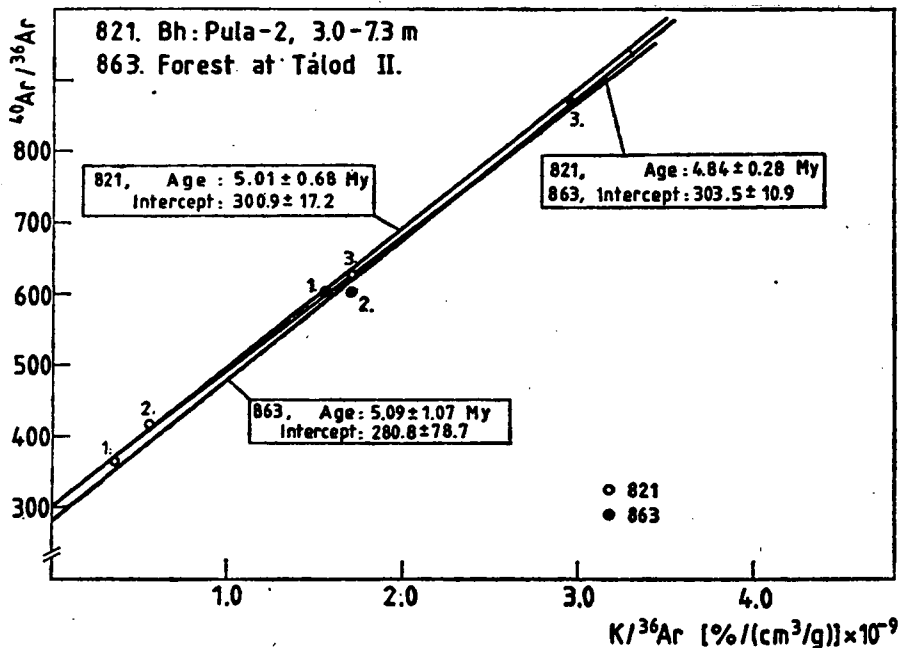
IX



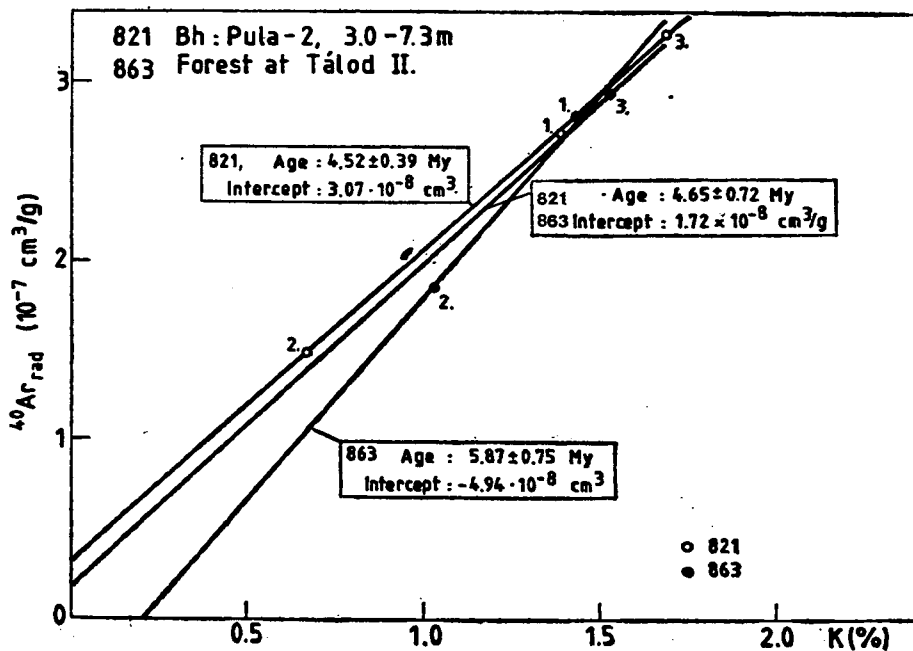
X



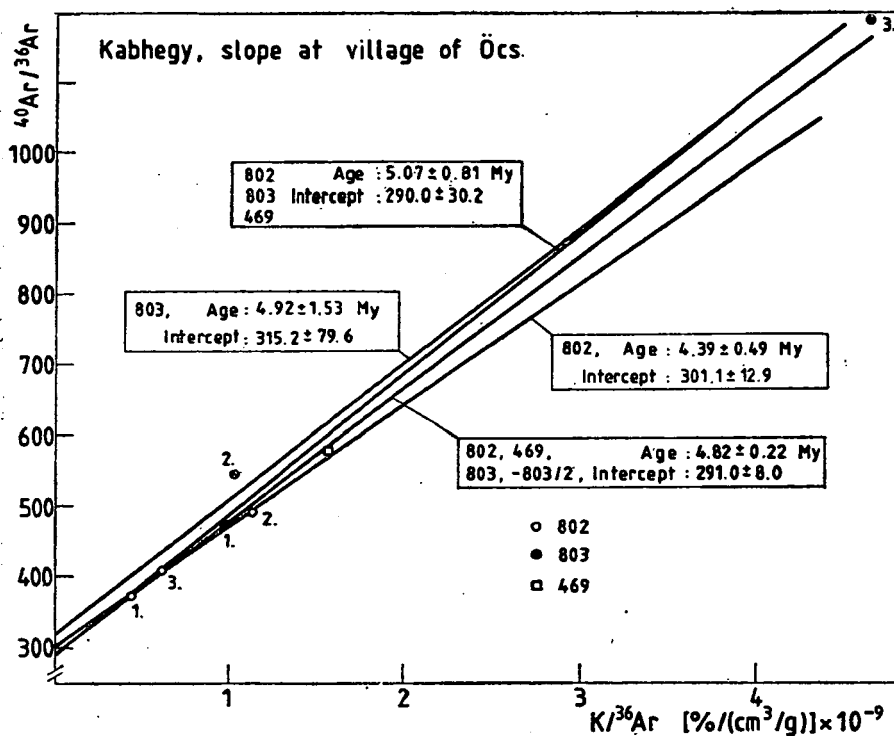
XI



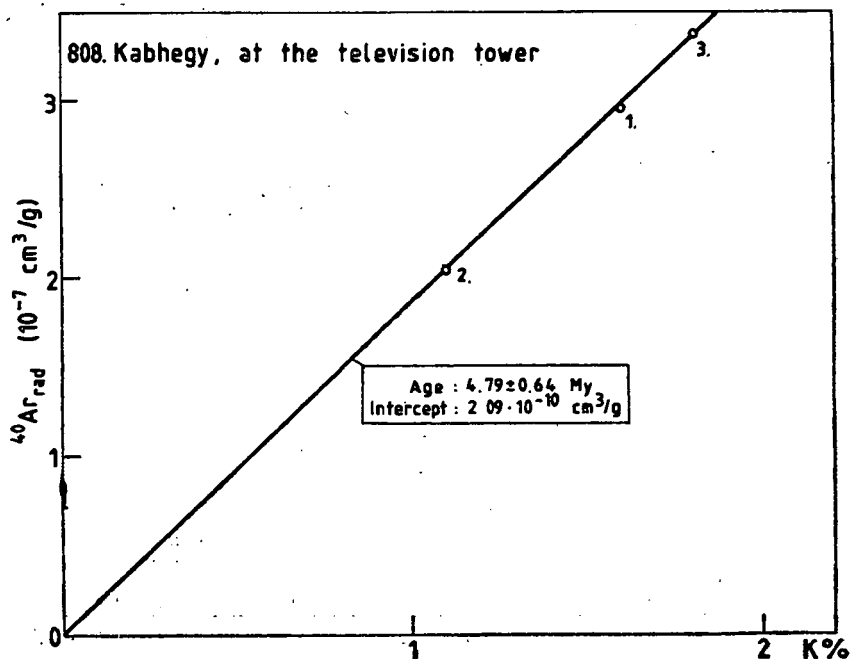
XII



### XIII

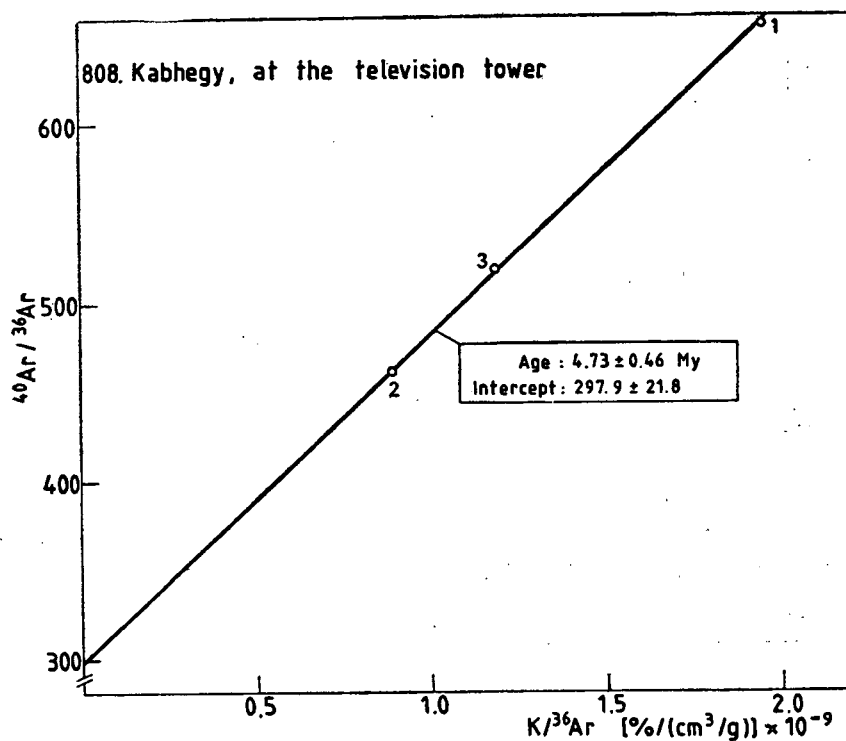


### XIV

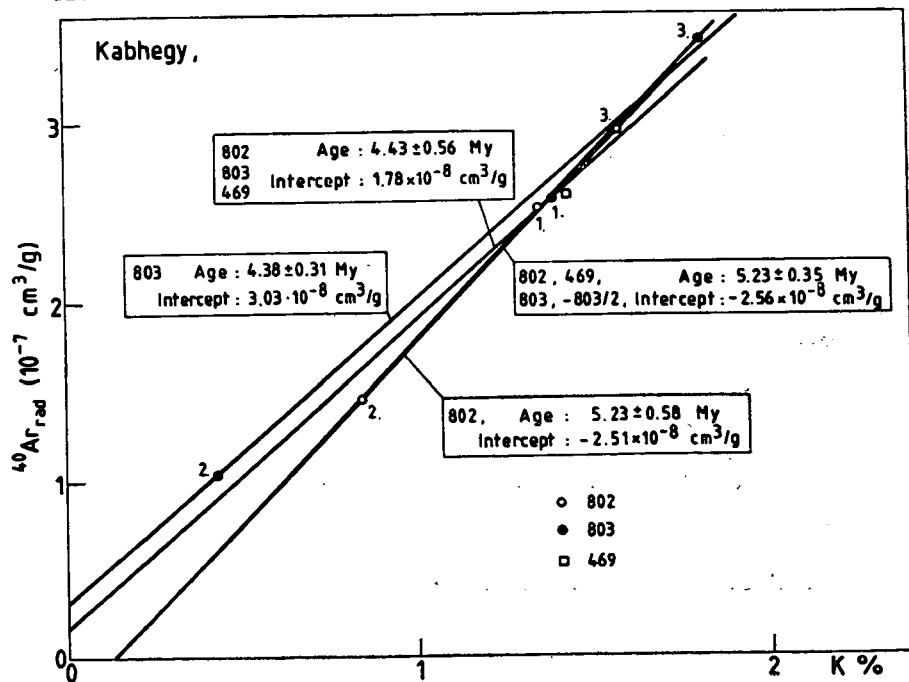




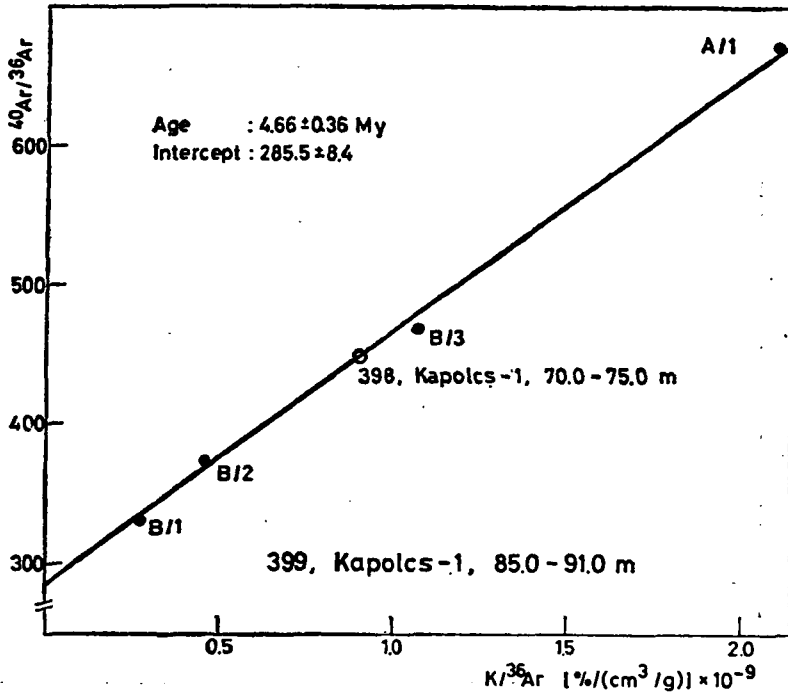
XV



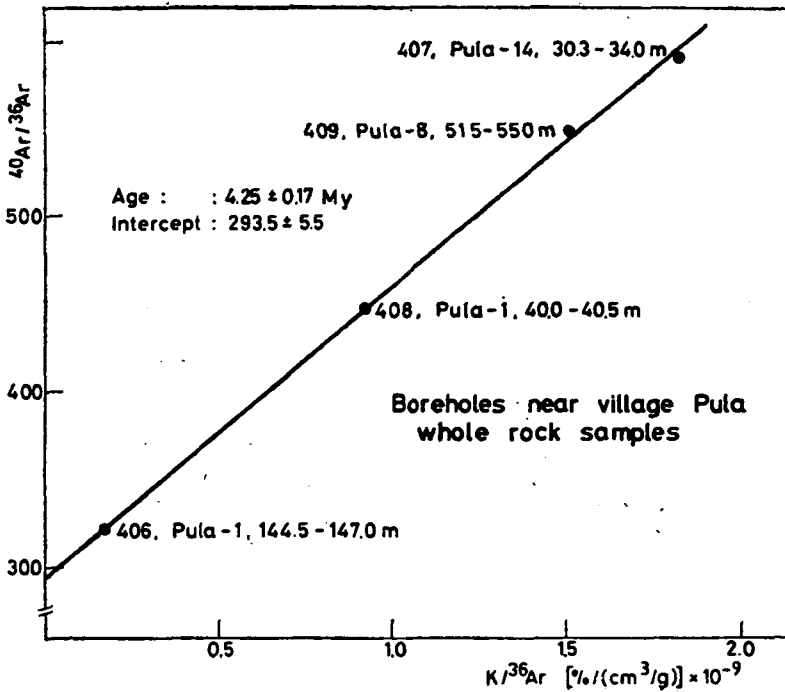
XVI



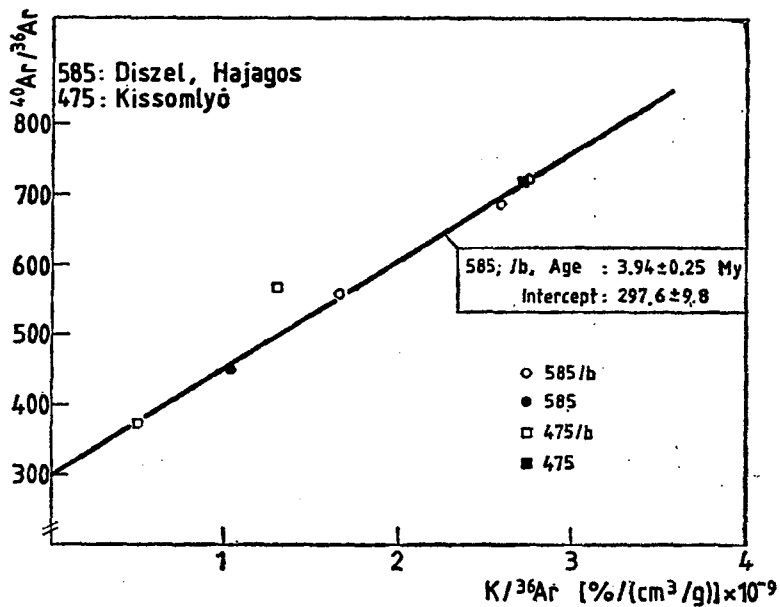
# XVII



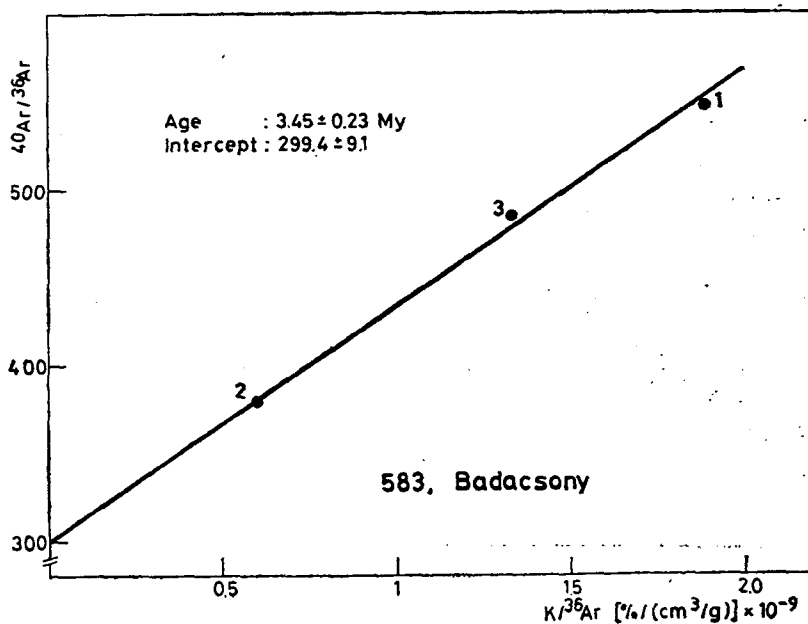
# XVIII



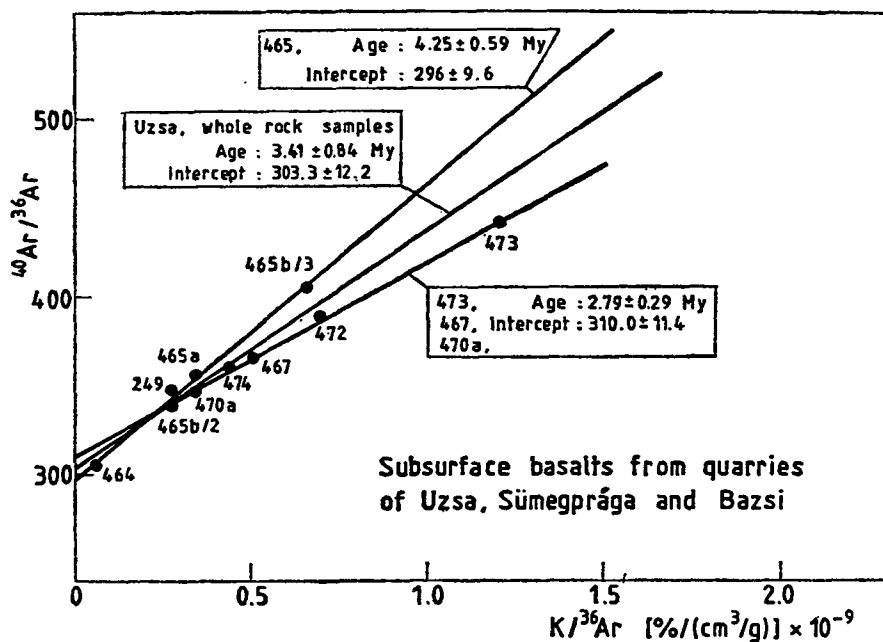
XIX



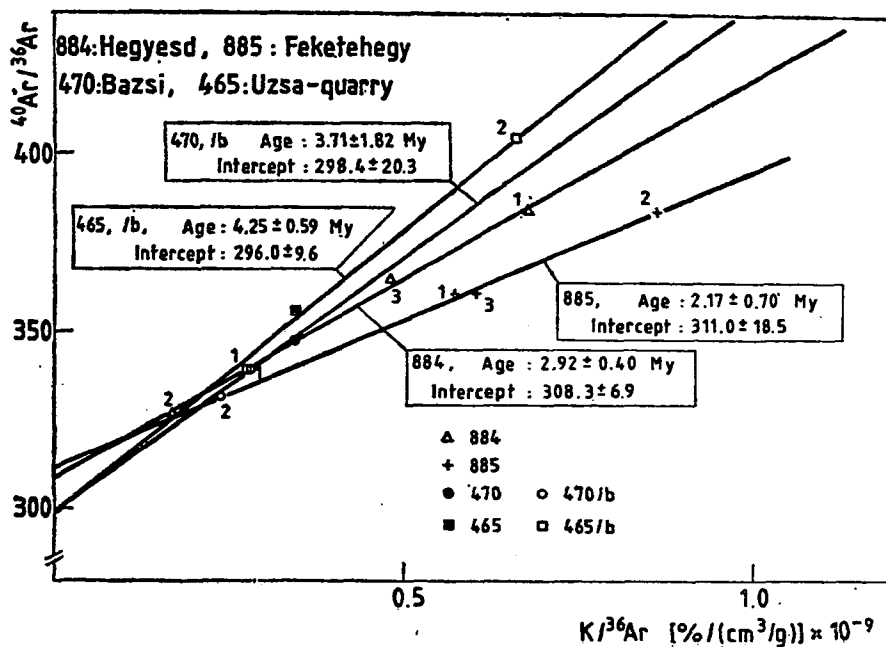
XX

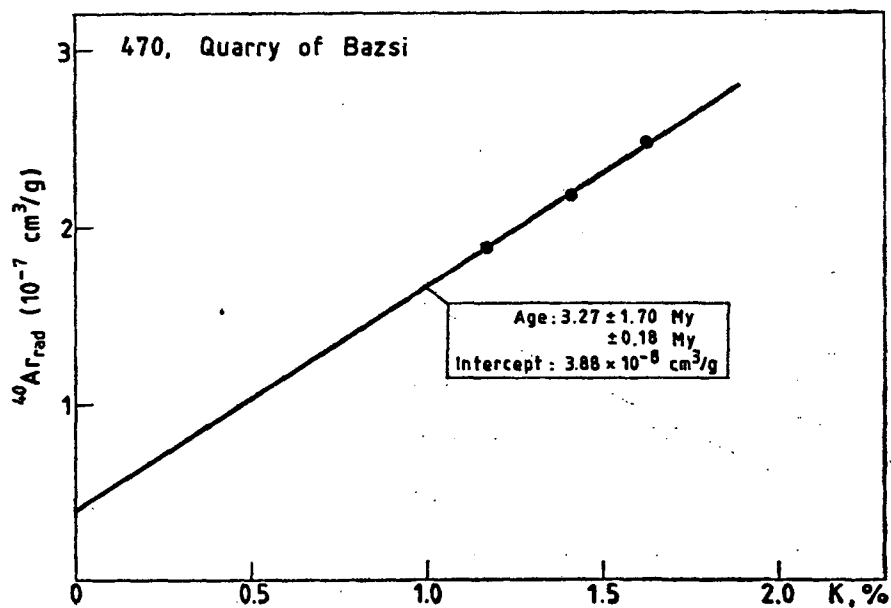
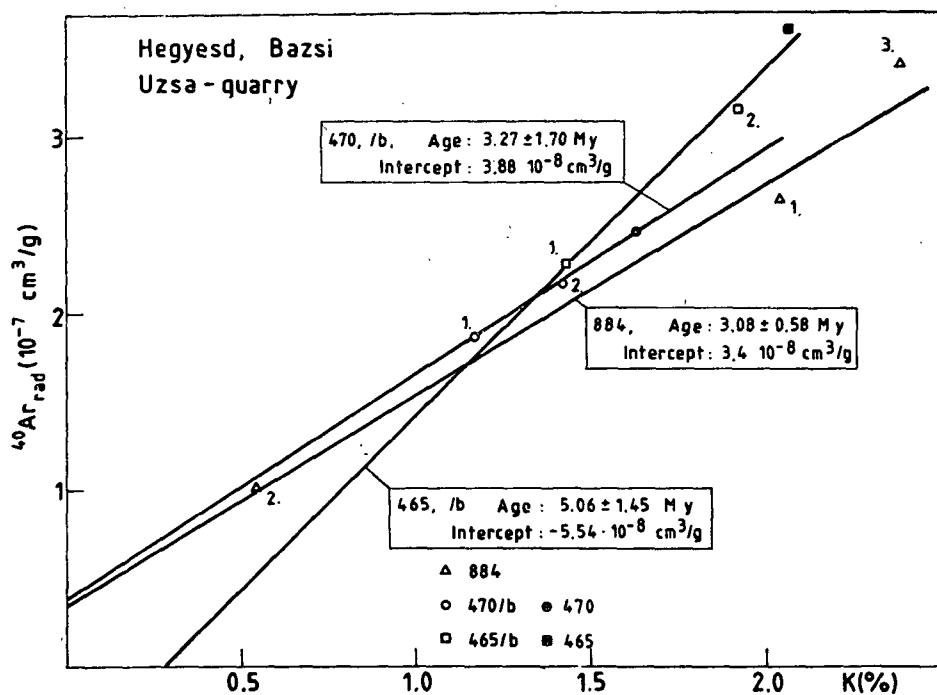


XXI

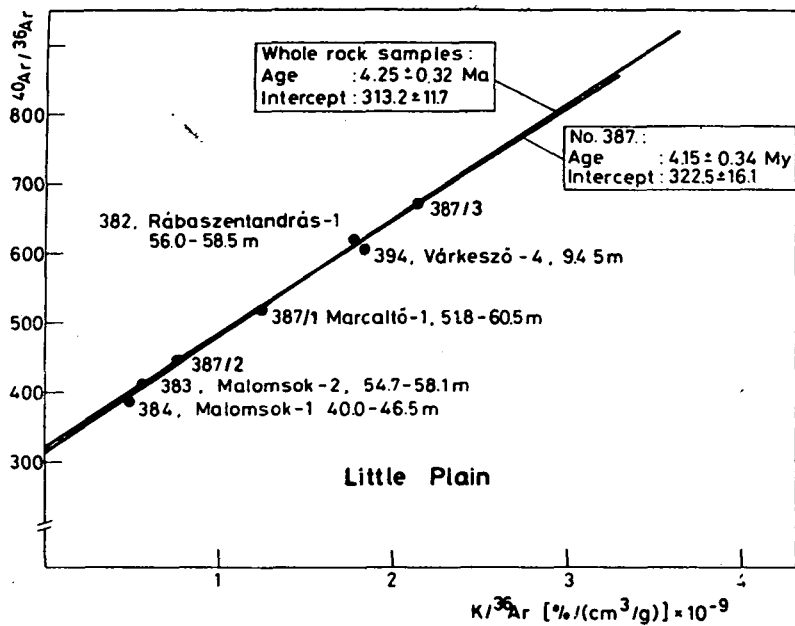


XXII

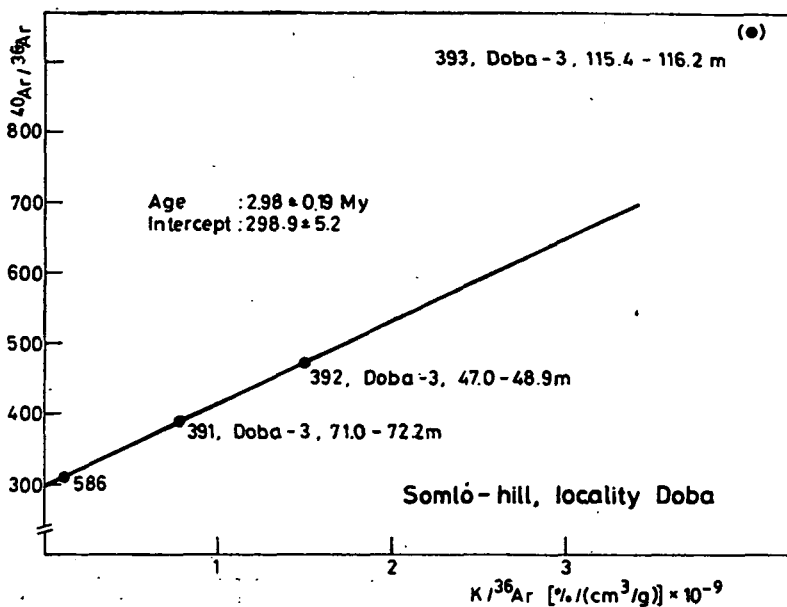




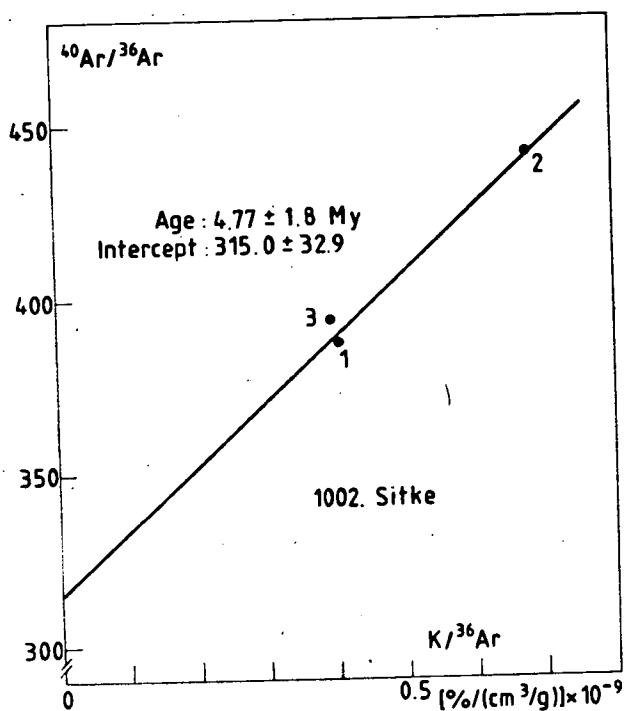
XXV



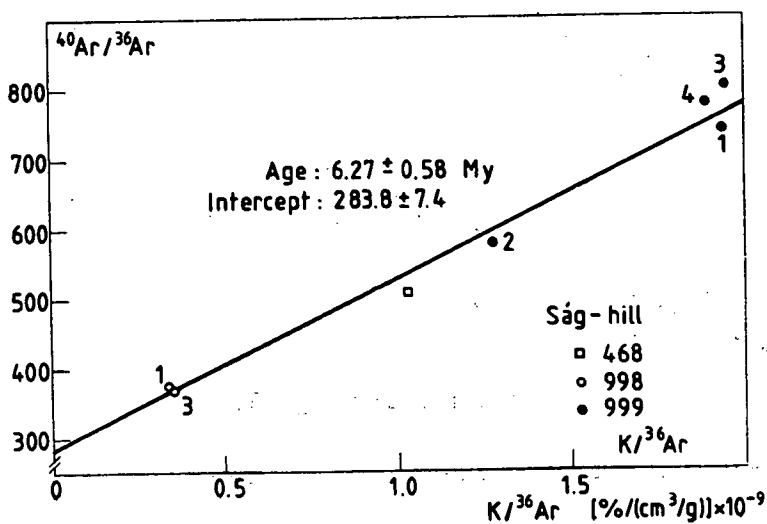
XXVI



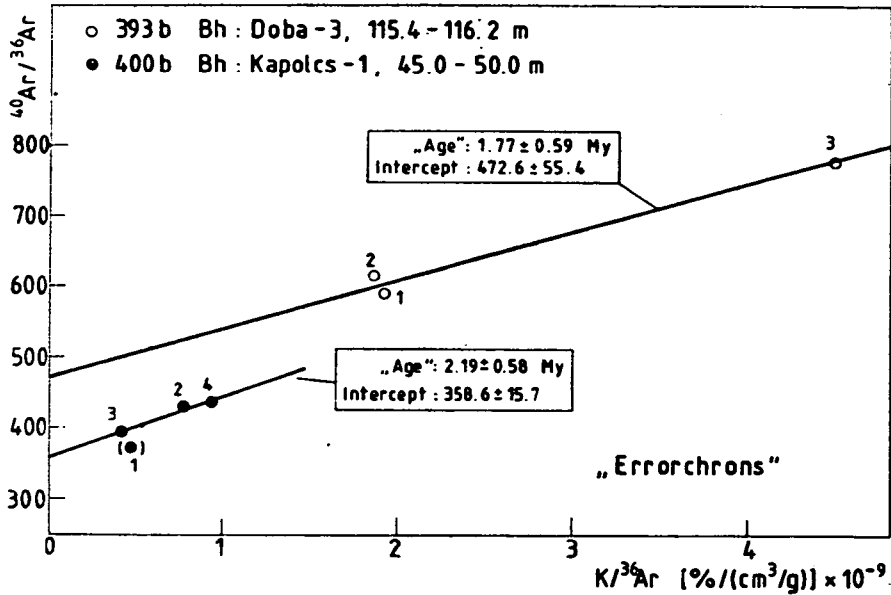
# XXVII



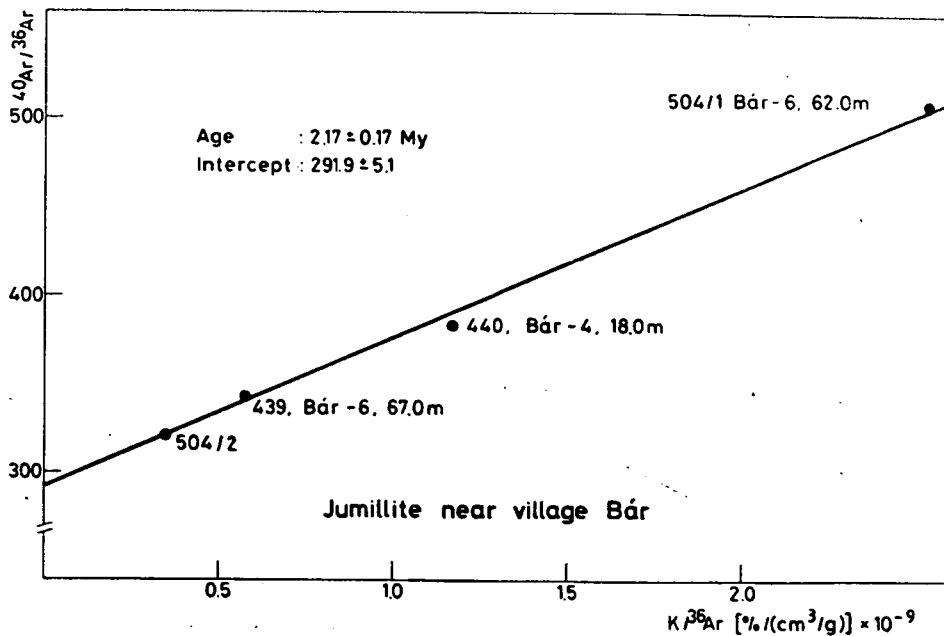
# XXVIII



XXIX

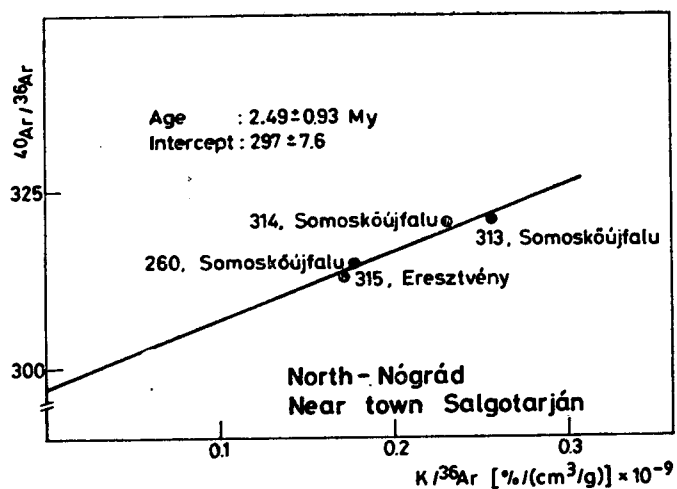


XXX

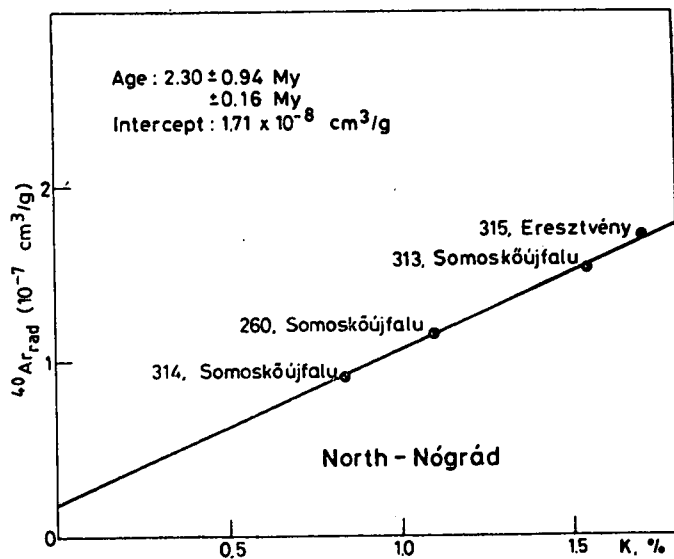




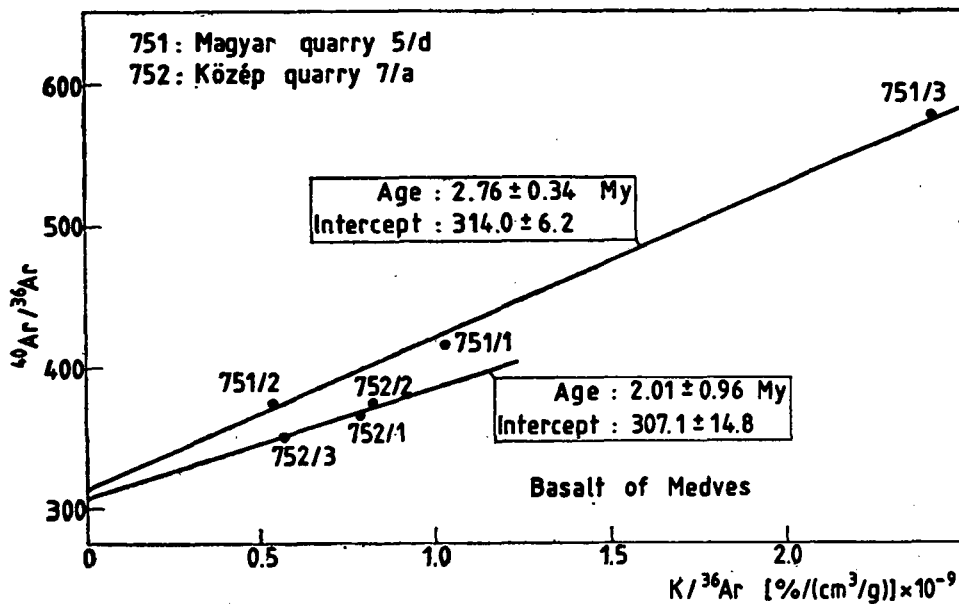
XXXI



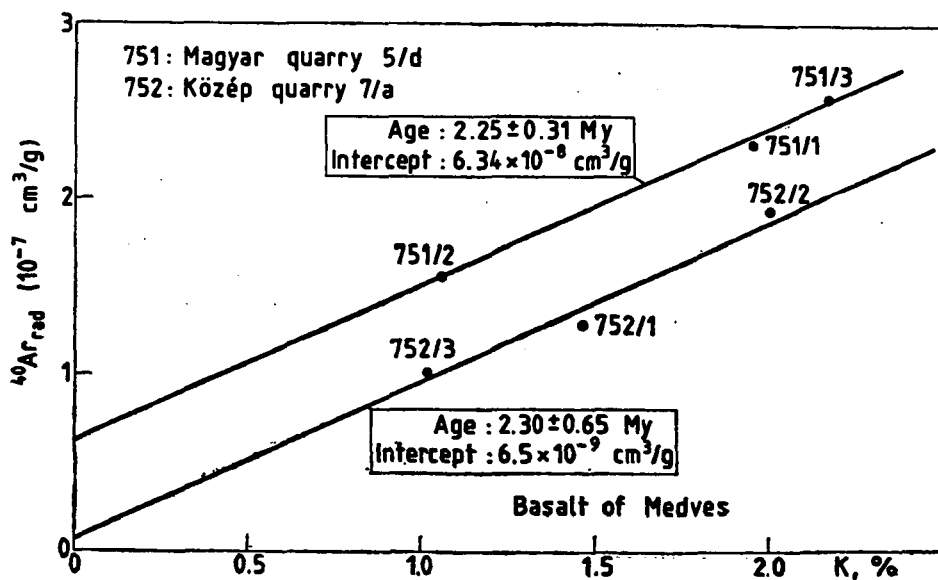
XXXII



XXXIII



XXXIV



## ORGANIC GEOCHEMICAL CHARACTERIZATION OF BROWN COALS BY THERMAL DEGRADATION AND MODIFIED ROCK-EVAL METHOD

M. HETÉNYI<sup>1</sup> and M. KEDVES<sup>2</sup>

<sup>1</sup>Department of Mineralogy, Geochemistry and Petrography,  
Attila József University

<sup>2</sup>Department of Botany, Attila József University

### ABSTRACT

The relationships between the organic geochemical features of brown coals and the peculiarities of the formation micro-environment determined on the basis of microscopic plant remnants of the samples have been studied.

Samples were brown coals of Eocene age from the Dorog and Tatabánya basins (Hungary, Transdanubia).

The organic matter falls between the types II and III (i.e. between oil prone and gas prone). The more exact position of the samples within the group is determined mainly by the macro-environment (i.e. the locality). Within a given locality some relationships could be observed also among the microenvironmental features.

The hydrocarbon genetic potential of the samples was characterized by experimental thermal degradation and step-by-step Rock-Eval pyrolysis. In case of Rock-Eval pyrolysis the isotherm temperature between the steps was increased by 20 °C. Based on the results it is plausible that the hydrocarbon genetic potential of brown coals and the oil quantity to be obtained by experimental thermal degradation are considerably influenced by the chemical-biological features of the micro-environment. The value of the gas-hydrocarbon genetic potential and its change as a function of temperature are unambiguously determined by the character of the micro-environment.

Keywords: modified Rock-Eval pyrolysis, brown coal, hydrocarbon genetic potential, thermal degradation, plant remnants.

### INTRODUCTION

Rock-Eval pyrolysis is a rapid and effective means of characterizing the quality and thermal maturity of kerogens and perspective source rocks. The procedure and apparatus has been developed by ESPITALIÉ *et al.*, (1977). In Rock-Eval pyrolysis pulverized rock samples are progressively heated to 550 °C under an inert atmosphere. The quantity of the hydrocarbons which have been released in this temperature programmed pyrolysis is mentioned as genetic potential (TISSOT and WELTE, 1984), petroleum potential (ESPITALIÉ, 1977) or petroleum generative potential (PETERS, 1986) of the sediments. During the assay, the hydrocarbons already present in the rock in a free or adsorbed state are volatilized at a moderate temperature. This is the first peak of the pyrogram (S1). The second peak of the pyrogram (S2) represents the hydrocarbons generated by the cracking of kerogen. The temperature at which the maximum cracking of the organic matter occurs is called  $T_{max}$ . The pyrolysis of the organic matter results in generating oxygen containing volatiles (S3), too. On the basis of S1, S2, S3,  $T_{max}$  and the total organic carbon content (TOC), the

<sup>1</sup> H—6701 Szeged, Pf. 651, Hungary

<sup>2</sup> H—6701 Szeged, Pf. 657, Hungary

This sample is very rich in sporomorphs, but the number of the species is few. The spores of tropical ferns (Schizaeaceae, *Anemia*, *Cicatricosisporites dorogensis*, Plate I—9) are dominant: 44.5%, the quantity of the “tranquillus type” palm pollen grains is nearby the same, 42.4% (Plate I—10, 11). Sporomorphs occurring in a small quantity: *Lygodium* (3.0%) tropical fern genus (Plate I—7, 8), *Cycadopites minor* (2.7%), *Cycadopites kyushuensis* (1.7%), “granulatus type” palm pollen grains (1.4%), (Plate I—12), Fagaceae *Cupuliferoipollenites pusillus* (1.4%).

This spore-pollen spectrum reflects the “tranquillus type” palm forest, with fern (*Anemia*-*Mohria*, *Lygodium*) undergrowth.

#### Sample No T—6

The plant tissue remnants (Plate II—3) are degraded, with a high quantity of fungous remnants. Very often the hyphae penetrate the tissue remnants (Plate II—4, 7). The resinous drops are few.

The sample is in general poor in sporomorphs, but the number of the species is relatively high. It is worth of mentioning that there is not a single species with predominant quantity. The important percentage of the palynomorphs is as follows: *Monocolpopollenites tranquillus* (Palmae) 24%, Fagaceae: *Cupuliferoipollenites pusillus* (20.0%), *C. oviformis* (15.5%), Myricaceae (20.0%), the presence of the pollen grains of the form-genus *Plicatopollis* (Juglandaceae) is also important.

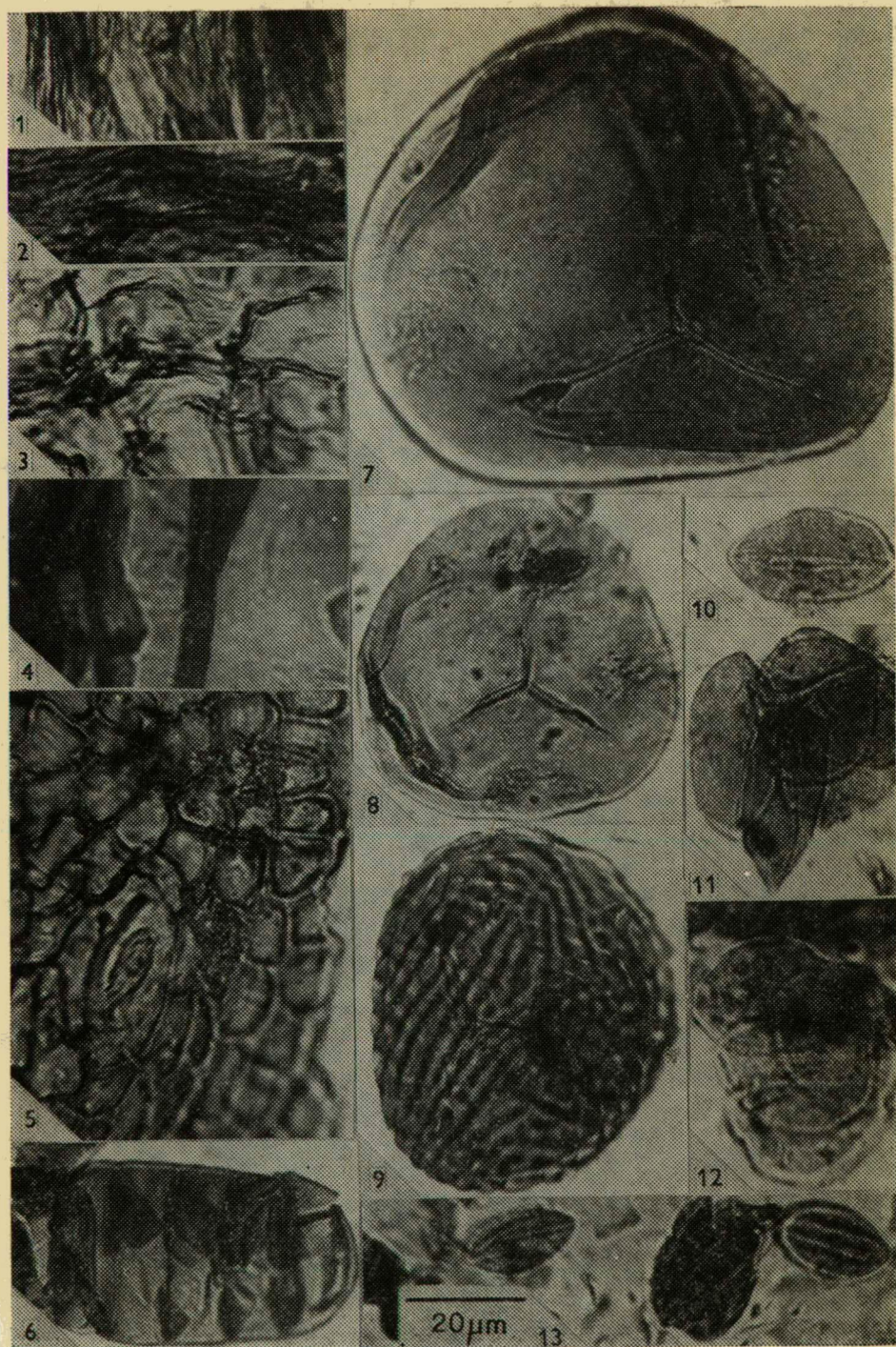
The destroyed organic material bleed with fungous hyphae indicates an intense biological activity during the sedimentation process. Before this there was a strong oxidation, as an antecedent of the microbial activity. The spore-pollen spectra suggest in inundated open swamp, the pollen grains fell in the sedimentary basin, from the vegetation zones of the river side.

## EXPLANATION OF PLATES

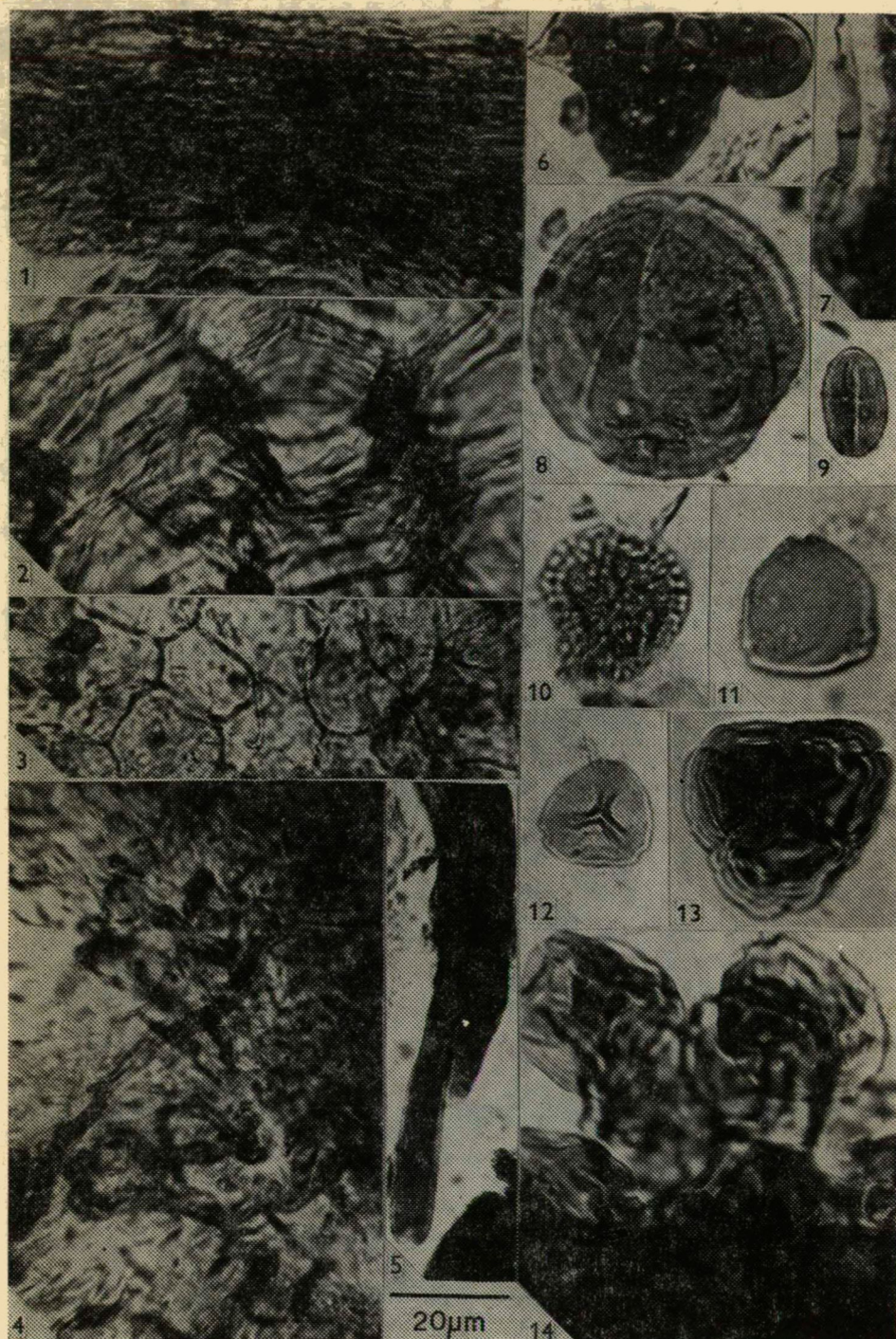
### Plate I

1. Degraded plant tissue remnants, fibres or vascular elements. Slide: D—3—1, cross-table number 13.3/111.2.
2. Remnants of vascular tissue. Slide: D—16—3, cross-table number, 19.2/118.3.
3. Degraded parenchyma cells. Slide: D—3—2, cross-table number, 19.7/113.2.
4. Burnt prosenchyma cells. Slide: D—16—2, cross-table number, 15.1/104.6.
5. Stoma bearing epidermis remnant. Slide: D—3—3, cross-table number, 21.8/104.0.
6. Fungous remnant, *Pluricellaesporites* fsp. Slide: D—3—1, cross-table number, 13.3/108.5.
7. *Leiotriletes dorogensis* (Kds. 1960) Kds. 1961, Schizaeaceae, cf. *Lygodium*. Slide: D—3—2' cross-table number, 9.6/103.8.
8. *Leiotriletes adriennis* (R. Pot. et Gell. 1933) W. Kr. 1959, Schizaeaceae, cf. *Lygodium*. Slide: D—3—1, cross-table number, 10.7/114.9.
9. *Cicatricosisporites dorogensis* R. Pot. et Gell. 1933 subfsp. *dorogensis*, Schizaeaceae, *Anemia*. Slide: D—3—1, cross-table number, 11.9/105.6.
10. *Monocolpopollenites tranquillus* (R. Pot. 1931) Th. et Pf. 1953 subfsp. *tranquillus*, Palmae. Slide: D—3—1, cross-table number 19.5/112.1.
11. *Monocolpopollenites tranquillus* (R. Pot. 1931) Th. et Pf. 1953 subfsp. *tranquillus*, Palmae. Slide: D—3—2, cross-table number, 13.6/113.1.
12. *Arecipites granulatus* (Kds. 1961) L. Rákosi 1973, Palmae, massula of pollen grains. Slide: D—3—2, cross-table number, 10.3/119.9.
13. *Cupuliferoideaipollenites liblarensis* (Thoms. in Pot., Thoms. and Thiery. 1950) R. Pot. 1960, Fagaceae v. Leguminosae (left), *Cupuliferoipollenites pusillus* (R. Pot. 1934) R. Pot. 1960, Fagaceae (right). Slide: D—16—1, cross-table number, 22.1/113.6.









## Organic geochemical features

To describe the geochemical features of the organic matter brown coals were chosen that display similar organic carbon contents. As it is shown in Table 1: TOC=65—73%, the hydrogen content varies between 5.7 and 6.7%. In favour of exact comparison, the elementary composition is given to moisture and ash-free state. Ash content varies within wide extreme values, i.e. between 6.8 and 28.9%. When comparing the two coal seams the samples from the Dörög basin (marked by D) display higher ash and H-contents than the samples from Tatabánya (marked by T). The ash contents of the latter ones shows only slight changes and their H-contents are nearly the same, i.e. 5.69, 5.84 and 5.89%. Concerning the organic carbon content, the TOC-contents show lowest and highest values in the D-samples and medium values in the T-samples. With respect to the two most significant element, i.e. C and H, the difference can be neglected.

TABLE I

*Moisture- and ash-content of samples, elemental analysis of organic matter (OM)*

Sample	Moisture %	Ash %	C %	Elemental analysis of OM		S %
				H %	N %	
D—16	8.66	19.70	73.22	6.39	0.15	4.61
T—1	13.64	7.03	71.05	5.84	0.61	3.03
T—2	14.37	6.77	72.48	5.69	0.93	5.33
D—3	8.94	28.87	65.44	6.74	0.43	7.88
T—6	11.28	13.73	68.84	5.89	2.63	5.73

## Plate II

1. Degraded plant tissue remnants, probably fibres or tracheids. Slide: T—1—1, cross-table number 18.1/106.7.
2. Thick walled parenchyma tissue remnants. Slide: T—1—1, cross-table number, 16.1/110.4.
3. Thin walled parenchyma cells. Slide: T—6—4, cross-table number, 17.4/109.4.
4. Hyphae penetrated into degraded plant tissue remnants. Slide: T—6—2, cross-table number, 11.4/105.2.
5. Fossilized resinous cell material. Slide: T—1—1, cross-table number, 18.2/103.8.
6. Resinous drop. Slide: T—2—3, cross-table number, 8.7/117.3.
7. Hyphae penetrated into degraded plant tissue remnants. Slide: T—6—2, cross-table number, 12.7/106.2.
8. Granotricolporites semiglobosus (Kds. 1963) Kds. 1974, Sterculiaceae. Slide: T—2—1, cross-table number, 9.3/118.4.
9. Cupuliferoipollenites pusillus (R. Pot. 1934) R. Pot. 1960, Fagaceae. Slide: T—1—3, cross-table number, 4.2/109.2.
10. Ilexpollenites margaritatus (R. Pot. 1931) Thg. 1937 f. medius, Aquifoliaceae, Ilex. Slide: T—2—3, cross-table number, 20.9/117.8.
11. Labraferoidaepollenites pseudogranulatus (Gladkova 1965) n. comb., Myricaceae. Slide: T—2—3, cross-table number, 9.9/115.6.
12. Plicatopollis lunatus Kds. 1974, Juglandaceae. Slide: T—2—3, cross-table number, 17.2/116.2.
13. Eriopites longisulcatus Wodeh. 1933, Ericaceae. Slide: T—1—1, cross-table number 17.2/113.3.
14. Eriopites longisulcatus Wodeh. 1933, Ericaceae. Immature massula of pollen grains. Slide: T—1—2, cross-table number 4.9/117.9.

Nevertheless, the quantitatively similar carbon and hydrogen contents imply remarkable qualitative difference. In harmony with the Rock-Eval records carried out by the usual programme (isothermal temperature = 300 °C) the organic geochemical features of the samples are different. All samples are immature, these did not reach the main CH-generation zone Fig. 1. As compared to the evolution path

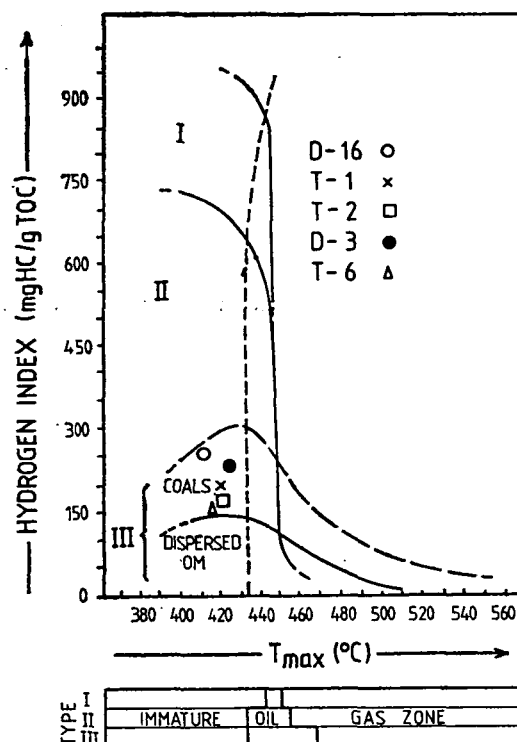


Fig. 1. Diagram of Hydrogen Index versus  $T_{max}$  for the brown coals examined

determined for the dispersed organic matter, based on the HI-OI indices all the five samples fall between type II and III (Fig. 2). Nevertheless, the H-index of the D-samples is higher than that of the T-samples, in harmony with the hydrogen content of the samples (Tables 1 and 2). The ability for pyrolysis of the organic matter is similar. The organic carbon content of the D-samples can be pyrolyzed to 20–22%, that of the T-samples to 13–17%. Within a given locality, e.g. comparing the three T-samples, the PC/TOC value is highest in the sample T—1 deriving from inundated deep swamp ecological conditions, and lowest in the sample T—6 formed in the environment characterized by intense microbial activity.

The genetic potential of the samples (Table 2) show definite relationship with the formation micro-environment. Sample D—16 deriving from an inundated deep swamp displays the highest genetic potential: 136 mg HC/g. The second highest value is displayed by the sample T—1 (114 mg HC/g) formed in very humid environment. The samples T—2 deriving from a myricaceous swamp, and D—3 referring



Rock-Eval pyrolysis results for brown coal samples (isothermal temperature = 300 °C) TABLE 2

Sample	T <sub>max</sub> °C	S1	S2	Gen. pot.	PI	S2/S3	PC/TOC	HI	OI
D—16	411	4.08	132.36	136.44	0.03	11.95	21.7	252	21
T—1	419	3.86	110.68	114.54	0.03	6.96	16.9	196	28
T—2	418	2.71	95.06	97.77	0.03	7.13	14.2	166	35
D—3	423	3.08	94.56	97.64	0.03	8.75	20.0	232	26
T—6	415	1.61	79.43	81.04	0.02	5.66	13.1	153	27

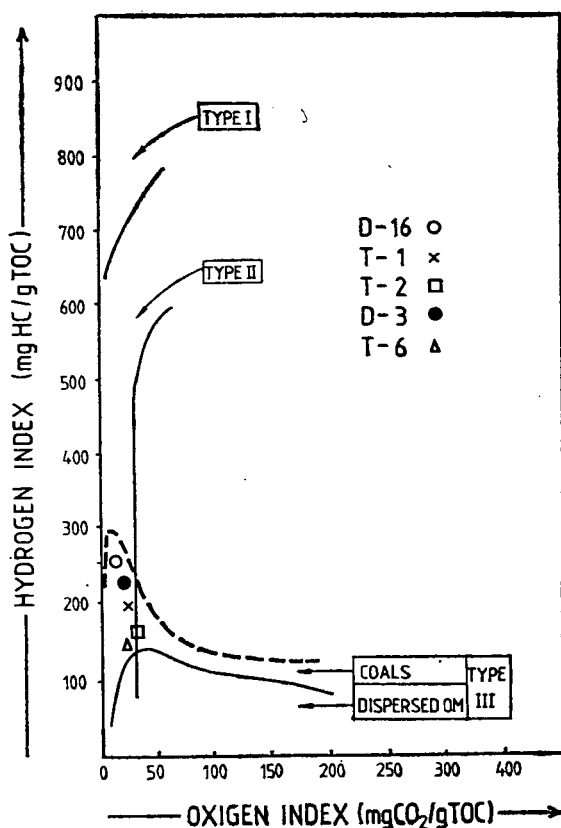


Fig. 2. Diagram of Hydrogen Index versus Oxygen Index for the brown coals examined

to tranquillus type palm forest show the same genetic potential (97.7 mg HC/g). The potential value is lowest in case of the sample T—6 (81 mg HC/g) the features of which referring to strong oxidation and high frequency biological activity.

Based on the H-index, on the genetic potential and on the PC/TOC ratio all the studied samples are favourable from the hydrocarbon generation point of view. In the HI-OI diagram (Fig. 2) these lie between the so-called oil prone and gas prone kerogens. Consequently, in the zone of catagenesis both oil and gas generation

can be expected from them. The S2/S3 values that are greater than 5 in all samples (Table 2) indicate also oil prone organic matter. PETERS (1986), however, stated that "the results overestimate the liquid-hydrocarbon-generative potential of these types of coals". Thus, in order to determine the liquid-hydrocarbon-genetic potential of the studied brown coal samples, experimental thermal degradation was carried out. Samples were heated at 500 °C for one hour, in inert gas atmosphere. Results are shown in Table 3. For comparison, the products of a type II, immature dispersed

TABLE 3

*Yield of thermal degradation (T = 500 °C. period = 1 hour)*

Sample	Unconverted matter %	Gas + Water %	Oil mg/g	Bitumen TOC
D—16	68	23.5	160	4.8
T—1	62	30.0	122	4.1
T—2	64	31.0	85	3.0
D—3	72	23.5	108	3.2
T—6	65	32.1	54	2.7
OM, type II. (Mecsek Mts)	92	6.8	163	47.0

organic matter developed under similar conditions, are also demonstrated. In the course of degradation relatively large amounts of oil were generated from the brown coal samples: 54—160 mg oil/g TOC. The quantity of liquid hydrocarbon generated from the sample D—16 is the same as that generated from the type II OM. Under the same conditions, 500—550 mg oil/g TOC was obtained from the oil shale containing kerogen of type II (HI = 440 mg HC/g TOC). About 40 mg oil/g TOC was generated by the lignite, displaying organic geochemical features similar to the kero-gens of type III (HETÉNYI, unpublished data).

The oil quantity generated from brown coals is also related to the plant remnants. Greatest amounts of oil were generated by the pyrolysis of samples D—16 and T—1. The oil production of the samples T—2 and D—3 shows medium values and lowest quantity of oil was generated during the thermal degradation of sample T—6 deriving from an environment of high biological activity. On the contrary, the total amounts of gas + water generated during the process did not show relationships to the palynological features. 23.5% gas + water was generated from the D-samples and 30—32% from the T-samples. This value represents the total amounts of water, hydrocarbon and non-hydrocarbon gases.

The S1 value provides information on the hydrocarbon gases, i.e. on the gas-hydrocarbon-genetic potential (measured in the course of Rock-Eval pyrolysis). Similarly to the genetic potential (S1 + S2), the S1 value shows relationship with the palynological features of the samples (Table 2). In order to study the change of gas-hydrocarbon quantity as a function of temperature, step-by-step Rock-Eval pyrolysis was carried out having changed the isothermal temperature by 20 °C between 180 and 340 °C.

The difference of data obtained by the lowest (180 °C) and highest (340 °C) isothermal temperature programme is shown in Table 4. Based on the change of the genetic potential, on the  $\Delta(S2/S3)$ , on the  $\Delta(PC/TOC)$  and on the  $\Delta HI$  value, the samples can be divided into two groups and the groups correspond to the localities. The measure of change concerning the data in relation with the genetic potential is

TABLE 4

*Change of the Rock-Eval pyrolysis data between  
180 °C and 340 °C isothermal temperature*

Sample	Change of data between 180—340 °C						
	S1	S2	Gen. pot.	PI	S2/S3	PC/TOC	HI
D—16	—22.46	49.29	26.83	—0.16	9.25	4.2	94
T—1	—18.03	26.30	8.27	—0.15	4.38	1.3	46
T—2	—12.54	19.06	6.52	—0.13	3.73	1.0	33
D—3	—11.16	21.65	10.46	—0.12	6.02	2.2	53
T—6	—9.41	16.93	7.52	—0.12	3.44	1.2	33

greater in the D- and smaller in the T-samples. At the same time, the change of the S1:  $\Delta S1$  (180°—340 °C) being characteristic rather of the gas-hydrocarbon-genetic potential shows relationship unambiguously with the palynological features of the samples.

The values of the change followed in the 20 °C steps are shown in Table 5. In this respect, the S1 value of the sample T—6 formed in an environment of strong biological activity displays different changes as compared to those of the other samples. In case of the sample in question, the gradual increase of  $\Delta S1$  can be observed as a function of the increasing temperature interval. In case of the other samples maxima can be observed between 220 and 240 °C.

TABLE 5

*Relative change of S1 between the following steps of modified Rock-Eval pyrolysis.  
(Difference of S1-values measured at 180° and 340 °C isothermal  
temperature = 100 %)*

Tempe- rature (°C)	Sample	— $\Delta S1$ (%)				
		D—16	T—1	T—2	D—3	T—6
180—200		0.9	0.9	0.6	0.1	0.4
200—220		0.4	1.2	0.6	1.1	0.2
220—240		3.3	5.5	4.4	3.4	1.7
240—260		1.4	1.4	0.1	1.0	1.9
260—280		5.5	6.2	3.3	5.1	3.1
280—300		6.5	6.2	12.7	15.2	9.4
300—320		39.3	20.2	23.3	15.9	22.0
320—340		42.7	58.4	55.0	58.2	61.3
180—340		22.46	18.03	12.54	11.16	9.41

The close interrelation between the palynological features and the change of the gas-hydrocarbon-genetic potential of the samples as a function of temperature can be clearly seen in Fig. 3. The S1 value is negligible and falls behind the determination limit between 180 and 200 °C, in case of all samples. The curves of the samples deriving from very humid inundated regions (D—16, T—1) are separated from those of the others. Three curve types can be distinguished after 220 °C: the curves of the mentioned inundated deep swamps, the curve of the fungiferous sample T—6 referring to the region of strong biological activity, and the common curve of samples

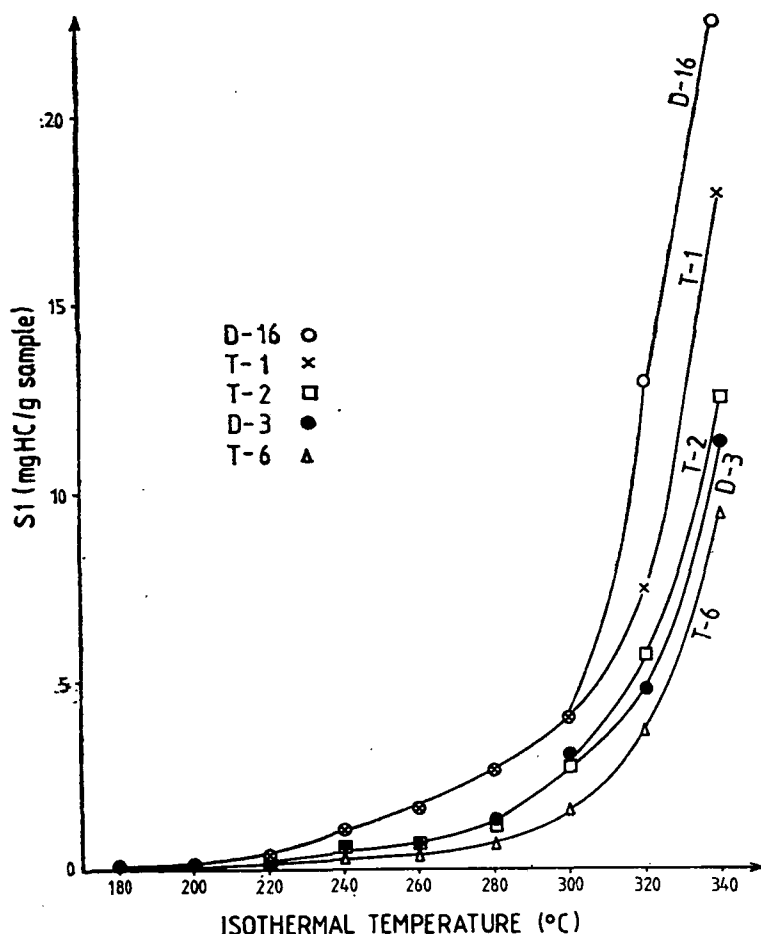


Fig. 3. The change of the gas-hydrocarbon-generative potential of the samples as a function of isothermal temperature

T—2 and D—3 being intermediary between the two preceding curves. Consequently, the hydrocarbon quantity generated between 220 and 300 °C is related first of all to the features of the environment of formation. Above 300 °C all samples display different curves, i.e. the individual features become predominating. At these temperatures (over 300 °C) probably small amounts of liquid hydrocarbon are also generated in addition to the gas-hydrocarbon. The sample sequence corresponds to the sequence obtained according to the S2 quantities (Table 2) by the Rock-Eval basic programme (isothermal temperature = 300 °C).

#### SUMMARY

The organic geochemical features of several Hungarian brown coals were studied by Rock-Eval pyrolysis and experimental thermal degradation. We tried to find relationships between these features and the microscopic plant remnants of the samples:

Brown coals derive from two different localities: Dorog and Tatabánya. In case of both localities samples were chosen that derive from periodically inundated deep swamp ecological conditions (D—16, T—1). One sample from each region formed in shallow moor characterized mostly by *tranquillus* type palm forest (D—3, T—2). The sample T—6 derives from an environment characterized by intense biological activity during sedimentation. In this sample great amounts of fungus remnants were found.

We tried to characterize the different environmental conditions by samples that display minimum differences with respect to the organic matter quantity. TOC equals 68—72% in the T-, and 65—73% in the D-samples.

As a first approximation, the quality of the organic matter proved to be similar. All samples are immature containing organic matter between type II and type III. Within the group, however, samples being closer either to type II or to type III could be distinguished. The D-samples were closer to type II and the T-samples to type III organic matter. Relationship between the H-index and the features of the microscopic plant remnants could be observed only within one locality.

The position of the samples in the evolution paths and the high S<sub>2</sub>/S<sub>3</sub> value indicated organic matter suitable to generate both gas and oil. By means of experimental thermal degradation 54—160 mg oil was generated from 1 g organic carbon. Greatest amounts of oil were generated during the pyrolysis of the samples deriving from swampy inundated region, and lowest amounts were experienced in case of samples deriving from the region of high frequency biological activity, independently of the locality.

The gas-hydrocarbon-genetic potential was studied by step-by-step Rock-Eval pyrolysis. The isothermal temperature was increased by 20 °C between 180 and 340 °C. At the beginning, the S<sub>1</sub> value proved to be negligible, between 200 and 300 °C isothermal temperatures it displayed close relationship with the features of the ecological conditions. The S<sub>1</sub> isothermal temperature curves of the samples that showed similar microscopic plant remnants coincide (Fig. 3). Above 300 °C isothermal temperature the curves become separated. In this range the increasing sequence of D<sub>1</sub> value is the same as that of S<sub>2</sub> value and roughly corresponds to the sequence of increasing oil production, as well.

The results of these investigations suggest that the microscopic plant remnants of the samples, i.e. the ecological conditions are related to the hydrocarbon-genetic potential of the organic matter. This relationship is characteristic especially in case of gas-hydrocarbon-genetic potential as a function of temperature.

#### ACKNOWLEDGEMENT

The authors express their gratitude to the Geochemical Research Laboratory of the Hungarian Academy of Sciences making available the samples investigated and to the Hungarian Geological Survey for the permission to publish this work.

#### REFERENCES

- ESPITALITÉ, J., MADEC, M. and TISSOT, B. (1977): Source rock characterization method for petroleum exploration. Offshore Technology Conference.  
ESPITALITÉ, J., DEROO, G. et MARQUIS, F. (1985): La pyrolyse Rock-Eval et ses applications, I—II. Revue de L'Institut Français du Pétrole 40, 5, 6 563—579, 755—784.

- ESPITALIÉ, J., DEROO, G. et MARQUIS, F. (1986): La pyrolyse Rock-Eval et ses applications, III Revue de L'Institut Français du Pétrole 41, 1, 73—79.
- FORSBERG, A., and BJØRØY, M. (1981): A sedimentological and organic geochemical study of the Botneheia formation, Svalbard, with special emphasis on the effects of weathering on the organic matter in shales. In: *Advances in Organic Geochemistry*, 1981, ed. by M. BJØRØY, 60—68.
- FREDERIKSEN, N. O. (1985): Review of Early Tertiary sporomorph paleoecology. — *AASP Contribution ser.*, 15, 92.
- KEDVES, M. (1960): Etudes palynologiques dans le bassin de Dorog — I. — *Pollen et Spores* 2/1, 89—118.
- KEDVES, M. (1963): Contribution à la flore éocène de la Hongrie sur la base des examens palynologiques des couches houillères du puits III. d'Oroszlány et du puits XV/b de Tatabánya. — *Acta Bot.* 9/1—2, 95—130.
- KEDVES, M. (1969): Palynological Studies on Hungarian Early Tertiary Deposits. — *Akadémiai Kiadó Budapest*.
- ORR, W. L. (1983): Comments in pyrolytic hydrocarbon yields in source-rock evaluation. In: M. Bjørøy et al, eds., *Advances in organic geochemistry*, 1981, New York, Wiley, 775—787.
- PETERS, K. E. (1986): Guidelines for evaluating petroleum source rock using programmed pyrolysis. *AAPG Bulletin* 70, 3, 318—329.
- RÁKOSI, L. (1973): Palynologie des formations paléogènes du bassin de Dorog. — *Ann. Inst. Geol. Publ. Hung.*, 55, 500—575.
- SAXBY, J. D., BENNETT, A. J. R., CORCORAN, J. F., LAMBERT, D. E. and RILEY, K. W. (1986): Petroleum generation: Simulation over six years of hydrocarbon formation from torbanite and brown coal in a subsiding basin. *Org. Geochem.*, 9, 2, 69—81.
- SPIRO, B. and AIZENSHTAT, Z. (1981): Natural combustion and pyrolysis of bituminous rocks at the margin of Hatrurium, Israel. In: *Advances in Organic Geochemistry*, 1981, ed. by M. BJØRØY, 799—807.
- TEICHMÜLLER, M. and DURAND, B. (1983): Fluorescence microscopical rank studies on liptinites and vitrinites in peat and coals, and comparison with results of the Rock-Eval pyrolysis. *Int. J. Coal Geol.*, 2, 197—230.
- TEICHMÜLLER, M. and R. TEICHMÜLLER (1979): Diagenesis of coal (coalification) In: G. LARSEN and G. V. CHILINGAR: *Diagenesis in sediments and sedimentary rocks. Developments in Sedimentology*, Elsevier, 1979, 207—218.
- VERHEYEN, T. V., JOHNS, R. B. and ESPITALIÉ, J. (1984): An evaluation of Rock-Eval pyrolysis for the study of Australian coals including their kerogen and humic acid fractions. *Geochimica et Cosmochimica Acta* 48, 63—70.
- TISSOT, B. P. and WELTE, D. H. (1984): *Petroleum formation and occurrence*: New York, Springer-Verlag, 699.

*Manuscript received, 5 September, 1986*

## TYPE AND EVOLUTION STAGE OF HUNGARIAN OIL SHALE KEROGENS

M. HETÉNYI and L. PÁPAY

Institute of Mineralogy, Geochemistry and Petrography,  
Attila József University

### ABSTRACT

The insoluble organic matter of some Hungarian oil shales (Upper Pannonian, maar type: Pula, Gércse, Várkesző, and Miocene, lagoon-type: Mecsek, Várpalota, Mátraszele) were investigated.

In spite of the same age and similar formation processes the maar-type oil-shale kerogens are different: the Pula kerogen proved to be an algal-derived organic matter of type I, of high conversion and H/C ratio, and good petroleum potential. On the contrary, the organic matter of Várkesző oil shale corresponds to type II and can be interpreted by presence of terrestrial plant remnants in the precursor material. The considerable difference between the Pula and Várkesző oil shales during the thermal decomposition in the evolution paths, apparent activation energy (Pula:  $146 \text{ kJmol}^{-1}$  and Várkesző  $75 \text{ kJmol}^{-1}$ ) and in the ratio of the gas and oil phases formed can be interpreted by the presence of terrestrial plant remnants in the precursor material of the Várkesző oil shale. The kerogen of Gércse oil shale can be considered as a transition between type I and II.

The lagoon-type oil shales contain kerogen of type II. The Corg content and petroleum potential, as well as the H/C atomic ratio and the HC-yield of the Várpalota oil shale is fairly high. During the pyrolysis it generates considerable amount of oil. The petroleum potential of oil shales from Mecsek and Mátraszele corresponds rather to a source rock of good quality.

### INTRODUCTION

In Hungary two types of oil shale formations had been found by the Hungarian Geological Survey (BENCE, JÁMBOR, PARTÉNYI, 1979; JÁMBOR and SOLTÍ, 1975, 1976; JÁMBOR, RAVASZ and SOLTÍ, 1982; SOLTÍ, 1980, 1985):

1. Maar-type oil shale beds generated as fillings in volcanic craters, and
2. Lagoon-type oil shale beds deposited in intramontane lagoons.

The maar-type oil shale formations were discovered in the course of investigating the tuff rings of Upper Pannonian basalt areas in Transdanubia (Hungary). The beds are of small size and medium to poor quality as compared to the international scale and they are insignificant as sources for energy and raw materials, respectively. Nevertheless, these oil shales serve as excellent model to investigate the characteristics of different organic matters and to study their artificial evolution (HETÉNYI, 1979, 1980, 1983; HETÉNYI, TÓTH, MILLEY, 1982). These provide the possibility to seek for relationships between the depositional environments, the composition of the precursor biomass and the type of the generating kerogen.

In the development of maar-type occurrences the isolation of the crater lake from the inland sea as well as the warm to temperate climate played an important role.

The intense weathering of the crater wall and thus the abundance of the crater lake in nutrients promoted the accumulation of the organic matter (BENCE *et al.*, 1979; HAJÓS, 1976; NAGY, 1976).

The oil shales in the intramontane basins are of poor quality. Their formation was influenced mainly by their isolation from the open sea and from the main sediment transporting currents. These are usually related to coal beds (SOLTI, 1982).

To analyse in detail the peculiarities of the organic matter, three samples were chosen from both environments. These are: those of maar-type from Pula, Gérce and Várkesző, and those of lagoon-type from Várpalota, Mecsek Mountains and Mátraszele.

## EXPERIMENTS

The oil shale samples were ground to grain size of 0,05—0,15 mm, the bitumen was extracted in a Soxhlet extractor by chloroform and by benzene-acetone-methanol mixture of 70:15:15 ratio.

Kerogen was isolated first by physical method, the remaining mineral components were destructed by means of chemical procedures.

The organic carbon content was determined at 1000 °C in oxygen atmosphere.

The CR/CT ratio was measured on the basis of the ASTM standard (CUMMINS *et al.*, 1972).

Experimental evolution was carried out between 300 and 500 °C under nitrogen atmosphere. Products were collected on a cooled trap and oil was separated from the water. The solid matter remained was extracted.

The organic matter of the oil shales as well as that of the degradation products and unconverted organic matter were characterized by the H/C atomic ratio and by Rock Eval pyrolysis (ESPITALIÉ *et al.*, 1977).

The shale oil was checked by IR and NMR method (PÁPAY, 1982).

## RESULTS

From economic point of view the most important features of the organic matter-bearing sedimentary rocks, among others that of the oil shales, are the quantity and chemical composition of hydrocarbons generated from them either by natural evolution or by experimental thermal degradation. Based on the organic matter content of the sediments and on the type and evolution stage of kerogen, the values of these characteristics can be estimated.

### 1. Quantity of organic matter

The organic matter content is usually characterized by the organic carbon content. Based on the average values of the Hungarian oil shales of medium to poor quality, their organic carbon contents vary between 10—13% and 2—7%, respectively (Table 1).

### 2. Evolution stage of kerogen

As it has been expected, the maturity of the kerogen of the oil shales studied corresponds to the zone of diagenesis (Table 2). The ratio of the diagenesis coefficient and the H/C atomic ratio of the kerogen concentrates (CR/CT equals to 0,1—0,5, the atomic ratio from 1,3 to 1,7) refer to this fact. As compared to the heteroatomic



Organic carbon content of the different Hungarian oil shales

TABLE 1

Age	Locality	Depths (m)	C <sub>org</sub> (%)	
			average	min.—max.
Upper Pannonian	Pula	4.5—39.5	13.4	0.3—45.7
	Gérce	4.0—68.3	6.6	0.1—15.5
	Várkesző	55.0—70.5	13.0	3.2—18.7
Badenian	Várpalota	3.1—14.0	10.9	4.1—26.3
Carpathian	Mecsek	surface exposure	4.3	—
Ottományian	Mátraszele	234.7—236.1	2.8	1.8—4.5

Evolution level of the Hungarian oil shale kerogens

TABLE 2

Locality	CR/CT	H/C atomic ratio	S2/S3	T <sub>max</sub>	HI mgHC gTOC
Pula	<0.10	1.7	15.7	442	745
Gérce	0.20	1.6	8.7	429	500
Várkesző	0.43	1.3	6.4	425	390
Várpalota	0.36	1.5	6.7	425	460
Mecsek	0.36	1.5	9.2	432	440
Mátraszele	0.53	1.3	6.8	428	370

products (S3), the quantity of hydrocarbon (S2) measured by Rock Eval pyrolysis is higher than five. The ratio indicates that the changes describing the main phase of hydrocarbon generation, that is the catagenesis, did not start yet. When plotting the maximal temperature of hydrocarbon generation (T<sub>max</sub>) against the H-index being in good correlation with the H/C atomic ratio, it can be seen that the samples are in the immature zone (Fig. 1).

The immaturity of this kerogen is evidenced by the position of the samples on the evolution path as well as the fact that by means of experimental degradation nearly the complete evolution path can be reproduced. Fig. 2 illustrates the artificial evolution paths of different types of kerogen obtained by experimental thermal degradation.

### 3. Type of kerogen

The evolution paths are suitable to determine the most important characteristic of kerogen, i.e. its type: As it can be seen in Fig. 2, based on the evolution paths the lagoon-type oil shale kerogens belong to type II. Nevertheless, considerable differences can be observed between the samples of the Mecsek Mountains, Mátraszele and the Várpalota samples. The latter starts with a higher H-index than the previous ones. Consequently, during its artificial evolution, as well as during the corresponding natural evolution under suitable conditions, this can or could produce

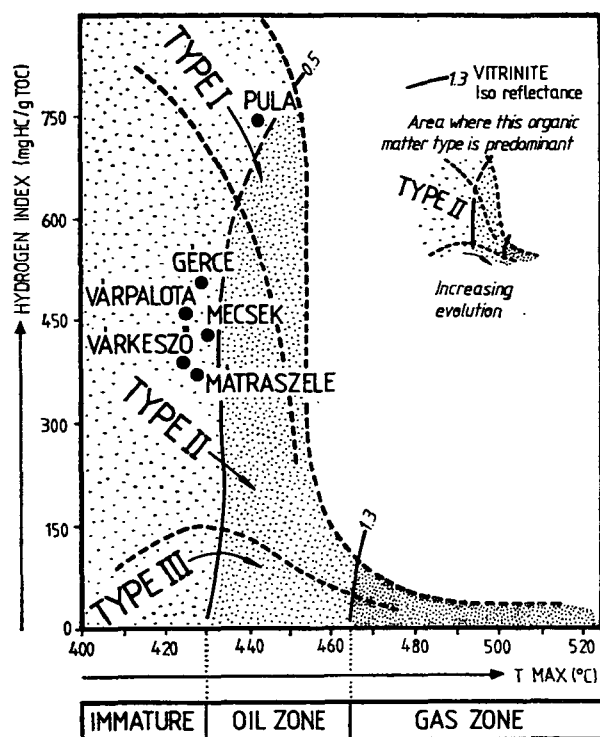


Fig. 1. Classification of the kerogens of the different Hungarian oil shales and characterization of their maturity in general HI—T<sub>max</sub> diagram

more hydrocarbons than the kerogen of the Mecsek or Mátraszele samples. Thus, under the same geological conditions the type of the organic matter of oil shales accumulated in intramontane lagoons is the same but due to smaller differences within the given type, these samples are of different economic values.

Among the oil shales generated in volcanic tuff rings the differences are much more emphasized. The kerogen of Pula can be ranged to type I, whereas the kerogen of Várkesző belongs to type II. The kerogen of Gerge seems to be transitional between them (HETÉNYI, 1985).

As a comparison, the experimental evolution paths of the sedimentary samples containing kerogen of type III, are also demonstrated in Fig. 2. These samples are sediments from the neighbourhood of the Mátraszele bed presumed formerly as oil shale indications but these cannot be considered to be oil shales due to their organic geochemical features, for example due to the type of organic matter.

The value which can be measured by Rock-Eval pyrolysis as well as the value which can be calculated from it are also suitable to characterize the type of the organic matter. Consequently, as to our opinion the type of kerogen of similar stage being at the beginning of evolution can be expressed numerically by the PC/TOC ratio (HETÉNYI, 1983). The ratio shows the proportion of the total organic carbon to that pyrolyzable by Rock Eval method. Based on the organic carbon content of 65% to be pyrolyzed by Rock Eval, the kerogen of the Pula oil shale belongs unambiguously

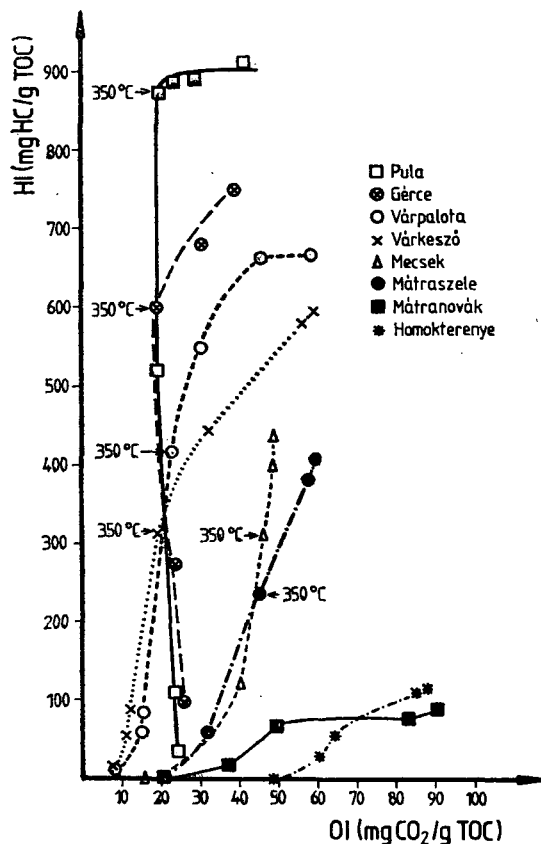


Fig. 2. Artificial evolution paths of the different Hungarian oil shales

to type I. The PC/TOC value of the samples of type III, varying between 12 and 13, considerably differs from this value. This is a medium value and shows some closeness in case of the kerogens of lagoon type oil shales and of the Várkesző oil shale kerogens, varying between 32 and 40 per cent. Based on this value, the kerogen of the Gércse oil shale seems to be transitional between the type I and II, but closer to type II having 47% PC/TOC value (Table 3).

When plotting the H-index as a function of  $T_{\max}$  (Fig. 1), all the oil shales are found in the field characterized by the organic matter of type II, except the Pula oil shale which, on the basis of these values, contains organic matter of type I.

Kerogen was isolated from the maar-type oil shale (Pula sand Várkesző) containing organic matter of two different types (type I and II), and from the most important lagoon-type bed (Várpalota) (Table 4). Isolation was carried out from the strata being most abundant in organic matter. In case of the Várkesző oil shale containing greater amounts of coalified plant remnants, organic matter-rich strata were chosen which contained greater quantities of plant remnants. As to our opinion the difference between the Pula and Várkesző kerogens can be attributed to the different

Characterization of the type of the organic matter in Hungarian oil shales  
and oil shale indications

TABLE 3

Locality	Type of organic matter	PC/TOC %	T <sub>max</sub> °C	HI mgHC g TOC
Pula	Type I	65	442	745
Gérce	Type(I)—II	47	429	500
Várkesző	Type II	38	425	390
Várpalota	Type II	40	425	460
Mecsek	Type II	38	432	440
Mátraszele	Type II	32	428	370
Mátranovák	Type III	13	432	140
Homokterenye	Type III	12	431	130

Characterization of the kerogens isolated from Hungarian oil shales

TABLE 4

Locality	Oil shale formation	H/C atomic ratio	CR/CT	Type of kerogen
Pula	maar-type	1.7	<0.10	Type I
Várkesző	maar-type	1.3	0.43	Type II
Várpalota	lagoon-type	1.5	0.36	Type II

proportion of mixing of the algal material constituting the biomass and of the higher plant remnants in the two samples (HETÉNYI, 1985).

As to the pollen analyses (NAGY, 1978; KEDVES, 1983) Botryococcus remnants are abundant in both beds, but the Pula oil shale shows extreme abundance. This is caused by the conditions favourable to the accumulation of Botryococcus braunii K. in the Pula oil shale. The uprushing water with carbonic acid produced by the sub-volcanic activity warmed the crater lake, producing favourable living conditions to the algae. The conservation of the huge amount of algal material accumulated in this manner was assured by the lack of destructive organism. The higher concentration and good preservation of the algae produced aliphatic polymer rich in hydrogen, that is the kerogen of type I. The organic matter of the Várkesző oil shale contains also large colonies of Botryococcus, the amount of it, however, being less than in the case of Pula. Further, the colonies are destructed due to the biologically active sedimentation environment. At the same time, the occasionally macroscopically identifiable higher plant remnants constitute the major part of the organic matter, being the precursors of the kerogen of type III. The mixing of the two extreme kerogen types, that is type I and III, resulted in kerogen which can be qualified as type II (HETÉNYI, 1983).

#### 4. Experimental simulation of the catagenesis

The different types of kerogen, that is the different precursor biomasses can be recognized in the course of the experimental evolution, as well.

Based on the experimental simulation of the catagenesis the apparent activation energy of the Pula and Várkesző kerogens shows a ratio of two-to-one (Table 5).

The composition of the precursor matter is reflected also in the quantities and qualities of the hydrocarbons formed during the kerogen evolution. The Pula oil shale generated 688 mg shale oil to 1 g organic carbon. The maar-type oil shale of Várkesző and the lagoon-type oil shale of Várpalota generated 400–450 mg shale oil to 1 g organic carbon (Table 5).

TABLE 5

*Artificial evolution of kerogens isolated from maar-type oil shales*

Locality	Pula	Várkesző
Type of kerogen	Type I	Type II
Temperature of degradation (°C)	500	500
Degradation-period (hours)	5	5
Oil yield (mg/g TOC)	688	425
Gas + water yield (mg/g TOC)	492	669
Ratio of conversion (%)	85	70
Apparent activation energy of catagenesis (kJmol <sup>-1</sup> )	146	75

The bitumen, being intermediary product of the evolution shows better the differences in the chemical composition of the kerogens than the shale oil. The H/C atomic ratios characterizing the bitumens are ranged between the values of 1,63–1,74 and 1,31–1,50 in case of the oil shales containing organic matter of type I and type II, respectively (Table 6).

TABLE 6

*H/C atomic ratio of bitumens formed by artificial evolution of the different oil shales (temperature: 350 °C)*

Degradation period (hours)	Maar-type oil shales		Lagoon-type oil shales	
	Pula	Várkesző	Várpalota	Mecsek
1	1.74	1.39	1.50	1.45
5	1.64	1.38	1.46	1.36
10	1.63	1.34	1.31	1.35

Shale oil is the most significant end-product generated during the pyrolysis. In case of the two maar-type kerogens the average length of the paraffin chain is very different in the shale oils. The lagoon-type kerogen shows transitional characteristics,

TABLE 7

*Characteristic values of shale oil yielded by thermal degradation of kerogens isolated from Hungarian oil shales (temperature: 500 °C)*

Locality	Type of kerogen	Length of the average paraffinic carbon skeleton *	H in the different carbon skeleton*		
			aliphatic %	alicyclic %	aromatic %
Pula	Type I	C <sub>16</sub>	60	30	10
Várkesző	Type II	C <sub>10</sub>	48	31	21
Várpalota	Type II	C <sub>13</sub>	55	27	18

\* Measured by NMR records

in this respect, too. The proportion of the aromatic compounds refers also to the similarity of the Várpalota and Várkesző organic matters. The proportion of the aromatic compounds amounts to about twenty percent in these cases, but only about ten percent in case of the Pula shale oil (Table 7).

## REFERENCES

- HAJÓS, M. (1976): Diatom flora in Upper Pannonian sediments of borehole Put—3 at Pula village (Transdanubia, Hungary). — Annual Report of the Hungarian Geological Institute of 1974 Budapest, p. 263—486.
- HETÉNYI, M. (1979): Thermal degradation of the oil shale kerogen of Pula (Hungary) at 473 and 573 K. — Acta Miner., Petr. Szeged, XXIV/1, p. 99—111.
- HETÉNYI, M. (1980): Thermal degradation of the organic matter of oil shale of Pula (Hungary) at 573—773 K. — Acta Miner. Petr., Szeged, XXIV/2, p. 301—314.
- HETÉNYI, M., TÓTH, I. and MILLEY, GY. (1982): On the role of temperature and pressure in the artificial evolution of organic matter of the Pula oil shale (Hungary). — Acta Miner. Petr., Szeged, XXV/2, p. 131—146.
- HETÉNYI, M. (1983): Experimental evolution of oil shales and kerogens isolated from oil shales. — Acta Miner. Petr., Szeged, XXVII/1, p. 73—85.
- HETÉNYI, M. (1985): Organic geochemical features of maar-type oil shales of Hungary. — Acta Miner. Petr., Szeged, XXVII, p. 145—152.
- JÁMBOR, Á. and SOLTÍ, G. (1975): Geological conditions of the Upper Pannonian oil shale deposit recovered in the Balaton Highland and at Kemeneshát, — Acta Miner. Petr., Szeged, XXII, p. 9—28.
- JÁMBOR, Á. and SOLTÍ, G. (1976): Geological conditions of the Upper Pannonian oil shale deposit recovered in the Balaton Highland and at Kemeneshát (Transdanubia, Hungary). — Annual Report of the Hungarian Geol. Institute of 1974, Budapest, p. 193—220.
- JÁMBOR, Á., RAVASZ, Cs. and SOLTÍ, G. (1982): Geological and lithological characteristics of oil shale deposits in Hungary. — 3rd All Union Meeting on the Geochemistry of Oil Shales, Tallinn.
- KEDVES, M. (1983): Étude paléobotanique sur les schistes pétrolière du tertiaire supérieur de Hongrie. — Revue de Micropaléontologie, 26/1, p. 48—53.
- NAGY, E. (1976): Palynological investigation of Transdanubian oil shale exploratory boreholes. — Annual Report of the Hungarian Geological Institute of 1974, Budapest, p. 247—262.
- PÁPAY, L. (1982): IR and NMR characterization of oil generated from some Hungarian oil shale at 773 K. — Acta Miner. Petr., Szeged, XXV/2, p. 147—156.
- SOLTÍ, G. (1980): The oil shale deposit of Várpalota. — Acta Miner. Petr., Szeged, XXIV/2, p. 289—300.
- SOLTÍ, G. (1981): The geyserite of Pula. — Annual Report of the Hungarian Geological Institute of 1970, Budapest, p. 241—247.
- SOLTÍ, G. (1985): Alginite (oil shale) exploration and utilization possibilities in Hungary. — Földtani Kutatás, XXVIII, p. 11—20.
- TISSOT, B., DURAND, B., ESPITALIÉ, J. and COMBAZ, A. (1974): Influence of the nature and diagenesis of organic matter in formation of petroleum. — Am. Assoc. Petr. Geol. Bull., 58, p. 499—506.
- TISSOT, B. P. and WELTE, D. H. (1978): Petroleum formation and occurrence. — Springer Verlag.
- TISSOT, B. P. (1984): Recent advances in petroleum geochemistry applied to hydrocarbon exploration. — Am. Assoc. Petr. Geol. Bull., 68, p. 545—563.

Manuscript received, 10 July, 1986



**B**20234

## Illustrations

Figures should be used only where they are essential to elucidate the text.

The illustrations should be numbered according to their sequence in the text, and in the text references should be made to each figure.

All illustrations should be given separately, not stuck on sheets and not folded. The number of the figure and the authors name should be noted on the reverse side of the photographs and on the lower frontside of drawings, indicating at the same time the top of the figure where it is necessary.

Captions for all figures should be given typewritten on a separate list at the end of the manuscript. Drawn text in the figures should be kept to a minimum.

Drawings should be made on tracing paper by Indian ink. The thickness of the lines and the size of the lettering should be big enough to allow a necessary reduction.

Photographs of good contrast and intensity on glossy paper are only acceptable. Colour photographs or drawings cannot be accepted.

Use bar scale on all illustrations instead of numerical scales that must be changed if reduction is necessary.

## References

All references to publications made in the text should be made by quoting the author's name (without initials) and year of publication in parenthesis.

The list of references at the end of the manuscript should be arranged alphabetically by author's names and chronologically per author.

If the referred publications are written by more than two authors, in the text only the name of the first author should be indicated, the other co-authors are denoted by "et al.", however, in the list of references the names of authors and all co-authors should be mentioned.

In the list of references all references should be written, e.g. Balogh, K., A. Barabás (1972): The Carboniferous and Permian of Hungary. *Acta Miner. Petr.*, Szeged, XX/2, 191—207.

At references to books beside the author's name, year of publication, title and the publishing house should also be mentioned.

In the case of references for symposium volumes, special issues or multi-authors books, the following system should be used: Roser, B. P., C. W. Childs, and G. P. Glasby (1980); Manganese in New Zealand. In: I. M. Varentsov and Gy. Grasselly (Editors): *Geology and Geochemistry of Manganese*, Vol. II Akadémiai Kiadó, Budapest, 199—211.

Manuscript that are not adequately prepared will be returned to the author(s).